Volcanic evolution of the Huka Group at Wairakei-Tauhara Geothermal Field, Taupo Volcanic Zone, New Zealand

Hamish James Cattell

A thesis submitted in partial fulfilment

of the requirements for the degree of

Doctor of Philosophy in Geological Sciences at the

University of Canterbury

2015

Abstract

Basin-hosted stratigraphy in volcanic arc settings reflects the interplay between ancient environments, volcanism, magmatism and tectonism. Lithostratigraphic variations within basins can be used to identify the location and timing of the processes contributing to their evolution. However, when deposits are hydrothermally altered, the use of many traditional analytical techniques for assessing their volcanic origin become impracticable, making analysis challenging. Examination then relies on an integrated mix of detailed macroscopic assessment and techniques utilising remaining stable magmatic phases. The Huka Group at Wairakei-Tauhara Geothermal Field (Wairakei-Tauhara) is primarily comprised of volcanic deposits preserving ~300 kyr of evolution in the Taupo Volcanic Zone (TVZ), New Zealand. Intensive geothermal well drilling in the field has identified the distribution and variation comprising its Waiora and Huka Falls Formations. The volcanic, structural and environmental history of the Huka Group, however, remains poorly understood. This thesis is concerned with identifying the stratigraphic and geothermal significance of the Huka Group from recent drill core samples at Wairakei-Tauhara. Drill core facies analysis confirm a spatially and temporally complex depositional history at the site. Deposits forming Waiora Formation were sourced from local explosive and effusive eruptions over ~100 kyrs within extensional basins hosting paleo-Lake Huka. Lacustrine and fluvial deposition prevailed for the following ~200 kyrs, as volcanism ceased, depositing the Huka Falls Formation. Frequent drilling of Huka Falls Formation has identified and thoroughly constrained facies variations of a local pyroclastic member, the Middle Huka Falls Formation. This eruption evolved as a series of water-supported, eruption-fed density currents from a sublacustrine vent in Tauhara transported beneath Lake Huka. Examined Huka Group core samples were hydrothermally altered and required the use of novel assessment techniques for comprehensive stratigraphic assessment. This alteration provided an opportunity to locally date the geothermal system within the Huka Group reservoir. Stratigraphic variations of resistant magmatic phenocrysts (feldspar) and immobile elements (Ti, Zr, V and Y) added new details of depositional processes and lithostratigraphy. Regional magmatic immobile element comparisons identified geochemical similarities within Huka Group ignimbrites that may have implications for the longevity and recurrence of caldera magma systems in TVZ. Geothermal activity

in the Waiora Formation reservoir was dated using pristine hydrothermal adularia and $^{40}Ar/^{39}Ar$ dating methods. Results recognised a young phase of the system's evolution (<30 ka) and the applicability of $^{40}Ar/^{39}Ar$ dating for use in geothermal chronology. Lastly, a conceptual evolutionary model for the Huka Group presents ~300 kyr of depositional processes, landscapes and structural events at Wairakei-Tauhara. The long-lived lacustrine setting is recognised to have been continually modified by episodic volcanism and gradual tectonism. Variations in Huka Group stratigraphy between the Wairakei and Tauhara Fields identify contemporaneous, but separate evolution of the underlying controlling horst (ridge) and graben (basin) structure. This study highlights the unique tectonic, magmatic, volcanic and sedimentary processes forming basins in the TVZ and improve our understanding on the geological evolution of geothermal systems. Techniques trialled in the study are demonstrated to be suitable for investigating altered volcanic materials and can be utilised elsewhere in the TVZ or other geothermal settings.

Acknowledgements

This thesis was the result of 3 ½ years of full-time research gratefully funded by the University of Canterbury (UC) PhD Scholarship, the Mason Trust Fund, GNS Science, Contact Energy, International Geothermal Association, the Geological Society of New Zealand and the Royal Society, Canterbury Branch.

This work was supervised by Jim Cole and Christopher Oze who together formed a perfectly balanced team. Their support, patience and quality feedback were invaluable throughout my undergraduate and postgraduate experiences and is a testament to their characters. External supervision by Greg Bignall (GNS) and Fabian Sepúlveda (Contact Energy) was critical in allowing work to progress and has been gratefully appreciated. Thanks to the always accommodating staff at GNS Wairakei for supplying me with beds, bikes and boots. Special thanks to Michael Rosenberg for the inspiration that helped get my work underway all those years ago and for assistance in the field/core shed.

The staff and my peers in the Department of Geological Sciences at UC have been a friendly wealth of knowledge and were always willing to help. Particular gratitude goes to the academic staff: Jarg Pettinga, Travis Horton, Ben Kennedy, Darren Gravley, David Bell and Kari Bassett for their advice and enthusiasm. Thanks to Pat Roberts and Janet Warburton for taking care of the paperwork with a smile. Thanks to the technical staff: Sacha Baldwin-Cunningham, Kerry Swanson and Chris Grimshaw for their proactive and amusing approach towards all things. Thanks Rob Spiers for teaching me how to make my thin sections by hand, Stephen Brown for all things XRF and XRD and Mike Flaws (Mechanical Engineering, UC) for being there in my moments of great peril with the SEM/EDS/C-coater.

Cheers to everyone who has come and gone during my time on the top floor of von Haast over the last 5 years: Allison J, Jonathan D, Tom G, Paul S, Flo B, Paul A, Jackie D, Nick R, Latasha T, Toni C, Matthew H, Emma R, Grace O's, Andrew W, Rebecca F... and the rest of you. Thanks to Louise Vick, Sarah Bastin and Heather Craig for being excellent office mates who did this marathon with me.

Thank you to my family for their endless care, support and interest in my work. Finally Jemma, your ongoing positivity and support kept me motivated every day of this journey. Thank you *all*.

Contents

List of Figures

List of Tables

1

Introduction

The central Taupo Volcanic Zone (TVZ) is a highly active volcanic region with thinned crust, shallow melt and high-temperature geothermal systems. They are the manifestations of complex inter-related magmatic, tectonic and volcanic processes occurring in TVZ. Drilling associated with the development of geothermal energy since the 1950s has provided direct insight into the deep stratigraphic and structural architecture of the TVZ. This allows once inaccessible deposits from its early geological history to now be comprehensively examined. In eastern TVZ, volcanic sequences >3 km thick have been drilled without intersecting basement rock that outcrops to the east and west of TVZ. Such thick volcanic sequences indicate that within concentrated depocentres, intense long-term net subsidence (>1.5 mm/yr; Wilson et al., 2010) has generated substantial accommodation space, infilled by volcanic products.

Drilling up to 3 km deep in the Wairakei-Tauhara Geothermal Field (Wairakei-Tauhara) in central TVZ intersects a well-established and detailed stratigraphic sequence defined by >300 wells (Rosenberg et al., 2009a). A significant proportion of the field's shallow to intermediate depth stratigraphy is comprise of the Huka Group (Grindley, 1959). The Huka Group is a lithologically variable mix of buried volcaniclastic, lava and lacustrine deposits 500 – 2500 m thick (Grindley, 1959; 1965; Rosenberg et al., 2009a). Its deposition occurred in a series of basin depocentres recording ~300 kyr of volcanic, sedimentary and tectonic evolution at eastern TVZ (Rosenberg et al., 2009a; Downs et al., 2014a; Wilson et al., 2010). Understanding the depositional record provides unprecedented insight on the geological evolution at Wairakei-Tauhara. This knowledge improves our broader awareness on the late regional evolution of central TVZ.

AIMS AND RESEARCH QUESTIONS

A common difficulty in investigating the geological history recorded by thick volcanic arc basin-fill sequences is the ability to recognise their stratigraphic complexity. The difficulty arises when their deposits contain few lithological variations and are buried or hydrothermally altered. This thesis investigates and evaluates the geological history of basin-fill volcaniclastic, sedimentary and lava deposits assigned to the Huka Group in the TVZ. These deposits represent ~300 kyr of depositional processes and environments in the TVZ during a period marked between by two regional caldera eruptions. It addresses questions on the distribution of strata reflecting eruption and depositional variations emplaced during this poorly understood period. As drilling progressed at Wairakei-Tauhara, it has become apparent early geological models and explanations were oversimplified and do not account or explain the geological variation now identified throughout the fields. Through rigorous investigation of recent core samples using a mix of traditional and new techniques, this research characterises the Huka Group at the Wairakei-Tauhara Geothermal Field to explain its geological history. Outcomes build on past ideas to provide a better understanding of the nature and order of volcanic, tectonic and geothermal events during this important period of TVZ evolution.

This thesis addresses five main aims comprising the following chapters. Each aim includes several specific research questions to be investigated. These are summarised in Table 1.1.

Table 1.1. Summary of thesis aims and questions to be addressed in this thesis.

Aims	Research questions	How could this be investigated?	
1. Characterise detailed Huka Group lithostratigraphy from continuous core samples.	*What were the dominant transport and depositional processes?* *How many emplacement events occurred?* *What contemporaneous depositional environments prevailed?*	Log field-wide core samples in macroscopic detail. Summarise common lithology types as a facies model and identify variations. Interpret spatially and temporally variable depositional events and environments from facies analysis.	**Chapter 2**
2. Investigate the detailed volcanic origins of the Middle Huka Falls Formation.	*What eruption processes do the facies variations represent?* *How did the eruption progress?* *What aspects of Lake Huka physiography can be inferred from this eruption?*	Log selected core samples and identify major lithofacies. Utilise available fresh samples to infer magmatic and volcanic conditions. Interpret the eruption mechanism and environments from facies and textural analysis.	**Chapter 3**
3. Trial methods to enhance the detail of altered volcanic stratigraphy.	*Can magmatic phases be utilised to differentiate separate visually similar emplacement units?* *Can immobile elements variations be used to infer possible magmatic source origins?*	Measure stratigraphic variations of stable magmatic crystal and element phases using modified petrographic and chemostratigraphic methods. Compare these variations with established lithostratigraphic models. Compare Huka Group immobile whole-rock chemistry with TVZ juvenile magma compositions.	**Chapter 4**
4. Locally constrain the timing of hydrothermal activity in the Huka Group host rocks.	*Can young hydrothermal minerals in the Huka Group be directly dated?* *What geothermal processes can affect mineral dating? Did they?* *How did the sampled deep mineralised fracture form?*	Trial $^{40}Ar/^{39}Ar$ dating on hydrothermal adularia from the Waiora Formation reservoir. Measure the influence of Ar loss by transient heating. Use stratigraphic relationships to infer the relative timing of the event.	**Chapter 5**
5. Present a complete field-wide conceptual interpretation of Huka Group deposition and environments.	*What landscapes were present during Huka Group deposition?* *What deposits can be used to constrain the relative timing of events?* *How did the field's structure and stratigraphic architecture evolve?*	Utilise new findings complementing existing sources. Interpret likely depositional environments, vent sources and structural modifications influencing the Huka Group. Correlate dated stratigraphic correlatives in TVZ to infer timing and subsidence rates at Wairakei-Tauhara.	**Chapter 6**

THESIS STRUCTURE

Chapters in this thesis have been written in stand-alone manuscript format, intended for peer review and publication. As a result, there is some repetition between successive chapters in their introduction and background sections. Methodology and terminology sections within chapters have been kept minimal for publication and are explained further in Appendix A2.1 (data files are in Appendix A2.2-2.8). Each chapter has a central focus on examining Huka Group stratigraphy. These are intended to provide a better understanding of its spatial variation and overcome some limitations of hydrothermal alteration to assess its volcanic, magmatic and tectonic geological history.

Chapters investigating the principal aims of this thesis are:

Chapter 1: *Introduction.* This provides the aims and purpose of the research. It provides context of the geological setting (TVZ), highlights key literature and identifies the field area locality (Wairakei-Tauhara).

Chapter 2: *Volcanic and sedimentary facies of the Huka Group arc-basin sequence, Wairakei-Tauhara Geothermal Field, New Zealand.* This chapter documents recent continuous drill core samples intersecting Huka Group in detail from Wairakei-Tauhara. Descriptions account for the lateral and vertical stratigraphic variations and the general depositional sequence to identify major prevailing depositional environments. Findings conclude volcanism and deposition were varied locally between Wairakei and Tauhara, but their depositional environments remained relatively similar and stable. The established stratigraphic model is used in the following chapters.

Chapter 3: *Eruptive origins of a lacustrine pyroclastic succession: Insights from the Middle Huka Falls Formation, Taupo Volcanic Zone, New Zealand.* This chapter focuses on the volcanic origins of the shallow volcaniclastic member of the Huka Falls Formation that is frequently drilled and stratigraphically well constrained. The Middle Huka Falls Formation is local to Wairakei-Tauhara. It is recognised to be the first entirely subaqueous eruption in the TVZ.

Chapter 4: *Targeting stable elements and crystal phases to enhance the stratigraphic detail of altered volcanic stratigraphy.* Limitations of visually assessing highly altered samples were identified during investigations in Chapter 2. This alteration precludes the use of traditional sedimentological

techniques. Here, new methods are trialled for applied techniques used to enhance the macroscopic stratigraphic detail of the core samples. This involved assessment of primary phenocryst sizes and chemostratigraphy of resistant magmatic phases to identify depositional variations. Results are consistent with the stratigraphic model and together enhance the stratigraphic macroscopic resolution.

Chapter 5: *$^{40}Ar/^{39}Ar$ dating of hydrothermal products from a continental arc setting.* Similar to the techniques trialled in Chapter 4, this chapter utilises established isotopic dating methods. Its effectiveness is trialled on hydrothermal adularia from the Huka Group reservoir providing age constraints to the geothermal system. Results successfully identified that the adularia was relatively young, broadening the applicability of the dating method, and suggest its formation may have coincided with young hydrothermal eruption fracturing.

Chapter 6: *Geological Evolution of the Huka Group Geothermal Reservoir, Wairakei-Tauhara Geothermal Field, New Zealand.* This chapter utilises findings from Chapters 2 – 5, together with existing data and literature, to present a full field-wide account of the geological and structural evolution of the Huka Group at Wairakei-Tauhara. Deposits suggest that ancient landscapes remained relatively stable throughout the coexisting inter-eruptive period. Its environments appear similar to specified landforms in present-day TVZ. Additionally, the basins underlying Wairakei and Tauhara are interpreted to have evolved somewhat independently by differential subsidence, erosion and deposition in response to gradual tectonism and episodic volcanism.

Chapter 7: *Summary.* Here the outcomes from the thesis contributing to the existing scientific field are reviewed.

GEOLOGICAL SETTING: TAUPO VOLCANIC ZONE (TVZ)

The field area for this research is the Wairakei-Tauhara Geothermal Field (Wairakei-Tauhara) located within the TVZ in the North Island of New Zealand (Fig. 1.1). The TVZ is a 300 km × 60 km rifted continental arc at the southernmost extension of the Tonga-Kermadec subduction system (Wilson et al., 1995). The system formed in response to the westerly oblique subduction of the Pacific Plate beneath the Australian Plate along the Hikurangi Margin and is further addressed by Cole & Lewis (1981).

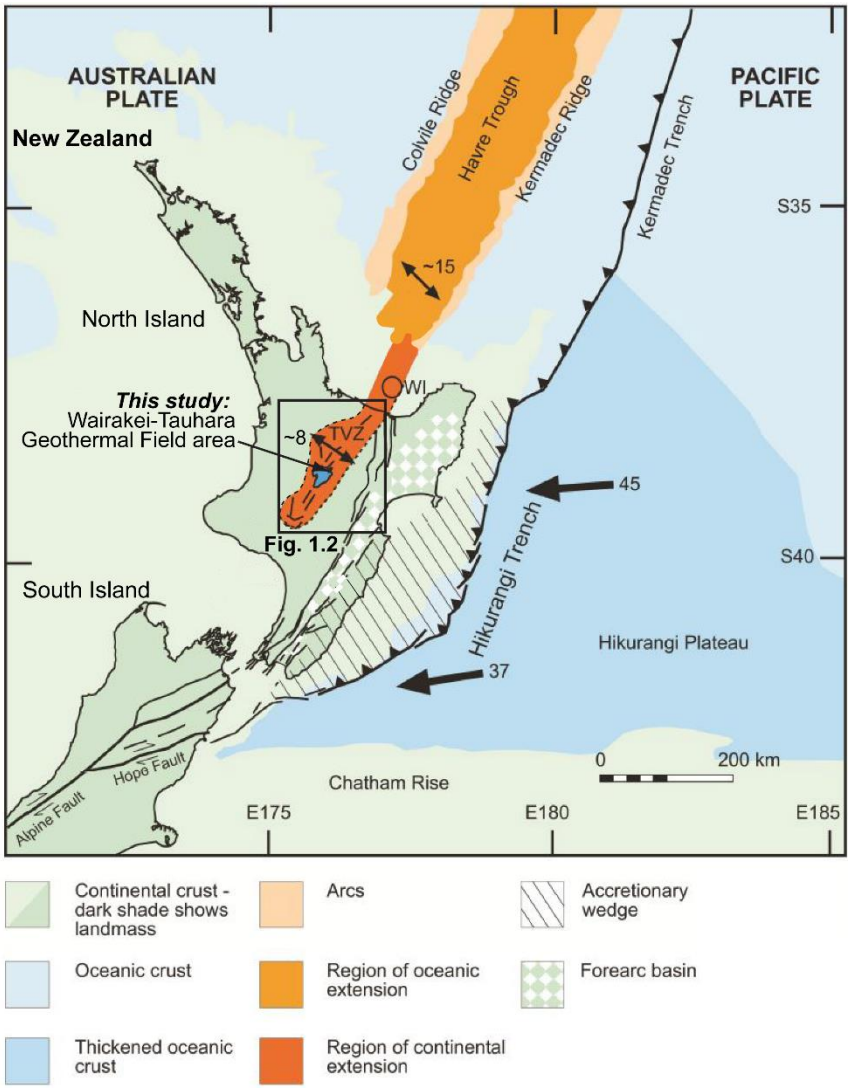

Figure 1.1. Map of North Island, New Zealand illustrating key tectonic features and locations of TVZ and Wairakei-Tauhara. Double arrows are extension direction along the TVZ and Havre Trough (Darby & Meertens 1995; Wallace et al., 2004). Single arrows are direction and relative rate of oblique convergence (in mm/yr) between Pacific and Australian plates. Abbreviations are: TVZ = Taupo Volcanic Zone, WI = White Island. Figure modified from Wilson et al. (2008).

A central segment of TVZ is the foremost focus of this research as its volcanism and tectonism have had direct influences on the research field site. Comprehensive reviews on the TVZ's structural and volcanic features are in Cole et al. (1995), Houghton et al. (1995), Wilson et al. (1995; 2009), Leonard et al. (2010), Rowland et al. (2010) and Seebeck et al. (2014).

Structure

Gravity studies indicate the TVZ is a broad depression of complex mosaic block faulting and local caldera and basin anomalies, flanked by metasedimentary greywacke basement (Fig. 1.2A; Mortimer, 1994; Bibby et al., 1995; Leonard et al., 2010). Together with extensional secular basins, these depressions serve as concentrated depocentres where thick stratigraphic sequences can accumulate. The influence of the structure on the stratigraphy at Wairakei-Tauhara is discussed in Chapters 2 and 6.

The Taupo Fault Belt basin (TFB) and Taupo-Reporoa Basin (TRB) in the TVZ are the major regional depocentres in which the Huka Group accumulated (Chapters 2 & 6; Fig. 1.2A; Downs et al., 2014a). The evolution of Kaiapo Graben (Grindley, 1965), the local southern sector of TFB underlying western Wairakei, is the focus of assessment here. Extensional strain in TVZ increases northeast along the strike of TVZ (Villamor & Berryman, 2001). It is principally accommodated by NE-SW-trending normal faults assigned to the 60 × 15 km TFB between Taupo and Okataina Volcanic Centres (Fig. 1.2A; Villamor & Berryman, 2001; Rowland & Sibson, 2001; Downs et al., 2014a). The TRB in eastern central TVZ is a 45 × 20 km structural basin between Lake Taupo to Waiotapu Geothermal Field (Fig. 1.2A; Downs et al., 2014a). In the west, TRB is bound by faulted horsts and in the east is the Kaingaroa Plateau. Northern and southern boundaries are marked by Reporoa and Whakamaru calderas, respectively (Nairn et al., 1994; Wilson et al., 1986; Downs et al., 2014b).

Volcanism

Northeastern and southwestern segments of TVZ contain andesite to dacite composite volcanoes, while the central 125 × 60 km segment is dominantly rhyolitic, erupted from large caldera centres (Fig. 1.2A; Houghton et al., 1995; Wilson et al., 1995). Silicic volcanism in the central TVZ has been the most active and productive on Earth over the last 350 kyr (Houghton et al., 1995; Wilson et al., 1995) after its commencement by at least ~1.9 Ma (Eastwood et al., 2013). The diverse range of volcanic eruption

styles and transport processes in TVZ referred to in this thesis (Appendix A1.1) are reviewed by Wilson et al. (1995). Volcanism associated with the evolution of Wairakei-Tauhara are covered in Chapters 2, 3 and 6.

Estimates suggest >10,000 km^3 of magma has erupted in TVZ mainly by >25 large eruptions (30 – >1500 km^3) from 8 caldera centres (Fig. 1.2A; Houghton et al., 1995; Wilson et al., 1995; 2009). Of the ~25 caldera eruptions, four are amongst the ten largest global Quaternary supereruptions (Fig. 1.3; Houghton et al., 1995; Wilson et al., 1995; 2009). Deposits generated by these events have created most of the stratigraphy in the TVZ, including Wairakei-Tauhara, by infilling TFB and TRB depocentres (Downs et al., 2014a). Caldera volcanism in central TVZ has historically occurred as vigorous, short-lived bursts of silicic volcanism from several vents (termed 'flare-ups') separated by long hiatus periods (Wilson et al., 2009). These major events destroy existing environments which gradually recover and re-establish during quiescent sedimentary periods (Smith, 1991; Smith et al., 1993; Manville & Wilson, 2004). A regional TVZ flare-up between ~349 – 281 ka generated >3000 km^3 of magma from 7 caldera centres (Fig. 1.3; Wilson et al., 2005; 2009; Gravley & Wilson, 2006; Gravley et al., 2009; Downs et al., 2014a). This period was contemporaneous with the commencement of Huka Group deposition during a relatively quiescent period at Wairakei-Tauhara.

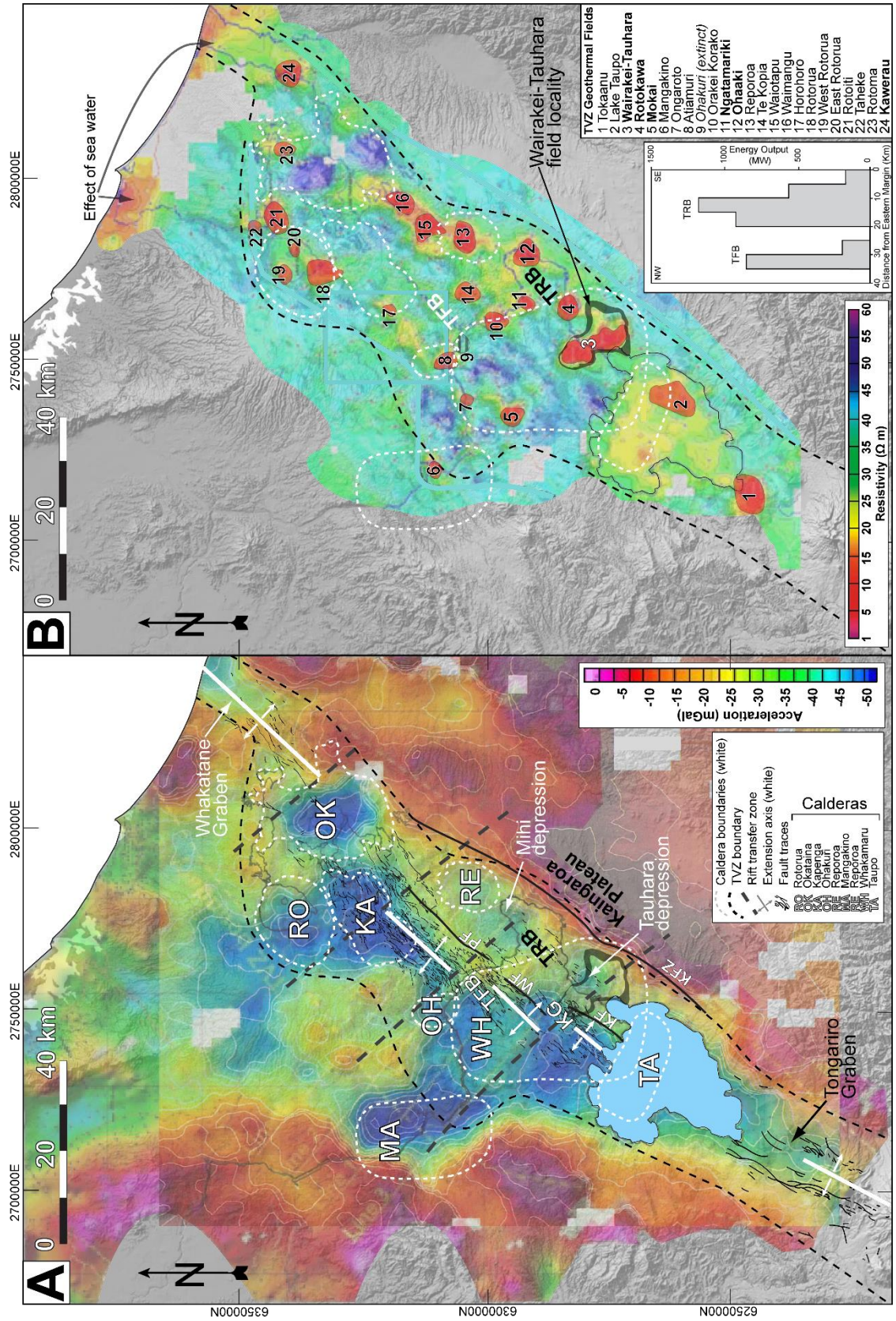

Figure 1.2. A. Residual Bouguer gravity anomaly map of TVZ from Bibby et al. (1995) and Soengkono (2011), overlain by TVZ volcanic centres from Wilson et al. (1995). Calderas offset from their gravity lows as they are defined by their deposit distribution. Rift transfer zones from Rowland and Sibson (2001); Mihi depression from Soengkono (2012); Tauhara depression is inferred in Chapter 6. Basins: TRB = Taupo-Reporoa Basin; TFB = Taupo Fault Belt basin; KG = Kaiapo Graben; Faults: PF = Paeroa Fault; WF = Whakaheke Fault; KF = Kaiapo Fault. **B.** Regional map of apparent resistivity with low resistivity zones (highlighted in red) identifying geothermal systems. Wairakei-Tauhara DC resistivity boundary is shown (Risk, 1984). *Insert* is the heat output from geothermal fields in the TFB and TRB belts. Figure modified from Bibby et al. (1995). Names in bold type are geothermal fields utilised for power production; those italicised are extinct systems.

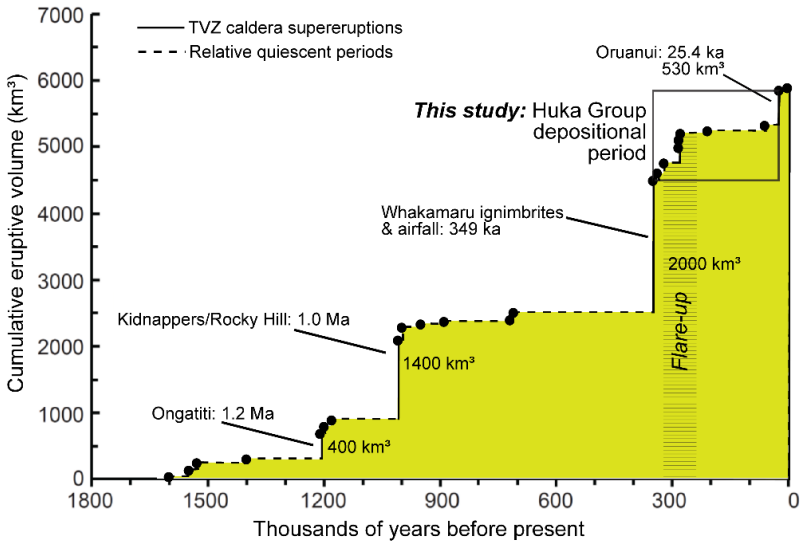

Figure 1.3. Cumulative eruptive volumes versus time for central TVZ during the past ~1800 ka of caldera-forming eruptions (black dots) and supereruptions (labelled) divided by hiatus of relatively quiescent depositional periods. Figure modified from Wilson et al. (2009).

Geothermal

The TVZ hosts 23 active high-temperature geothermal systems (>250 °C) delineated by electrical direct current (DC) resistivity methods (Fig. 1.2B; Bibby et al., 1995). Collectively the fields form two broadly parallel western and eastern belts of conductivity separated by a central region of relatively resistant crust in the TFB (Fig. 1.2B *insert*; Bibby et al., 1995; Rowland et al., 2012). Comprehensive reviews on the distribution and structure of geothermal fields in TVZ are provided by Bibby et al. (1995), Rowland and Sibson (2004), and Rowland et al. (2010; 2012). The Wairakei-Tauhara geothermal system and its field development are covered in Grindley (1965), Bibby et al. (1995), Bolton (2009) and Sepúlveda et al. (2012). The geological influence of the Huka Group on the Wairakei-Tauhara geothermal system are discussed in Chapters 5 and 6.

FIELD AREA: WAIRAKEI-TAUHARA GEOTHERMAL FIELD

Wairakei-Tauhara is located northeast of Lake Taupo in the central TVZ (Fig. 1.2B). The geothermal field refers to the area above a geothermal system defined at the near-surface by a DC resistivity boundary delineating the resource and drilling area (from Risk, 1984). The geothermal system is the natural entity that at Wairakei-Tauhara is thought to reflect the location of a primordial magmatic heat source within the crust (Wilson et al., 2015). The structural and stratigraphic architecture of Wairakei

Geothermal Field is outlined in the influential publication by Grindley (1965) that contains the foundations for the field's present day geological architecture. The reviewed stratigraphy of Wairakei-Tauhara by Rosenberg et al. (2009a) and updated by Bignall et al. (2010a) is used and adapted in this thesis. Detailed stratigraphy of the Huka Group and other relevant formations are discussed in Chapter 2.

Preamble:

The general stratigraphy at Wairakei-Tauhara has been recently refined by Rosenberg et al. (2009a). However, the complex variation and distribution of the Huka Group have only previously been summarised in geotechnical drilling reports (e.g., Rosenberg et al., 2009b). Geothermal drilling in 2009 generated ~5 km of continuous drill core from eleven wells that are ideal for investigating Huka Group lithostratigraphy in new detail.

Here in ***Chapter 2****, I utilise 4.2 km of recently drilled core samples to introduce the lithostratigraphy of the Huka Group. Drill core samples are logged in new detail (physical and photograph examination), their clast componentry are measured and a resulting facies model is applied to each well location. The resulting facies model is used to identify the number of depositional events that comprise Huka Group, each reflecting ancient depositional environments, transport processes and volcanic events at Wairakei-Tauhara.*

This chapter has been written as a sedimentological-type manuscript of the drill core samples. Graphic logs are intended to be used as visual references for the highly detailed text descriptions. The chapter has previously been submitted to the New Zealand Journal of Geology and Geophysics and has been edited addressing the reviewers' recommended revisions. During the time of thesis submission, the revised co-authored manuscript was accepted awaiting print.

2

Volcanic and sedimentary facies of the Huka Group arc-basin sequence, Wairakei-Tauhara Geothermal Field, New Zealand

H.J. Cattell, J.W. Cole and C. Oze

Department of Geological Sciences, University of Canterbury. Christchurch 8140, New Zealand

ABSTRACT

Detailed facies analyses of intra-arc basin stratigraphy provide spatial and temporal insights into the nature and timing of volcanic, sedimentary and tectonic events. Rift and caldera basins hosting lakes in the central Taupo Volcanic Zone (TVZ) continental arc preserve a sequence of locally- and regionally-sourced volcanic deposits and interbedded lacustrine sediments. A series of new continuous core samples intersecting the Huka Group from Wairakei-Tauhara Geothermal Fields in the TVZ has provided a unique opportunity to study ~300 kyrs of local arc volcanism, sedimentary processes and ancient surface environments. Results from facies analysis demonstrate that the Huka Group commenced with a large ignimbrite (Waiora Ignimbrite Member) emplaced onto faulted relief covered by an ancient lake, Lake Huka. Graded volcaniclastic facies, lavas and sediments comprising the Waiora Volcaniclastics Member then accumulated in the basins over the next ~100 kyrs. A spatially variable switch from volcaniclastic (Waiora Volcaniclastics Member) to lacustrine sediments followed (Huka Falls Formation). Excluding an intra-lake phreatomagmatic eruption (Middle Huka Falls Formation), these siltstones reflect a ~200 kyr local pyroclastic hiatus. Late Huka Group deposition became gradually more fluvial as rivers prograded marginal areas of the lake until the Oruanui eruption at 25.4 ka. The drill core samples provide new insights into processes and environments associated with the Huka Group. These insights enhance our understanding of the geological history at Wairakei-Tauhara Geothermal Fields and contribute to our knowledge of the ancient processes occurring during evolution of the TVZ.

INTRODUCTION

Diverse volcanic and sedimentary deposits accumulating in subsiding intra-arc rift and volcano-tectonic basins preserve insights into detailed depositional processes and the nature of the sediment-generating mechanism (Smith et al., 1993; Manville et al., 2009; Downs et al., 2014a). Resulting deposits reflect details of the transport processes, prevailing environments and regional tectonics. Volcanism and tectonism dominantly influence the stratigraphic architecture and sedimentary processes in arc environments by generating and remobilising abundant clastic material and creating accommodation space (Manville et al., 2009; Manville, 2010). Lakes hosted within depocentres (e.g., rift or caldera basins) commonly preserve thick sequences of syn-eruptive material interbedded with inter-eruptive sediments (Smith, 1991), turbidites and diatomaceous silts (van der Marel, 1947; Brathwaite, 2003).

Identifying the source vent environment of volcanic deposits preserved in ancient basins remains challenging due to lithologically-similar deposits and deposit burial. Lavas and volcaniclastic material filling these depocentres may be transported to lakes from subaerial vents (Cas & Wright, 1991; Freundt, 2003; Allen et al., 2012; Jutzeler et al., 2014) or directly erupted beneath the lake (Busby-Spera, 1986; Allen & McPhie, 2009; Valenzuela et al., 2011; Downs et al., in press; Chapter 3). Facies analysis of abundant drilled samples is necessary for understanding ancient depositional processes and paleo-environments in volcanic arc settings (e.g., Fisher & Schmincke, 1984; Cas & Wright, 1987; Kano et al., 1993; Song & Lo, 2002; Paulick et al., 2004; Sohn et al., 2013).

Contemporaneous, silicic continental arc volcanism and extensional tectonism in central Taupo Volcanic Zone (TVZ), New Zealand, promotes the development of regional caldera and rift basins filled by ephemeral and long-lived lakes (Manville, 2001; Manville et al., 2007). The Huka Group (Grindley, 1959; 1965) in the Wairakei-Tauhara Geothermal Field (Wairakei-Tauhara), TVZ, records ~300 kyrs of volcanic, volcaniclastic and sedimentary deposition in a paleo-Lake Huka, the predecessor to present-day Lake Taupo (Grange, 1937; Grindley, 1965; Healy, 1965; Smith et al., 1993; Manville & Wilson, 2004; Manville et al., 2007; Rosenberg et al., 2009a; Downs et al., 2014a; in press). Pioneering studies broadly interpreted the Huka Group as *"aggradational pumiceous deposits [emplaced] in a subsiding volcano-tectonic basin"* (Grindley, 1965) and *"material erupted into a lake that was rapidly re-deposited after the eruption"* (Healy, 1965). Both explanations are correct, however, stratigraphic

insights gained from recently drilled core in Wairakei-Tauhara (e.g., Rosenberg et al., 2009b) suggest they are oversimplified and geographically limited. Through core sample facies analysis together with the established local stratigraphy of Wairakei-Tauhara (Rosenberg et al., 2009a; Bignall et al., 2010a), the history of the Huka Group including volcanic events, transport processes and depositional environments can now be comprehensively examined and interpreted.

Outcomes from this detailed investigation find the thick, lithologically variable Huka Group sequence resulted from a spatially and temporally complex interplay between regional extension, lacustrine reworking and explosive and effusive volcanism. These provide the framework for refining current stratigraphic models and for paleo-environmental reconstructions of the central TVZ.

WAIRAKEI-TAUHARA GEOTHERMAL FIELD (WAIRAKEI-TAUHARA)

Wairakei-Tauhara is defined by an electrical DC resistivity boundary (Risk, 1984) located northeast of Lake Taupo on the eastern edge of TVZ (Figs. 2.1 & 2.2A).

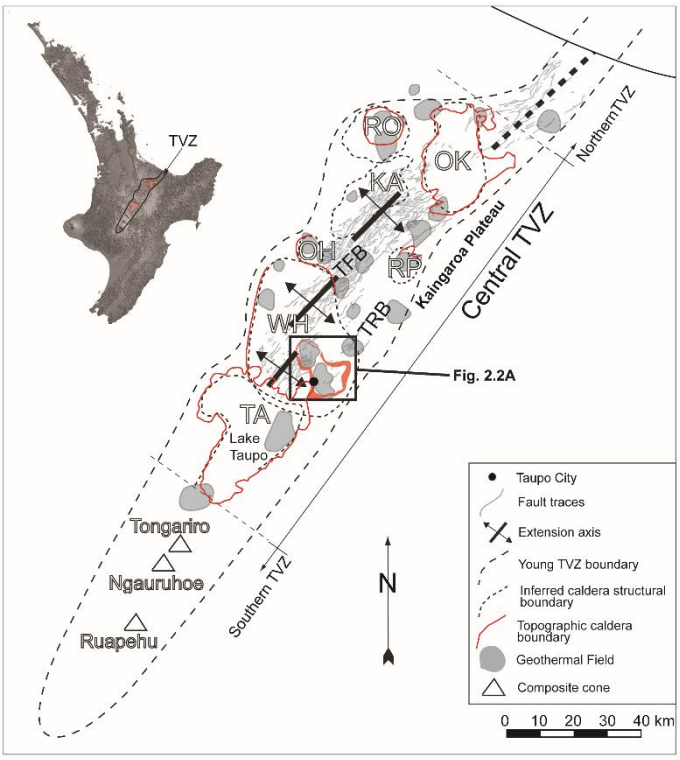

Figure 2.1. Location of Wairakei-Tauhara and features within the young TVZ boundary (Wilson et al., 1995). Young central TVZ eruptive centres are: OK = Okataina, RO = Rotorua, KA = Kapenga, OH = Ohakuri, RP = Reporoa, WH = Whakamaru and TA = Taupo. Abbreviations: TFB = Taupo Fault Belt basin and extension axes, TRB = Taupo-Reporoa Basin. *Insert* shows location of the TVZ, central North Island, New Zealand. Faults are from GNS Active Fault Database (http://maps.gns.cri.nz/website/af/viewer.htm). Extension axis and figure modified from Rowland and Sibson (2001), caldera topography from Leonard et al. (2010).

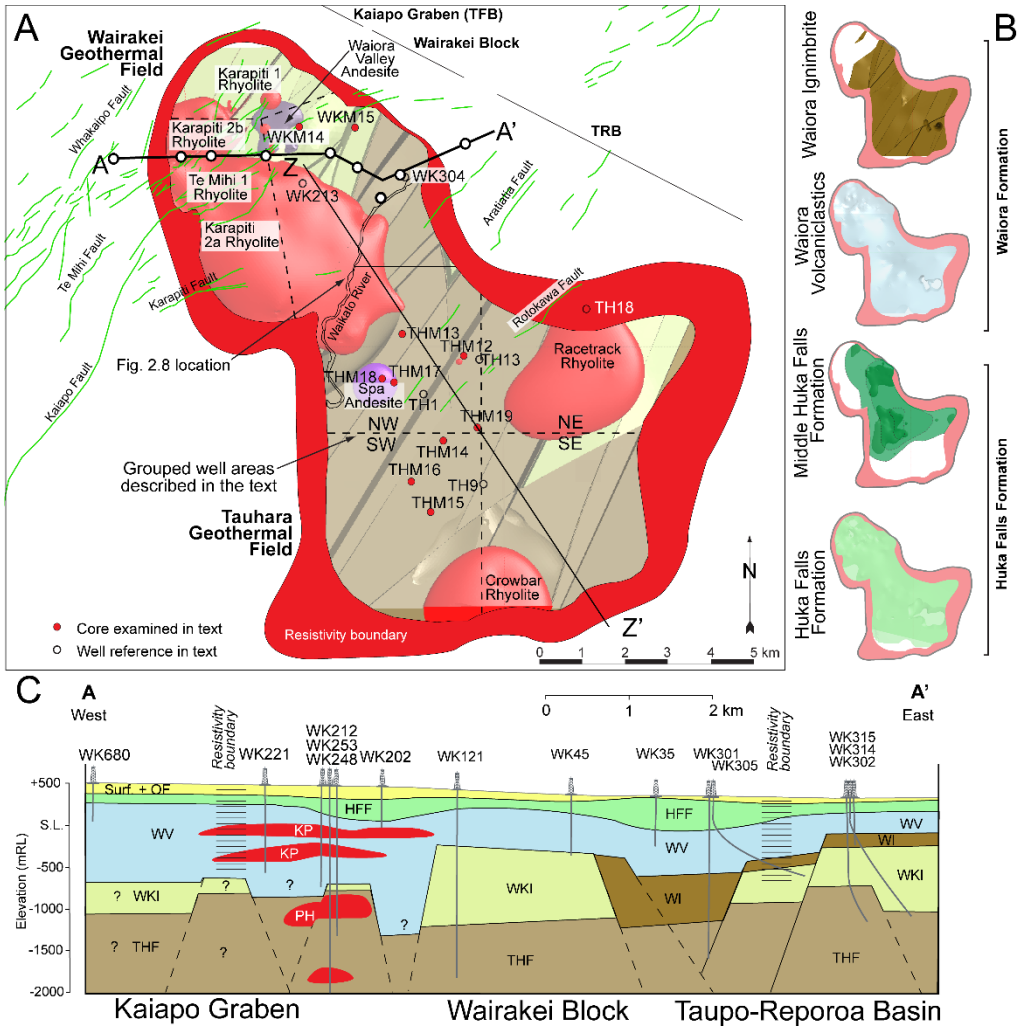

Figure 2.2. A. The Wairakei-Tauhara Geothermal Field DC resistivity boundary (Risk, 1984). Shown are well locations used in this thesis (dots) and regions of grouped wells described in the text (dashed boundaries), surface fault traces (green lines), the location of major lavas (red & purple; see Fig. 2.3) and the deep structure (TRB = Taupo-Reporoa Basin). Cross section A – A' is in Fig. 2.2B and Z – Z' is Fig. 2.9A-C. Geological units and fault structure modified from Alcaraz et al. (2010). **B.** Known and inferred geographic distribution of modelled Huka Group stratigraphy at Wairakei-Tauhara. **C.** A – A' cross is modified from Rosenberg et al. (2009a) illustrating the interpreted structure of the field and stratigraphic units from drilling (see Fig. 2.3 caption for abbreviations). Faults are used (dashed where inferred) to show major controls on thickness and distribution of deep formations. Elevation in mRL is metres relative to average sea level.

Stratigraphy

Sixty years of drilling for geothermal investigations have generated significant geological data for refining the geological model at Wairakei-Tauhara. Stratigraphy in the field has been reviewed by Rosenberg et al. (2009a; updated by Bignall et al., 2010a) and its use here is summarised by Fig. 2.3.

The Huka Group in Wairakei-Tauhara includes all deposits above Wairakei Ignimbrite (formal localised Whakamaru Group member; Grindley, 1960; 1982; Wilson et al., 1986) and below the

Oruanui Formation (Fig. 2.3; Wilson, 2001). The Waiora Formation is a widespread succession of thickly bedded uncorrelated ignimbrites, reworked volcaniclastic and lacustrine sediments. The sequence is ~400 m thick in the Wairakei field, and is between 800 – 2100 m thick in the Tauhara field. Four Waiora Formation members have been identified in the Wairakei-defined Type Section (Grindley, 1965; modified by Rosenberg et al., 2009a). These members, abbreviated $Wa_{\#}$, include Wa_1: 500 – 1500 m welded and unwelded ignimbrites; Wa_2: 50 – 150 m of reworked quartz-rich sediments; $Wa_{3\text{-}4}$: 350 – 500 m of undifferentiated pumice breccia and interbedded siltstone; Wa_5: 100 – 150 m of quartz-bearing pumiceous ignimbrite (Fig. 2.3; Grindley 1965; Rosenberg et al., 2009a).

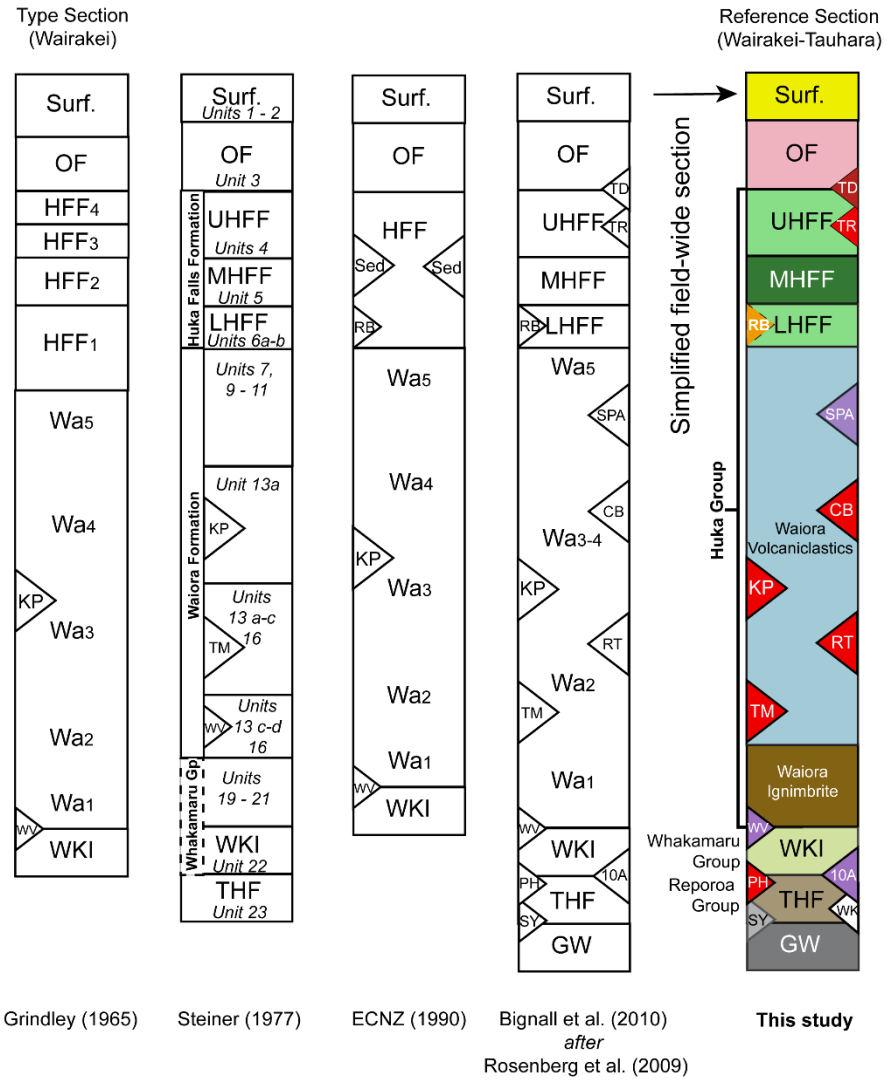

Figure 2.3. Changing stratigraphic columns for Wairakei and Wairakei-Tauhara following increased drilling and improved understanding of the subsurface architecture. A field-wide framework model modified after Bignall et al. (2010a) is used across Wairakei-Tauhara. Abbreviations: Surf = surficial sediments, OF = Oruanui Formation, U/M/L/HFF = Upper/Middle/Lower Huka Falls Formation, TD= Tauhara Dacite, TR = Trig Rhyolite, RB = Rautehuia Breccia, Wa_x = Waiora Formation members, Spa = Spa Andesite, CB = Crown Breccia, KP = Karapiti Rhyolites, RT = Racetrack Rhyolite, TM = Te Mihi Rhyolites, WV = Waiora Valley Andesite, WKI = Wairakei Ignimbrite, 10A = 10A Andesite, PH = Poihipi Rhyolite, THF = Tahorakuri Formation, WK = Waikora Formation, SY = Stockyard Ignimbrite, GW = Greywacke. Note: the stratigraphic colour code is different from the lithofacies colour code introduced in Fig. 2.4A.

Multiple andesite and rhyolite lavas and local eruption breccias have also been intersected in the Huka Group (Fig. 2.2C; Rosenberg et al., 2009a). In this investigation two major cored lavas, Racetrack Rhyolite and Spa Andesite, are examined (Fig. 2.3; Rosenberg et al., 2009a). The Huka Falls Formation is a comparatively thin (150 – 300 m) veneer of overlying massive to thinly bedded siltstone, sandstone and pumice vitric lapilli-tuff (Fig. 2.2C). Rosenberg et al. (2009a) re-defined lower, middle and upper units (referred to here as stratigraphic members). Lower and Upper Huka Falls Formation are widespread siltstone and sandstone beds (Fig. 2.2B). The Middle Huka Falls Formation is a laterally-confined pyroclastic unit that is absent in western Wairakei and southern Tauhara (Fig. 2.2B; Chapter 3).

Structure and faults

Early gravity, magnetic, structural and aerial imaging investigations (e.g., Grindley, 1960; 1965; Healy et al., 1964; Hochstein & Hunt, 1980; Hunt et al., 2009) identified Wairakei-Tauhara to be situated over a broad basement depression infilled by ≥3 km of low density volcanic and sedimentary deposits (Hunt et al., 2009; Rosenberg et al., 2009a; McNamara et al., 2013). Field mapping, aerial photography and surface ruptures recognise six major NE-SW-trending fault zones intersecting Wairakei-Tauhara: Whakaipo, Te Mihi, Kaiapo, Karapiti, Aratiatia and Rotokawa Fault Zones (Fig. 2.2A; Grindley, 1965).

The deep structure of Wairakei-Tauhara consists of a central Wairakei Block. To the northwest it is bound by the local down-faulted Kaiapo Graben sector of the regional Taupo Fault Belt (TFB; Villamor and Berryman, 2001; Downs et al., in press) beneath Wairakei. In the southeast, Wairakei Block is bound by Taupo-Reporoa Basin (TRB; Downs et al., 2014a) beneath Tauhara (Figs. 2.1 & 2.2C; Grindley, 1965). Rosenberg et al. (2009a) suggested the structure of Wairakei-Tauhara to be a series of horsts and grabens (Fig. 2.2C). Wilson et al. (2010) and Downs et al. (2014a) also proposed the presence of a long-lived horst running down central TVZ delineating the western and eastern respective margins of TRB and TFB (Fig. 2.1). Within TRB, Huka Group is a thick undifferentiated buried sequence with few outcrops preventing detailed stratigraphic correlation with Wairakei-Tauhara (Downs et al., 2014a).

The field is situated within the inferred southern boundary of Whakamaru caldera (Fig. 2.1; Wilson et al., 1986). Tectonic and volcano-tectonic overprinting has led to difficulties identifying deeply drilled structures and the relative influence of faulting mechanisms (e.g., Fig. 2.2C). Previously, offset Wairakei Ignimbrite has been explained by local uplift and tilting of NNE-SSW-trending fault blocks (Healy, 1984; Grindley, 1961), activity on a major caldera fault (Grindley, 1982; Wood, 1995; Wood & Browne, 2000; Wood et al., 1997) and structurally-concentrated erosion (Rosenberg et al., 2009a). Here, structural and stratigraphic interpretations from core assessments also support intense structurally-concentrated erosion explored further in Chapter 6.

TERMINOLOGY AND METHODOLOGY

Terminology

This thesis uses standard sedimentary grain-size terminology for non-volcanic deposits. Volcaniclastic grain-size terminology is after White and Houghton (2006; e.g., tuff/ash, lapilli-tuff/lapilli; Appendix A1.1). In the present study, reworked volcanogenic deposits (usually assigned sedimentary terminology) cannot be consistently differentiated from primary volcaniclastic deposits and are both assigned volcaniclastic terminology. The term *ignimbrite* is an interpreted small-to large-volume, welded to unwelded pyroclastic deposit describing an eruption-fed deposit emplaced by *pyroclastic density currents* (Fisher, 1961). When pyroclastic density currents enter a water body interstitial gas can become quickly replaced to form *water-supported volcaniclastic density currents* depositing unwelded pyroclastic deposits (e.g., Cas & Wright, 1991; McPhie & Allen, 2003; Allen et al., 2012; Jutzeler et al., 2014).

Samples and core logging

The Huka Group was investigated from eleven continuously cored wells (totalling 4.2 km of core). Drilling was commissioned by Contact Energy and drill cores were logged by GNS Science for a geothermal subsidence investigation in 2008 – 2009 (Rosenberg et al., 2009b; Bromley et al., 2010). Selected geological well reports summarising stratigraphy, petrography and drilling were provided by Contact Energy. Two of the examined cores are from wells in northern Wairakei and nine are from Tauhara Geothermal Field (Fig. 2.2A). Five wells are deeply drilled (>500 m) intersecting both Waiora

and Huka Falls Formations (WKM14, WKM15, THM16, THM18 and TH18). The remainder intersect only the Huka Falls Formation (THM12, THM13, THM14, THM15, THM17 and THM19).

Core samples were preferably examined over cuttings fragments from Wairakei-Tauhara because of their preserved textures and bedding contacts for examining depositional processes and environments. Cores are 1 m × 6 cm with a high sample recovery (calculated ~95 %). Continuous core photograph assessments provided an efficient method for logging lithostratigraphy and minimising disturbance to the sample (Glynn-Morris & Winmill, 2009). Supplementary physical assessments were undertaken on selected fine grained strata. Clasts are defined here as coarse particles (>5 mm) that are visible in core photographs. Smaller particles are considered part of the altered matrix. Clast volume, sorting and roundness were estimated using a standard volume and sorting comparative chart and clast type. The apparent long and short axes of the ten largest clasts were measured per 5 m interval (stored core box) using image analysis Java software, ImageJ (total ~5000 clasts; Appendix A2.3).

PROPOSED HUKA GROUP REFERENCE SECTION: WELL WKM15

Multiple detailed stratigraphic models have been previously proposed for Wairakei (Fig. 2.3; Grindley, 1965; Steiner, 1977; Healy, 1984; ECNZ, 1990; Wood & Browne, 2000; Rosenberg et al., 2009a; Bignall et al., 2010a). Lithostratigraphic units comprising the Huka Group were originally defined in 1960 at central Wairakei Type Section well WK213 (Fig. 2.2A) which was cored at 50 ft. (~15 m) intervals (Grindley, 1965). Results from continued widespread drilling has since identified that the detailed Type Section applies only locally to Wairakei. Lithologies across Wairakei-Tauhara are too variable for the Type Section to be confidently applied field-wide (Rosenberg et al., 2009a). A Huka Group Reference Section is required that recognises the lateral variation, utilises the current stratigraphic understanding and complements the existing Type Section (Grindley, 1965; Rosenberg et al., 2009a).

Well WKM15 (Fig. 2.2A) is selected for the Reference Section due to its near-complete core recovery intersecting all Huka Group formations and members (Rosenberg et al., 2009b). The vertical geotechnical well was cored to 596.1 m (elevation -231 mRL) in March 2009 and is located 1.5 km northeast of the Wairakei Power Station (6282529.84N, 2779235.87E; Rosenberg et al., 2009b).

Stratigraphy of WKM15 is summarised in Rosenberg et al. (2009b) and its detailed lithostratigraphy is documented in the following lithofacies section.

For lateral stratigraphic correlation across the fields, the Reference Section defines the Waiora Formation as including a *Waiora Ignimbrite* Member that directly correlates with Waiora Formation Wa_1 (Rosenberg et al., 2009a). An overlying *Waiora Volcaniclastics* Member correlates with combined Wa_2, Wa_{3-4} and Wa_5 (Fig. 2.3; Rosenberg et al., 2009a). In the latter, use of the term 'Volcaniclastics' refers to the dominant succession of volcanogenic deposits comprising the succession and is not intended to imply that it is an exclusively volcaniclastic lithotype.

In WKM15, Waiora Ignimbrite (490 – 596.1 m) consists of nine consolidated pumice and rhyolite lapilli-tuff beds totalling 90 m, capped by 18 m of fine tuff. In Tauhara, the member is known to be >1500 m thick (TH9; Milicich et al., 2008a) and consist of more than 4 ignimbrite sheets (Wood, 1994a). The Waiora Volcaniclastics Member (225 – 490 m) contains at least eight major volcaniclastic pumice and lithic lapilli-tuff units (20 – 40 m). Local to Wairakei-Tauhara, the Huka Falls Formation contains three members defined in Rosenberg et al. (2009a), present in the the Reference Section (~73 – 225 m). Well WKM15 contains 28 m of Lower Huka Falls Formation siltstone and sandstone, 62 m of Middle Huka Falls Formation pumice lapilli-tuff and 62 m of Upper Huka Falls Formation siltstone, fine and pebbly sandstone.

Previously there has been ambiguity in assigning a stratigraphic boundary to the lowermost Lower Huka Falls Formation contact across Wairakei-Tauhara (described in Rosenberg et al., 2009b). Uncertainty arises when shallow elevation siltstones (>0 mRL), typically assigned to Huka Falls Formation, are gradational with Waiora Volcaniclastics. In this study, Huka Falls Formation is distinguished from Waiora Volcaniclastics by its dominant brown (authigenic bioclastic) or white (siliciclastic) siltstone and sandstone over coarser grained volcanogenic lithologies. However, a difficulty occurs when reworked volcaniclastic units are interbedded with thin siltstone beds beneath the Huka Falls Formation. The Reference Section excludes these minor interbedded siltstones from Lower Huka Falls Formation, assigning them instead to Waiora Volcaniclastics.

LITHOFACIES TYPE OVERVIEW

Nine common lithofacies groupings occur in the eleven examined Huka Group core samples (Fig. 2.4A). Lithofacies classification criteria includes grain size, textures, matrix composition and clast componentry as outlined in Table 2.1 (i.e., denoted by acronym suffix, e.g., -bp = polymict breccia). The colour-coded lithofacies and photograph examples are shown in Fig. 2.4A. Depositional relationships between the lithofacies (Fig. 2.4B) are described in terms of four facies associations (i.e., acronym prefix, e.g., V- = volcaniclastic association; Table 2.1).

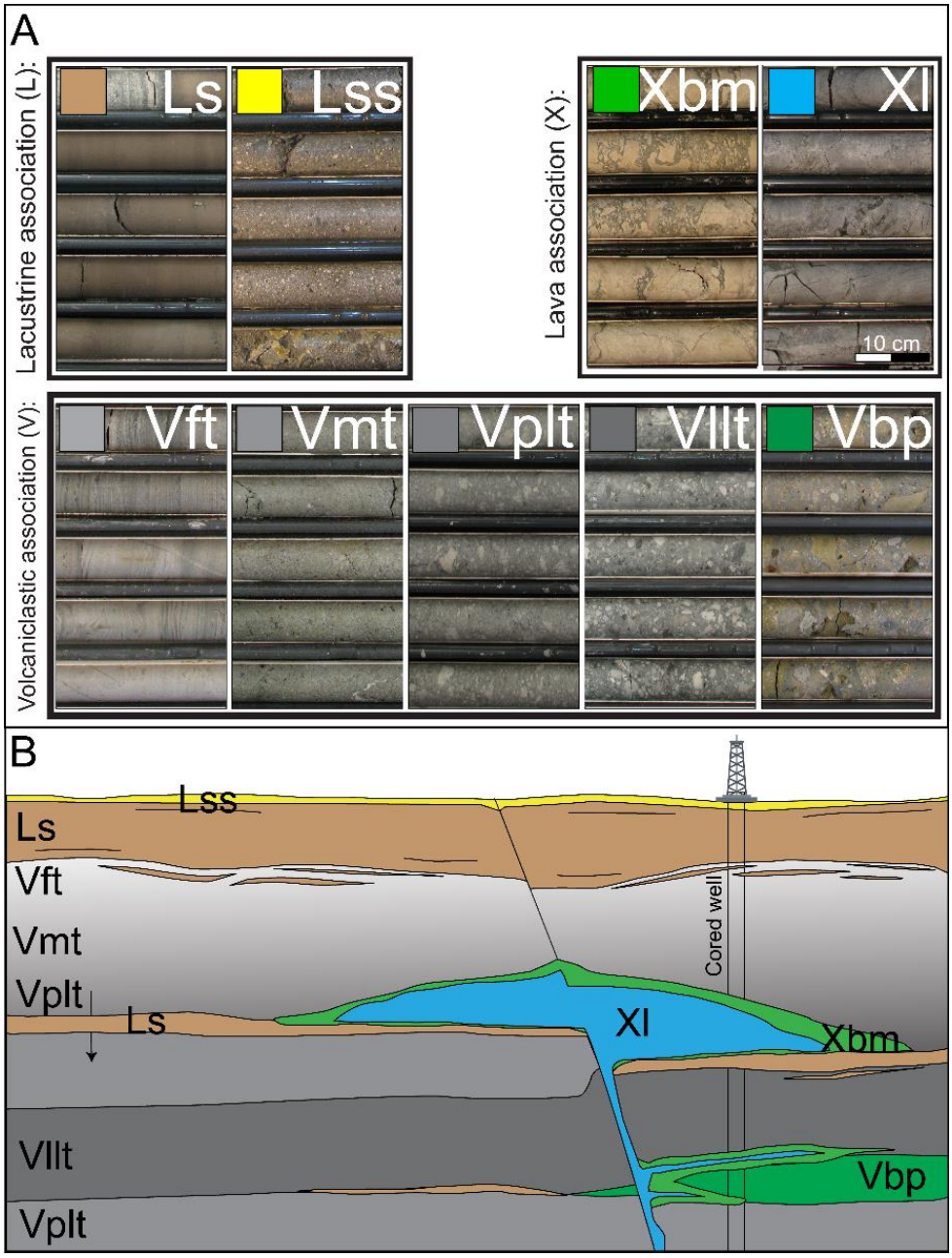

Figure 2.4. A. Core sample examples of lithofacies and lithofacies associations in the Huka Group. Ls = Lacustrine siltstone, Lss = Lacustrine sandy and pebbly siltstone, Vft = Volcaniclastic fine tuff, Vmt = Volcaniclastic medium tuff, Vplt = Volcaniclastic pumice lapilli-tuff, Vllt = Volcaniclastic lithic and pumice lapilli-tuff, Xbm = Lava monomict breccia, Vbp = Volcaniclastic polymict breccia, Xl = coherent lava. **B.** Schematic illustration showing a simplified conceptual relationship of the lithofacies in the Huka Group. Note: the lithofacies colour code shown here is different from the in stratigraphic colour code in Figs. 2.2A-C & 2.3.

Siltstone lithofacies

Lithofacies Ls (siltstone)

Lithofacies Ls includes red-brown, light and dark brown siltstone consisting of siliciclastic, minor bioclastic (diatoms, organics) and subordinate sandy sediments (Fig. 2.4A). Units are up to 100 m thick and often have gradational lower and sharp upper contacts. Textures are both massive to thinly bedded (planar or deformed, amalgamated) or interbedded with no significant clast content (<5 vol.%).

Lithofacies Lss (sandy and pebbly siltstone)

Lithofacies Lss (Fig. 2.4A) is recognised by containing a silty to medium sand matrix that supports >5 % clasts. The facies is usually grey-brown to dark brown and typically grades from or occurs within lithofacies Ls forming units up to 100 m thick. Clasts are subrounded, poorly sorted lithologically variable volcanogenic pebbles (andesite, scoria, rhyolite, pumice, siltstone and greywacke fragments).

Fine grained volcaniclastic lithofacies

Lithofacies Vft and Vmt (fine and medium tuffs)

Vitric and vitroclastic particles up to and including fine tuff grain-size comprise facies Vft, while medium tuffs of the same composition comprise facies Vmt. These facies are usually absent of clasts, often massive or thinly bedded (Fig. 2.4A) and are typically white-grey to light green. Facies Vft are usually 5 – 10 m thick while Vmt can be >20 m. Facies Vmt often grades up into facies Vmt and often overlies pumice lapilli-tuff facies Vplt (Fig. 2.4B).

Lithofacies Vplt (pumice lapilli-tuffs)

Lithofacies Vplt is a pumice lapilli-tuff characterised by the presence of ash to coarse lapilli-sized pumice clasts (typically 10 vol.%) and minor lithic clasts (<2 %) supported by a medium vitric tuff matrix (Fig. 2.4A). Pumice clasts are porphyritic to aphinitic and distinguished by their characteristic altered ‘bleached’ white colour forming clays (destroying vesicular textures). Clasts are poorly to well sorted, normally to reversely graded and are angular, ragged, lenticular (compacted) or boxy shapes. Clasts (> 5 mm) can be observed in photographs, while smaller particles are highly altered and cannot usually be differentiated from the altered matrix. Facies Vplt forms are a few tens of metres thick grading from underlying facies Vllt (with rare siltstone rip-up clasts), or occurs as separate, non-graded

units with sharp contacts. None of the assessed lithofacies show any evidence of welding, but have been weakly to moderately lithified by consolidation above ~700 m depth and are highly cemented below this depth.

Lithofacies Vllt (lithic and pumice lapilli-tuffs)

Lithofaces Vllt is lithologically diverse and spatially complex. Clasts comprising the facies are normally graded, subangular to subrounded, poorly to moderately sorted and are matrix-supported (2 – 70 vol.%; rarely clast-supported). Dominant lithic clasts appear mostly derived from underlying units and include siltstone, lavas, tuffs and very rare plutonic lithics. Pumice clasts are usually present in facies Vllt, but are less common than lithic clasts. Units are 1 – 100 m thick, thickly bedded to massive and are shades of off-white, grey, green and brown. Lower contacts are notably sharp (likely erosional), or are otherwise normally graded from underlying coarser lithofacies Vbp. When upper contacts commonly grade normally into facies Vplt over 2 – 10 m, an association with primary magmatic activity is indicated. Facies Vllt with no association with Vplt can be phreatic deposits, reworked sediments, or magmatic deposits with no Vplt (juvenile clasts) preserved. Under this facies, primary eruptive deposits and reworked volcanogenic sediments comprising facies Vllt cannot be confidently distinguished by photograph identification. Here they are described together, both using primary volcaniclastic grain size terminology.

Breccia lithofacies

Lithofacies Xbm

Coarse breccias are consolidated deposits comprised of poorly sorted, coarse lapilli and block-sized clasts totalling 20 – 50 vol.% of the lithofacies (Fig. 2.4A). Lithofacies Xbm (monomict breccias) and Vbp (polymict breccias) are separate lithofacies as they each give insights into the fragmentation and emplacement mechanisms. Facies Xbm in wells TH18 and THM18 are usually clast-supported with subordinate vitroclastic, clastic or fine tuff-sized matrix fill. Clasts are hypocrystalline or pumiceous textures. Basal contacts are sharp and heavily replaced and mineralised and upper contacts are normally graded.

Lithofacies Vbp

Lithofacies Vbp consist of poorly sorted, coarse lapilli- and dominant block-sized clasts of mixed lithologies comprising ≥50 vol.% (Fig. 2.4A) in wells THM12, THM14, THM15, and THM18. Clasts are subangular to angular and may form normally graded or massive very thick bedding. Commonly, units are 20 – 40 m thick and gradationally underlie or are interbedded with lithofacies Vllt. Lithofacies Vbp (dominant block) and Vllt (dominant lapilli) are differentiated only by clast size.

Coherent lava lithofacies

Lithofacies Xl

Massive, highly fractured to intact, dense, coherent hypocrystalline rhyolite (plagioclase, oxides, ± quartz) and andesite (plagioclase, pyroxene, oxides, ± biotite, amphibole) lavas comprise lithofacies Xl. Coherent rhyolites and andesites are porphyritic to aphyric, vesicular and often flow banded (Fig. 2.4A). Upper or basal sections of these lithofacies are highly brecciated (facies Xbm) and hydrothermally altered masking lithological contacts. Intact internal facies Xl remain fresh and holocrystalline. Together facies Xl and Xbm comprise the lava facies association, lithofacies X.

Deposit types & relationships				Interpretation	
Facies	***Associations***	***Lithological description (Fig. 2.4A)***	***Stratigraphic occurrence & lateral variation***	***Inferred transport & environment***	***Interpreted deposit type***
Silt (Ls)	Lacustrine (L)	Brown, organic-rich silt and fine sand. Moderate consolidation, massive to thinly bedded, well sorted, minor coarser sediments (<5vol.%). Sharp-intercalated lower & upper progressively gradational contact (<5m).	The facies dominates Huka Falls Formation (>200 m; excluding Middle Huka Falls Formation), thinner beds occur in Waiora Formation (5-15m). Intersected in all drill cores and occurs in a few localised outcrops. Lithogroup Ls rip-up clasts occur in the Volcaniclastic association, or is intruded by Xbm (hyaloclastite) at depth.	Lacustrine suspension near the centre of a ~200 m deep lake. Distribution reflects long-lived (Huka Group duration) Lake Huka with local depositional environments. Variably drilled Huka Falls Formation elevations suggest post-emplacement faulting.	Massive/weakly bedded form reflects progressive accumulation of suspended diatoms, clay & organic particles. Bedded form (e.g., in outcrops) is a turbidite succession.
Sandy & pebbly silt (Lss)	Lacustrine (L)	This facies is the same as Ls, but is mixed/interbedded with significant sand & pebbles (5-50vol.%). Clasts are subrounded, lithologically variable (andesite, scoria, rhyolite, pumice, tuff, mudstone, accretionary lapilli, greywacke), matrix-supported.	In TH18 is 10 & 30cm thick river gravel beds (253 & 261m depths). Overlying pebble zone is 90m (upper Lower, Middle & Upper Huka Falls Formation) of poorly sorted clasts in weakly defined medium beds. Thin Lss beds occasionally occur in uppermost Huka Falls Formation (e.g., WKM14).	Shallowing lake margin near localised prograding fluvial delta.	Lacustrine mixed suspension & terrigenous detritus & fluvial bedload pebbles.
Volcaniclastic fine tuff (Vft)	Volcaniclastic (V)	Largely indistinguishable fine grained volcaniclastic (±sedimentary) deposits divided by modal grain size. Vft consists of grey-white pumice-vitric/vitroclastic up to and including fine tuff. No significant clast content. Thinly bedded or soft sediment deformation present.	Grades from Vft capping graded volcaniclastic successions (1-2m). In Wairakei domain, Huka Group consists of ≥8 major volcaniclastic deposits. More localised lithological diversity in Tauhara domains.	Deposited in the lake centre, below wave base (~200 m). Suspension deposits are winnowed from subaerial &/or subaqueous density currents.	Hydraulically-deposited fine vitric-pumiceous & clastic ash suspension capping coarser underlying volcaniclastic associations.
Volcaniclastic medium tuff (Vmt)	Volcaniclastic (V)	Coarser equivalent of Vft. Fine to coarse sand, grey-white, pumice-vitric/vitroclastic.	Vmt comprises the Middle Huka Falls Formation in WKM14 (12.5m). It forms the matrix of, and grades from, Vplt and Vllt.	i) Lake-wide deposition from subaerially- &/or subaqueously-sourced suspended density currents.	i) Hydraulically-deposited medium vitric-pumiceous & clastic ash suspension
				ii) Lake-wide deposition from resedimented volcanogenic density currents associated suspension.	ii) Hydraulically-reworked medium clastic sand.
Volcaniclastic pumice lapilli-tuff (Vplt)	Volcaniclastic (V)	Vplt consists of Vmt and pumice clasts (1-10vol.%) and subordinate lithics (<2vol.%). Units are grey-white and a few tens of metres thick. Pumice occurs to 55vol.%. Matrix-supported clasts are porphyritic to aphanitic and are angular, ragged and lenticular or boxy shapes. Pumice is altered to white clay.	Commonly grades from Vllt and into Vmt. May contain Ls rip-up clasts. Vplt comprises much of the Waiora Volcaniclastics and Middle Huka Falls Formation. Middle Huka Falls Formation is absent in TH18. Middle Huka Falls Formation often consists of graded Vllt ±Vbp (25m), Vplt (70m) and Vft-Vmt (10m) facies.	i) Lake-wide deposition from subaerially- &/or subaqueously-sourced density currents.	i) Hydraulically-deposited medium vitric-pumiceous & clastic ash. Middle Huka Falls Formation deposition was confined to the deeper lake.
				ii) Lake-wide deposition from resedimented volcanogenic density currents.	ii) Hydraulically- reworked medium clastic ash suspension.
Volcaniclastic lithic lapilli-tuff (Vllt)	Volcaniclastic (V)	Vllt consists of up to medium lapilli-sized (~2-16mm), poorly-moderately sorted lithic and pumice clasts (~2-70vol.%). Units are white-grey and green. Lithic compositions reflect underlying volcaniclastic units or identify the presence of shallow plutons. Pyroclastic units contain basal rip-up clasts and pumice <5vol.%. Units are 1-100m, normally graded, thickly bedded to massive and typically matrix supported. Sharp (erosional?) lower Vllt contacts grade normally into overlying Vplt or Vmt. Clasts <5mm are poorly accounted for in photograph analyses.	Waiora Ignimbrite in northern Wairakei consists of ~10 density graded Vllt-Vplt beds (~70m) underlain and capped by Ls-Vft (~20m). Beds contain pink (vapour phase?), green and white subrounded lithic and compacted pumice clasts. Waiora Volcaniclastics in northern Wairakei (~300m) contains at least 6 and up to 9 lithogroup V units. At least 3 hydrothermal eruption beds occur in deep THM18 (>840m). Vllt sediments occur above lavas (THM18, TH18).	i) Lake-wide deposition from subaerially- &/or subaqueously-sourced density currents. Subaerial flows entering Lake Huka were controlled by source or shoreline conditions.	i) Graded equivalent of a co-ignimbrite lithic lag, neptunian breccias or a hydrothermal breccia.
				ii) Lake-wide deposition from resedimented volcaniclastic (e.g. lava clastic carapace) &/or volcanogenic density currents. Coarse Vllt and Xbm associations represent proximal facies.	ii) Reworked co-ignimbrite, hydrothermal breccia, polymict conglomerate.
Coarse monomict breccias (Xbm, Lbm)	Lava (X) and Lacustrine (L)	White, grey, green and brown units. Clasts are often clast-supported up to cobble size (16–64mm) and of a single lithology (>50vol.%). Basal contacts are sharp and altered, upper contacts are normally graded. Clasts are poorly sorted, angular-subangular.	Intra-formational glassy breccias occur within and overlie facies Xl (THM18). Lavas: Spa Andesite (THM18): 3 main breccia zones, clasts inherited from tortoise-shell jointed lava. Racetrack Rhyolite (TH18): jigsaw-fit, cobble-sized clast breccia, upper altered 100m, lower highly brecciated 35m.	i) Lake-wide deposition associated with & proximal to coherent lava (facies Xl), therefore, no significant transport component.	i) Autobrecciation lava dome or flow carapace.
		White, porphyritic, jigsaw-fit, ragged (pumiceous?) breccia beds (60vol.%) occur in a grey to dark silt matrix.	Sharply occur within lithogroup Ls facies (TH18, and THM18). White pumiceous breccia proximal to Xl and interbedded with Ls.	ii) Hyaloclastite contacts wet coherent, unconsolidated siltstone as an intrusion or lava carapace.	ii) Syn-volcanic hyaloclastite quenched intrusions.
Coarse polymict breccias (Vbp)	Volcaniclastic (V)	Clasts (20->50vol.%) are clast-supported, dominantly cobble-sized (>64mm), mixed lithology (accidental and accessory), poorly sorted and angular. Sharp unit basal contacts typically underlie emplacement units. Upper sections are normally graded. Overall very thickly bedded (20–40m).	Vertically/laterally gradational with finer grained (<<64mm) lithogroup Vllt. Occurs beneath the Middle Huka Falls Formation grading vertically and laterally into Vllt.	Lake-wide deposition from subaerially- &/or subaqueously-sourced phreatic/hydrothermal, phreatomagmatic or magmatic eruption density currents. Accumulations represent proximal facies.	Equivalent to a co-ignimbrite lithic lag or neptunian breccias or a (phreatic) hydrothermal eruption breccia.
Coherent lavas (Xl)	Lava (X)	Massive, fractured to intact, coherent hypocrystalline lavas. Porphyritic to aphanitic, vesicular (often flow banded). Upper and lower contacts are highly altered while the central cores remain fresh.	Intersected lavas: Racetrack Rhyolite (TH18, ~2km long, 45m flow-banded zones, vesicular, lower 35m glassy breccia carapace and 30cm pumaceous fall layer, sharply overlies Ls). Unnamed lava (TH18, 24m lava, 22m hyaloclastite breccia carapace, flow banded, porphyritic). Spa Andesite (THM18, 200m thick, 61wt.% SiO_2, vesicular, flow-banded, tortoise-shell fractured, intra-formational Xbm zones, overlies Ls).	Largely sublacustrine deposition flowing or extruded from unknown (fault-related?), buried (sublacustrine?) source vents. Intra-formational breccia zones denote external carapaces or divide successive sheared flow units.	Lava flows (<10 m thick & elongate) & lava domes (>>10 m thick).

Table 2.1. Summary and descriptions of lithofacies and facies associations identified in Huka Group cores at Wairakei-Tauhara. Facies are represented by an acronym and colour code (Fig. 2.4A-B) illustrated in graphic facies logs (Figs. 2.6-2.7). An interpretation is provided for the transport or depositional mechanism of the facies and a depositional environment is inferred.

HUKA GROUP LITHOFACIES ASSOCIATIONS

The following sections describe Huka Group lithofacies in three parts. Firstly, main facies associations are introduced in the Waiora Ignimbrite, Waiora Volcaniclastics and Huka Falls Formation (Table 2.1). Secondly, in each the overall depositional setting for the facies associations are collectively summarised (Table 2.1) with more rigorous depositional interpretations made in the discussion. Lastly, specific characteristics of the Reference Section well (WKM15) and lateral variation between wells (geographically grouped in Fig. 2.2A) are individually described in detail. These detailed text descriptions of core samples are summarised overall by facies log illustrations in Figs. 2.6-2.7.

WAIORA IGNIMBRITE

Volcaniclastic facies association description

The Waiora Ignimbrite contains a dominant facies association of density graded, very thick diffusely bedded (5 – 10 m) facies Vplt and Vllt, consistent with hydraulic grading (e.g., Manville et al., 1998; 2002). Overlying the main facies are moderately to thinly bedded facies Vmt and Vft. Facies Vllt consists of normally graded lithic lapilli-tuff, vitroclastic tuff that can be intensely silicified (cemented). The facies is white-grey, light green to pink-brown, reflecting the primary lithology and variable secondary hydrothermal mineral assemblages. Lithic clasts are usually ≤ 10 mm, 10 – 30 vol.% and include white-pink banded rhyolite, andesite and siltstone rip-up clasts. Clasts are homogeneously dispersed forming massive units or are concentrated at the base of beds. Poorly graded to weakly reversely graded, dominant juvenile pumice clasts (20 – 50 vol.%) include fiamme (compacted), blocky pumice and ragged blocky morphologies (Fig. 2.5A-D). Pumice clasts are white, light green or pink. At lowermost WKM14 is 15 cm of facies Vplt (Fig. 2.5A; a ‘pumice zone’). This zone is distinctly devoid of dense lithics and has a sharp upper contact with facies Vllt, and a sharp basal contact with lacustrine siltstone.

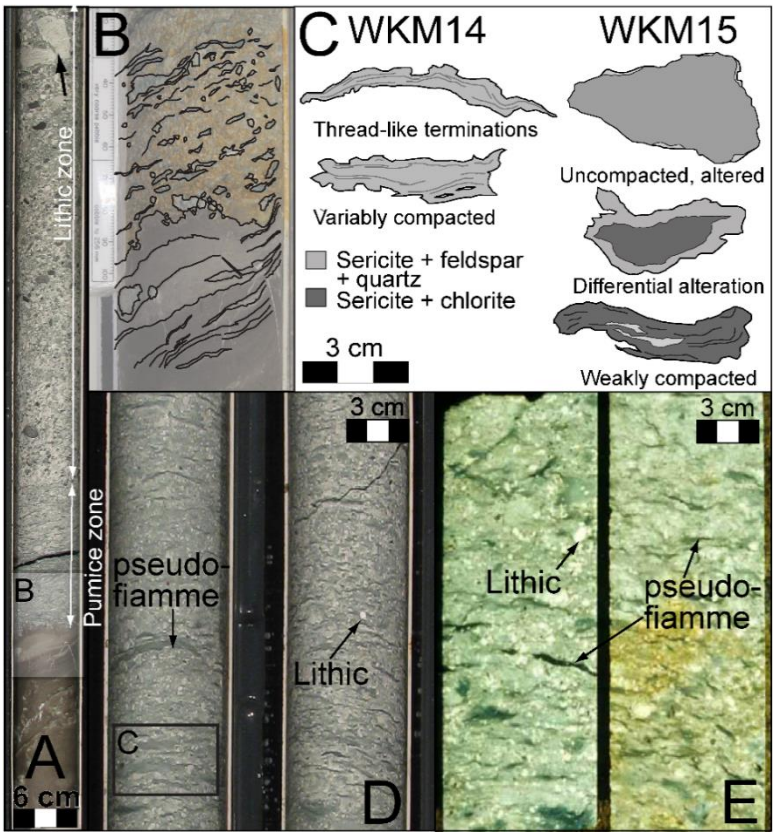

Figure 2.5. Compacted pumice ignimbrite textures in: **A.** lowermost Waiora Ignimbrite (WKM14) pyroclastic facies (pumice and lithic zones) overlying a lacustrine facies. Black arrow points to two large subrounded rhyolite lithics. **B.** Close-up of the irregular erosional and loading pyroclastic and lacustrine contact in A. **C**. Comparison of altered and compacted Waiora Ignimbrite pumice textures in WKM14 and WKM15. Similar post-emplacement compaction textures between **D.** Waiora Ignimbrite (WKM14), northeastern Wairakei and **E.** Green Tuff Belt, Japan (Gifkins et al., 2005a).

Lacustrine facies association description

Waiora Ignimbrite contains a facies association of thin planar to disturbed bedded siliciclastic (and minor bioclastic) facies Ls, with minor mixed or interbedded facies Vmt or Vft. Siltstone lithologies comprising much of the facies is brown to dark brown. The thinly bedded facies vertically grades from underlying facies Vft cap emplacement units, and implies a return to gradual lacustrine sedimentation.

Depositional setting of Waiora Ignimbrite lithofacies

Hydraulic grading, thick bedding, rip-up clasts and a lacustrine facies association of the volcaniclastic facies indicate that episodic volcaniclastic density currents (Table 2.1) interacted with a prevailing lacustrine environment, Lake Huka. However, given the available evidence, the source vent environment (either subaerial or subaqueous) remains difficult to identify. Presence of the discrete basal 'pumice zone' at the base of the facies (Fig. 2.5A; facies Vplt) suggests either a pumice-rich current

component advanced along with (i.e., by 'pumice flotsam'; Branney & Kokelaar, 2002), or an early pumice-rich current completely preceded (Fisher, 1979), main emplacement flows.

Waiora Ignimbrite is both welded (in central and southern Tauhara Field) and unwelded (northeast Wairakei; Rosenberg et al., 2009a). The geographic distribution of welding could have been influenced by the location of Lake Huka cooling interacting flows. However, welding intensity correlates with the overlying unit thickness, suggesting syn-emplacement compaction was a major control (*cf*. Whakamaru ignimbrites; Wilson et al., 1986).

Thread-like pumice (well WKM14) and selectively altered pumice textures (well WKM15; Fig. 2.5C) in Waiora Ignimbrite at northeastern Wairakei are interpreted as diagenetic 'pseudo-fiamme' (Fig. 2.5D). These lack the plastically-deformed Y- and U-shaped bubble-wall shards of true welding formed by hot emplacement (forming eutaxitic fiamme; Gifkins et al., 2005a). Similar diagenetic 'pseudo-fiamme' textures have been identified in Japan's Green Tuff Belt (Fig. 2.5E; Gifkins et al., 2005a). The shape of pseudo-fiamme reflect the clast's original morphology, differential compaction against competent clasts and variable clast alteration (Gifkins et al., 2005a). High-temperature alteration mineralogy from hydrothermal processes in Waiora Ignimbrite (>230 °C; Rosenberg et al., 2009b) probably increased the rate of selective pumice dissolution and compaction.

Capping the bedded volcaniclastic sequence are laminated and thinly bedded lithofacies Vmt, Vft and Ls notably absent of pumice clasts. These deposits represent material winnowed from subaqueous density currents and progressively settled through the water column (i.e., equivalent to subaerial pyroclastic co-ignimbrite ash clouds; Kokelaar et al., 2007). 'Background' sedimentation of facies Ls following large volcaniclastic emplacement reflect a return inter-eruptive periods in the stratigraphic record.

Reference section lithofacies distribution

Well WKM15 intersected only a relatively thin (100 m), but complete uppermost sheet of Waiora Ignimbrite at Wairakei-Tauhara (Fig. 2.6B, unit 1; Rosenberg et al., 2009b). The ignimbrite sheet consists of approximately nine, ~10 m thick density-size graded beds totalling 90 m (Fig. 2.6B; grouped facies in unit 1). Clasts are normally graded rhyolite, andesite and basalt lithics (facies Vllt) that grade

into reversely graded ragged pumice (facies Vplt). The mean measured largest clast size is 1.5 cm, while a uniquely large lithic clast (6.6 cm) occurs near the base of Waiora Ignimbrite in WKM15 indicating transporting currents retained coherency and some carrying capacity. Overlying thickly bedded facies Vllt is 20 m of thinly bedded facies Vft and Vmt (Fig. 2.6B). Bedding and grain-size characteristics unequivocally identify these facies as a water-settled suspension deposit. Unlike WKM14, there is no overlying lacustrine facies (Fig. 2.6B, uppermost unit 1). The deposit shows no signs of erosion, and reworking is restricted to the uppermost suspension unit.

Lateral variation

Northeastern Wairakei

Lithological variations between the uppermost Waiora sheet intersected by wells WKM15 and WKM14 are minor (Fig. 2.6A-B). Waiora Ignimbrite in WKM14 consists of ten angular, poorly sorted beds of variably compacted pumice and rhyolite lapilli-tuff (facies Vllt; Fig. 2.6A, unit 1). Individual beds are 5 – 10 m thick totalling 75 m. In WKM14 there are fewer lithic lapilli clasts, and more pumice clasts with poorly sorted, reverse grading due to their higher compaction. At the base is an irregular, sharp, likely erosional contact with a lacustrine facies (Fig. 2.5A-B). The 15 cm thick pumice zone at the base of WKM14 (Fig. 2.5A) is overlain by a dominant thickly bedded pumice and lithic lapilli tuff (facies Vllt; Fig. 2.5A, lithic zone). Within 1 m of the lower sharp contact are two particularly coarse, angular-subangular lithic clasts (both 4.2 cm long; Fig. 5A). At 3.2 m above the contact is a 10 cm long siltstone rip-up clast, probably eroded from the underlying lacustrine facies. Overlying the bedded Waiora Ignimbrite unit is 10 m of facies Vft grading into a 10 m thick bedded lacustrine facies association (Fig. 2.6A, unit 2).

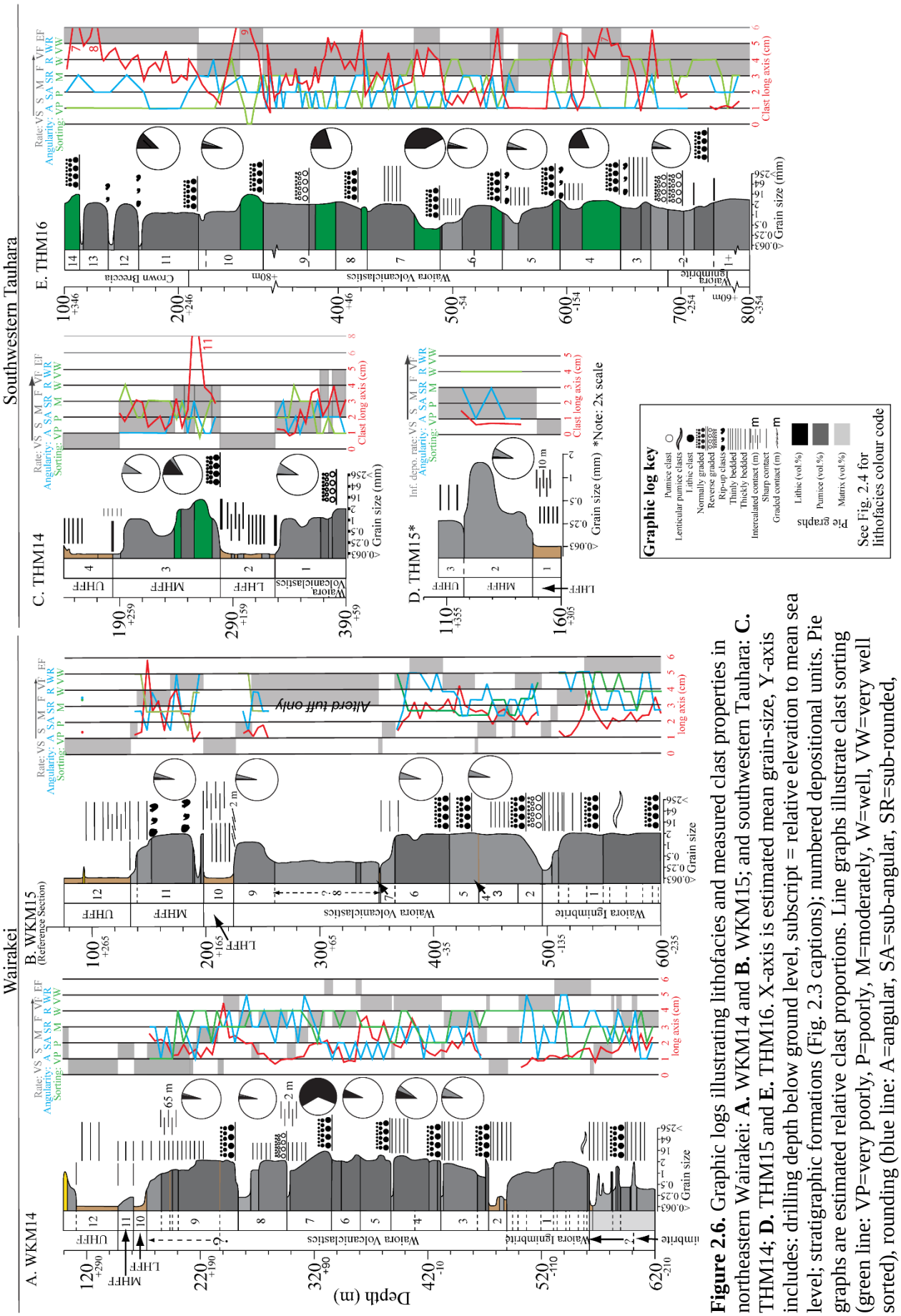

Figure 2.6. Graphic logs illustrating lithofacies and measured clast properties in northeastern Wairakei: **A.** WKM14 and **B.** WKM15; and southwestern Tauhara: **C.** THM14; **D.** THM15 and **E.** THM16. X-axis is estimated mean grain-size, Y-axis includes: drilling depth below ground level, subscript = relative elevation to mean sea level; stratigraphic formations (Fig. 2.3 captions); numbered depositional units. Pie graphs are estimated relative clast proportions. Line graphs illustrate clast sorting (green line: VP=very poorly, P=poorly, M=moderately, W=well, VW=very well sorted), rounding (blue line: A=angular, SA=sub-angular, SR=sub-rounded, R=rounded, WR=well rounded), average size of 10 largest clasts (red line) and inferred relative depositional rate (grey boxes: VS =very slow, S=slow, M=moderate, F=fast, VF=very fast, EF=extremely fast).

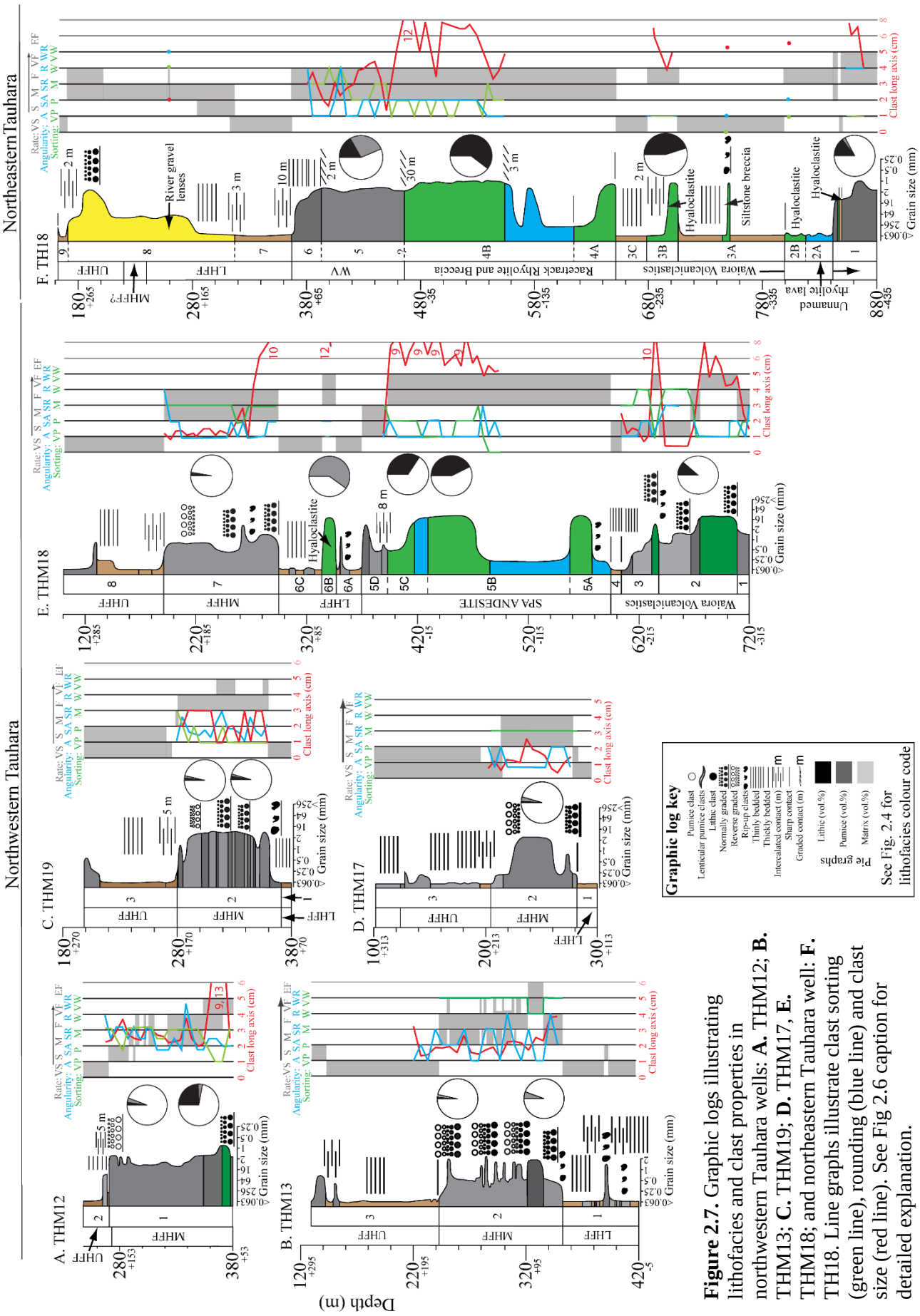

Figure 2.7. Graphic logs illustrating lithofacies and clast properties in northwestern Tauhara wells: **A.** THM12; **B.** THM13; **C.** THM19; **D.** THM17, **E.** THM18; and northeastern Tauhara well: **F.** TH18. Line graphs illustrate clast sorting (green line), rounding (blue line) and clast size (red line). See Fig 2.6 caption for detailed explanation.

Southwestern Tauhara

Only shallow depth (WKM14, WKM15) to intermediate depth Waiora Ignimbrite was assessed from cores in this study (THM16; Fig. 2.6E, units 1+ & 2). Seventy metres of Waiora Ignimbrite at the base of well THM16 in southwestern Tauhara contains alteration pseudo-textures, fine and medium pumice fiamme and rhyolite lithic lapilli (facies Vllt) in a heavily silicified matrix. Intense alteration of the deep Tauhara sample precluded detailed macroscopic interpretation limiting its depositional interpretation (Chapters 4 and 5).

WAIORA VOLCANICLASTICS

Volcaniclastic facies association

Waiora Volcaniclastics contains a highly variable vertical and lateral lithostratigraphic variations dominated by lithic lapilli-tuff (facies Vllt). Volcaniclastic facies associations are often underlain by breccia (facies Vbp), or pumice and lithic lapilli-tuffs (facies Vllt). These then normally grade into pumice lapilli-tuffs (facies Vplt) and bedded facies Vft and Vmt. Depositional units are 40 – 60 m thick. All deposits display evidence for subaqueous primary deposition (e.g., size-density grading) or reworking (e.g., thin bedding, cross-bedding).

Lacustrine association

Well sorted siltstone (facies Ls) of the lacustrine association are thin, dark brown beds (10 cm thick) interbedded with volcaniclastic facies, or as thick massive units (10s – 100 m). Siltstones are well sorted siliciclastic lithologies (light colour) with a variable bioclastic component (dark brown).

Lava association

Facies associated with lava extrusion or intrusive emplacement include coherent lava (facies Xl), monomict breccias (facies Xbm) and related sediments (facies Vllt; Fig. 2.4A). Massive, closely fractured to coherent, flow banded hypocrystalline andesitic or rhyolitic lavas are up to 180 m thick. Minor separate flow units 60 – 80 m thick are identified and may be internally divided by 20 – 50 m thick jigsaw-fit breccia facies Xbm.

Depositional setting of Waiora Volcaniclastics lithofacies

Dominating Waiora Volcaniclastics are graded sequences of facies Vbp and Vllt; facies Vplt and facies Vft and Vmt representing individual volcaniclastic emplacement events (e.g., Fig. 2.4B). Their thick bedding and significant juvenile material are consistent with deposits from explosive magmatic or phreatomagmatic density currents. Conversely, breccia facies lacking juvenile pumice, but rich in altered polymict lithics (facies Vbp, Vllt or Vmt) are interpreted as hydrothermal (phreatic) eruptions deposits. Coarse polymict breccias (facies Vbp) vertically grading into lithic lapilli-tuffs (facies Vllt) may identify the locality of a nearby source vent (e.g., lag breccia, Walker, 1985; hydrothermal breccia, Browne & Lawless, 2001; or neptunian breccia, Allen & McPhie, 2009).

Well-developed normal grading and bedding identified in facies Vplt and Vllt (and lesser Vmt-Vft) throughout Waiora Volcaniclastics is hydraulic density grading, supporting continual lacustrine deposition. Well sorted and bedded facies Ls reflects progressive water-settled deposition of fine grained particles remobilised by volcaniclastic turbidites (e.g., Schneider et al., 2001). Additionally, absence of extra-basinal pyroclastics (e.g., Allen et al., 2012), reworked clasts (facies Vllt) and preserved bedding further suggest deposition occurred deep in a lake where detrital input and water currents were low (Smith et al., 1993; Nelson & Lister, 1995).

The thickness and internal structure of lava facies in Waiora Volcaniclastics support either a flow, a composite flow or a dome type morphology. Relationships between the lava and surrounding facies help characterise their emplacement style (i.e., extrusive or intrusive) and extrusive setting (i.e., subaerial or subaqueous). Lava association lithofacies Xbm includes autobreccia and hyaloclastite breccias (Fig. 2.4B). Surrounding lithofacies Xbm are quenched hyaloclastite carapaces (facies Vllt) 20 – 40 m thick. Carapaces are bedded and have reworked and sharp contacts with lacustrine facies.

Reference section lithofacies distribution

Deposition of Waiora Volcaniclastics was the result of intra-basinal depositional events. Graded Vmt-Vft and Ls beds in WKM15 (Fig. 2.6B, units 1, 4, 7) demonstrate that the 290 m thick Waiora Volcaniclastics is comprised of at least six volcaniclastic emplacement events (Fig. 2.6B, units 2, 3, 5, 6, 8, 9; lithofacies Vplt and Vllt). Hydrothermal alteration of the volcaniclastic facies can, however,

obscure unit boundaries and may conceal additional emplacement units (e.g., Fig. 2.6D, unit 8; Chapter 4). Most depositional units are a graded facies Vllt-Vplt-Vmt sequence. All are hydraulically graded and bedded supporting continuous Waiora Volcaniclastics subaqueous emplacement. No lava facies occur in the reference well.

Lateral variation

Northeast Wairakei

Well WKM14 contains a similar Waiora Volcaniclastics sequence to WKM15 (Fig. 2.6A-B). The 330 m thick sequence consists of bedded facies Vllt, 2 beds of facies Vplt and 80 m of highly altered, undifferentiated facies Vft (likely containing several unidentified beds; Fig. 2.6B, unit 8). The uppermost 65 m (facies Vllt) contains thinly interbedded facies Ls (Fig. 2.6B, unit 9).

Northwest Tauhara

In contrast to Waiora Volcaniclastics in Wairakei, lithologies comprising the Tauhara cores are mainly locally sourced facies (e.g., facies Xl and Vbp). In well THM18, the lowermost volcaniclastic facies (Fig. 2.7E, units 1 – 3) includes three layered units of moderately to very well sorted, normally graded facies Vbp, Vllt and Vmt. The lowermost (>8 m thick) and middle unit (75 m thick) are not bedded. The upper unit (36 m thick) is thinly bedded and interbedded with <10 m of facies Ls. The absence of observed juvenile material and grading characteristics suggest a proximal, subaqueous hydrothermal eruption source (Browne & Lawless, 2001). Well-developed normal grading in the lower two units reflects hydraulic sorting. Thin bedding observed in the third unit suggest water current strengths may have increased as deposition progressed (Fig. 2.7E, unit 3).

Overlying the hydrothermal eruption deposits in THM18 is a 200 m thick, 3-layer, tortoise-shell-jointed composite lava flow (Fig. 2.7E, facies Xl, unit 5A-C; McPhie et al., 1993, p. 32). Each layer includes an overlying jigsaw-fit autobreccia facies (facies Xbm) of similar thickness. Capping facies Xbm is 25 m of thinly bedded, reworked facies Vllt carapace with minor accidental clasts in the lava facies (Fig. 2.7E, unit 5D; Prasetyo et al., 2012). Above Spa Andesite and its reworked carapace is a 75 m thick dominantly lacustrine facies sequence (Fig. 2.7E, units 6A-C). The lacustrine facies

contains small density current deposits (facies Vft, unit 6A), a hyaloclastite breccia (facies Xbm, unit 6B) and two, 7 m thick, interbedded facies Vplt (unit 6C).

Northeast Tauhara

Well TH18 contains ~500 m of volcaniclastic, lacustrine and lava facies. At its base is a highly altered and reworked volcaniclastic facies (Fig. 2.7F, unit 1) overlaid by ~200 m of lacustrine and interbedded lava facies (Fig. 2.7F, unit 4A-5). The lava facies includes a pale grey, variably-orientated flow banded, 24 m thick 'Unnamed' rhyolitic lava (facies Xl, TH18; Ramirez et al., 2009). Overlying the lava is a 22 m thick, hyaloclastite carapace (facies Xbm) sharply contacting facies Ls (Fig. 2.7F, unit 2). The remaining 150 m is lacustrine facies (Fig. 2.7F, unit 3A-C) and is comprised of thinly bedded facies Ls, minor interbedded facies Vft, a disturbed siltstone breccia (3 m) and 30 m of jigsaw-fit hyaloclastite (Fig. 2.7F, unit 3B). The lava facies is a 185 m thick rhyolite (Fig. 2.7F, unit 4; Racetrack Rhyolite). The 60 m thick massive portion (facies Xl) is flow-banded, vesicular and weakly porphyritic to glassy. Facies Xl is enveloped by a significant 35 m thick lower and 80 m thick upper glassy breccia (facies Xbm) that could be a combination of quench and mechanical shear (i.e., intrusional) in origin.

Southwest Tauhara

Above Waiora Ignimbrite in well THM16 are repeated volcaniclastic deposits. Eight, 30 – 60 m thick, normally graded sequences of facies Vbp, Vllt and Vmt beds (Fig. 2.6E, units 3 – 10) are identified beneath the much younger (post-Oruanui) Crown Breccia hydrothermal eruption unit (Fig. 2.6E, units 11 - 14; Rosenberg et al., 2009b). An apparent lack of juvenile pumice, the high proportion of accessory lithic clasts and the repetitive nature of the deposit support a proximal hydrothermal (phreatic) eruption origin, similar to that in THM18. No lacustrine facies are preserved between the successive deposits indicating eruptions were periodically eroding any contemporaneous facies Ls. The origin of Crown Breccia and underlying eruption deposits is discussed further in Chapter 5.

HUKA FALLS FORMATION

Lacustrine association

Lacustrine facies in the Huka Falls Formation contain massive to thinly bedded bioclastic to siliciclastic siltstone and sandstone (facies Ls) with minor to no visible volcanogenic clasts (<5 vol.%). Interbedded

facies Vft are present. These are likely reworked sediments or distal air-fall tephra. The facies association is comprised of either singular thin beds (10 cm) up to thinly bedded very thick units (10 – 100 m). Lower contacts are gradational and upper contacts are sharp and likely erosional. Within volcaniclastic facies overlying the lacustrine association are minor lithofacies Ls rip-up clasts derived from the weakly consolidated underlying substrate. Clast-bearing facies Lss contains sediments of mixed composition that are usually subrounded to rounded. Identified at a single well location (TH18) is facies Lss with interbedded clast-supported lenses of rounded pebbles.

Volcaniclastic association

The Huka Falls Formation volcaniclastic association consists of ~100 m thick bedded, hydraulically graded facies. Facies Vbp (or the normally graded equivalent, facies Vllt) in a basal section contains most of the Huka Falls Formation lithic content. Overlying the breccia is facies Vplt, the volumetrically dominant fraction of the volcaniclastic association. Juvenile pumice lapilli (10 vol.%) are altered, crystal-rich, mostly ragged forms. The supporting matrix is white-grey vitric tuff with minor lithic lapilli (<5 vol.%). Capping the dominant pumice lapilli-tuff are bedded facies Vmt-Vft.

Depositional setting of Huka Falls Formation lithofacies

The massive to weakly bedded siltstone textures identify continuous water-settled lacustrine sedimentation (e.g., Schneider et al., 2001). Cored samples are compositionally and texturally similar to the thinly bedded (~5 cm thick) outcrops along the Waikato River (Fig. 2.2A) and are interpreted as sublacustrine turbidite gravity current deposits transported deep in the Lake Huka (Fig. 2.8A-B; e.g., Cas & Wright, 1987, p. 325). Soft sediment deformation and intra-formational rip-up clasts are identified in the Huka Falls Formation outcrops. In the outcrops, the bedded siltstone and sandstones are sharply overlaid by >1 m of 10 – 20 cm thick beds of planar and tabular cross-bedded, fine to coarse fluvial sands (Fig. 2.8B-C). These sands together with rounded pebble lenses in TH18 (facies Lss) identify shallow lacustrine environments prograded by fluvial activity. Middle Huka Falls Formation was emplaced by density currents beneath Lake Huka (interpreted in Chapter 3).

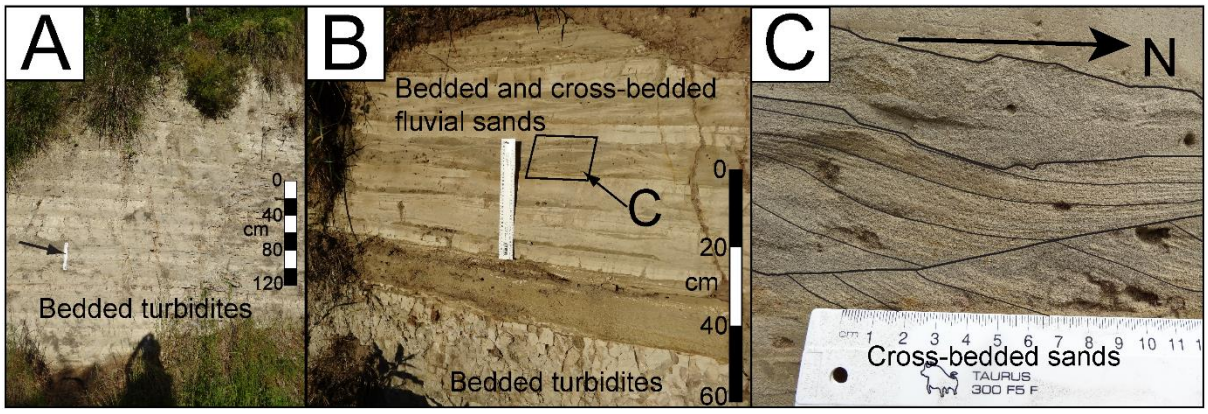

Figure 2.8. Outcrops of the Upper Huka Falls Formation near Huka Falls Scenic Lookout, Taupo. **A.** Wide view of a thick succession of the bedded silt and fine sand amalgamated turbidite beds. **B.** Beds of thinly bedded and cross-bedded fluvial sands sharply overly thinly bedded silt and fine sand beds. **C.** Close-up of Fig. 2.8B cross-bedding in the fluvial sands. Paleo-flow direction is approximately north.

Reference section lithofacies distribution

Well WKM15 intersects relatively thin Huka Falls Formation members (Fig. 2.6B, unit 10 – 12). A sharp lower contact separates the Waiora Volcaniclastics from Lower Huka Falls Formation siltstone (facies Ls). The 29 m thick lacustrine facies consists of thinly bedded facies Ls with interbedded (<1 cm – 1 m thick) facies Vft (Fig. 2.6B, unit 10). The 65 m thick volcaniclastic facies (Middle Huka Falls Formation) commences with several 2 m thick Vplt and Vmt beds with siltstone rip-up clasts. Forty metres of overlying massive facies Vplt contains large (10 cm diameter) siltstone rip-up clasts. The sequence is capped by 12 m of Vmt and 3 m of massive to laminated Vft (Fig. 2.6B, unit 11). The return to a lacustrine facies (facies Ls; Upper Huka Falls Formation) is marked by a sharp contact above which facies Ls contains 15 m of thinly interbedded facies Vft. Above this is dark brown, thinly bedded facies Ls (30 m thick) and 20 m of more massive facies Ls. These two are sharply separated by a 2 m bed of pebbly facies Vllt (Fig. 2.6B, unit 12).

Lateral variation

Northeast Wairakei

In WKM14, twelve metres of lacustrine facies lie above a gradational lower contact (1 m thick) at 173 m depth (Fig. 2.6A, unit 10). This facies association contains lithofacies Ls interbedded with facies Vft and Vmt. Thinly bedded, green-grey facies Vmt to laminated Vft (13 m thick) in WKM14 comprise a relatively thin volcaniclastic association (Fig. 2.6A, unit 11). The overlying lacustrine association

consists of a massive, 10 m thick facies Ls with interbedded facies Vft (Fig. 2.6A, unit 12). These include 27 m of overlying thinly bedded facies Ls, 9 m of green, bedded facies Vmt and 4 m of facies Lss.

Northwest Tauhara

Multiple shallow wells intersecting Huka Falls Formation at Wairakei-Tauhara provide good constraints on its lateral facies variation (Rosenberg et al., 2009b). A similar drilled sequence as that seen in surface outcrops occurs throughout most of Tauhara (Fig. 2.7A-E; THM12, THM13, THM17 and THM18). Sharply overlying the Lower Huka Falls Formation lacustrine facies in THM12 is a uniquely coarse grained volcaniclastic Middle Huka Falls Formation breccia facies (facies Vbp; Fig. 2.7A, unit 1; Rosenberg et al., 2009b; Chapter 3). Throughout Tauhara, Middle Huka Falls Formation contains a ~60 – 80 m thick massive facies Vplt unit. However, size-density clast grading in THM13 and THM19 records 5 – 10 m thick bedding (Fig. 2.7B-C, both unit 2).

Northeast Tauhara

Well TH18 intersects a distinctive facies sequence (Fig. 2.7F). The lower 10 m of the lacustrine association at 370 m depth contains interbedded facies Ls and Vmt (Fig. 2.7F, unit 7). The overlying 65 m is massive to thinly bedded facies Lss with increasing sand content upwards (Fig. 2.7F, unit 8). Interbedded within facies Lss at 253 and 261 m depth are, respectively, 10 and 30 cm thick, clast-supported rounded pebble beds. The volcaniclastic facies is absent in TH18 (Chapter 3).

Southwest Tauhara

The shallow lacustrine and volcaniclastic sequence in THM16 is replaced by facies Vbp-Vllt-Vmt of the younger Crown Breccia hydrothermal eruption deposits (Fig. 2.6E, units ~11-14; Rosenberg et al., 2009b). In wells THM14 and THM15, facies Ls in the Lower and Upper Huka Falls Formation is interbedded with thin facies Vmt beds together comprising 10 – 50 m thick units (Fig. 2.6C-D; respectively, units 2 and 3).

In the Upper Huka Falls Formation, facies Ls usually consists of a lower 10 – 20 m massive siltstone, overlaid by 20 – 60 m of bedded siltstone and fine sand, capped by 20 m of mixed silt, sand- and pebble-sized clasts (recognised by Grindley, 1965). Within the 100 m thick volcaniclastic facies in

THM14 is a coarse breccia lithofacies Vbp grading normally into bedded facies Vllt, Vplt and Vmt/Vft (Fig. 2.6C, units 3) similar to THM12. Capping the volcaniclastic association is laminated and deformed facies Vft (~2 m thick) sharply contacting an overlying lacustrine facies. The Middle Huka Falls Formation thins laterally towards southern Tauhara in THM15 (Fig. 2.6D).

DISCUSSION

Emplacement and paleo-environments

Facies distributions in Huka Group core and outcrop samples reflect a history of high spatial depositional variation across Wairakei-Tauhara. Deposits identify ancient interactions between effusive and explosive volcanism and paleo-Lake Huka gradually generating voluminous basin-fill material. Interpreted Huka Group depositional processes and prevailing environments over ~300 kyr are summarised as conceptual paleo-geographic cross-section reconstructions in Fig. 2.9A-C.

Of foremost relevance to understanding lacustrine volcaniclastic deposits is distinguishing deposition by subaerial flows entering subaqueous settings (Freundt, 2003; Jutzeler et al., 2014) or directly from subaqueous eruptions (Allen & McPhie, 2009). Both vent sources typically produce texturally- and compositionally-similar deposits (Freundt, 2003; Allen et al., 2012); however, recent advances in the field of subaqueous volcanism has significantly improved our understanding in recognising useful diagnostic features (Valenzuela et al., 2011; Rosa et al., 2009; 2010; Shane & Wright, 2011; Allen & McPhie, 2009; Allen et al., 2012; Schindlbeck et al., 2013; Jutzeler et al., 2014). When sample types are small (e.g., drill samples) and their spatial extent is limited, definitive eruption characteristics are less apparent and are inferred based on textural evidence, including that observed by hydrothermal alteration.

Waiora Ignimbrite

The distribution of Waiora Ignimbrite across Wairakei-Tauhara (Fig. 2.2B) reflects a complex emplacement and post-emplacement history. In southern Tauhara, wells have intersected >1500 m of Waiora Ignimbrite consisting of 3 or 4 thick flow sheets (100 – 400 m thick; Wood 1994a; Milicich et al., 2008a). In contrast, Waiora Ignimbrite examined in this study at northeastern Wairakei is comparatively thin (Fig. 2.6A-B; 100 m), conformable and lacks evidence for reworking between its

beds. These features suggest this Waiora Ignimbrite at Wairakei is only a single late eruptive capping a sequence of earlier thick sheets previously intersected by deep drilling in Tauhara. Based on their drilled distribution, the early sheets likely filled TRB underlying the modern Tauhara field allowing the late sheet to overtop the basin (Figs. 2.2C & 2.9A). This sheet is inferred to have originally been thinly emplaced in Wairakei, but has subsequently been eroded. Unique facies associations and density grading in the late sheet (best observed in WKM15) confirm sublacustrine deposition and the early establishment of Lake Huka across Wairakei-Tauhara.

Within Waiora Ignimbrite are abundant pumice clasts that must have been denser than water to have sunk during density current deposition (Manville et al., 1998; 2002). Pumice sinking occurs when clasts are either erupted dense (<60 vol.% vesicularity; Cas & Wright, 1991; Manville et al., 1998; 2002; White, 2001), when hot pumice from a subaerial vent are emplaced into water (Cas & Wright, 1991; Allen et al., 2012; Jutzeler et al., 2014) or when pumice are erupted subaqueously becoming waterlogged and sink (Kano et al., 1996; Allen et al., 2008; Allen & McPhie, 2009). Hydrothermal alteration to the structure of pumice clasts in Waiora Ignimbrite prevents assessment of possible hot-state emplacement textures (e.g., Cas & Wright, 1991) making the vent environment difficult to constrain. However, preserved beds of reversely graded pumice in the ignimbrite beds imply that as density sorting gradually formed, pumice clasts had initial, but short-lived buoyancy. Clasts were waterlogged by increasing size, then sank to deposit a reversely size graded fabric (Kano et al., 1996; Manville et al., 1998; 2002). Reversely graded pumice fabrics can, however, occur in hot pumice derived from both subaqueous and subaerial environments.

The irregular sharp (likely erosional and loaded) lower lithological contact and presence of rip-up clasts (Fig. 2.5A-B) suggest the saturated siltstone substrate was overrun by erosive volcaniclastic density currents depositing Waiora Ignimbrite. Transporting currents were moderately coherent, water-supported, density-stratified and capable of supporting fine to (rare) coarse lithic, pumice and rip-up clasts (Fig. 2.5A). At the base of Waiora Ignimbrite in WKM14, the compacted pumice zone (Fig. 2.5A) fits an interpretation involving a density stratified waterlogged pumice rich-flow beneath the main overriding flow. Moderately sorted lithic lapilli and the fine ash suspension cap comprising Waiora Ignimbrite support fines-winnowing and density stratification during the transport phase.

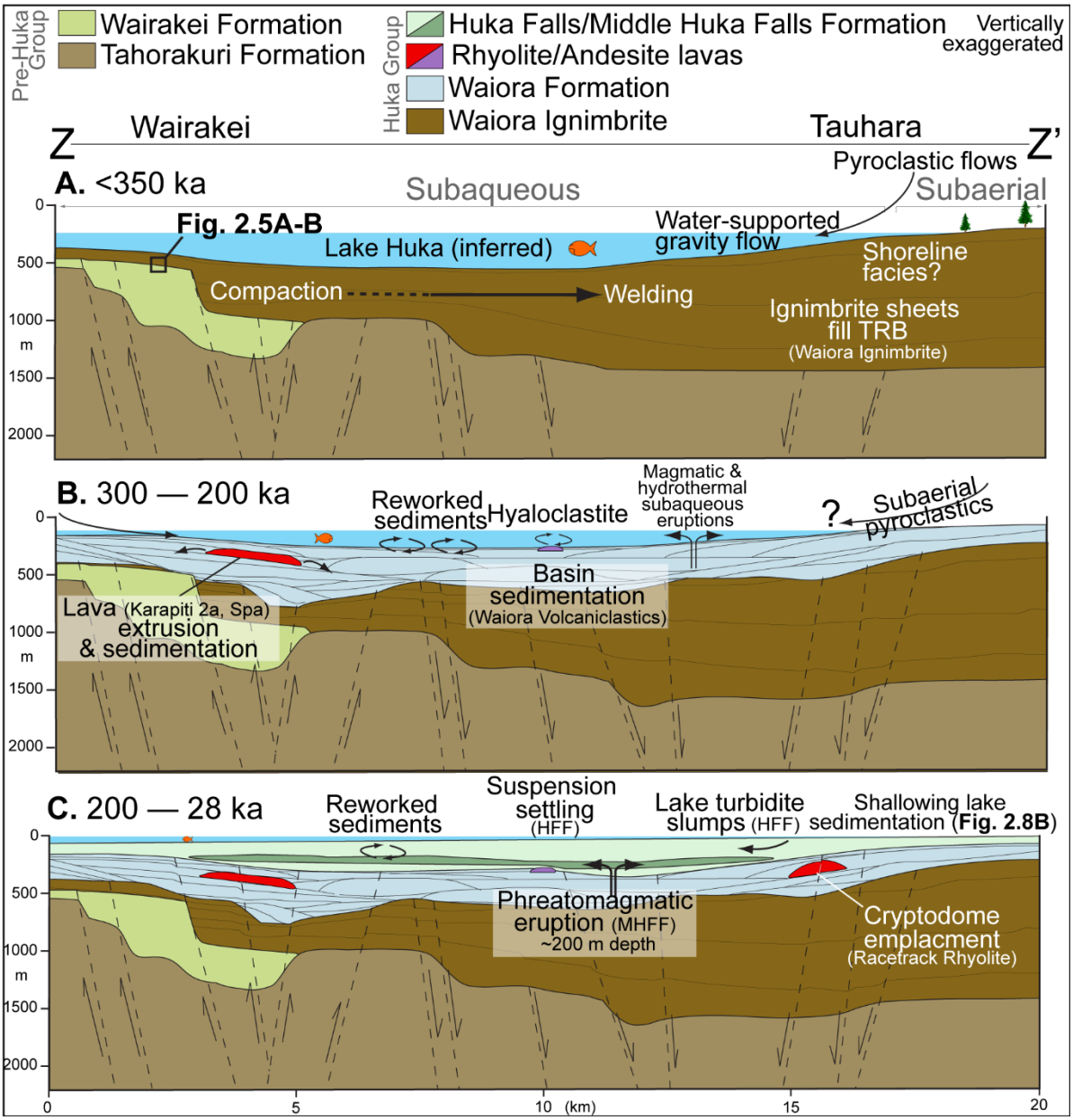

Figure 2.9. Northwest-southeast conceptual cross section Z – Z' (intersecting Fig. 2.2A) of depositional environments at Wairakei-Tauhara and stratigraphic relationships of the Huka Group sequence between **A.** <350 ka, **B.** 300 – 200 ka and **C.** 200 – 28 ka. TRB = Taupo-Reporoa Basin. 'Fig. 2.5A-B' in stage 'A.' conceptually identifies the location of Waiora Ignimbrite sample shown in Fig. 2.5.

Lateral welding variations in Waiora Ignimbrite indicate currents were initially of high mass-flux and contained hot interstitial gas (Kokelaar & Busby, 1992; Kokelaar & Königer, 2000; Kokelaar et al., 2007). Subaqueous welding could have been possible beneath Lake Huka if flows retained sufficient heat and subsequent syn-eruptive lithostatic compaction was high (e.g., Cas & Wright, 1987; 1991; Kokelaar and Busby, 1992; Kokelaar and Königer, 2000). Localities in the field where welding is absent, such as in northern Wairakei (WKM14 and WKM15), could identify areas where hot gas in

transporting currents had been replaced by water, retarding welding, as they mixed in Lake Huka (Fiske, 1963; Fiske & Matsuda, 1964; Whitham, 1989; Cole & Decelles, 1991; Freundt, 2003).

The lithostratigraphic architecture and structure of ignimbrite deposits are understood to record evolution of the transporting current's lower depositional boundary (Branney & Kokelaar, 2002). In the Waiora Ignimbrite sheet, 9 stacked graded units (5 – 10 m thick) could have formed by either ~9 separate but consecutive density current pulses, or by a singular sustained current with an unstable lower flow boundary resulting in double grading (diffusely-stratified lapilli-tuff of Branney & Kokelaar, 2002). The relatively sharp contacts between these successive beds and their well-developed internal density grading supports emplacement by the former mechanism (Dr R. Cas pers. comm. 2014).

While it has been established that the lacustrine facies and suspension cap identify lacustrine deposition of Waiora Ignimbrite, the location of the vent source remains unresolved: was this sheet erupted beneath Lake Huka, or did it flow into the lake? Identifying a vent source environments can be difficult as individual textures are often are not always exclusively diagnostic (Allen et al., 2012). Together, textures that can support subaqueous emplacement deposits include rounded clasts, well-developed grading and sorting, a shoreline breccia facies, terrestrial or shallow-water lithics, elutriated fines and vesicular pumices (White, 2000; Schneider et al., 2004; Allen et al., 2012). Identification of density graded bedding and subrounded lithic clasts in Waiora Ignimbrite support its deposition as into the lake by an initial, but limited, abrasive subaerial transport phase (e.g., Ohanapecosh Formation; Jutzeler et al., 2014). Since pumice clasts are susceptible to abrasion and rounding during subaerial transport (Allen et al., 2012), angular to subangular Waiora Ignimbrite pumice clast (compacted) morphologies may have formed following a (inferred) subaerial transport, perhaps by quench fragmentation and brecciation upon entering Lake Huka.

Following this premise, subaerial pyroclastic flows transporting late stage Waiora Ignimbrite must have been dense enough to enter Lake Huka (Fig. 2.9A). Flows are inferred to have become quenched, fragmented, waterlogged and hydraulically sorted at the Lake Huka shoreline. Flows continued as cooled water-supported density currents eroding and loading the saturated, but coherent underlying lake sediments (e.g., Pavey Ark andesitic ignimbrite, Kokelaar et al., 2007). After the final currents were deposited , turbulence in Lake Huka ceased allowing winnowed suspended ash (Freundt,

2003) to settle from the water column forming the 20 m thick suspension cap (facies Vft). Continued sedimentation of facies Ls identified in WKM14 (Fig. 2.6A, unit 2) suggests the lake entirely accommodated this ignimbrite sheet. The lake depth is inferred to have been >100 m and must have submerged Wairakei block in northern Wairakei.

Waiora Volcaniclastics

Waiora Volcaniclastics is a 400 – 500 m thick sequence of lithologically-variable volcaniclastic, lava and lacustrine facies. Interbedded in Waiora Volcaniclastics are fine grained volcaniclastic (facies Vft) with thin lacustrine suspension beds (facies Ls) that record inter-eruptive periods. In northern Wairakei, these beds are used to identify between 6 and 9 major volcaniclastic emplacement events comprising Waiora Volcaniclastics (Fig. 2.6A-B). Dominating Waiora Volcaniclastics are pumice-rich volcaniclastic facies (facies Vllt or Vplt) with or without basal rip-up clasts that recognise erosive density current transport deep in Lake Huka (Fig. 2.9B). Clast textures and near-uniform clast componentry comprising volcaniclastic facies support mainly primary intra-basinal(?) sources. Lateral facies and vent source correlation is typically not possible due to rapid lateral facies variations and variable hydrothermal alteration intensities (Rosenberg et al., 2009a; Downs et al., in press).

Occurrences of locally coarse facies Vbp in core samples recognise locations of nearby hydrothermal eruption vents (Browne & Lawless, 2001). Facies associations, hydraulic grading and bedding textures interpret hydrothermal eruption deposits in THM18 (Fig. 2.7E; units 1 – 3) and THM16 (Fig. 2.6E; units 4 – 10) suggest that the proximal vents were also submerged. Eruptions at THM18 must have ceased before extrusion of Spa Andesite as evident by interbedded lacustrine facies accumulations (Fig. 2.7E, unit 4). Stratigraphic relationships at THM16 indicate hydrothermal eruptions were repetitive and excavated overlying Huka Group strata (Fig. 2.6E, unit 4 – 14; Rosenberg et al., 2009b).

Interbedded lava facies in the Waiora Formation are less intensely altered than volcaniclastic facies preserving important extrusional textures. Spa Andesite at northwestern Tauhara is a composite lava flow (facies Xl) divided by brecciation textures (facies Xbm; Fig. 2.7E, unit 5A-C). Together with flow banding and facies relationships, these support subaqueous lava extrusion within or into prevailing

Lake Huka (Fig. 2.9B). Conspicuous tortoise-shell joints and jigsaw-breccia led Rosenberg et al. (2009b) to infer it as 3 ropy, pahoehoe-type lava flows. Flow banding textures are often implied to be an indicator of subaerial extrusion. However, Tian and Shan (2011) and Milicich et al. (2013) have identified that these textures are also common in subvolcanic intrusions such as cryptodomes and laccoliths. The presence of flow banding in 'Unnamed' and Racetrack Rhyolite in TH18 (Fig. 2.7F, units 2, 4) is subordinate to the lavas' sharp lithological contacts and their exceptionally thick facies Xbm. These characteristics best fit an interpretation of high shearing and cooling emplacement by subvolcanic intrusion, but would benefit from relative chronological assessments, such as U-Pb on stable magmatic zircon (e.g., Milicich et al., 2013).

Huka Falls Formation

The widespread occurrence of lacustrine siltstones and hydraulically reworked volcaniclastic deposits in the TVZ stratigraphic record (e.g., Grange, 1937; Grindley, 1965; 1986; Healy, 1965) indicate that bothlong-lived and ephemeral lakes have long been present (Manville, 2001; 2007; Manville & Wilson, 2004). Present-day and ancient lakes hosted by caldera depressions and large rift basins are the most significant sedimentary depocentres in TVZ (Fig. 2.1; Langridge, 1990; Smith et al., 1993; Leonard, 2003; Downs et al., in press). Their distribution in TVZ reflects the locations of local to regional base-levels controlled by tectonic subsidence, volcano-tectonic subsidence or volcanogenic damming (Manville et al., 2007; 2009; 2010).

Distribution of the Huka Falls Formation (Grindley, 1959; 1965) in Wairakei-Tauhara and TRB represent the footprint of Lake Huka (Fig. 2.1) controlled by NE-SW-trending faults overprinting caldera structures (Manville & Wilson, 2004). Details on the form(s), distribution, controls and evolution of Lake Huka remain unresolved due to limited geological evidence, but are indirectly inferred using interbedded volcaniclastic deposits.

Previous studies of the Huka Falls Formation at Wairakei-Tauhara have identified several key aspects reflecting deposition and environments in Lake Huka. Grindley (1965) recognised the variable stratigraphic boundary and lithological contact between Waiora Volcaniclastics and Huka Falls Formation to be diachronous. Huka Falls Formation is older in the basins, where it first progressively

accumulated (TFB and TRB) prior to 190 ka (Rosenberg et al., 2009a), than it is on the ridges (Wairakei Block). Locally thick occurrences such as in central Tauhara (300 m thick, THM19; Ramirez & Rosenberg, 2009) and adjacent to the Waikato River (200 m thick, WK304) probably reflect local zones of tectonic subsidence (Rotokawa and Aratiatia Faults; Fig. 2.2A) where lithofacies Ls was able to thickly accumulate in the deep lake. Sedimentation by suspension settling (e.g., Smith et al., 1993) and volcanogenic turbidites (e.g., Schneider et al., 2001) correspond with a deep area of the lake (>100 m) once covering the Wairakei-Tauhara area. West and east of Wairakei-Tauhara, Huka Falls Formation thins (<50 m, TH9) and coarser grained sediments become more common (Fig. 2.7F; TH18) in areas where the lake is interpreted to have been shallower.

The origin of the Middle Huka Falls Formation has been recognised from regular well site locations that constrain its distribution, facies and the overall low hydrothermal alteration intensity (e.g., Rosenberg et al., 2009b; Chapter 3). The member sharply overlies Lower Huka Falls Formation (facies Ls) with a contact lithologically similar to the deeper contact in Fig. 2.5B. Three graded lithofacies are consistently recognised including a proximal coarse breccia (Fig. 7A; facies Vplt and Vllt), a medial pumice lapilli-tuff facies (facies Vplt) and an ash suspension facies (facies Vmt and Vft). These detailed volcanic origins of the Middle Huka Falls Formation are explored in Chapter 3 using a separate facies model.

Above the bedded Huka Falls Formation, facies Ls outcrops near Taupo are planar bedded and tabular cross-bedded fluvial sands (e.g., Fig. 2.8A-B). These sediments may identify an area in late Lake Huka that became overrun by shallow rivers connecting northern and southern portions of the regional lake (Manville & Wilson, 2004). Prograding fluvial environments (facies Lss) intersected in several northern Wairakei-Tauhara wells (e.g., TH18, WKM14) reflect an increase in fluvial activity, prograding into lacustrine environments (Fig. 2.9C; Takemura & Kamp, 1991).

Improvement to existing insights

The detailed lithological assessments made from recently drilled core samples enhance and provide new details to existing general interpretations of the depositional history at Wairakei-Tauhara (e.g., Martin, 1961; Grindley, 1960; 1965; 1982; Healy et al., 1964; Healy, 1965; 1984; Takemura & Kamp, 1991; Wood, 1994a; 1998; Wood & Browne, 2000; Rosenberg et al., 2009a; Bignall et al., 2010a). Additional insights are provided on the long-lived, but dynamic structure of Lake Huka in the area (Chapters 3 and 6). Volcaniclastic textures throughout the group reflect a continuous history of hydraulic sorting and reworking in Lake Huka followed by differential lithostatic compaction and hydrothermal alteration. Evidence for late fluvial progradation suggests the basin was filling and shallowing prior to the 25.4 ka Oruanui eruption which destroyed the lake (Manville & Wilson, 2004). New interpretations of the timing and nature of geological events at Wairakei-Tauhara continue to enhance our broader regional knowledge of the productivity and magnitude of volcanism during the evolution of the central TVZ.

SUMMARY

The lithostratigraphic sequence of the Waiora and Huka Falls Formations (Huka Group) in the Wairakei-Tauhara Geothermal Field is described using facies analysis of eleven recently drilled cores. Interpreted facies associations provide a new detailed account of the depositional sequence over ~300 kyr. Textures in the thickly bedded and graded uppermost Waiora Ignimbrite identify that multiple pyroclastic density currents were deposited into paleo-Lake Huka. The thick, overlying accumulation of volcaniclastic, volcanic and sedimentary beds comprising Waiora Volcaniclastics represent small subaqueous density currents, extra-basinal pyroclastic flows, lavas and their sediments filling the basin over approximately ~100 kyrs. A following ~200 kyr period of volcanic quiescence is reflected by the Huka Falls Formation lake sediments. Quiescence was briefly interrupted by a small phreatomagmatic eruption in the lake (Middle Huka Falls Formation); however, lacustrine deposition resumed and became increasingly fluvial due to basin aggradation. Understanding the Huka Group record provides new refined insights of activity in the TVZ and a detailed architectural understanding that serves as a foundation for further detailed geological investigations in the Wairakei-Tauhara Geothermal Field area and elsewhere in TVZ.

Preamble:

In the previous chapter, a detailed lithostratigraphic summary of the Huka Group from core samples was presented. This recognised the sequence of prevailing depositional environments and processes at the core sites. One shallow unit in particular, the Middle Huka Falls Formation (MHFF), could be readily recognised and laterally correlated given its shallow elevation and lithostratigraphic constraints.

Here in ***Chapter 3****, the frequently drilled member becomes the focus of assessment. High preservation of the MHFF gives the most detailed and complete insight of the styles and environments contributing to the late Huka Group. This chapter examines its volcanic deposits using a facies model providing details of MHFF eruptive conditions. The model is specific to MHFF and is different to that in Chapter 2. Outcomes identify a subaqueous eruption style and setting unique in TVZ. However, given the prevailing environments identified in Chapter 2, similar processes were likely common in the Huka Group's history.*

This chapter includes some introductory overlap with previous Chapter 2 for it to be a stand-alone manuscript. The chapter has been reviewed and published in the New Zealand Journal of Geology and Geophysics as:

- *Cattell H.J., Cole J.C., Oze C., Allen S.R. 2014. Eruptive origins of a lacustrine pyroclastic succession: insights from the middle Huka Falls Formation, Taupo Volcanic Zone, New Zealand. New Zealand Journal of Geology and Geophysics 57: 331–343.*

This chapter is similar to the published version and where appropriate references to previous chapters have been included.

Deputy Vice-Chancellor's Office
Postgraduate Office

UNIVERSITY OF CANTERBURY
Te Whare Wānanga o Waitaha
CHRISTCHURCH NEW ZEALAND

Co-Authorship Form

This form is to accompany the submission of any thesis that contains research reported in co-authored work that has been published, accepted for publication, or submitted for publication. A copy of this form should be included for each co-authored work that is included in the thesis. Completed forms should be included at the front (after the thesis abstract) of each copy of the thesis submitted for examination and library deposit.

Please indicate the chapter/section/pages of this thesis that are extracted from co-authored work and provide details of the publication or submission from the extract comes:

Chapter 3: *Eruptive origins of a lacustrine pyroclastic Succession: insights from the Middle Huka Falls Formation, Taupo Volcanic Zone, New Zealand.*

Published in: 2014 New Zealand Journal of Geology and Geophysics 57: 331–343.

Please detail the nature and extent (%) of contribution by the candidate:

Hamish has undertaken all of the fieldwork, interpretation and laboratory analysis (90%). The co-authors provided advice and discussion on volcanic processes and helped with editing of the final manuscript (10%).

Certification by Co-authors:
If there is more than one co-author then a single co-author can sign on behalf of all
The undersigned certifies that:

- The above statement correctly reflects the nature and extent of the PhD candidate's contribution to this co-authored work
- In cases where the candidate was the lead author of the co-authored work he or she wrote the text

Name: *J. W. Cole* Signature: 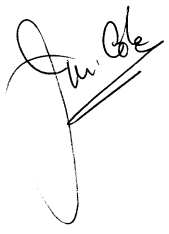 Date: *9/04/2015*

3

Eruptive origins of a lacustrine pyroclastic succession: insights from the Middle Huka Falls Formation, Taupo Volcanic Zone, New Zealand

H.J. Cattell[1]; J.W. Cole[1]; C. Oze[1] and S.R Allen [2]

[1] Department of Geological Sciences, University of Canterbury. Christchurch 8140, New Zealand

[2] ARC centre of Excellence in Ore Deposits and School of Earth Sciences, University of Tasmania, Hobart, Tasmania 7001, Australia

ABSTRACT

Current and ancestral lakes within the central Taupo Volcanic Zone (TVZ) provide depocentres for pyroclastic deposits. They, therefore, provide a reliable record of eruption history. These lakes can also be the source of explosive eruptions that directly feed pyroclast-rich density currents. Lithofacies characteristics of pyroclastic deposits give insight for discriminating between eruption-fed and resedimented facies. The most frequently recognised styles of subaqueous eruptions in the TVZ are shallow-water phreatomagmatic and phreatoplinian eruptions that form subaerial eruption columns. However, deeper source conditions (>150 m water depth), could have generated subaqueous explosive eruptions feeding water-supported pyroclast-rich density currents, similar to neptunian eruptions. Such deep-water eruptions have not previously been recognised in the TVZ. Here, we study a subsurface deposit, the Middle Huka Falls Formation (MHFF), in the Wairakei-Tauhara Geothermal Fields, TVZ, which we interpret to be the product of a relatively deep-water pyroclastic eruption (150 – 250 m depth). The largely subsurface Huka Falls Formation records past sedimentary and volcaniclastic deposition in a late form of long-lived ancient Lake Huka. Deposits examined in drill cores from eight wells reveal a lithic-rich lower unit, a dominant middle pumice lapilli-tuff unit and an overlying bedded tuff unit. A locally-thick coarse lithic lapilli-tuff (lower unit) near well THM12 suggests a nearby source vent locality vent beneath Lake Huka. This research provides an understanding on the origin of the MHFF deposit and offers insights for evaluating and interpreting the diversity of subaqueous volcanic lake deposits elsewhere.

INTRODUCTION

Extensional volcanic arc settings commonly host long-lived or ephemeral lakes formed by either structurally-controlled subsidence, subsidence following explosive eruptions or by volcanic eruptions blocking water outflows (Manville et al., 2007; 2009; 2010). Lakes and marine basins within or close to volcanic centres are depocentres for extra- or intra-basinal pyroclastic deposits and serve as a record of eruptive activity (e.g., Cas et al., 1990, 2001; Nelson & Lister, 1995; Manville, 2001). In some cases, the pyroclastic deposits that punctuate background sedimentation are thick, massive to graded, pumice-rich density currents fed directly from volcanic eruptions. The source of these eruptions can be from either relatively deep (≥150 m) subaqueous vents, or hot pyroclastic flows traversing the shoreline from a subaerial vent (Cas & Wright, 1991; White, 2000; Allen & McPhie, 2009; Allen et al., 2012; Jutzeler et al., 2014). Identifying the vent setting can be problematic as material from both sources turbulently mix with water and are transported in water-supported mass flows, ultimately producing similar deposits. Additionally, ancient deposits may be poorly preserved due to reworking, hydrothermal alteration and segmented uplift and exposure, further prohibiting identification. Detailed lithological examination is a key method for determining transport and depositional processes as well for inferring eruption conditions of pyroclastic deposits (e.g., Cas & Wright, 1987; McPhie et al., 1993). Pumice rounding, lithic clast type and clast distribution are important attributes allowing the two different origins to be identified (Allen and McPhie, 2009, Allen et al., 2012).

The central Taupo Volcanic Zone (TVZ), New Zealand, hosts large and deep lakes (<1 – 45 km long; <40 – 185 m deep). Explosive caldera-forming eruptions in the TVZ generated current Lake Taupo and Lake Rotorua and volcanic damming formed Lake Rotoiti, Lake Tarawera and Lake Okataina (Manville et al., 2007). The position, thickness and orientation of lacustrine deposits assigned to the Huka Falls Formation (HFF; Grindley, 1959; 1965) define the distribution of ancient Lake Huka, the ancestor of Lake Taupo (Fig. 3.1; Smith et al., 1993; Manville & Wilson, 2004; Rosenberg et al., 2009a). Drilling in Wairakei-Tauhara Geothermal Fields (Wairakei-Tauhara) in the TVZ has cored over 300 vertical metres of HFF. The Huka Falls Formation Middle Member (MHFF; Rosenberg et al., 2009a) is thick, entirely subsurface pyroclastic deposit enclosed by lacustrine sediments. Recent drilling

at Wairakei-Tauhara has intersected MHFF in eight cored wells returning new samples that present a unique opportunity to examine its stratigraphy in detail.

Here, detailed facies analysis of distinct MHFF units together with lithological and geochemical quantitative parameters are used to identify a vent location and infer eruption and transport processes. The results provide new insight into the past, likely frequent, interactions between lakes and explosive volcanism in the TVZ.

GEOLOGICAL SETTING AND STRATIGRAPHY

The central Taupo Volcanic Zone

The TVZ is an active volcano-tectonic intracontinental rift system in the central North Island, New Zealand, where volcanic activity commenced ~2 Ma (Fig. 3.1; Wilson et al., 1995). Offshore subduction causing continental rifting and crustal thinning in TVZ has concentrated silicic-dominated, explosive caldera-forming eruptions and smaller effusive dome eruptions to this zone. The commencement of activity at Whakamaru caldera (0.35 Ma) and present-day active vents define a late geographic area enveloping TVZ termed 'young TVZ' (Fig. 3.1; Wilson et al., 1995; Downs et al., 2014a). Deposition of HFF occurred in this young TVZ period between ~350 kyr – 28 kyr (Rosenberg & Kilgour, 2003; Rosenberg et al., 2009a).

Present-day TVZ contains numerous volcanic centres and lake-filled basins, providing an environment where pyroclastic deposits are concentrated (Manville & Wilson, 2004; Manville et al., 2007). Distributions of HFF from surface outcrops and drilling between southern Lake Taupo and Reporoa caldera in the Taupo-Reporoa Basin (TRB) preserve the location of an ancient lake, Lake Huka (Fig. 3.1; Smith et al., 1993; Manville & Wilson, 2004; Manville et al., 2007; Rosenberg et al., 2009a; Downs et al., 2014a). The full extent and number of lakes comprising Lake Huka, however, remains uncertain. Repeated regional faulting overprinting caldera structures in TRB is suggested to be the main structural control (Fig. 3.1; Manville & Wilson, 2004; Rosenberg et al., 2009a; Downs et al., 2014a).

Volcanic vents submerged by lakes in TVZ have previously been identified as the source of phreatomagmatic eruptions (e.g., early Ohakuri fall deposits; Gravley, 2004; Gravley et al., 2007; Downs et al., in press) and high intensity phreatoplinian eruptions (e.g., Oruanui, Hatepe and Rotongaio

deposits; Self & Sparks, 1978; Walker, 1981; Wilson, 1993). However, vents sourced in deep water where the eruption column is largely subaqueous have not previously been documented for TVZ.

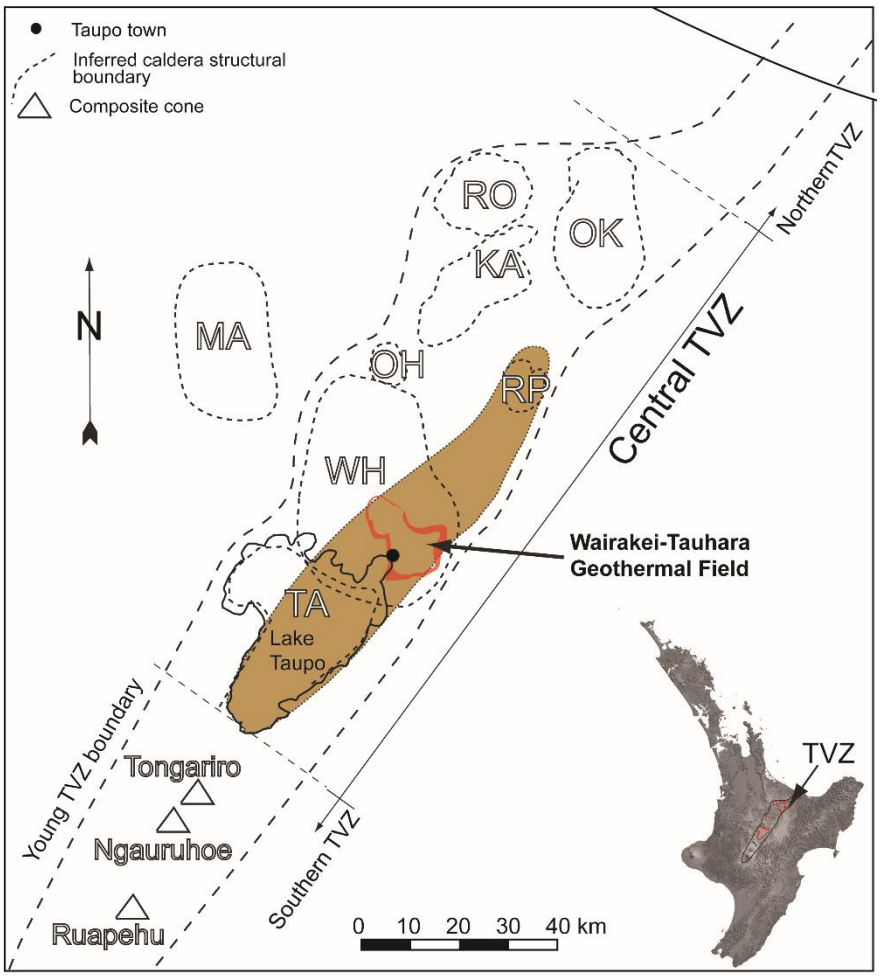

Figure 3.1. Main figure is the Taupo Volcanic Zone (TVZ), vent centres and the extent of HFF deposits (brown area) from Manville and Wilson (2007) approximating the extent of ancient Lake Huka. The young TVZ boundary is shown enveloping eruptive centres: OK = Okataina, RO = Rotorua, KA = Kapenga, OH = Ohakuri, RP = Reporoa, WH = Whakamaru and TA = Taupo. MA = Mangakino is from an older phase of TVZ. Figure modified from Wilson et al. (1995). *Insert* shows location of the TVZ, central North Island, New Zealand.

The Wairakei-Tauhara Geothermal Fields and Huka Falls Formation

The Wairakei-Tauhara Geothermal Fields are defined by a single DC resistivity boundary northeast of Lake Taupo in the TVZ (Fig. 3.2A; Risk, 1984). Extensive well drilling in 2009 by Contact Energy confirmed most major stratigraphic units are laterally continuous between the two adjacent fields (Rosenberg et al., 2009a; 2009b; Bignall et al., 2010a). Comprising the shallow stratigraphy is the HFF: a relatively thin, lacustrine succession above the Waiora Formation and beneath the Oruanui Formation (at elevations +400 – +100 mRL; Grindley, 1965). Throughout most of Wairakei-Tauhara, HFF consists

of three lithostratigraphic members: Lower (LHFF) and Upper (UHFF) separated by Middle (MHFF) (Fig. 3.2B; Rosenberg et al., 2009a).

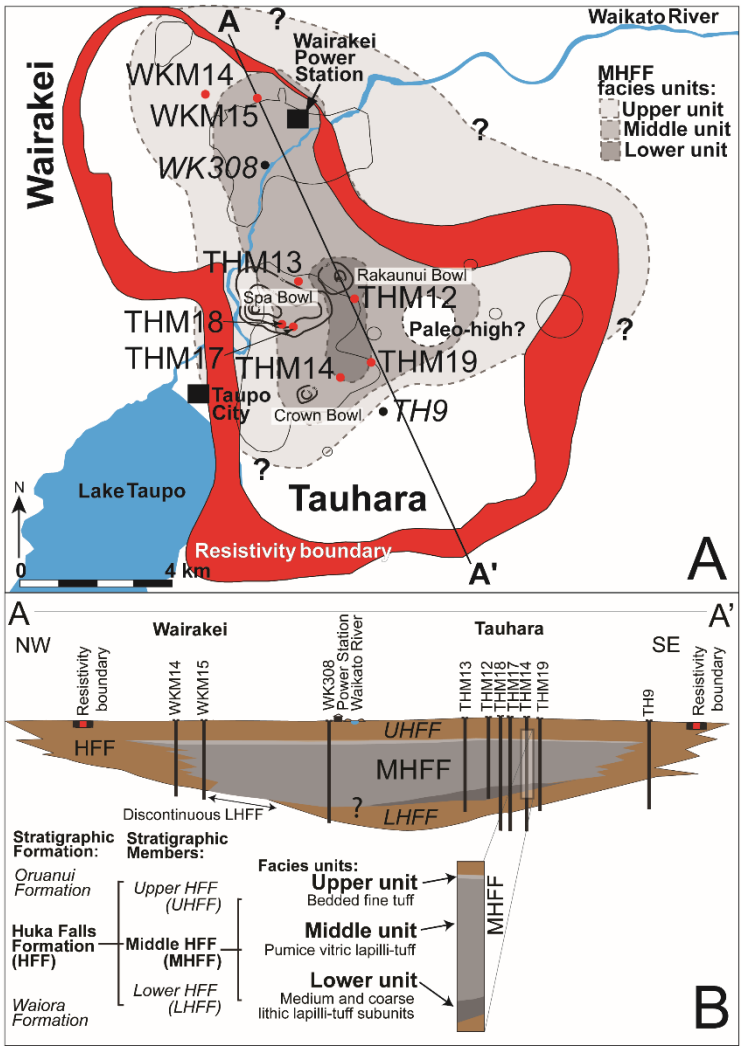

Figure 3.2. A. Wairakei-Tauhara Geothermal Fields as defined by a DC resistivity boundary (Risk, 1984). Shades of grey infer distributions of three MHFF units defined in the text. Red dots = analysed cored locations, black dots = wells described in the text, thin black lines = 3D modelled MHFF locations from drilling data, thick solid black lines = subsidence bowls from Bromley et al. (2009). **B.** Conceptual lithostratigraphic architecture of HFF through line A – A' in Fig. 3.2A (vertically exaggerated). Tree diagram insert is the stratigraphic relationship between stratigraphic formations (Grindley, 1965), HFF members (Rosenberg et al., 2009a) and MHFF facies units (this chapter).

The LHFF is a bedded to laminated volcanogenic sandstone and lacustrine siltstone. Geology well logs suggest that the buried member is discontinuous between Wairakei and Tauhara (Fig. 3.2B; Rosenberg et al., 2009a). In contrast, UHFF is comprised of lacustrine siltstone and fine grained volcaniclastic detritus. It is less lithologically variable than LHFF (Rosenberg et al., 2009b) and has some localised surface outcrops (Chapter 2). The dividing MHFF is a vitric tuff supporting angular pumice clasts and normally graded dense lithic clasts. This member is completely buried and is ≤100

m thick in cored Tauhara wells. However, near Wairakei Power Station (Figs. 3.2A-B), MHFF is reportedly 200 m thick (Rosenberg et al., 2009a). From this area, well logs identify that it is mainly confined within the Wairakei-Tauhara DC resistivity boundary, pinching out towards the north, west and gradually to the southeast (Fig. 3.2A-B; Rae, 2007; Rosenberg et al., 2009a). Beyond the field's resistivity boundary to the northeast where little drilling has occurred MHFF distribution is poorly constrained.

Geological models utilising well log data calculate a MHFF deposit volume of ~6 km^3 from uncorrelated drilled areas (S. Alcaraz, pers. comm. 2013). The model significantly underestimates the total volume by not inferring correlation between wells in the field. A realistic total volume is ~10 km^3, over a ~100 km^2 area (Fig. 3.2A). This volume characterises it as a 'smaller' scale explosive eruption in the TVZ. Characteristic 'large' volume eruptions (30 – >300 km^3) in TVZ form thick, widespread ignimbrites and are associated with calderas (Wilson et al., 1995).

METHODS AND MATERIALS

Core samples

The MHFF deposit was examined in all eight continuously cored wells drilled in both Wairakei and Tauhara Geothermal Fields (wells THM12-14, THM17-19, WKM14-15; Fig. 3.2; Rosenberg et al., 2009b). Cores were 6.3 cm in diameter (HQ size) with a ~95 % recovery rate and are stored at Contact Energy's Wairakei Steam Field core shed. Core samples were used rather than cuttings for assessing MHFF because they better preserve important rock textures, grain sizes and lithostratigraphic relationships. Examination of the cores included physical examination and assessment of high-resolution (8 MP) digital photographs of all the core provided by Contact Energy (Glynn-Morris & Winmill, 2009). Drill cores are hydrothermally altered, containing an intermediate argillic alteration assemblage (illite-smectite, illite, chlorite, pyrite, calcite and quartz vein fill; Browne & Ellis, 1970; Rosenberg et al., 2009b). The alteration minerals replaced ferromagnesian mineralogy, volcanic glass and weakly cemented the rock, restricting the use of comprehensive vesicularity and traditional grain size assessments.

Measurements of *in situ* clast sorting, rounding and volume were made used standard clast assessment charts. At 5 m intervals, the ten largest clasts were measured in two-dimensions along their apparent long axis using a ruler. Measurements at each 5 m interval were averaged to characterise the relative transport conditions at that stratigraphic level. The large clast population (1 – >6 cm) was the focus of this assessment. Small particles (<5 mm) were common but difficult to identify in core photographs, so were described as the altered sample matrix (<5 mm) rather than as clasts (>5 mm).

Supplementary samples and laboratory methods

In addition to the core samples, phenocrysts separated from altered pumice and dense lithic clasts (including rare granodiorite) and matrix samples were collected for examination from well THM12. In addition, a washed sample of rotary-drilled MHFF pumice cuttings from well WK308 (Fig. 3.2A) was provided by Michael Rosenberg, GNS Science. Cuttings were loose, small mixed chip fragments (≤1 cm diameter) collected at 10 m intervals over 75 m from between 105 – 180 m depth. They had no significant hydrothermal alteration making them better suited for whole-rock geochemistry and micro-vesicularity analyses.

Dense lithic clasts, separated phenocrysts and fresh pumice chips were impregnated in resin, thin sectioned and examined by microscopy to identify lithologies and micro-textures. Pumice micro-vesicularity and crystallinity was estimated from 12 randomly selected thin section samples. Thin sections were imaged using photomicroscopy at 4× magnification, SEM backscattered images (BSI) and backscattered electron images (BSE; 95×, 100× and 250× magnifications at 15 kV accelerating voltage). Their small size precluded meaningful Archimedes' principle vesicularity measurements (Houghton & Wilson, 1989). Pumice chip buoyancy was assessed by examining the relative settling behaviour of 100 randomly selected 6 – 8 mm chips (sieved -3 φ to -2.5 φ) in water and over a 24 hour period.

Minor pumice phenocryst phases removed from altered pumice clasts (clay) were confirmed using a JEOL 7000F Scanning Electron Microscopy (SEM) and Energy-Dispersive X-ray Spectroscopy (SEM-EDS) at the University of Canterbury (test conditions: 15 kV accelerating voltage, 0.59 nA at 5000 counts per second). Whole-rock major and trace element geochemistry of the pumice chips and

granodiorite lithic clasts were assessed by X-ray Fluorescence Spectroscopy (XRF) using a Philips PW2400 XRF at the University of Canterbury. Analytical procedures are outlined by Norrish and Chappell (1967).

LITHOFACIES DESCRIPTIONS

MHFF cores preserve three distinct vertically and laterally graded facies reflecting stages of an eruption (Fig. 3.3). Intersected within a single well, the layered facies are believed to represent waxing and waning of the eruptive magnitude and evolving flow conditions in a single eruption event. Units include a lower unit 25 – 35 m thick is rich in coarse lithics, a dominant middle unit of pumice lapilli-tuff (~60 m thick) and a widespread upper fine tuff unit contains (3 – 10 m thick). The following sections summarise their lithological variations.

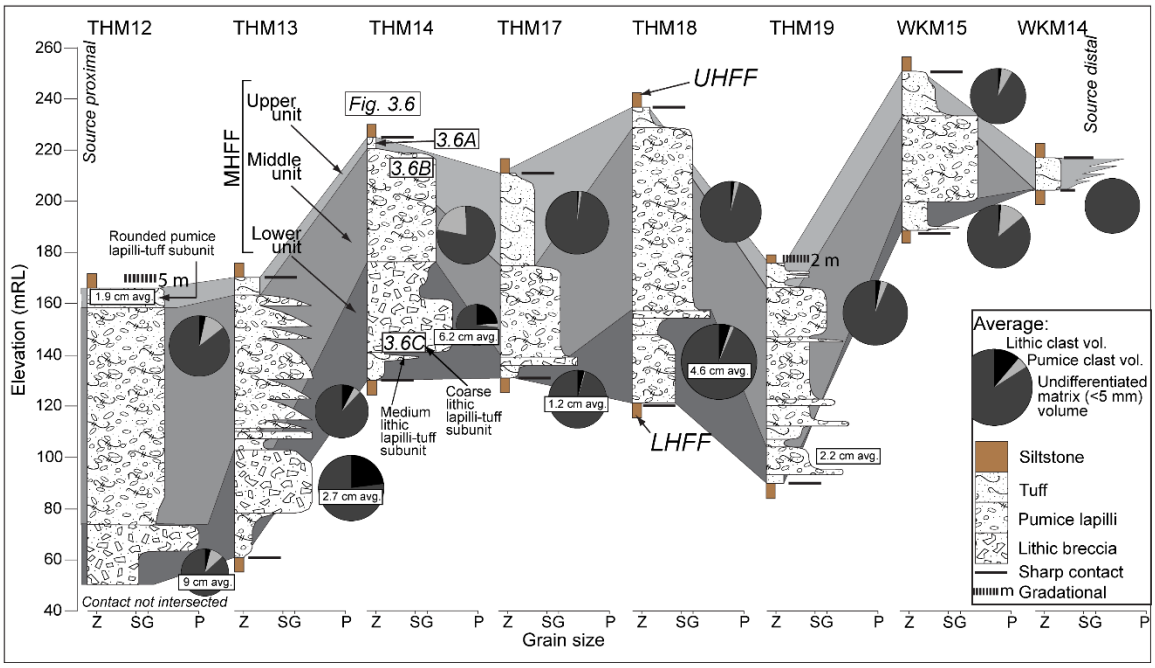

Figure 3.3. Graphic logs of cores summarising the distribution of MHFF facies units and estimated clast proportions (pie charts). Measurements in boxes are the average clast size in the coarse lithic lapilli-tuff unit. Grain size abbreviations: Z = silt, S = sand, G = granule and P = pebble. Avg. = average. 'Fig.3.6A-C' text boxes identify the stratigraphic locations of core photos in Fig. 3.6.

Lower unit: medium pumice lapilli-tuff and coarse lithic and pumice lapilli-tuff.

A sharp, planar contact with LHFF defines the base of MHFF in all cores, but was not intersected by drilling in THM12. The contact is overlaid by the lower unit facies in Tauhara wells. This unit can

consist of two parts including an underlying medium pumice-lithic lapilli-tuff subunit and a coarse lithic lapilli-tuff subunit (Fig. 3.2B). No lower unit occurs in wells WKM14 and WKM15.

The lower medium pumice-lithic lapilli-tuff subunit typically contains ≤5 vol.% lithic lapilli and ≤15 vol.% pumice lapilli clasts in a vitric tuff matrix. Well THM19 contains the largest (≥16 mm) and most concentrated clasts (40 vol.%) than the other core samples. Between wells, lateral sorting of the subunit ranges from very poor (THM19), poor to moderate (THM12-14) to well sorted (THM17 and THM18).

Over 1 – 2 m, the reversely graded medium pumice-lithic lapilli-tuff subunit grades into the overlying coarse lithic (and minor pumice) lapilli-tuff subunit. Medium to coarse lapilli clasts in the overlying subunit are subangular, poorly sorted and matrix-supported (30 – 50 vol.%). Clast lithologies are rhyolite (~25 vol.%), basalt (~5 vol.%), silicified volcaniclastics (~15 vol.%), siltstone (~10 vol.%) and granodiorite (<<1 vol.%). In well THM12, the subunit is exceptionally coarse grained (coarse lapilli-tuff to breccia) and is most lithologically diverse (≤30 cm clasts, average 9 cm). The subunit is clast-supported in wells THM12 and THM14 (Fig. 3.6C), totalling ~10 m thick and grades normally over a further 10 – 20 m. These wells contain rare, large, angular and blocky white pumice clasts (<2 vol.%) among the clast-supported lithic content. The coarseness, angularity and sorting of the coarse lithic lapilli-tuff subunit suggests a near source proximity. In other wells, clasts in this subunit are moderately coarse in THM18 (<4.6 cm) to finer grained and better sorted in THM13 (<2.7 cm), THM19 (<2.2 cm), THM17 (<1.2 cm).

Middle unit: pumice lapilli-tuff

The middle unit is comprised of massive to thickly bedded (2 – 5 m) to massive pumice vitric lapilli-tuff. In the cored wells it is up to 68 m thick (Fig. 3.3). Dominant medium pumice lapilli clasts (~15 vol.% up to ~40 vol.%) are moderately to poorly sorted with angular, ragged and lenticular shapes (Fig. 3.4B). Pumice clasts are normally graded to massive and hydrothermally altered, destroying vesicular textures. In wells where the unit is bedded, up to eight 5 m thick beds can be identified. The base of each bed is usually has a sharp (sheared?) contact with some concentrated, normally graded medium lithic lapilli (3 – 5 vol.%), overlaid by pumice vitric lapilli-tuff (10 vol.%) and capped by fine tuff (wells

THM13, THM18, THM19 and THM12 upper 20 m). In THM14, pumice lapilli are largest (<2.3 cm), abundant (≤40 vol.%) and are ragged and lenticular forms (Fig. 3.6B). Pumice clasts are rare or absent in THM17 (uppermost 30 m), THM12 (lower 65 m) and WKM15. The middle unit is absent altogether in WKM14.

Upper unit: thinly bedded fine tuff

Overlying the pumice lapilli-tuff is fine grained tuff comprising the 5 – 10 m thick upper unit (Fig. 3.5). The tuff is thinly bedded to laminated (Fig. 3.6A; 0.4 cm beds) and contains minor flame and other soft sediment deformation structures (e.g., THM14 and THM18; Fig. 3.4A). The widespread prevalence of this subordinate fine grained unit between wells indicates that it is the most distal to source. Well THM12 singularly contains two ~3 m thick beds of concentrated pumice lapilli (35 vol.%) assigned to a localised rounded pumice lapilli-tuff subunit (Fig. 3.5). The beds have sharp bases with the MHFF tuff and are both normally graded. Pumice within these beds are ~2 cm diameter. Within the overlying UHFF siltstone are sharply interbedded, 2 – 30 cm thick, extremely fine tuff beds.

Figure 3.4. Core samples from well THM14 showing the three MHFF units. **A.** an upper distal unit of fine vitric tuff (187 – 190 m depth); **B.** a middle medial unit of angular pumice lapilli and vitric tuff (208 – 211 m depth); and **C.** a lower proximal unit of coarse lithic lapilli-tuff (266 – 269 m depth).

RESULTS

Pumice crystallinity, composition and micro-vesicularity

Petrographic observations identify MHFF fresh pumice chips as weakly porphyritic (~5 vol.%, non-dense-rock equivalent) containing primary plagioclase, quartz, amphibole and accessory pyrite. Separated phenocrysts from the altered pumices contain large (>500 μm), normally zoned and euhedral plagioclase (~60 % total), quartz (~30 % total), a circular-shaped Ca-Ti silicate identified as leucoxene by SEM-EDS (~7 % total), and accessory pyrite (3 % total). No ferromagnesian minerals are preserved. The MHFF matrix contains silicified and devitrified (formerly) glassy bubble wall fragments, pumice shards and subordinate lithic fragments.

Whole-rock XRF results identified whole-rock compositions of the MHFF pumice chips and granodiorite lithic clasts to be very similar, supporting a co-magmatic relationship (Fig. 3.3; Appendix A2.4). Minor apparent variations (in major and high-field strength trace elements) could be explained by incompatibility and fractionation of a common melt between early plutonic crystallisation (granodiorite lithics) and later magmatic volcanism (pumice chips). However, more comprehensive geochemical analyses are needed to confidently confirm the relationship.

Wt.%	Pumice chips	Granodiorite lithic
SiO_2	75.03	73.51
TiO_2	0.29	0.36
Al_2O_3	13.46	14.35
Fe_2O_3	2.23	1.60
MnO	0.07	0.05
MgO	0.40	0.51
CaO	1.82	2.55
Na_2O	3.47	4.35
K_2O	3.17	2.63
P_2O_5	0.06	0.09
***Total**	**100.00**	**100.00**

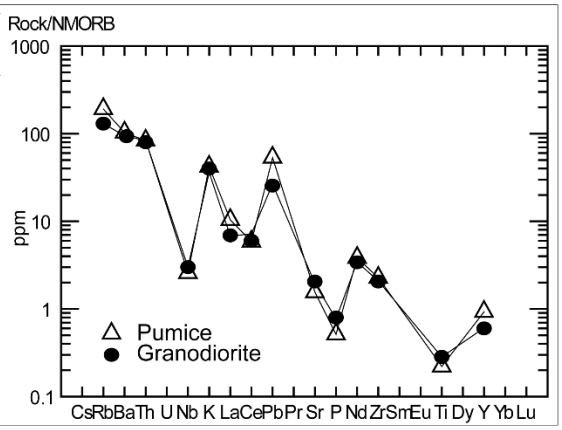

Figure 3.5. Whole-rock major element (in weight percent; Wt.%) and trace element chemistry of fresh pumice chips (WK308) and granodiorite lithic clasts (THM12). Elemental similarities in the table (*recalculated LOI totals) and spider diagram support a co-magmatic relationship.

Micro-vesicularity measurements identified moderately vesicular pumice chips (40 – 60 % vesicles; see Houghton & Wilson, 1989) consisting of spherical and dominantly elongate cylindrical vesicle domains (Fig. 3.4A–C). Vesicles are uniformly small (20 – 75 μm diameter) and elongate

(aspect ratios of >8:1). Less common medium sized vesicles (75 – 150 µm) are more spherical or weakly elongate (ratio of 2:1). Some show evidence for coalescence. Rare, large vesicles (>150 µm) are less elongate (ratios of 4:1). Pumice chip samples are devoid of larger vesicles >0.5 mm in diameter. Large vesicles were probably present in the original pumice clasts, although likely sparsely, but are inferred to have been preferentially destroyed during mechanical drilling of the well forming the chip fragments. The majority (63 %) of the chips remained floating after 24 hours of buoyancy tests, suggesting specific gravities <1 g/cm^{-3} and original vesicularities of ≥54 % (DRE density estimated 2.2 g/cm^3, Allen & McPhie, 2003) (equation from Houghton & Wilson, 1989; Manville et al., 1998). Those that sank were the fraction of smaller sized chips (<8 mm) comprised of small vesicles.

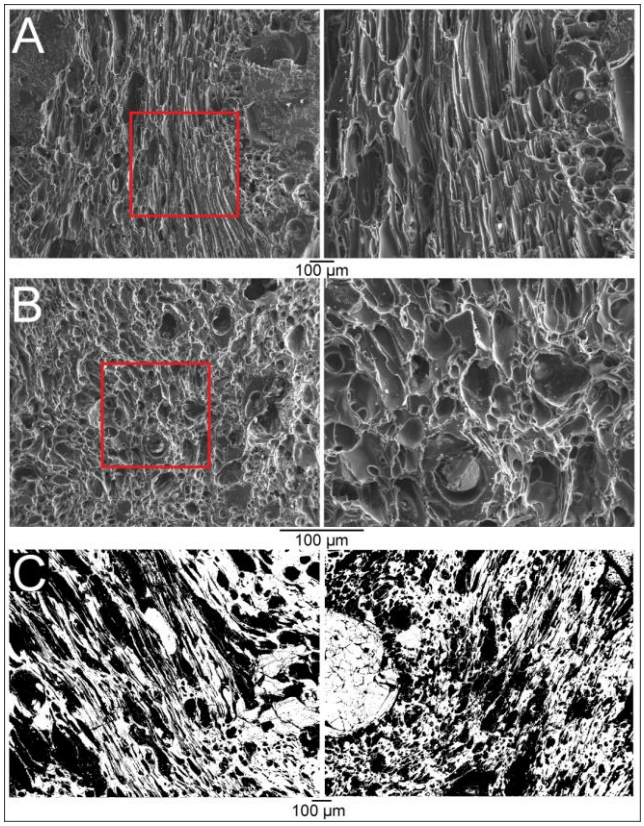

Figure 3.6. SEM images of a single fresh pumice chip sample from the MHFF from well WK308. **A.** Oblique BSI image of cylindrical vesicles at 95× and 250× magnification; **B.** Top-down perspective BSI image of circular vesicles (looking down cylindrical vesicles) at 95× and 250× magnification; **C.** BSE binary images of micro-vesicularity at 100× magnification where vesicles are black and dense phases are white (glass and crystals). Red square shows the magnified area of in the right BSI image.

Lithic clast componentry

Lithic clasts are concentrated in the MHFF lower unit. Lithics are typically medium lapilli size (THM13), but range from coarse ash to block (in THM12 and THM14). Lithics in the middle unit are

rare (≤5 vol.%). Large rare siltstone clasts (>10 cm) present in the lower and middle units and are consistent with rip-up clasts derived from the underlying LHFF substrate. The presence of granodiorite clasts between wells are proportional with the coarseness and thickness of the lower unit. Those in THM12 were largest and most angular (typically ≤4 cm, up to 13 cm). They were smaller (<2 cm) and less abundant in wells THM13 and THM14. Granodiorite clasts consisted of plagioclase (~50 %), quartz (~30 %), alkali-feldspar (~15 %), biotite (~5 %) and accessory hornblende, chlorite, magnetite, zircon, apatite, sericite and calcite. Granodioritic lithic clasts have been previously identified in several other pyroclastic units in TVZ (e.g., Ewart & Cole, 1967; Beresford, 1997; Brown et al., 1998b; Gravley, 2004; Downs et al., in press) and support the presence of widespread shallow intrusions throughout the TVZ (Browne et al., 1992; Chambefort et al., 2014).

DISCUSSION

Source environment and transport conditions

In Wairakei-Tauhara, spacing of geothermal wells indicate that the MHFF is thick (200 m), but drilling suggests it is not very widespread (Fig. 3.2A–B) suggesting a confined depositional setting. The deposit is enveloped by lacustrine siltstones and has no known subaerial correlative. A lack of reworked facies in the upper unit implies that transport, sorting and deposition all occurred subaqueously. Such thick and graded subaqueous pumiceous deposits may be deposited into a subaqueous setting with water-supported density currents (e.g., Allen et al., 2012; Kokelaar et al., 2012), or they are directly fed within the subaqueous setting (e.g., Allen & McPhie, 2009). Density currents from pyroclastic flows traversing the shoreline can produce deposits that can include a shoreline lithic breccia, including subaerial accidental clasts and abraded, subrounded pumice clasts (Fig. 3.7A; e.g., Znp tephra deposits, Allen et al., 2012); however, none of these features have been identified in MHFF. In subaqueous eruptions, coarse lithic clasts tend to quickly drop from the eruption column, depositing near source to form proximal lithic breccias. Pumice clasts remain characteristically angular, as clast impacts and abrasion during subaqueous transport are buffered by water (Kokelaar et al., 2012). Turbulence within eruption columns and density currents winnow ash fines into the water column to form water-settled suspension deposits. Resulting density layered deposits are generated by turbulent mixing and hydraulic sorting

forming a vertically stratified facies sequence. The MHFF has these features and so is most consistent with a subaqueous explosive eruption source (Fig. 3.8).

Textures in the MHFF (albeit poorly preserved) lack evidence for hot deposition (e.g., welding, pumice fiamme and eutaxitic texture), most common in subaerial settings. They are instead most typical of subaqueous explosive eruptions where the column mixes with water (Cas & Wright, 1991).

The MHFF is interpreted here to be the product of an eruption-fed subaqueous density current. Its sharp underlying contact and lower rip-up clasts are inferred to be the result of shearing and erosion at the head of the transporting current over the lacustrine substrate (LHFF). Density grading, weak bedding and the overall thick nature of the deposit is typical of deposits from sustained, high-density turbidity currents (Lowe, 1982). Conformable normal grading between the three stacked MHFF facies suggest that emplacement occurred from a single waxing and waning eruption event. Facies preserve the magnitude of the eruption source and evolving transport flow conditions (forming proximal, medial and distal facies; Fig. 3.6A-C). Early deposition of the medium lithic-pumice lapilli-tuff subunit may indicate that initial deposition was by concentrated erosive currents fed by a dense column, initially restricted by the diameter of the vent.

Following the eruption onset, a rapid increase in eruption energy is interpreted to have eroded the conduit walls, clearing the vent to deposit the lower unit (coarse lithic-pumice lapilli-tuff subunit). The coarsest lithic and waterlogged pumice clasts quickly dropped out of transporting currents becoming density stratified. Deposits accumulated near the vent forming a basal breccia analogous to either a lithic lag breccia (subaerial or shallow eruptions; Walker, 1985) or a neptunian lithic breccia (deep explosive eruptions; Allen & McPhie, 2009). Given that the ancient lake floor was presumably relatively flat-lying where deposition occurred, Rosenberg et al. (2009b) inferred THM12 to be the most proximal known locality to the MHFF source vent based on the coarse and lithologically diverse clast-rich MHFF lower unit intersected. Dense clast concentrations in THM14 (Fig. 3.4C) suggest it is also ‘near’ source, but is probably more distal than THM12. Pumice and granodiorite compositions support a co-magmatic relationship. The latter may have been sourced from a shallow intrusion intersected by ascending magma or is otherwise reworked from older volcanic deposits. The vent location near well THM12 coincides with present-day Rakaunui subsidence bowl (Bromley et al., 2009). Like other local

subsidence bowls (e.g., Crown Road subsidence bowl; Bromley et al., 2009), Rakaunui bowl may too reflect the location of a vent, perhaps the MHFF source.

After the vent had stabilised, the main eruptive phase fed water-supported density currents rich in pumice and coarse ash. Critically, the resulting middle unit is weakly bedded with ≥8 beds underlain by minor thin lithic clast beds. Density layering reflects transport density stratification, intensified by an unstable collapsing eruption column feeding multiple currents. Absence of the middle unit in the most distal section (WKM14) either suggests that currents become exhausted, due to lateral run-out dilution, or that the lake shallowed, blocking density current transport and deposition. In western Wairakei Field, presence of only the distal facies suggest that main density currents at these locations were waning. Coarser lacustrine facies in eastern Tauhara Field identify an area of the lake that was too shallow for weak currents to continue transport.

Following passage of the main gravity currents, reducing lake turbulence allowed suspended fines to passively settle through the water column forming the thinly bedded fine tuff upper unit. The rounded pumice lapilli-tuff subunit in THM12 suggest a history of abrasive grain collisions. Abrasion could have occurred in floating pumice rafts, or near the lake shoreline (Allen & McPhie, 2009). A pumice raft would have required clasts to rise through the water column while hot and buoyant, then to cool at the lake surface, becoming waterlogged and sinking to the lake floor. Alternatively, rolling and abrasion of saturated pumice near the higher-energy shoreline followed by subaqueous re-sedimentation may also explain the rounded pumice subunit. The sharp underlying contact best supports deposition by re-sedimentation.

Interbedded tuffs in the directly overlying siltstone (UHFF) must have been deposited a considerable time after the eruption given the low rate of lacustrine sedimentation (e.g., <0.3 mm/yr in Lake Taupo; Nelson & Lister, 1995). These beds are most likely re-sedimented MHFF from the upper unit (or sourced elsewhere), but could also be preserved younger airfall tephra.

Eruption depth

Facies characteristics in the MHFF provide insight into the depositional setting and source. The lack of evidence for reworking of the MHFF, and contrasting pyroclastic (MHFF) and lacustrine depositional

rates (UHFF) suggest the up to 200 m thick unit was deposited entirely within Lake Huka. The contact between MHFF and UHFF is conformable suggesting Lake Huka was ≥100 m deep in Tauhara to fully accommodate emplacement. The maximum depth of its modern-day (although caldera lake) equivalent, Lake Taupo, at 150 – 185 m deep may be a plausible depth for the Lake Huka vent. We therefore infer an eruption from a subaqueous vent between 150 – 250 m depth.

Inferred eruption style and explosivity

The bedded MHFF internal facies arrangement (Fig. 3.7D) is similar to that deposited from a deep, volatile-rich, high intensity neptunian style eruption (Fig. 3.7B; e.g., Mount Read Volcanics, McPhie & Allen, 2003; Allen & McPhie, 2009). The MHFF can be similarly divided into multiple density graded beds suggesting a fluctuating clast supply from an unsteady eruption column feeding density stratified currents. The absence of a known (or preserved) subaerial component and the lack of accretionary lapilli could indicate that the lake depth (150 – 250 m) was sufficient to supress development of a vertical subaerial column.

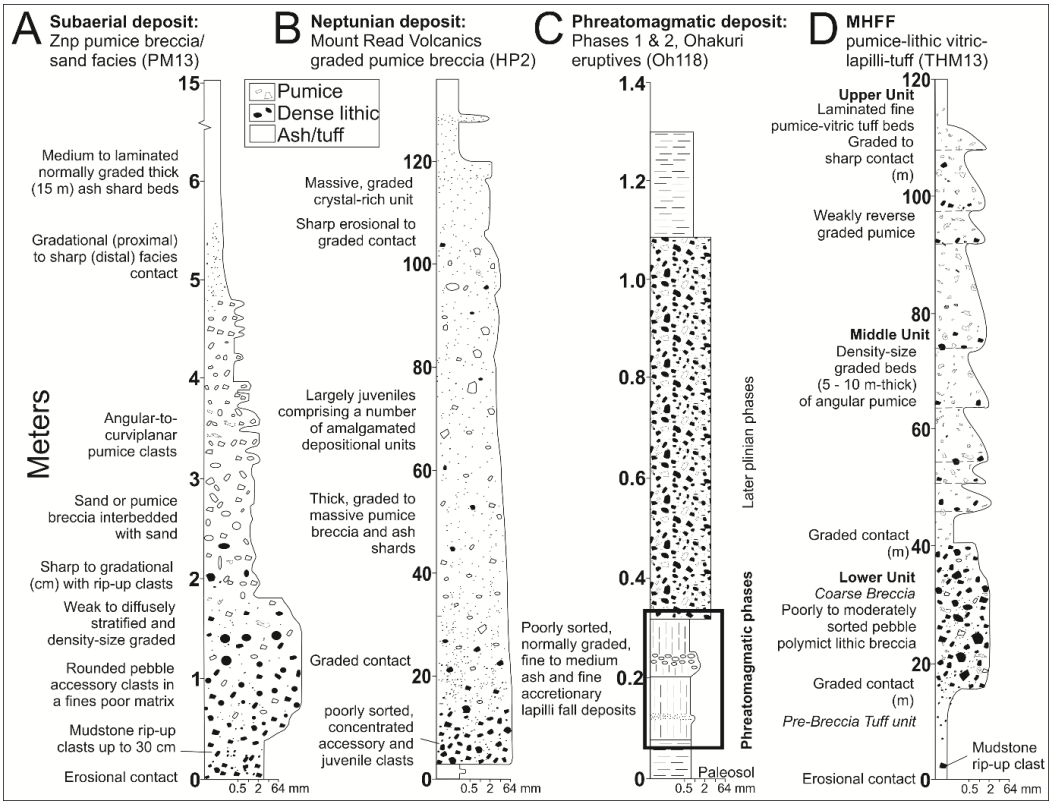

Figure 3.7. Comparison of facies architectures between different source eruption styles and vent environments, including: **A.** a subaerial to subaqueous transported deposit (Znp marine tephra, PM13; Allen et al., 2012); **B.** a neptunian deposit (graded pumice breccias from the Mount Read Volcanics, HP2; McPhie & Allen 2003; Allen & McPhie 2009) and **C.** a phreatomagmatic deposit (Ohakuri eruptives; Gravley 2004) compared with **D.** the MHFF (in THM13; Fig. 3.1).

Lithological aspects of the middle unit could, however, also support a shallower water (<30 m) phreatomagmatic origin. Voluminous fine ash (tuff) as present in the MHFF is more typical of highly efficient fragmentation by phreatomagmatic eruptions from unconfined magma-water interactions (Allen and McPhie, 2009). Explosive phreatomagmatic eruptions produce eruption columns that breach the water surface generating subaerial plumes (e.g., Houghton et al., 2000; Wilson, 2001; Gravley, 2004). Resulting subaerial pyroclastic density current and fall deposits are commonly widespread and dominated by juvenile ash shards, low or variably vesicular pumice, accretionary lapilli and subordinate lithics (Houghton et al., 2000). Unsteady water-magma interactions, more common in lower intensity phreatomagmatic eruption phases, can generate discrete episodic layered deposit packages (Fig. 3.7C; e.g., Ohakuri Phase 1 & 2; Gravley, 2004). High fines preserved in the middle unit suggest that the transporting density currents had some level of coherency when transported in the subaqueous setting.

The moderately (micro-) vesicular pumice chips with elongate vesicles reflect a history of melt shearing and stretching during ascent prior to significant exsolution and quenching (Cashman et al., 2000). These textural characteristics are consistent with both phreatomagmatic and neptunian eruption origins, but supressed and terminated vesiculation is most consistent with deep-water eruptions (Cashman et al., 2000; Allen & McPhie, 2009). Major vesicle and juvenile jointing textures useful for fragmentation analysis are not preserved; however, the high overall fines indicate the eruption water depth (inferred 150 – 250 m) and hydrostatic confining pressure were insufficient to suppress fragmentation (and possibly vesiculation; Allen & McPhie, 2009; Fig. 3.8).

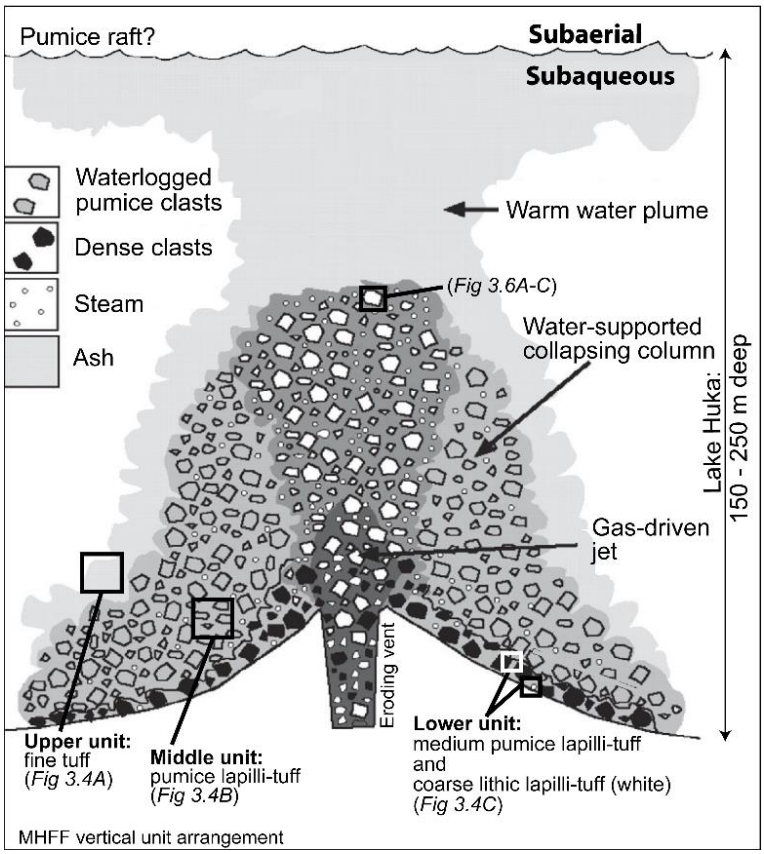

Figure 3.8. Conceptualised MHFF eruption dynamics showing laterally variable and stacked lithofacies deposited from a 150 – 200 m deep vent in Lake Huka. Figure modified from Allen and McPhie (2009).

To account for the MHFF deposit characteristics, the subaqueous eruption is inferred to have had archetypical phreatomagmatic-style magmatic and fragmentation mechanisms (efficient magmatic and quench fragmentation, moderately high vesicularity, limited confining pressure). The eruption then likely developed via neptunian-like processes (Fig. 3.8; relatively deep, subaqueous confined, flow dynamics). The MHFF deposit reinforces the continuum of hydrovolcanic eruption styles that are the result of complex interactions between variable magmatic, ambient vent and water conditions (e.g., Kokelaar, 1983; 1986; Walker & Croasdale, 1971; Walker 1973; Self & Sparks, 1978; Allen & McPhie, 2009; Cas & Van Otterloo, 2011).

CONCLUSIONS

Lithofacies analysis of core samples provides insight for inferring the vent setting, eruption style and transport and depositional processes for the MHFF deposit from Wairakei-Tauhara Geothermal Field. Deposited within the ancient Lake Huka, the MHFF records a pyroclastic succession which we interpret to have been directly fed by a subaqueous explosive eruption from a vent inferred between 150 – 250 m depth. The explosive eruption generated abundant ash, lithic and highly vesicular pumice lapilli transported within an almost exclusively subaqueous eruption column. The explosive eruption deposited a proximal, vent clearing, coarse lithic lapilli-tuff in central Tauhara Geothermal Field (THM12). Vent clearing deposition was followed by deposition from a collapsing, turbulent eruption column feeding water-supported gravity currents, progressively emplacing the pumice lapilli-tuff. Suspended ash settled when the eruption ceased. The MHFF appears to have a relatively high matrix content (70 – 90 vol.%) compared to deposits from high intensity, deep-water subaqueous (neptunian) eruptions. Results highlight the potential complexity encountered when discriminating the provenance of subaqueous volcaniclastic deposits. Evidence stemming from the primary eruption and transport processes provides new insight into assessing interactions between lakes and volcanism in the TVZ.

Preamble:

In Chapter 2, facies analysis of Huka Group core samples were presented as a lithostratigraphic model for Wairakei-Tauhara. In Chapter 3, the eruption history of the late Middle Huka Falls Formation was specifically investigated from comprehensive samples and its well-constrained stratigraphy. Facies models highlight high lateral and vertical lithological variation in the Huka Group, reflecting diverse vent sources and depositional environments. In these chapters, Lake Huka which existed across Wairakei-Tauhara is identified to have interacted with volcanic processes influencing deposition of the Huka Group. However, during core inspections primary lithological variations were found to be difficult to identify in intensely altered zones. As a consequence, the appearance and detailed insight into the Waiora Formation could be compromised.

In an effort to enhance stratigraphy and depositional insights of thick altered volcanic strata, ***Chapter 4*** *investigates the effectiveness of measuring variations in alteration-resistant magmatic crystals and immobile elements. During volcaniclastic transport in the aqueous setting, density graded particles become preserved in the final deposit as a normally or reversely graded fabric. Here, the size and volume distribution of primary feldspar phenocrysts are measured in two continuous cores by photomicrograph analysis. The distribution of immobile elements Ti and Zr concentrated in dense, primary ilmenite/titanite and zircon crystals are measured in multiple cores. Measurement methods used a mix of laboratory XRF, portable XRF and EDS. Finally, immobile element variations in the altered Huka Group are briefly compared with regional magmas to identify their use of identifying possible magmatic correlatives in the TVZ.*

A condensed version of this chapter focused on chemostratigraphy has been reviewed by Geochemistry: Environment, Exploration, Analysis. Material has been edited in response to two reviewers' comments. It is in preparation for resubmission.

Deputy Vice-Chancellor's Office
Postgraduate Office

UNIVERSITY OF CANTERBURY
Te Whare Wānanga o Waitaha
CHRISTCHURCH NEW ZEALAND

Co-Authorship Form

This form is to accompany the submission of any thesis that contains research reported in co-authored work that has been published, accepted for publication, or submitted for publication. A copy of this form should be included for each co-authored work that is included in the thesis. Completed forms should be included at the front (after the thesis abstract) of each copy of the thesis submitted for examination and library deposit.

Please indicate the chapter/section/pages of this thesis that are extracted from co-authored work and provide details of the publication or submission from the extract comes:

Chapter 4: *Enhancing the resolution of altered volcanic stratigraphy in the Wairakei-Tauhara Geothermal Field using phenocryst and immobile element measurements.*

Please detail the nature and extent (%) of contribution by the candidate:

Hamish has undertaken sample collection, geochemical and petrographic preparation, analysis and interpretation (90%). The co-author (10 %) provided discussion and advised on editorial matters.

Certification by Co-authors:
If there is more than one co-author then a single co-author can sign on behalf of all
The undersigned certifies that:

- The above statement correctly reflects the nature and extent of the PhD candidate's contribution to this co-authored work
- In cases where the candidate was the lead author of the co-authored work he or she wrote the text

Name: *C. Oze* Signature: 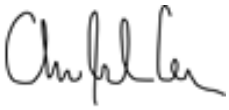 Date: *14/04/2015*

4

Enhancing the resolution of altered volcanic stratigraphy in the Wairakei-Tauhara Geothermal Field using phenocryst and immobile element measurements

Hamish Cattell and Christopher Oze

Department of Geological Sciences, University of Canterbury, Christchurch 8140, New Zealand

ABSTRACT

Thick stratigraphy comprised of multiple volcanic deposits can be difficult to accurately log when successive units are lithologically similar or hydrothermally altered. As a consequence, resulting lithostratigraphic logs may not contain the stratigraphic resolution required for investigating volcanic-hosted resources or for detailed geological reconstructions. By measuring stratigraphic variations of magmatic phases least affected by hydrothermal alteration, their resulting stratigraphic trends identifying the structure of the magmatic deposit can be used to enhance lithostratigraphic models. The Huka Group at Wairakei-Tauhara Geothermal Field in the Taupo Volcanic Zone contains >500 m of hydrothermally altered volcanic and sedimentary deposits. Continuous core samples have provided detail of its lithostratigraphic variation. Hydrothermal alteration has, however, variably modified the appearance of volcaniclastic strata, potentially reducing macroscopic variations and limits the use of visible magmatic components for charactering and interpreting its geological history. This investigation measures the stratigraphic distribution of resistant feldspar phenocrysts (size and volume) and immobile elements (Ti, Zr, V and Y) in Huka Group volcanic strata to enhance its stratigraphic resolution. Phenocrysts measurements identified stratigraphic variations consistent with macroscopic clast grading, useful for identifying the host lithology. Chemostratigraphy successfully used a mix of laboratory and field-portable geochemical methods for gathering comprehensive data tracing stratigraphic variations. Variations in Ti/Zr identified host rock lithofacies, detailed grading textures, graded

depositional units and formational boundaries when primary magmatic variations were present. Regional magmatic comparisons with the Huka Group are made using immobile elements. Outcomes support mainly local magma sources for the Huka Group, except for an early ignimbrite that is consistent with an earlier Whakamaru-type magma. Overall, the use of alteration-resistant phenocrysts and immobile elements with field-based geochemical methods can be highly effective approaches for better understanding hydrothermally altered volcanic sequences at geothermal fields.

INTRODUCTION

Identifying the lithological variation that comprises volcanic sequences is fundamental for developing accurate and detailed stratigraphic models in volcanic settings. These models can find use in volcanic-hosted resource exploration or contribute to reconstructing a region's volcanic history. Lithostratigraphic models require detailed visual assessment and interpretation of lithological and textural variations. However, when volcanic strata occur in hydrothermal settings, moderate to intense hydrothermal alteration can modify their original mineralogy, whole-rock geochemistry and visual appearance, potentially compromising development of lithostratigraphic models. Previous investigations have successfully used stratigraphic variations of stable magmatic phenocrysts (Allen & McPhie, 2003) and immobile elements (e.g., MacLean & Barrett, 1993; Barrett & MacLean, 1994; Gifkins, 2001; Gifkins & Allen, 2001; Large et al., 2001) to enhance insights of hydrothermally altered volcanic strata.

The Huka Group at Wairakei-Tauhara Geothermal Field (Wairakei-Tauhara) in the Taupo Volcanic Zone (TVZ), New Zealand (Fig. 4.1A), hosts a thick sequence of volcanic and sedimentary deposits emplaced over ~300 kyr (Rosenberg et al., 2009a). Recent coring has provided unprecedented insight into the field's stratigraphy (Fig. 4.1B) and lithostratigraphy for investigating its geological evolution (Chapter 2). However, overprinting hydrothermal alteration to the cored samples have variably reduced the deposit's original petrographic and macroscopic variations necessary for more for detailed characterisation. Previous investigations at Wairakei-Tauhara have identified that plagioclase phenocrysts and magmatic high-field strength elements (Ti, Zr, V and Y) can remain stable during low to moderate intensity hydrothermal alteration at the sampled depths (Steiner, 1977; Youngman, 1988). Within Huka Group strata, magmatic

crystals and elements can potentially preserve unique spatial and temporal magmatic variations enhancing stratigraphic models and identifying magmatic relationships.

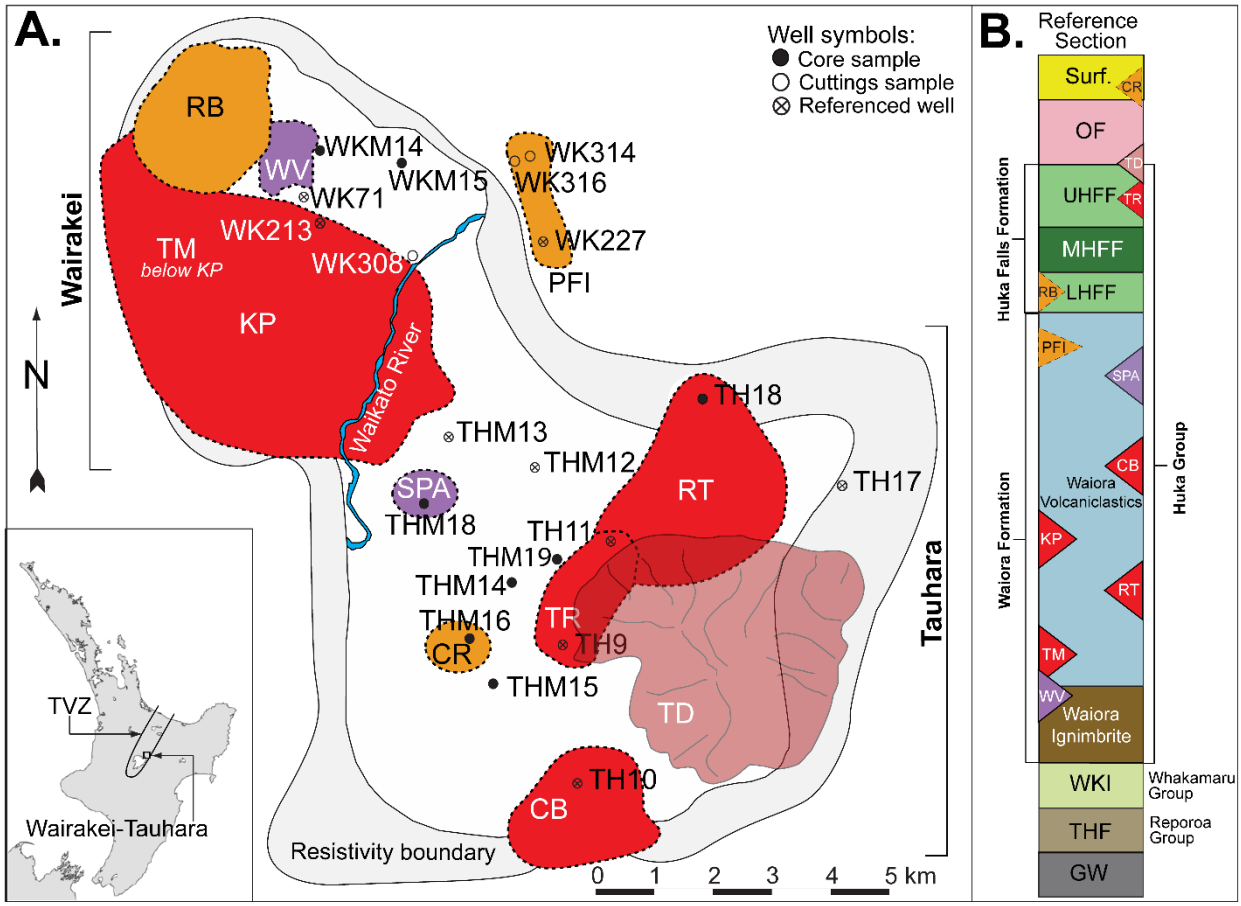

Figure 4.1. A. Wairakei-Tauhara area is defined by a DC electrical resistivity boundary and inferred Huka Group lava, local breccia and ignimbrite locations (coloured; Fig. 4.1B) are from a 3D Geological model by Contact Energy. Labelled dots are drilled wells and sample locations. See Fig. 4.1B caption for abbreviations. *Insert:* location of Wairakei-Tauhara Geothermal Field within the TVZ, New Zealand. **B.** Summarised stratigraphy at Wairakei-Tauhara highlighting the investigated Huka Group. Abbreviations: Surf. – surficial deposits; OF – Oruanui Formation, TD – Tauhara Dacite; TR – Trig Rhyolite; U/M/LHFF – Upper, Middle and Lower Huka Falls Formation; CR – Crown Breccia; RB – Rautehuia Breccia; PFI – Polo Flats Ignimbrite; SPA – Spa Andesite; CB – Crowbar Rhyolite; KP – Karapiti Rhyolite; RT – Racetrack Rhyolite; TM – Te Mihi Rhyolite; WV – Wairoa Valley Andesite; WKI – Wairakei Ignimbrite; THF – Tahorakuri Formation; GW – Greywacke basement. Stratigraphy modified from Bignall et al. (2010a).

Utilising stratigraphic measurements of phenocryst sizes, their volume and immobile element chemostratigraphy, these stable magmatic components are targeted and stratigraphic variations are interpreted for improving lithostratigraphy and depositional understanding of the Huka Group. Crystal volume and phenocrysts size variations are determined using thin section image analysis. Chemostratigraphic variations (Ti and Zr) use a mix comprehensive field-portable X-Ray Fluorescence (pXRF) supplemented with laboratory X-Ray Fluorescence (lab XRF) and Energy-Dispersive X-ray Spectroscopy (EDS). Previous

use of pXRF for scientific investigations has thoroughly established that it is less accurate than lab XRF (e.g., Craig et al., 2007; Goodale et al., 2012; Hall et al., 2014). Its proven high precision (consistency) and rapid analysis of unprepared samples, however, make it a potentially valuable tool for detecting chemostratigraphic immobile element variations in thick volcanic strata (e.g., Piercey & Devine, 2014).

MATERIALS AND METHODS

Samples and phenocryst measurements

Sixty-seven small core samples (<50 g) were collected from wells WKM14 and WKM15 (Fig. 4.1A), both intersecting the Huka Group and Wairakei Ignimbrite (Fig. 4.1B) between 100 – 620 m depth (Appendix A2.2). Several additional Huka Group core samples were available for the investigation from TH18 (554 – 641 m) and THM18 (493 and 588 m; Fig. 4.1A). Raw Huka Group cuttings samples from wells WK314 and WK316 (Fig. 4.1A) with no previous drying or crushing preparation were geochemically analysed for whole-rock compositions by a portable X-Ray Fluorescence Spectrometry. No samples were collected for further laboratory analysis. Detailed lithostratigraphy of the cored wells is described in Chapter 2 (Fig. 4.1B). Well stratigraphy and hydrothermal alteration is originally documented in geological reports by Rosenberg et al. (2009b), Ramirez et al. (2009) and Milicich et al. (2008b; 2009). Alteration intensity is defined as ‘weak’ (primary textures and >75% primary minerals preserved), ‘intermediate’ (most primary textures and 50% primary minerals preserved), or ‘strong’ (all primary textures and minerals overprinted). Alteration in the Huka Falls Formation samples are consistent with weak to intermediate ‘argillic’ assemblages (illite, illite-smectite, pyrite, Fe-oxides, chlorite, calcite, quartz veins). With depth, alteration rank and intensity increase to intermediate ‘propylitic’ in the Waiora Formation (illite-smectite, chlorite, calcite, adularia).

Using methods from Allen and McPhie (2003), thin sections were made of each of the core samples from WKM14 and WKM15 and at least 4 photomicrographs were taken of each under 1.5× magnification. Photomicrograph images were used to measure the size (perimeter) and maximum length of the 10 largest phenocrysts and estimate the total crystal volume in 2-dimensions (Appendix A2.5). Crystal size and volume estimates were then averaged for each sample. The sample standard deviation (SD) is estimated by volume estimate variations between multiple photographs of the same sample. The SD is taken as a measure of

sample crystal size sorting (higher SD = poor sorting) and crystal distribution uniformity within each sample (low SD = uniformly dispersed crystals between sample photographs).

Immobile element measurements

Laboratory X-Ray Fluorescence (lab XRF)

Samples were analysed by whole-rock laboratory X-Ray Fluorescence (lab XRF) for chemostratigraphic and bivariate magmatic analysis of immobile elements. Sample preparation involved drying, crushing and hand picking of foreign lithics leaving only the finest grained material (≤2 mm) for milling. Material was milled for 4 minutes in a tungsten carbide swing mill (samples >2.5 g/cm^3) or an agate ball mill (samples <2.5 g/cm^3). The latter was preferentially used to restrict sample preparation contamination (Potts, 1987; Gifkins et al., 2005b). Analyses were undertaken at the University of Canterbury using a Phillips PW2400 Sequential Wavelength Dispersive XRF using analytical methods outlined by Norrish and Chappell (1967) as well as by Norrish and Hutton (1969). Loss on ignition (LOI) result totals were not recalculated to 100 weight percent (wt.%) because they are considered impractical for hydrothermally altered rocks, particularly when dealing with elemental ratios, and may introduce further error (Gifkins et al., 2005b). Most analyses were near 100 wt.%. Immobile elements TiO_2 and Zr were used for chemostratigraphic analysis and Zr, V and Y for comparing the compositions of regional magmas. Major element results in wt.% (Appendix A2.4) were converted to oxide-free states in parts per million (ppm) for comparison with portable X-Ray Fluorescence results (in ppm).

Portable X-Ray Fluorescence (pXRF)

Portable X-Ray Fluorescence Spectrometry (pXRF) is commonly applied to mineral exploration (e.g., Gazley et al., 2011), archaeology (e.g., Sheppard et al., 2011) and environmental analyses (e.g., Peinado et al., 2010), and has only recently been trialled in geothermal stratigraphy (Mauriohooho et al., 2014a; 2014b; this study). The merits and limitations of using pXRF for scientific investigations has been comprehensively covered in previous studies and is beyond the scope of the present investigation (see papers in: *Geochemistry: Exploration, Environment, Analysis* 2014, special volume, 14, no. 2-3).

In this study, an Innov-X Alpha Series pXRF with a 10 – 40 kV X-ray tube (10 – 50 µA current) was used with a customisable detection time between 0 – 120 seconds (s). Analyses were set at 60 s for lab

tests (dry samples) and 90 s for *in situ* field tests (moist samples) using recommendations by Hall et al. (2014; Appendix A1.2 & A2.1). The pXRF uesd was capable of analysing up to 20 elements (atomic number, Z, <22) using the factory-set Soil Mode, although only Ti and Zr were to be used for chemostratigraphy measurements. Higher power pXRFs with 50 kV X-ray tubes are capable of analysing >40 elements (Z >12; i.e., they can detect multiple immobile elements), but were not available for this investigation. Approximately 350 core, cuttings and prepared powder samples were analysed 3 – 4 times (total 1250 analyses; Appendix A2.4). Results from repeat tests were averaged to identify variations and reduce the effect of (unprepared) sample inhomogeneity due to the pXRF's small analysis area (~0.7 mm diameter; Potts et al., 1997). The finest grained matrix of *in situ* core samples most representative of the stratigraphic unit (at 10 – 20 m interval) and largest representative cuttings (at 10 – 15 m interval) were preferentially analysed to reduce the pXRF targeting large clasts.

Energy-dispersive X-ray spectroscopy (EDS)

Energy-Dispersive X-ray Spectroscopy (EDS) assessed the microscopic distribution and host mineral phases of Ti and Zr in selected thin sectioned samples. These host phases are directly targeted by the pXRF, therefore, an awareness of their distribution is necessary to validate the pXRF method. Two representative thin sections were examined by EDS including shallow MHFF (sample WKM15_23) and deep Waiora Ignimbrite samples (sample WKM15_60). These samples were selected to represent the range of hydrothermal rank and various alteration styles and intensity (argillic to intermediate propylitic; Rosenberg et al., 2009b) that may promote mobility of Ti and Zr in the Huka Group core samples. Mineral analysis used an Oxford Instruments X-Max^N EDS coupled with a JEOL 6400 Scanning Electron Microscope (SEM test conditions: 37× magnification, 20 nA beam current at 15 kV accelerating voltage).

RESULTS

Phenocryst measurements

Assessments of 67 thin sections from wells WKM14 and WKM15 identified magmatic andesine feldspar by its twinning, zoning and a tabular crystal habit or as fragmented forms (Appendix A2.7-2.8). Subordinate magmatic quartz phenocrysts were recognised by common embayed and curved morphologies and undulose textures. Highest quartz content in Huka Group occurs in the Waiora Ignimbrite (5 %).

Overall, phenocrysts size in Huka Group volcaniclastic deposits is 2.7 times their average length. This is less than the 3.0 times measured by Allen and McPhie (2003) in lavas and may reflect the increased exposure and mechanical breakage of crystals in turbulent volcaniclastic density currents prior to deposition. Largest measured phenocrysts, and their highest volumes, occur concentrated at the base of lithic and pumice lapilli-tuff beds (clast-rich) where they are typically poorly sorted (high size SD) and non-uniformly distributed (high volume SD; Fig. 4.2A, unit 1 base). Smaller, broken crystals are common in fine and medium tuff suspension facies where they are typically well sorted (low size SD) and more uniformly distributed (low volume SD; Fig. 4.2B, unit 1 top). Phenocryst volumes are measured between <1 – 29 total volume % (vol.%), with a mean value in Huka Group of 5 vol.%. Crystal length and size measurements show similar vertical trends, while volume measurements are more independent (Fig. 4.2A-B). Volume trends tend to reflect the host rock lithology (Fig. 4.2A-B). For example, they are low in primary volcaniclastic deposits and high when concentrated in re-deposited volcanogenic sandstones.

Mean crystal volumes are 4.9 vol.% in the Waiora Ignimbrite (number of samples, n = 24) and 7.5 vol.% in the MHFF (n = 5). The Waiora Volcaniclastics (n = 20) have lower crystal volumes averaging 3.2 vol.%. Phenocrysts in samples from WKM14 are larger and more variable than in WKM15 (Fig. 4.2A); however, given that more samples were available for WKM15, its crystal measurement trend is more detailed (Fig. 4.2B).

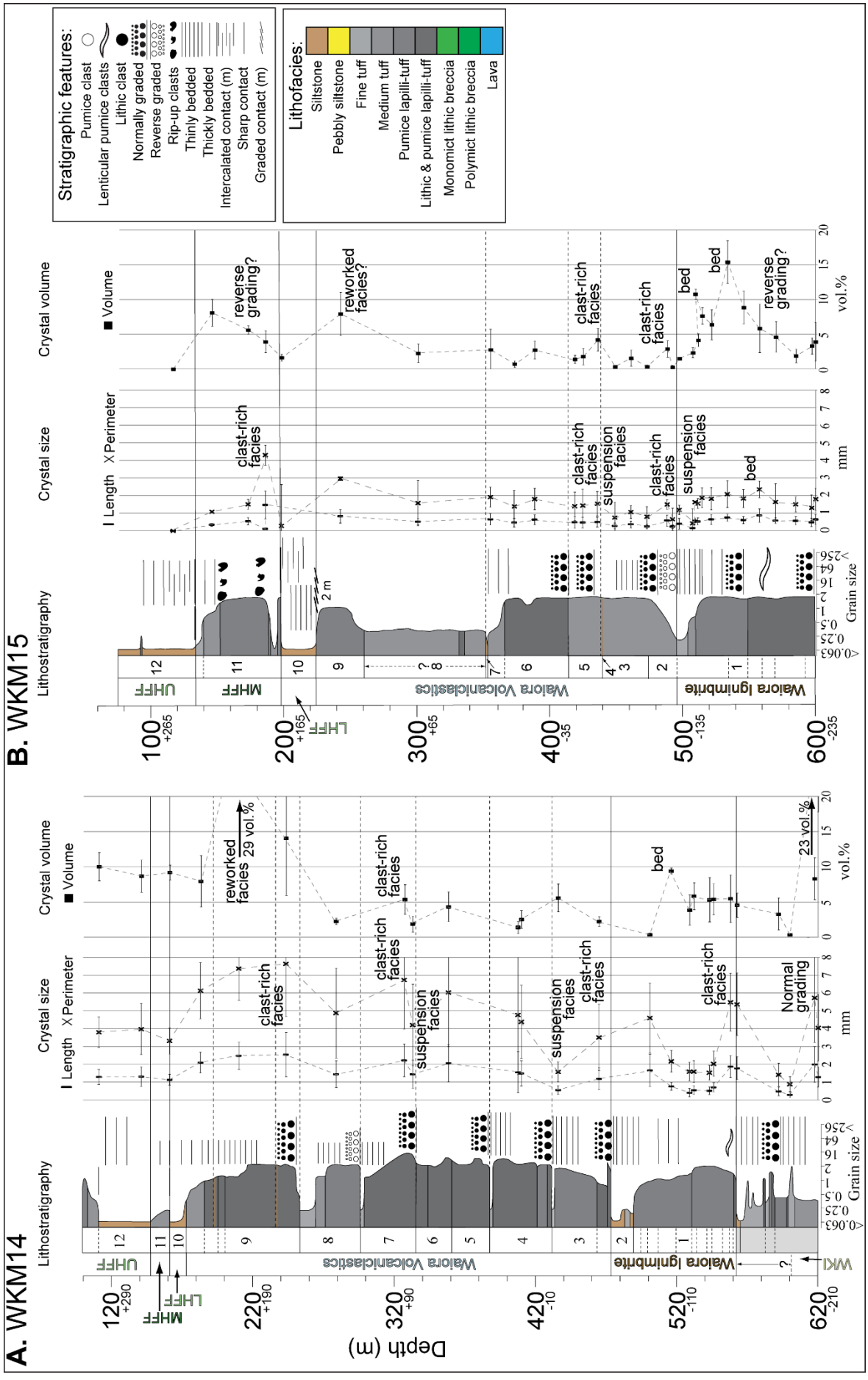

Figure 4.2. Physical phenocrysts size variations compared with Huka Group lithostratigraphic logs in wells **A.** WKM14 (n = 26) and **B.** WKM15 (n = 31). Phenocryst size (length and perimeter) and volume measurements are averaged from image analysis measurements. Error bars are the standard deviation (SD) between thin section measurements. Logs are in metres depth (m) and elevation in metres below mean sea level (subscript, mRL). Numbered units are visually identified depositional units. Formation name abbreviations are explained in Fig. 4.1B caption.

Immobile element chemostratigraphy

Identifying Ti and Zr host crystals and immobility

Results from EDS analyses identify crystal hosts and the distribution of elements Ti and Zr within selected MHFF (WKM15_23) and Waiora Ignimbrite samples (WKM15_60; Appendix A2.6). In the MHFF, Ti is concentrated in magmatic ilmenite ($FeTiO_3$) and Zr in zircon crystals ($ZrSiO_4$; Fig. 4.3A), both are magmatic in origin. The Waiora Ignimbrite sample contains larger grains of magmatic titanite ($CaTiSiO_5$) and small, matrix-disseminated leucoxene (TiO_2) that contain most of the sample Ti content. Similarly, Zr was concentrated in small zircon crystals (Fig. 4.3B). Titanium-bearing oxide and silicate magmatic phases (e.g., biotite, augite, hornblende, ilmenite, titanite, magnetite, titanomagnetite and volcanic glass) commonly alter to hydrothermal products in geothermal settings (e.g., leucoxene species, rutile, titanite/sphene; Thompson & Thompson 1996). Leucoxene can occur as an accessory mineral in both magmatic and hydrothermal environments (Cuney & Friedrich, 1987). The disseminated distribution of leucoxene identified in Waiora Ignimbrite, together with its poorly crystalline structure and small size, makes it most consistent with crystallisation from a hydrothermal fluid. However, since negligible Ti mass change has been previously demonstrated in moderately intense hydrothermal alteration settings (propylitic zone; Steiner, 1977; Youngman, 1988), Ti must be conserved within the host rock during hydrothermal phase changes, such as the isochemical reaction between hydrated volcanic glass and hydrothermal leucoxene (e.g., Bignall et al., 1996).

Youngman (1988) made a rigorous attempt to practically demonstrate whole-rock elements displaying mass transfer in the Wairakei-Tauhara reservoir, and those that do not. Chemical and XRF methods were used for estimating mass transfer by comparing unaltered (out-field well WK227) and altered samples (in-field wells WK71, 216; TH1, 2 and 4). Difficulties encountered in practically determining mass transfer include, sampling from the same lateral (and compositional) unit, and accounting for primary compositional variations between laterally ‘equivalent’ samples (i.e., variation not due to mass transfer). The method required samples to be recalculated to a constant volume, accounting for bulk density variations. Unfortunately, only a small Huka Group sample suite was available, restricted by difficult sample access (drilled) and few identifiable lateral correlatives. The small suite resulted in overly broad stratigraphic

compositional variations where whole-rock compositions had to be averaged for the Huka Falls and Waiora Formations, rather than for more detailed internal units. Altered samples exceeding one SD from the average unaltered composition are statistically considered to have undergone some 'significant' mass transfer. The difference were calculated for elements exceeding the average unaltered value by more than one SD. Elemental variations within one SD were assigned a zero value (see Youngman, 1988; Appendix 4, Table 4)

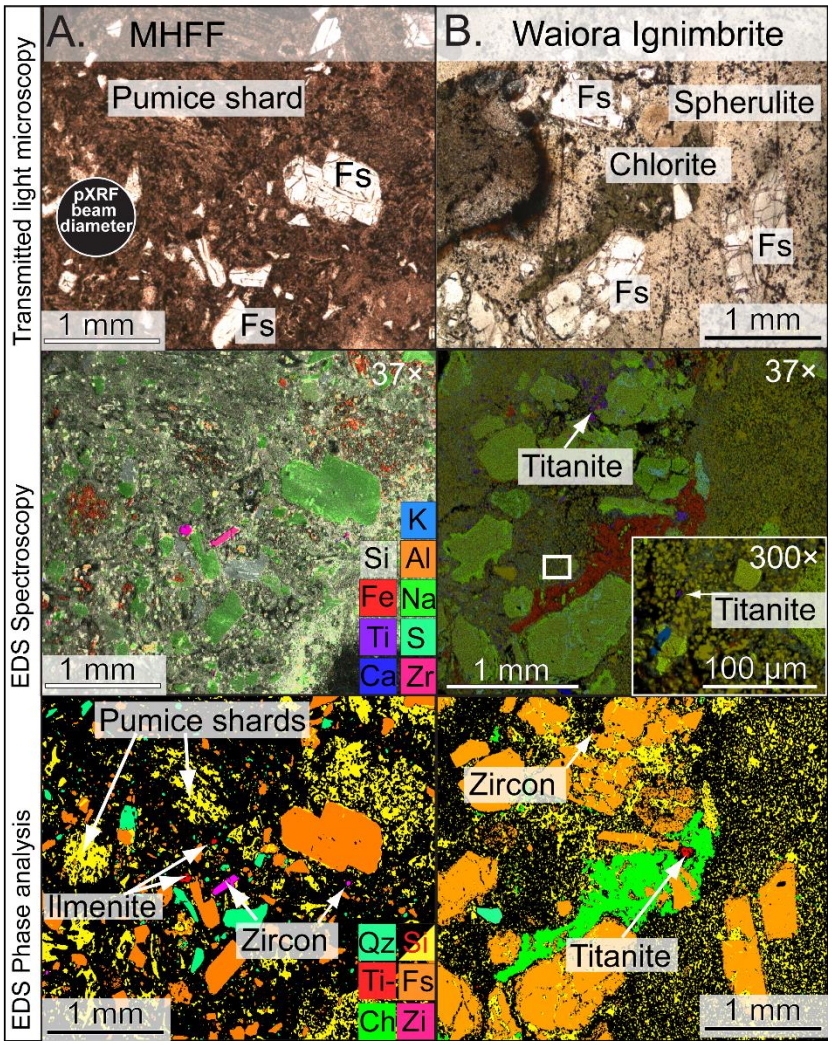

Figure 4.3. Comparison of thin section methods imaging on the two selected samples **A.** MHFF (WKM15_23; 189 m) and **B.** Waiora Ignimbrite (WKM15_60; 522 m). Plain polarised transmitted light microscopy investigates mineralogy, EDS spectroscopy shows the spatial distribution of elements, and EDS phase analysis infers the composition of crystal phases analysed by pXRF (portable X-ray fluorescence). K – Zr are respective atomic elements in Fig. 4.3A-B. Mineral abbreviations: Qz = quartz, Fs – plagioclase feldspars; Si = silica-rich glass, pumice or silicification; Ti- = Ti-bearing oxide or silicate; Ch = chlorite; Zi = zircon.

Youngman (1988) measured elemental variations between unaltered and altered samples into one of three groups: little or no significant mass transfer detected (immobile); some mass transfer detected, but attributed to primary variation (primary variation); and significant mass transfer detected (mobile components). Elements Y and V were assigned to 'no significant mass transfer', while variations detected in TiO_2 and Zr are attributed to 'primary compositional variations'. These site-specific results are consistent with the expected element mobility for the shallow Wairakei-Tauhara system, and are considered appropriate for identifying suitable chemostratigraphic immobile elements.

Barrett and MacLean (1994) propose that a highly correlated bivariate linear trend (regression coefficient, $r \geq 0.85$) can identify the chemical immobility of trace elements. The method is most effective in rocks with compositional homogeneities, such as lavas and primary pumice lapilli-tuffs (Gifkins et al., 2005b); however, few accurate lab XRF analyses are available for Huka Group lavas and volcaniclastics. Chemical imobility in the inhomogeneous volcaniclastic MHFF and Waiora Ignimbrite is examined using lab XRF, supplemented with less accurate pXRF data (Fig. 4.4A-B). Results indicate that Ti concentrations are typically ten times the concentration of Zr in MHFF (n = 12).

A strong correlation detected between Ti and Zr (r = 0.92; Fig. 4.4A) support immobility in the intermediate argillic alteration zone. Collectively, correlation of results from Waiora Ignimbrite samples (n = 35) in the weak-intermediate propylitic alteration zone appears low (r = 0.47; Fig. 4.4B). However, due to the nature of the sample used, some sample interpretation can justify the correlation. Three distinct Waiora Ignimbrite sample data sets are identified corresponding with density graded (macroscopically visible) lithologies each containing variable Ti- and Zr-bearing minerals (Fig. 4.4B). The main trend (r = 0.96, n = 16) corresponds with a 'least contaminated' dominant central pumice lapilli-tuff lithology. Sample WKM15_60 analysed by EDS with matrix-disseminated titanite and leucoxene grains (containing magmatic Ti) occurs in the central lithology (Fig. 4.3B). The correlation for the central lithology is strong, supporting Ti and Zr immobility at depth (≤600 m) in the weakly propylitic alteration zone. Above the main trend, Ti is enriched (n = 9) and corresponds with a physically stratified lithic-rich basal lapilli-tuff containing Ti-rich lithic clasts. Below the main trend, samples comprising rhyolite shard-rich tuff are depleted in Ti (n = 20) relative to Zr (Fig. 4.4A-B). Despite variable hydrothermal alteration intensities, compositions of Ti and Zr

in the altered samples are interpreted to preserve the host unit's magmatic genesis and are, therefore, suitable chemostratigraphic tracers in the Huka Group, at least to the depth of the cored samples.

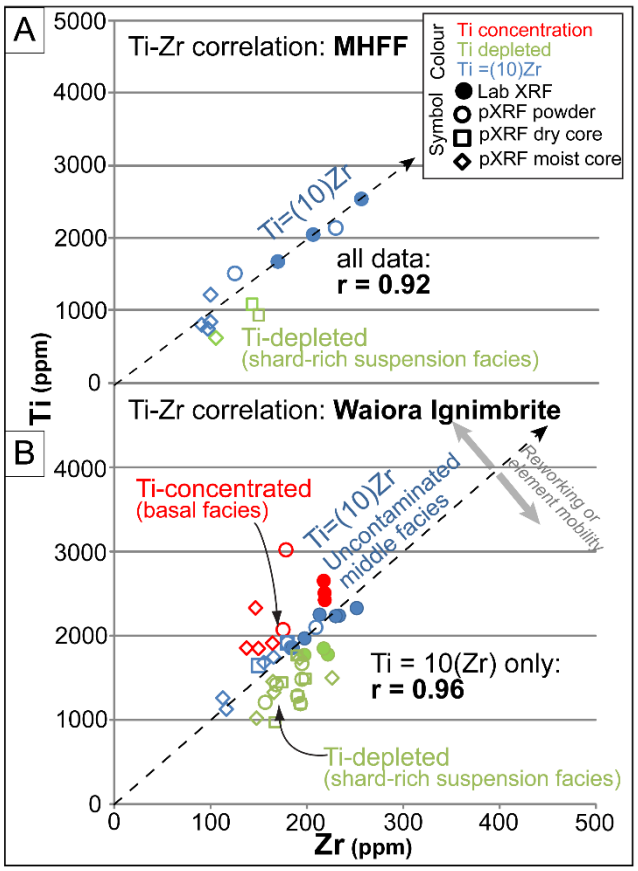

Figure 4.4. Element correlation coefficients of well WKM14 and WKM15 samples from the **A.** Middle Huka Falls formation (MHFF) between 140 – 160 m depth and **B.** Waiora Ignimbrite (WKM15) between 500 – 600 m depth. Data shows the relative concentrations (mobility) between elements Ti and Zr in the selected formations. An r value ≥0.85 is recommended by Barrett and MacLean (1994), for homogeneous and variably altered volcanics. The volcaniclastic MHFF achieves this value whereas the Waiora Ignimbrite falls short, most likely due to interpreted stratification grading and contamination. Data point colours identify relative Ti concentrations and symbol shape are the analysis types (closed = lab XRF; open = pXRF) – see accompanying key.

Chemostratigraphy of altered volcanic stratigraphy using lab XRF and pXRF

Numerous studies have confirmed pXRF to be capable of providing precise compositional data (e.g., Craig et al., 2007; Goodale et al., 2012; Hall et al., 2014; Piercey & Devine, 2014) usually of lower accuracy than lab XRF, as suggested in Fig. 4.5 (Appendix A2.1). The precision of pXRF, largely irrespective of detection time, makes it a useful tool in chemostratigraphy because it is able to rapidly and consistently identify relative variations between (magmatically-dissimilar) stratigraphic units. By increasing the detection time of the pXRF, the analysed sample concentration and limiting effects of sample moisture on pXRF detection are reduced (Appendix A1.2; Ge et al., 2005). The overall limiting factor on pXRF accuracy and precision

remains the properties of *in situ* samples (grain size and moisture). Errors in the pXRF data are primarily due to unfavourable sample types. Sample type errors can be reduced by averaging multiple analyses per sample (Potts et al., 1997; Forster et al., 2011).

Chemostratigraphic logs of the Huka Group (core and cuttings samples) identify that both pXRF and lab XRF successfully identified stratigraphic variations in Ti/Zr and Zr (Figs. 4.6-4.8). Variations identify the stratigraphic distribution of Ti- (ilmenite, titanite and leucoxene) and Zr-concentrated (zircon) crystals within single and between successive depositional units. Depositional controls influencing the distribution of Ti and Zr and their stratigraphic variations shown in Figs. 4.6-4.8 are described in the discussion.

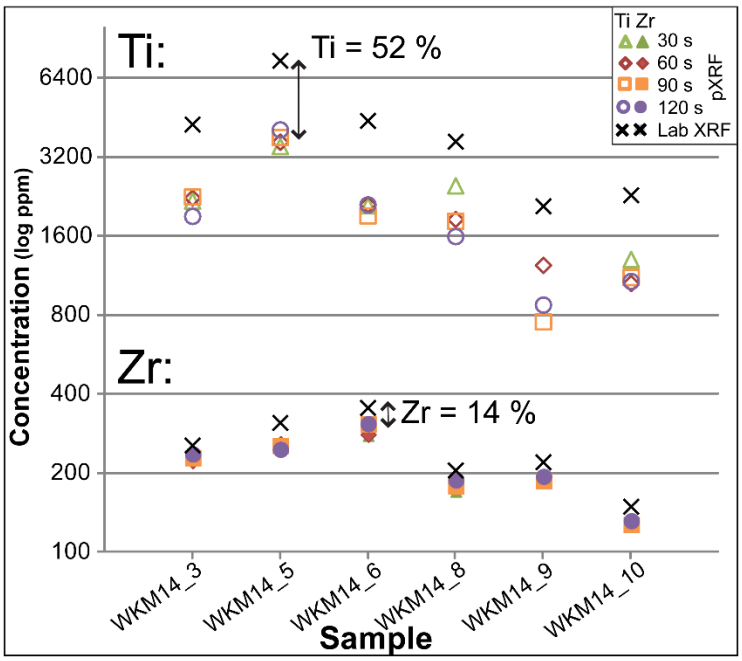

Figure 4.5. Variations between pXRF count times and lab XRF values in Ti and Zr concentrations (ppm) from six selected Huka Group powder samples. Percentage is the mean accuracy of the pXRF concentration compared to the lab XRF value (i.e., pXRF mean Ti detection is 48 % of the lab XRF value). The similar consistent trends reflects the high precision of pXRF. See key for data point symbol and colour types.

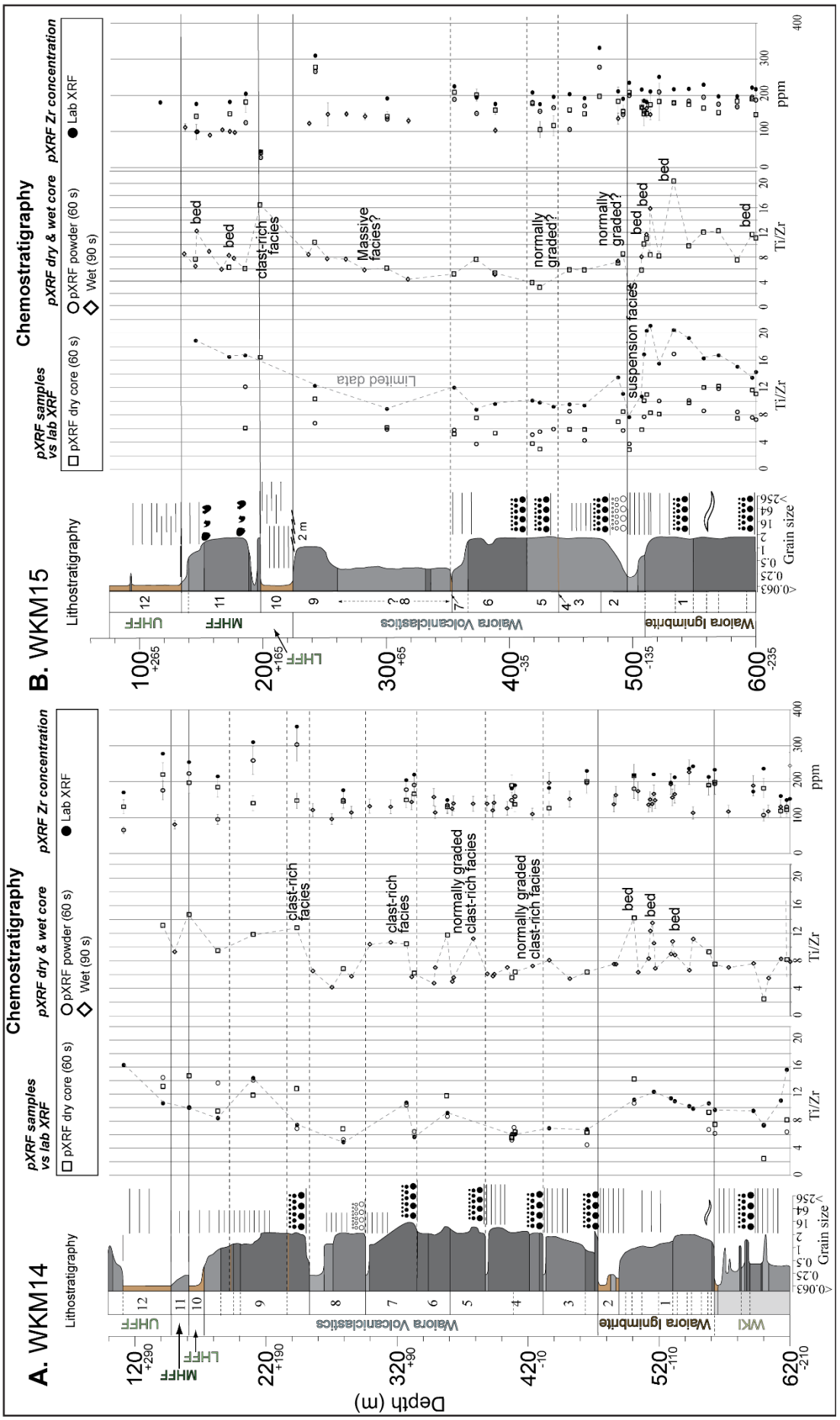

Figure 4.6. Chemostratigraphic immobile element logs of Wairakei wells: **A.** WKM14 and **B.** WKM15 enhancing stratigraphic details. See Fig. 4.1B for stratigraphy abbreviations and Fig. 4.2 for the lithofacies colour key. Data point key shows the analysis and sample types of each data point. Logs are 1) Ti/Zr (lab XRF and dry pXRF), 2) Ti/Zr (dry and moist pXRF) and 3) Zr (lab and pXRF). Annotations are possible interpretations of the data trends. Inferred dashed trends are not equivalent as different samples and sample numbers were often analysed between each method. Error bars are the SD variation between repeat pXRF Zr analyses.

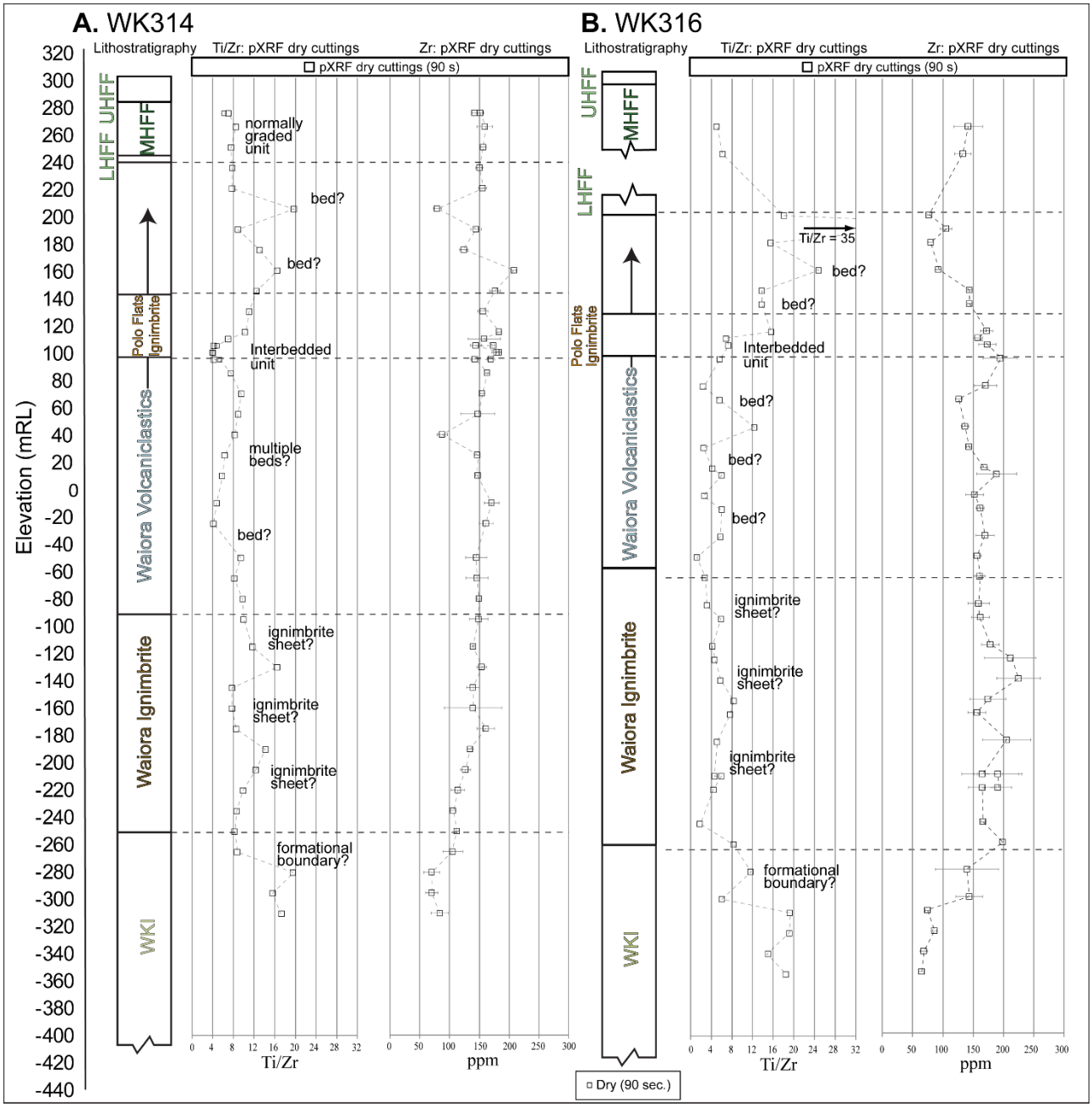

Figure 4.7. Adjacent out-field cuttings wells: **A.** WKM314 and **B.** WK316 in mRL elevation. Annotations are possible data trend interpretations. See Fig. 4.1B for stratigraphy abbreviations.

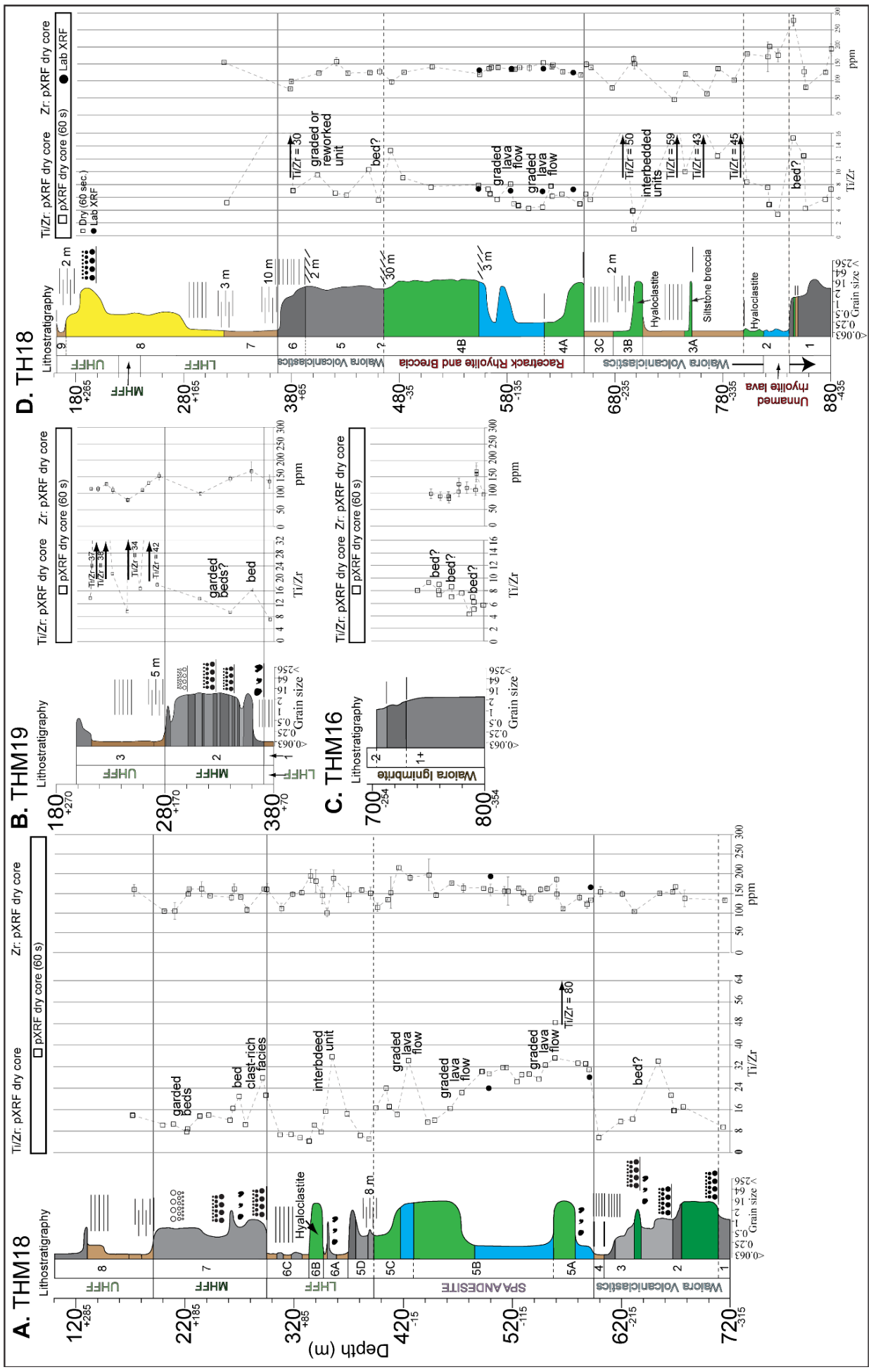

Figure 4.8. Chemostratigraphic immobile element logs of Tauhara wells **A.** THM18, **B.** THM19 and **C.** lowermost THM16, **D.** TH18. Annotations are possible data trend interpretations. See Fig. 4.1B for stratigraphy abbreviations and Fig. 4.2 for the lithofacies colour key.

Regional magmatic comparison using immobile elements

Immobile element geochemistry of altered Huka Group samples from Wairakei-Tauhara are compared with regional whole-rock magma compositions to identify possible magmatic source origins (e.g., Brown et al., 1998a). Whole-rock immobile elements Zr, V and Y (Youngman, 1988) are examined in ignimbrite samples from Waiora Ignimbrite, Waiora Volcaniclastics (WKM14, WKM15 and THM16) and Polo Flats Ignimbrite (informal new name, WK314; Fig. 4.1A). The latter was previously implied to be a Kaingaroa Ignimbrite correlative at Wairakei-Tauhara (Nairn et al., 1994; Wood, 1994a). Regional magmas, represented as juvenile pumices, which are temporally or geographically relevant to the Huka Group include these nearby: Reporoa (Kaingaroa Ignimbrite), Ohakuri (Ohakuri Formation), Taupo (Oruanui Formation) and Whakamaru calderas (including Whakamaru, Rangitaiki and Paeroa units). Because of the poor preservation, availability and correlation of Huka Group pumice samples at Wairakei-Tauhara Geothermal Field, prepared volcaniclastic lithologies are used. Due to physical sorting, winnowing and entrainment contamination by lithic clasts during ignimbrite transport, compositional trends are expected to be slightly dissimilar (e.g., enriched in Zr, V and Y), but somewhat reflective of a juvenile correlative. Such enrichment is shown between Rangitaiki pumice and ignimbrite sample types in Fig. 4.9A-B.

Of the Huka Group samples, Polo Flats Ignimbrite (Fig. 4.1A) has higher Y and Zr/V, which distinguish it from the previously inferred Kaingaroa pumice correlative (Fig. 4.9A-B). Waiora Volcaniclastics (WKM14, WKM15) span Y 20 – 40 and Zr 150 – 240. These are slightly more enriched than Waiora Ignimbrite, but are overall depleted relative to Ohakuri pumice (Fig. 4.9A). Waiora Volcaniclastics Zr/V values are widely dispersed (Fig. 4.9B). The late Waiora Ignimbrite sheet (WKM14, WKM15) has values clustered between Y 20 – 32 and Zr 175 – 250 (Fig. 4.9A). The earlier sheet is less enriched and has lower values. Waiora Ignimbrite Zr/V values mainly overlap fields of the Whakamaru Group (Fig. 4.9B). Both pumice and ignimbrite fields are provided for the Rangitaiki member (Fig. 4.9A-B; Brown, 1994), the latter being enriched in both Y and Zr, possibly through lithic clast contamination. Three Wairakei Ignimbrite samples from directly beneath the Huka Group (WKM14) consistently overlap the Whakamaru Group Rangitaiki Member (pumice sample).

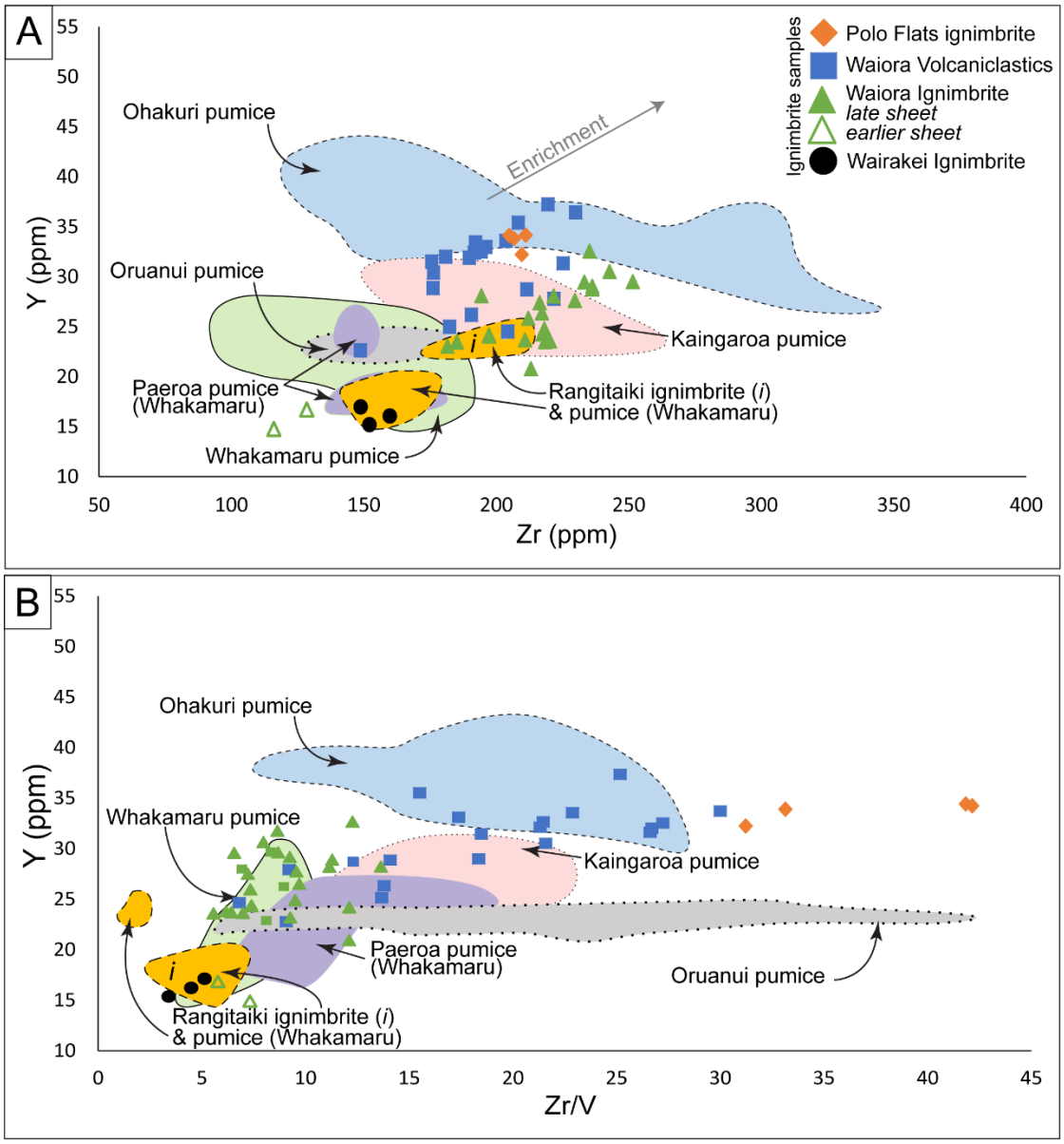

Figure 4.9. Whole-rock immobile trace element bivariate plots **A.** Y vs. Zr and **B.** Y vs. Zr/V of Huka Group and other ignimbrite samples from Wairakei-Tauhara compared with juvenile pumice fields of the Ohakuri Formation (n = 102; Gravley, 2004), Kaingaroa Ignimbrite (n = 77; Beresford, 1997), Oruanui Formation (n = 135; Wilson et al., 2006), Whakamaru Group (n = 53), Rangitaiki Ignimbrite (pumice (n = 17) and ignimbrite (n = 3); Brown, 1994) and Paeroa Ignimbrite (n = 24; Downs et al., 2014a; 2014b).

DISCUSSION

Evaluation of phenocryst measurements for enhancing stratigraphy

In moderate to intensely altered strata where lithological identification may be restricted by the effects of alteration (e.g., replacement and cementation), detailed phenocryst measurements can be used to identify the host lithology (Allen & McPhie, 2003). Stratigraphic variations in crystal size and length measurements are an indication of crystal physical preservation following eruption, transport and diagenesis (Fisher & Schmincke, 1984; Cas & Wright, 1987; Best & Christiansen, 1997). Large euhedral crystals are preserved when they are hosted within clasts protecting them from (size-reducing) breakage. In volcaniclastic deposits comprising Waiora Ignimbrite, largest crystal measurements coincide with clast-rich units, such as basal lithic breccias or capping pumice rafts (Chapter 2). Smaller and more uniform crystal sizes occur in the main overlying volcaniclastic unit where free crystal forms are exposed to mechanical breakage.

Crystal volume variations are consistent with lithostratigraphic density grading (clast size variations in Chapter 2). Similar to large crystal size trends, peaks in crystal volume coincide with lithologies concentrated in dense lithic clast and crystal material. Volume trends are more reliable indicators of stratigraphic grading because sorting and grading processes act consistently on the particle size and density properties of both clasts and crystals (i.e., unlike crystal size variations variably influenced by host clast properties). In the upper Waiora Formation, crystal volumes are enriched in reworked volcanogenic sandstones. These deposits are concentrated in dense crystals by winnowing of vitric or vitroclastic fines.

Overall, phenocryst measurements record details of the host lithotype and stratigraphic grading trends. Identification of these properties may make the technique useful when macroscopic textures are obscured restricting visual assessment, such as by hydrothermal alteration (Allen & McPhie, 2003). However, comprehensive sampling, presence of non-altered preserved phenocrysts, time-consuming thin section preparation and detailed image analysis are required to accurately capture stratigraphic variations. Its use is better suited to thin volcanic successions (i.e., 10s of metres) where the necessary resolution is more easily achieved. In thick volcanic successions, rapid data collection methods such as pXRF chemostratigraphy are more appropriate.

Immobile element analysis in the Huka Group

Use of pXRF for chemostratigraphy

Chemostratigraphy requires a large data set to detect and identify detailed stratigraphic variations. This investigation has highlighted the value of using pXRF for gathering large consistent data sets given its field portability, short analysis time and need for limited (to no) sample preparation. The non-invasive method is also efficient and inexpensive compared to lab XRF. Highlighting the rapid use of pXRF, over 200 analyses of drill core and cuttings samples at 90 s detection times were able to be gathered over an 8 hour period during this investigation. However, the lack of preparation required the 'most unit representative' lithologies to be targeted by the pXRF (e.g., sample matrix) and repeat analyses made to identify the influence of sample inhomogeneity (Potts et al., 1997). Chemostratigraphic analytical intervals should be selected to reflect the variety of macroscopic details such as bedding. For example, five meter thick bedding in the Waiora Ignimbrite required ~4 pXRF targets per bed to detect its variation. Higher specification pXRF models (45 – 50 kV) equipped with sensitive detectors or a gas purge are able to detect a range of elements ($Z>12$) beyond the detection limit of the pXRF used here. These sensitive devices are preferable for chemostratigraphic and other magma evolution and alteration studies where light and high-field strength elements are of interest.

Huka Group chemostratigraphy findings

Chemostratigraphic analysis of the Huka Group has identified trends between depositional units that, together with EDS and discernible stratigraphic variations (Chapter 2), can enhance existing stratigraphic resolution. Chemical trends are intended for comparison within and between local depositional units within a well (i.e., short data trends), rather than for identifying whole well chemostratigraphic trends. Variations in Ti and Zr concentrations within Huka Group strata are subtle, attesting only slight compositional variations between the rhyolite volcaniclastic deposits. The geochemical similarity permits interwell correlations in the Huka Group, except over short distances. Similar Ti/Zr trends can, however, be recognised between adjacent wells (<1 km apart) even when several samples from slightly different stratigraphic positions are analysed (e.g., between WKM14 and WKM15, WK314 and WK316).

When chemostratigraphic resolution is high relative to the overall deposit thickness, separate depositional units or internal facies variations can be recognised. These are identified as distinct variations

in Ti/Zr stratigraphic signatures (e.g., gradual or sharp) and approximate the distribution of dense titanite/ilmenite/leucoxene and zircon crystals. In volcaniclastic deposits, distinct distributions of these dense phases within single depositional units reflect the physical properties and processes within the transporting current. Depositional characteristics recognised from the deposit may include the currents' degree of coherency, the development of density stratification, winnowing of fines content and addition of accidental clasts modifying the original magmatic composition (Gifkins et al., 2005b). Chemostratigraphy can also identify individual beds when they are underlain with concentrated, normally graded titanite/ilmenite and zircon crystals (basal facies) and support their emplacement by density stratified mass flows (e.g., Large et al., 2001). This can be observed in Waiora Ignimbrite (Fig. 4.6A-B) and proximal facies of the MHFF (Fig. 4.8A). In these units, sharp Ti/Zr variations are detected and consistent with multiple normally graded beds deposited by recurring density stratified currents.

Wide Ti/Zr variations in the Waiora Formation may identify thick composite ignimbrite sheets. Chemical variations coinciding with established stratigraphic formational boundaries could be used to identify separate eruptives. Mauriohooho et al. (2014a) found immobile element Y (Youngman, 1988) could be used to discriminate between Waiora Ignimbrite and Volcaniclastics Members in Tauhara. Variations of Zr in cuttings wells WK314 and WK316 (Fig. 4.7A-B) appear to distinguish Wairakei Ignimbrite (low Zr) from Waiora Ignimbrite (higher Zr). Within these wells, high analytical resolution using Ti/Zr successfully detected the base of the interbedded Polo Flats Ignimbrite (Fig. 4.7A-B). Slightly higher total Zr detected in the late Waiora Ignimbrite sheet (Fig. 4.6A-B; WKM14, WKM15, 150 – 200 ppm) compared with earlier sheets drilled (~100 ppm; Figs. 4.7A-B & 8C) suggest it may be a more evolved eruptive.

Deposits with apparent gradual linear Ti/Zr signatures can reflect overall normal (negative Ti/Zr slope) or reverse grading (positive slope). Static Ti/Zr trends (i.e., units with homogeneous distributions of the dense crystals) support emplacement by a non-stratified depositional process or possible reworking of these units evenly dispersing the dense crystals. Both of these apparent trends are detected in beds comprising Waiora Volcaniclastics (Fig. 4.6A-B). Lateral MHFF facies variations are recorded by chemostratigraphy between the bedded proximal facies (sharp Ti/Zr variations; Fig. 4.8A-B) and its massive distal facies (near static Ti/Zr; Fig. 4.7A-B).

Lavas in the Huka Group have more gradual chemostratigraphic variations than inhomogeneous volcaniclastic strata. Massive Spa Andesite lava facies (Fig. 4.8A) have consistent (near static) Ti/Zr values whereas the intervening breccia carapace facies is more irregular. The 8 composite lava flows and dividing autobreccia increase in Zr with reducing elevation (125 – 200 ppm) and decrease in Ti (~5000 – 3000 ppm), perhaps reflecting withdrawal from a compositionally zoned magma. In contrast, the massive lava and carapace breccia facies comprising Racetrack Rhyolite (Fig. 4.8D) has a near static Ti/Zr signature further supporting (from Chapter 2) emplacement by a single, non-stratified (intrusion) event.

Regional magmatic comparison overview

Comparable whole-rock trace element compositions between the Huka Group ignimbrites from Wairakei-Tauhara and regionally-sourced juvenile pumice have identified possible magmatic correlations in TVZ. Dissimilar immobile element chemistry between Polo Flats Ignimbrite and ~281 ka Kaingaroa Ignimbrites (Fig. 4.9A-B; Downs et al., 2014a) suggest the two are chemically distinct units. This outcome is consistent with their dissimilar mineral chemistry previously identified by Beresford (1997). No clear magmatic correlative(s) are yet identified for the beds comprising Waiora Volcaniclastics. Waiora Volcaniclastics samples appear overall compositionally related, supporting the interpretation of local magmatic and eruptive sources comprising the member. Geochemical similarities between Polo Flats Ignimbrite and Waiora Volcaniclastics suggest the former may be from a local magmatic source (Fig. 4.9A-B). Its shallow interbedded locality within Waiora Volcaniclastics (Fig. 4.7A-B) suggests it is younger than the previously inferred Kaingaroa Ignimbrite correlative.

Trace element compositions of Waiora Ignimbrite samples clustering near the Whakamaru ignimbrite field (Fig. 4.9A-B) may support a common magmatic source. A Whakamaru source vent for Waiora Ignimbrite is also supported by stratigraphic (temporal) and petrographic relationships with other Whakamaru Group members (Martin, 1961; Grindley, 1965; 1982; Wilson et al., 1986; Wood, 1994a). The three Wairakei Ignimbrite samples from beneath the Huka Group are geochemically consistent with the Whakamaru Group Rangitaiki Member pumice (Fig. 4.9A-B). These outcomes could indicate following the 349 ka and 339 ka eruptions (Downs et al., 2014a), Whakamaru-type magmatism may have been more prolonged than previously identified by contributing to the early Huka Group. Geochemical and

chronological assessments of fresh Huka Group pumice samples unavailable for this investigation would better establish these relationships (e.g., Rosenberg et al., 2014).

Overall, the use of immobile element geochemistry has proven to be a useful tool for measuring stratigraphic variation and identifying similarities between magmatic suites. Detailed analytical spacing and large precise data sets are key to overcome some the difficulties of analysing altered volcanic deposits. Use of pXRF calibrated against accurate laboratory methods is demonstrated to be an effective tool for collecting comprehensive geochemical data when precision is required. Use of these techniques are intended to complement lithostratigraphy (Chapter 2) by enhancing detail otherwise compromised by alteration.

SUMMARY

Magmatic feldspar phenocryst measurements and chemostratigraphic immobile element variations can be used to analyse detailed stratigraphy and magmatic relationships in altered volcanic strata. These techniques were tested to enhance the stratigraphic understanding of the hydrothermally altered Huka Group at Wairakei-Tauhara Geothermal Field. Results identified vertical variations in drill samples reflecting separate depositional processes or magmatic events. Large data sets are fundamental to the outcomes of both techniques for overcoming the detail-limiting effects of alteration. This favours the use of chemostratigraphy together with field-portable geochemical methods (pXRF) for mass data collection. New insight has been gained in the Huka Group, enhancing existing lithostratigraphy, on volcanic transport processes and magmatic sources. Similarities in immobile element comparisons suggest Huka Group may be mainly locally sourced, except for the commencing ignimbrite. The Waiora Ignimbrite is chemically consistent with material from a previously active caldera source and may highlight a void in our current understanding in the progression of early volcanism in central TVZ.

Preamble:

This chapter was conceived following the identification of hydrothermal minerals during the Huka Group core logging stage (Chapter 2). The hydrothermal minerals are coarse, rhombic crystals of fracture-lining adularia – some of the most pristine samples identified before at Wairakei-Tauhara. Their identification led to an application-type approach developed in Chapter 5 investigating the timing of the hydrothermal system hosted within the Huka Group reservoir. Recent advances in the apparatus and techniques used in $^{40}Ar/^{39}Ar$ dating after Verati et al. (2013) suggested these products, despite their young age and high atmospheric contamination, could provide direct constraints on the system's evolution.

Results from $^{40}Ar/^{39}Ar$ dating were much younger than previously measured and directly correspond with a young local phase of the geothermal system's evolution. This has implications for the influence of late volcanic episodes and magmatic heat inputs affecting the Wairakei-Tauhara system.

This chapter has been written as a short article type in preparation for submission to GSA Geology. At the time of thesis submission, data are undergoing continued laboratory refinement prior to peer review of the article.

Deputy Vice-Chancellor's Office
Postgraduate Office

UNIVERSITY OF CANTERBURY
Te Whare Wānanga o Waitaha
CHRISTCHURCH NEW ZEALAND

Co-Authorship Form

This form is to accompany the submission of any thesis that contains research reported in co-authored work that has been published, accepted for publication, or submitted for publication. A copy of this form should be included for each co-authored work that is included in the thesis. Completed forms should be included at the front (after the thesis abstract) of each copy of the thesis submitted for examination and library deposit.

Please indicate the chapter/section/pages of this thesis that are extracted from co-authored work and provide details of the publication or submission from the extract comes:

Chapter 5: $^{40}Ar/^{39}Ar$ dating of hydrothermal products from a continental arc setting.

Please detail the nature and extent (%) of contribution by the candidate:

Hamish has undertaken core logging, sample collection, sample sorting and interpretation (80%). The co-authors (20 %) carried out the laboratory preparation and analysis at Stanford University and advised on data interpretation.

Certification by Co-authors:
If there is more than one co-author then a single co-author can sign on behalf of all
The undersigned certifies that:

- The above statement correctly reflects the nature and extent of the PhD candidate's contribution to this co-authored work
- In cases where the candidate was the lead author of the co-authored work he or she wrote the text

Name: *C. Oze* Signature:  Date: *14/04/2015*

5

$^{40}Ar/^{39}Ar$ dating of hydrothermal products from a continental arc setting

Hamish Cattell[1], Christopher Oze[1] and Martin Grove[2]

[1]Department of Geological Sciences, University of Canterbury, Christchurch 8140, New Zealand
[2]Department of Geological and Environmental Sciences, Stanford University, Stanford, CA, 94305, USA

ABSTRACT

Geothermal systems in the Taupo Volcanic Zone evolve over hundreds of thousands of years by repetitive intrusions at ten to hundred thousand year periods. The timing of these systems are based on previous U-Th dating of hydrothermal calcite, Ar/Ar dating of hydrothermal hornblende and indirect correlation of dated stratigraphy. An alternative to the previously dated minerals is the use of hydrothermal adularia that may provide reliable temporal constraints on the evolution of geothermal systems. Here, we trial $^{40}Ar/^{39}Ar$ dating of hydrothermal adularia from a single mineralised fracture against an existing U-Th mean age of 99 ka in the Tauhara Geothermal System to identify its level of activity. Our results identify that adularia mineralisation occurred <30 ka (mean age 15 ±10 ka) relating to a younger stage of geothermal activity, and is the presently youngest dated hydrothermal silicate, validated by thermal diffusion models. This outcome identifies that $^{40}Ar/^{39}Ar$ dating can be suitable for evaluating complex hydrothermal minerals. Overall, we provide a new tool to successfully assess the timing of geothermal systems using $^{40}Ar/^{39}Ar$ dating on hydrothermal adularia.

INTRODUCTION

Geothermal fields are geographically stable features that exhibit thermal variability throughout their geological lifetimes (Bibby et al., 1995; Arehart et al., 2002; Milicich et al., 2014). Establishing their ages and timing of evolutionary events is often limited by geological evidence, and remains a central subject of debate at many active geothermal fields. Radiometric dating of hydrothermal fluids and minerals is a challenging task and is often controversial, particularly when they are young and active. These restrictions have limited the number of previous studies attempting to date both fossil geothermal systems (e.g., Brockamp et al., 2003; Arancibia et al., 2006; Hames et al., 2009; Gasquet et al., 2010; Márton et al., 2010; Mauk & Hall, 2010; Mauk et al., 2011) and active geothermal systems (e.g., Grimes et al., 1998; Dalrymple & Grove, 1999; Arehart et al., 2002; Villa et al., 2006; Verati et al., 2013).

Twenty-three active geothermal systems and at least two known fossil systems are hosted in New Zealand's Taupo Volcanic Zone (TVZ; Bibby et al., 1995). The rifted continental arc forms the southernmost expression of the Tonga-Kermadec subduction system and is a locus for highly productive silicic volcanism over 2 Myr (Wilson et al., 1995). Indirect geological evidence of the geothermal systems in the TVZ suggest they have evolved over several hundred-thousand years, maintained by repetitive heat pulses from local magmatic intrusions at tens of thousands of years (Grindley, 1965; Browne, 1979; Wood, 1994a; Chambefort et al., 2014; Milicich et al., 2014).

Recent drill core from the Tauhara sector of the joint Wairakei and Tauhara Geothermal Fields (Wairakei-Tauhara), TVZ (Fig. 5.1), has intersected a mineralised fracture containing large adularia crystals, a low-temperature form of alkali-feldspar ($KAlSi_3O_8$), commonly with a hydrothermal genesis. Hydrothermal adularia presents an ideal opportunity to directly date the geothermal system. Recent advances in the $^{40}Ar/^{39}Ar$ dating method (Jourdan et al., 2014) have reduced some of the existing challenges of dating young materials and now permit its application for use on more complex geological materials. Previous investigations directly dating TVZ geothermal systems using U-Th and $^{40}Ar/^{39}Ar$ methods support continual thermal replenishment (Grimes et al., 1998; Arehart et al., 2002), but they lack the age resolution to accurately investigate the system's late evolution (<100 ka).

Here we conduct $^{40}Ar/^{39}Ar$ dating and assess the effect of thermally-promoted argon diffusion on a single fracture containing hydrothermal adularia from an active geothermal system. Results could provide a direct time constraint for the system and insight into its prolonged evolution. Overall outcomes may support Ar stability in the analysed samples under the inferred geothermal conditions and yield a comparatively young age supporting the ongoing renewal of the Tauhara geothermal system.

SAMPLES AND METHODOLOGIES

Sample collection and preparation

Four core fragments containing hydrothermal adularia were collected between 774 and 786 m depth along a mineralised fracture in well THM16 from Tauhara Geothermal Field (Fig. 5.1; samples: 16_774.3, 16_775.4, 16_778.73, 16_785.85). Intersected between 760 – 790 m depth, the fracture is near-vertical with an aperture of 0.5 – 1 cm and has vertical offset of 1 – 2 cm (Fig. 5.2A). Lining the fracture is a hydrothermal mineral assemblage of quartz, adularia forming a 0.5 cm thick mineralised layer (Fig. 5.2A-B), accessory pyrite, calcite and wairakite ± epidote and hematite. Fracture lining includes drusy well-formed radiating prismatic quartz (transparent) and minor disseminated pyrite. No mineral layering or crustiform-type banding was observed suggesting co-mineralisation following fracture formation. Below 774m depth diamond- and wedge-shaped adularia (cloudy white) is the dominant mineral with minor quartz. Some surfaces contain uniformly small dursy quartz or adularia crystals (<1-2 mm long), others surfaces are non-uniformly sized with large crystals up to ~5 mm long. Rare patches of red leached hematite occasionally stain the otherwise clean crystallised surfaces. The mineralised fracture occurs in a ~310 ka light brown pumice and lithic lapilli-tuff ignimbrite of the lowermost Waiora Formation drilled between 730 – >800 m depth in THM16 (Rosenberg et al., 2009a; 2014). The ignimbrite host rock is intensely silicified and contains a propylitic mineral association (chlorite, kaolinite, micro-quartz, adularia, pyrite, calcite, wairakite, epidote), with no petrographic evidence for thermal overprinting. Overlying the ignimbrite are lacustrine-deposited tuffs and at least eight local hydrothermal eruption breccias of the upper Waiora Formation (210 – 730 m) followed by at least four further hydrothermal eruption deposits of Crown Breccia (44 – 210 m; Rosenberg et al., 2009b; Chapter 2).

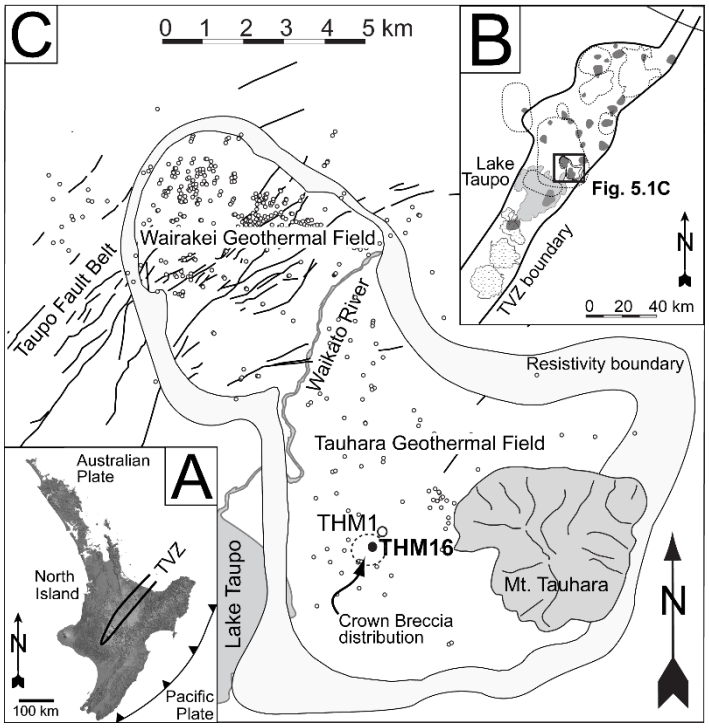

Figure 5.1. A. Map showing the location of the Taupo Volcanic Zone (TVZ) and the offshore subduction setting at North Island, New Zealand. **B.** The geographical boundary of young TVZ (from Wilson et al., 1995) illustrating the distribution of the southern cone volcanoes (speckled), eight caldera centres (dashed lines), 25 identified geothermal systems (grey dots) and central Lake Taupo (light grey area). Box denotes location of Wairakei-Tauhara Geothermal Field (Wairakei-Tauhara). **C.** Geographic architecture of Wairakei-Tauhara defined by an electrical DC resistivity boundary and bisected by the Waikato River and Taupo Fault Belt (solid lines). Open circles are drilled wells and those described in the text are labelled. Inferred distribution of Crown Breccia is shown by dashed circle.

From the collected core fragments, large grains of adularia were handpicked from the mineralized surface under a binocular microscope (Fig. 5.2C). Adularia crystals are typically <1 – 3 mm long, cloudy white to transparent, rhombic-shaped and free from intergrowths, making them easy to distinguish from prismatic quartz. Four mineral separates each contained 40 – 50 adularia grains (50 – 100 mg) and were each rinsed in deionised water. Petrological microscopy and Energy-Dispersive X-ray spectroscopy (EDS) assessment were undertaken on selected adularia crystals at the University of Canterbury to identify crystal textures and confirm their composition. An Oxford Instruments X-Max EDS was used coupled with a JEOL 6400 Scanning Electron Microscope set at 45× magnification, 15 mm working distance with a 20 nA beam current and 20 kV accelerating voltage.

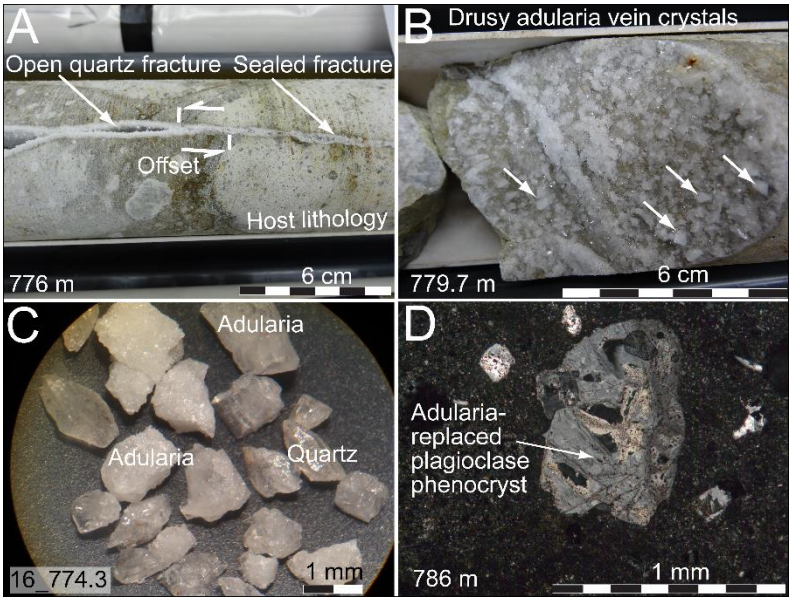

Figure 5.2. Photographs of the samples used. **A.** Section of THM16 drill core (6.3 cm diameter) with an offset mineralized fracture containing hydrothermal quartz in Waiora Formation ignimbrite host rock at 776 m depth. **B.** Cored fracture surface with the drusy rhombic adularia highlighted (arrows) at 779.7 m collected for analysis. **C.** Adularia and quartz crystals under binocular microscope before handpicking of sample 16_774.3. **D.** Thin section of host rock from 786 m depth under cross-polarised light at 10× magnification showing patchy feldspar pseudomorph and groundmass replaced by pervasive hydrothermal adularia and quartz, respectively.

$^{40}Ar/^{39}Ar$ dating

The $^{40}Ar/^{39}Ar$ analysis of the adularia samples were performed at Stanford University with analytical procedures outlined in Hacker et al. (1996). Mineral separates were packed in pure copper foil and interspersed in evacuated glass tubes with a neutron fluence monitor (27.92 ± 0.17 Ma Taylor Creek sanidine; Duffield & Dalrymple, 1990) and kalsilite glass to monitor Ca and K neutron-induced interferences. Irradiation took place at the Oregon State University TRIGA reactor. Twenty-two 400 – 700 µm adularia grains were fused per sample using a Spectra Physics 2016 Ar ion laser. Samples were step-heated and isotopes were measured using a MAP 216 mass spectrometer. Measured abundances of K-derived ^{40}Ar ($^{40}Ar_k$) were corrected using the zero age kalsilite glass baseline standard. The correction factor measured $(^{40}Ar/^{39}Ar)_K$: 4.937×10^{-03} ± 1.623×10^{-03}. Corrections to the measured $^{40}Ar/^{39}Ar$ for the atmospheric $^{40}Ar/^{39}Ar$ component were calculated under the assumption that initial argon was of atmospheric composition.

^{39}Ar diffusional loss with transient heating

$^{40}Ar/^{39}Ar$ dates are mainly cooling ages below a ‘closure temperature’ at a time when radiogenic ^{40}Ar ($^{40}Ar^*$) accumulates and is retained in the crystal. A difficulty in interpreting the resulting $^{40}Ar/^{39}Ar$ age

of the adularia samples may be due to diffusive loss of $^{40}Ar^*$ in the mobile geothermal setting. Argon retention is investigated here by isothermal heating experiments on abundantly available ^{39}Ar within the adularia samples to evaluate the diffusion sensitivity of Ar to transient heating histories. The ^{39}Ar fractional loss diffusion results will provide the basis for best-fit validation of the $^{40}Ar/^{39}Ar$ age of adularia crystallisation or indicate modification by a reheating event. Packed mineral separates were incrementally step heated following methods by Lovera et al. (1997).

RESULTS

Adularia petrography

Thin sections of the adularia crystals show patchy tile-like and sector twinning at the crystal cores and euhedral crystals have compositionally zoned outermost rims. No significant fluid inclusions or impurities were visible at 40× magnification. In the host rock, the dominant matrix and void spaces were intensely silicified by secondary quartz, while primary feldspar is replaced by patchy adularia pseudomorphs (Fig. 5.2D). Chemical EDS results confirmed the crystals are K-rich adularia consisting of: Si (56 wt.%), K (29 wt.%) and Al (15 wt.%) and are similar to results by Steiner (1970).

$^{40}Ar/^{39}Ar$ results

Results from the four hydrothermal adularia samples measured by $^{40}Ar/^{39}Ar$ (n = 87) yielded an inverse isochron average age of 15 ±10 ka (2σ standard deviation; mean square weighted deviate, MSWD = 1.17), presented in Fig. 5.3. In the samples, Ar near the atmospheric composition ($^{40}Ar/^{36}Ar$ = 295.5) was very high (~99 %) with only a trace $^{40}Ar^*$ detected. With the atmospheric correction applied, Fig. 5.3 shows the result of the high atmospheric contamination causing clustering of the data points and resulting in a wide extrapolated data spread at 2σ. Calculated ages for individual samples are similar to the inverse isochron age but are individually imprecise, making only the inverse isochron age valid.

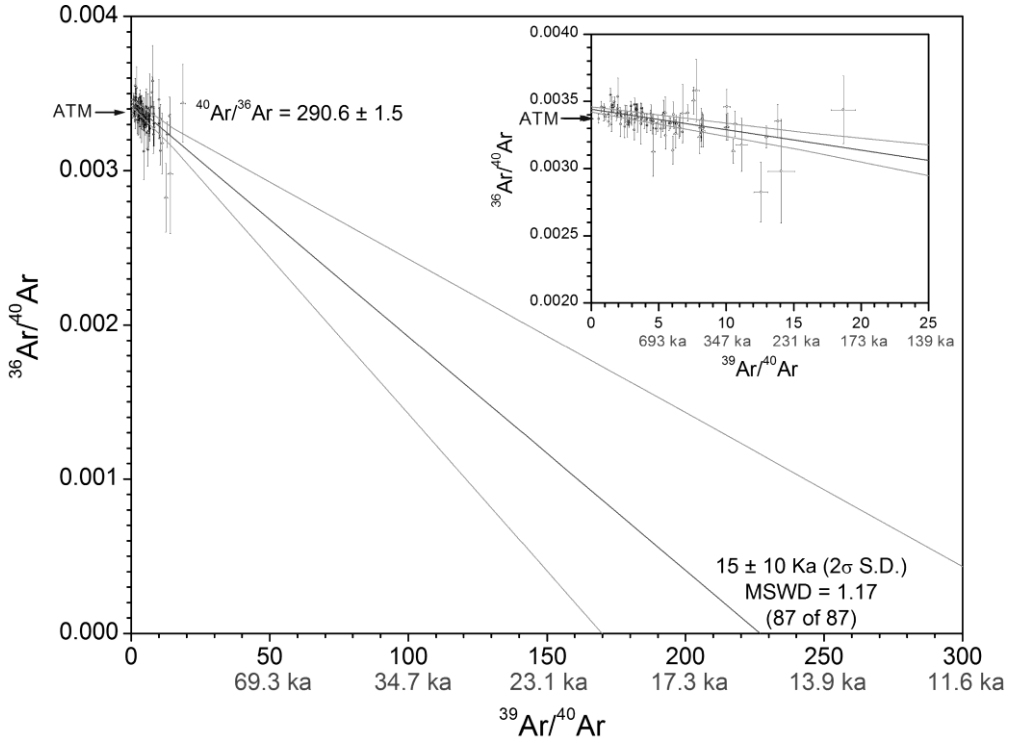

Figure 5.3. Inverse isochron plot showing all results (4 samples, n = 87 measurements). No data has been omitted from the overall data set. The upper and lower projected lines are 95% confidence bands. The ages in ka are shown on the ^{39}Ar /^{40}Ar x-axis. The central line is the extrapolated best-fit corresponding with a mean age of 15 ± 10 ka (2σ standard deviation (S.D.); mean square weighted deviate (MSWD) = 1.17). Note: the best-fit y-intercept ($^{40}Ar/^{36}Ar$ = 290.6) is different from atmospheric composition (ATM; $^{40}Ar/^{36}Ar$ = 295.5). *Insert* at the right shows the detail of the data close to the y-axis.

^{39}Ar diffusional loss

The effect of transient heating on adularia Ar diffusion and the $^{40}Ar/^{39}Ar$ age is modelled as fractional loss profiles using two exemplary crystal sizes (50 – 500 µm diameter) shown in Fig. 5.4A-B. Contours are diffusional fractional losses of ^{39}Ar as a function of the increased temperature spike (°C) over the heating duration (years). These models assume spherical diffusion geometry with activation energy (E) = 42.4 kcal/mol and a diffusion coefficient (D_0) = $\log_{10}$ -2.99. Short-term events are modelled for up to a 10 kyr-long high-temperature heating event (Fig. 5.4A-B, $\log_{10}$ 4). Longer transient heating events are highly unlikely to be thermodynamically sustainable at such depths within a geothermal system. The 50 µm model indicates that over 10 kyr transient heat pulses below ~300 °C promote little Ar loss (5 –10 %; Fig. 5.4A) and little loss over the same heating period occurs below ~350 °C for the 500 µm model (>5 %; Fig. 5.4B).

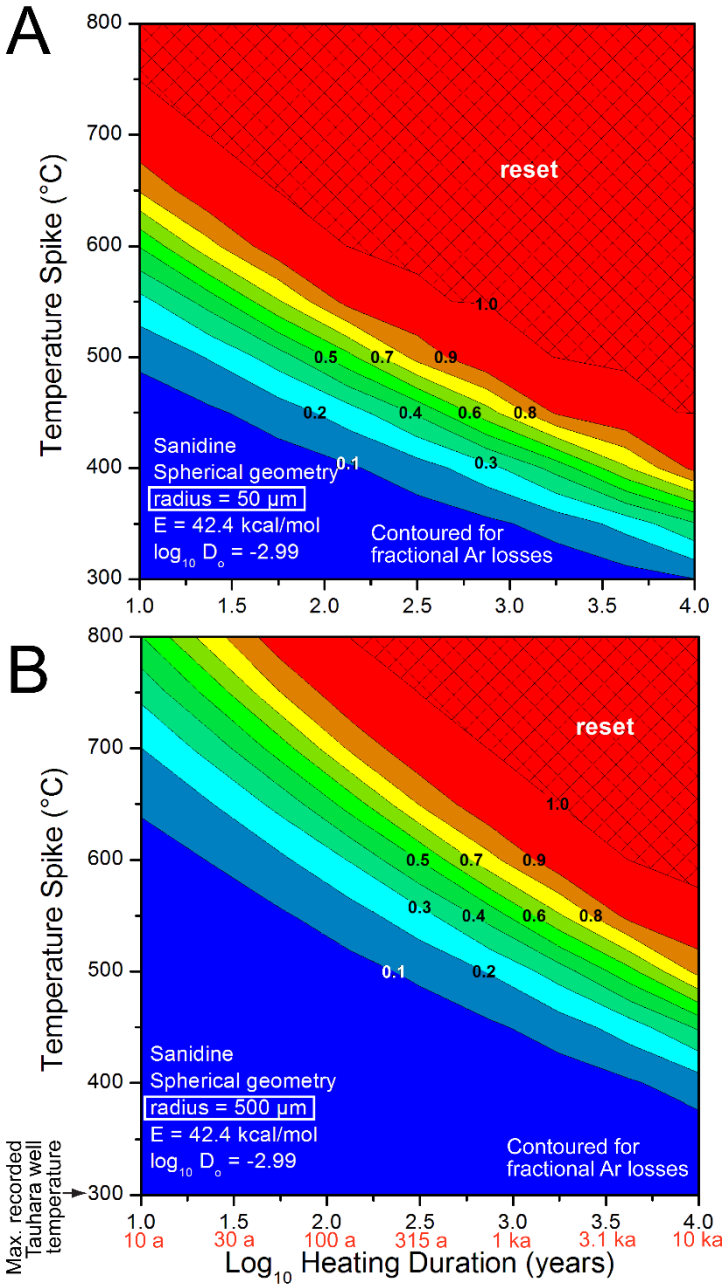

Figure 5.4. Modelled fractional loss profiles of the response of Ar loss from adularia during transient heating events for spherical geometry crystals at a radius of **A.** 50 µm and **B.** 500 µm. Contours are the percent of Ar lost at the given heating duration in years (a and ka) and temperature. Abbreviations = activation energy (E) and diffusion coefficient (D_0). The maximum (Max.) temperature measured at Tauhara (Contact Energy, 2010) is show in in Fig. 5.4B.

DISCUSSION

The obtained $^{40}Ar/^{39}Ar$ age of 15 ±10 ka (2σ) suggests the fracturing and mineralisation event is geologically young relative to the apparent ages previously presented for TVZ geothermal systems (>200 ka; Warakei, Grindley, 1965; Kawerau, Browne, 1979; Waiotapu, Reporoa, Wood, 1994b; Tauhara, Arehart et al., 2002). A young age identifies late continued evolution of the Tauhara

geothermal system and supports the principal concept in the TVZ of continual system evolution previously suggested to consist of thermal waxing and waning periods (e.g., Milicich et al., 2014; Chambefort et al., 2014).

High atmospheric contamination in the analysed adularia samples is likely due to their contact with meteoric and hydrothermal fluids measured near the atmospheric ratio ($^{36}Ar/^{40}Ar$ 292 – 311; Mazor et al., 1990). Extrapolation of the clustered data results in a low precision age; nevertheless, the 2σ error spans a relatively narrow total age range (Fig. 5.3). Examination of all of the data points identified no line of best-fit can be extrapolated older than ~30 ka. Given the compositional limitations of the samples, we confidently suggest this age to be a maximum plausible age for the adularia samples. However, while the apparent adularia $^{40}Ar/^{39}Ar$ age has been constrained, the effects on the age by processes within the geothermal setting including uptake of excess ^{40}Ar ($^{40}Ar_E$) during crystallisation and thermally induced ^{40}Ar loss by reheating must be explored to validate the age and use of the $^{40}Ar/^{39}Ar$ method.

$^{40}Ar_E$ is common in hydrothermal systems associated with magmatic heat source intrusions (Kelley et al., 1986). Addition of $^{40}Ar_E$ to the mineral lattice or in trapped fluid inclusions would increase the apparent age of the adularia. In hydrothermal fluids from surface geothermal fumaroles at Wairakei-Tauhara, low non-atmospheric ($\leq 5.2\times10^{-4}$ ppm) and atmospheric ^{40}Ar (2×10^{-4} – 2×10^{-3} ppm) concentrations have been measured (Mazor et al., 1990). Kelley et al. (1986) and Kelley (2002) found K-feldspar with trapped $^{40}Ar_E$ from hydrothermal fluids up to 0.1 – 1 ppm would increase the $^{40}Ar/^{39}Ar$ age by between 1 – 10 ka. Such concentrations are beyond the levels measured at Wairakei-Tauhara and would be accommodated within the reported 2σ error. Extrapolation of the results intersects the inverse isochron $^{36}Ar/^{40}Ar$ axis slightly above the atmospheric ratio identify a small presence of $^{40}Ar_E$ in the samples, but its effect is alleviated by using the $^{40}Ar/^{39}Ar$ method on highly K-rich minerals (Kelley, 2002).

Fractional losses of ^{40}Ar by thermally-promoted diffusion would reduce the apparent crystallisation age reflecting timing of the heating event. High temperature ‘pulses’ from the deep geothermal reservoir interacting with the adularia samples may have been sufficient to have induced Ar loss. The introduced hydrothermal mineral assemblage suggests crystallisation occurred at >230 °C

(Steiner, 1977; White & Hedenquist, 1990; Rosenberg et al., 2009b). In well THM16 at the sample depth the well temperature was measured at 200 °C. Maximum measured temperatures in the Tauhara field are slightly over 300 °C at depth (TH12; 1500 m depth; Contact Energy, 2010). Thermal conditions beyond deep drilling at Wairakei-Tauhara (maximum 3 km) are poorly understood, but extrapolation of known thermal gradients (20 °C/km) from deeper geothermal wells (McNabb, 1992) to 8 km depth suggest temperatures between 350 – 400 °C may occur at great depth (Kissling & Weir, 2005). We infer this temperature range as a maximum possible 'thermal pulse' for testing the feasibility of thermally-promoted Ar loss. The diffusion models (Fig. 5.4A-B) show the effect of heating on promoting Ar diffusion in small (50 µm) and larger crystals (500 µm). The analysed 400 – 700 µm adularia samples are best represent by the 500 µm model.

An existing U-Th age by Grimes et al. (1998) from Tauhara well THM1 (Fig. 5.1C) returned a hydrothermal calcite age of 99 ±44 ka. Using the 500 µm diffusion model, had adularia crystallisation occurred at 100 ka, and a 1,000 year long transient heating event of 400 °C followed at approximately 10 ka, the crystallisation age would be reduced by 5% (Fig. 5.4B; [100-10 ka]×0.05 = 4.5 ka; neglecting radiogenic ingrowth during the event). Diffusional losses from the 500 µm model indicate that 1,000 years of heating at 650 °C or 10 kyr of heating at 550 °C are required to reduce the age of the adularia from 100 ka to near the 15 ka $^{40}Ar/^{39}Ar$ age. Even at the lower confidence interval age value of Grimes et al. (1998) of 55 ka and assuming a smaller modelled crystal size (50 µm; Fig. 5.4A), the models suggest a 10 kyr transient heating event and temperatures >375 °C are required to reduce the age to 15 ka value. Overall, the models demonstrate that adularia requires either small diffusive transport distances (Fig. 5.4A) or protracted heating at very high temperature (Fig. 5.4B) to induce ^{39}Ar loss. In the Tauhara geothermal system, these values are excessive attesting the measured $^{40}Ar/^{39}Ar$ age of 15 ± 10 ka is consistent with crystallisation.

The fracturing mechanism could be consistent with a volcanic or hydrothermal eruption event (Nelson & Giles, 1985; Henneberger & Browne, 1988). In the overlying Crown Breccia hydrothermal eruption deposit, accessory lithic clasts from the 25.4 ka Oruanui Formation (Wilson, 2001; Rosenberg et al., 2009b; Vandergoes et al., 2013) support a Crown Breccia eruption age that could be consistent with the adularia $^{40}Ar/^{39}Ar$ age. The eruption focal depth could also be reflected by the fracture depth

at 550 m below the Crown Breccia depositional surface, a depth consistent with other TVZ hydrothermal eruptions (~450 m deep; Browne & Lawless, 2001). We infer, therefore, that fracturing at the sample depth (760 – 790 m) is due to hydraulic fracturing associated with Crown Breccia hydrothermal eruptions (Fig. 5.5). Such over-pressurisation fracturing and brecciation can initially enhance reservoir rock permeability, but promotes hydrothermal mineralisation sealing fractures and reducing permeability (Nelson & Giles, 1985; Henneberger & Browne, 1988; Browne & Lawless, 2001).

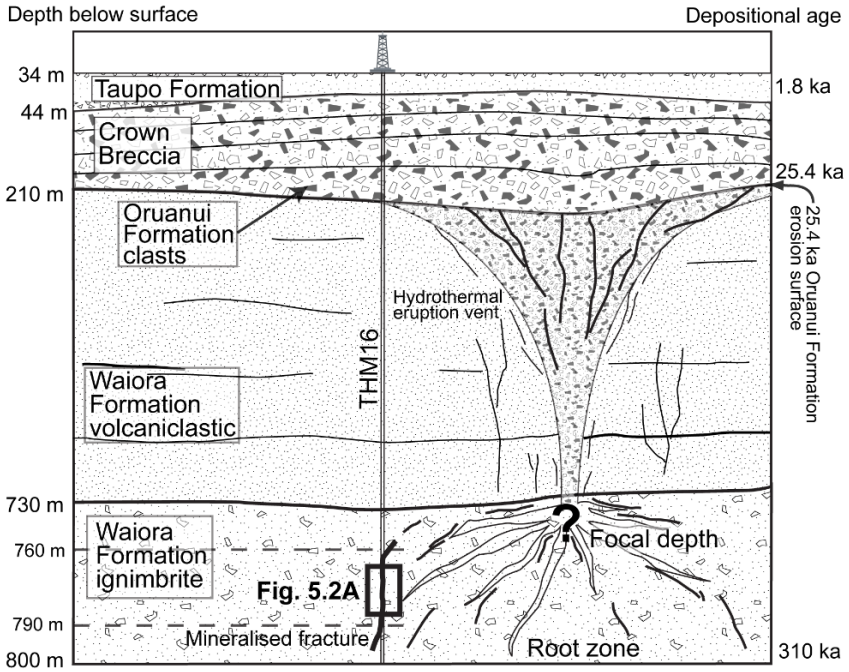

Figure 5.5. Conceptual illustration of the post-25.4 ka Crown Breccia vent and the stratigraphy of well THM16 (Rosenberg et al., 2009b). The proposed mechanism and interpreted location is shown for the < 30 ka mineralised fracture containing hydrothermal adularia.

Enhanced permeability by fracturing and fault movement in part regulates the longevity of geothermal systems in the TVZ (Browne & Lawless, 2001; Kissling et al., 2015). Together with fluid recharge and repeated heating intrusions (Milicich et al., 2014), the presented age is consistent with present-day active TVZ geothermal surface features identifying the systems to be continually evolving features with a level of natural self-sustainability. Overall we have presented a $^{40}Ar/^{39}Ar$ dating method suitable for directly assessing the age of young hydrothermal adularia to refine the timing of activity in complex geothermal environments. The method has successfully constrained the age of hydrothermal activity and can provide relative insight into the timing of reservoir fracturing and responsible mechanisms.

Preamble:

In Chapters 2 and 3, the detailed stratigraphic sequence of the Huka Group was characterised from drill core samples where the volcanic history was interpreted. In Chapter 4, the altered stratigraphic sequence was examined in detail. Results confirmed previously identified macroscopic textures and added detail of magmatic and transport emplacement processes. Chapter 5 deviated from previous lithostratigraphic assessments to locally assess the timing of the geothermal system within the Huka Group reservoir. At the local sample site in the Tauhara field, the system was measured to be much younger than previous assessments.

Collectively, these chapters provide refined insights into the geological and geothermal evolution of the Huka Group reservoir at the cored localities. These interpretations can now be applied to the existing field-wide stratigraphic model interpreted from >300 wells, mainly defined from cuttings samples. Here in ***Chapter 6****, findings from earlier chapters are combined with existing field-wide data to present a complete geological evolutionary model of the Huka Group at Wairakei-Tauhara. The order of deposition is explained and structural modifications in the field are summarised. Prevailing and contributing depositional environments (landscapes) resulting influenced by tectonism and volcanism are evaluated using present-day analogues in TVZ.*

This chapter will form the basis of a paper that will be submitted to the Journal of Volcanology and Geothermal Research. For the chapter to be a stand-alone manuscript, background content overlaps with Chapter 2. In the submitted manuscript, references to unpublished work will be omitted.

Deputy Vice-Chancellor's Office
Postgraduate Office

UNIVERSITY OF CANTERBURY
Te Whare Wānanga o Waitaha
CHRISTCHURCH NEW ZEALAND

Co-Authorship Form

This form is to accompany the submission of any thesis that contains research reported in co-authored work that has been published, accepted for publication, or submitted for publication. A copy of this form should be included for each co-authored work that is included in the thesis. Completed forms should be included at the front (after the thesis abstract) of each copy of the thesis submitted for examination and library deposit.

Please indicate the chapter/section/pages of this thesis that are extracted from co-authored work and provide details of the publication or submission from the extract comes:

Chapter 6: *Geological evolution of the Huka Group geothermal reservoir at Wairakei-Tauhara Geothermal Field, New Zealand.*

Please detail the nature and extent (%) of contribution by the candidate:

Hamish has undertaken all of the analysis, interpretation and writing (90%). The co-authors provided advice and helped with editing of the final manuscript (10%).

Certification by Co-authors:
If there is more than one co-author then a single co-author can sign on behalf of all
The undersigned certifies that:

- The above statement correctly reflects the nature and extent of the PhD candidate's contribution to this co-authored work
- In cases where the candidate was the lead author of the co-authored work he or she wrote the text

Name: *J. W. Cole* Signature: 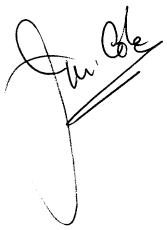 Date: *9/04/2015*

6

Geological evolution of the Huka Group geothermal reservoir at Wairakei-Tauhara Geothermal Field, New Zealand

H.J. Cattell; J.W. Cole and C. Oze

Department of Geological Sciences, University of Canterbury. Christchurch 8140, New Zealand

ABSTRACT

Geological settings characterised by contemporaneous continental arc volcanism and extensional tectonism can generate voluminous deposits that concentrate in subsiding basin depocentres. Basin-fill deposits can provide a detailed record of ancient eruptions, tectonism and depositional environments. Ancient basins frequently host geothermal resources and, therefore, require a detailed stratigraphic and structural understanding for their utilisation. Abundant, widespread and deep drilling at Wairakei-Tauhara Geothermal Field (Wairakei-Tauhara) in the Taupo Volcanic Zone (TVZ) has allowed the detailed stratigraphic framework to be established. Drilling up to 3 km deep has intersected the Huka Group, structurally hosted in the regional parallel Taupo Fault Belt basin (TFB; Kaiapo Graben sector) and Taupo-Reporoa Basin (TRB) intersecting Whakamaru caldera. Detailed Huka Group lithostratigraphy supplemented with existing drilling data from Wairakei-Tauhara has allowed ~300 kyr of volcanic and structural events and surface environments to be interpreted. Outcomes identify that the unique stratigraphic architecture in the basins underlying Wairakei-Tauhara evolved independently by localised subsidence, deposition and erosion events. Inferred chronological constraints suggest net subsidence and erosion at TRB (6 – 8 mm/yr) was approximately twice the rate at Kaiapo Graben (3 – 4 mm/yr) during Huka Group deposition. The continually subsiding basins hosted lacustrine-dominated environments, likely comparable to landscapes in present-day TVZ. This study improves our knowledge of past TVZ volcanism, tectonism and ancient environments in caldera inter-eruptive periods. Similar mechanisms to those presented could be valuable in explaining stratigraphy and the evolution of other rifted arc settings.

INTRODUCTION

In volcanic areas with numerous active source vents, thick spatially complex volcanic and sedimentary stratigraphic sequences accumulate with time. For these deposits to be preserved, emplacement needs to occur in subsiding tectonic or volcano-tectonic depocentres where erosion and reworking are typically low. Such permeable basins also commonly host valuable geothermal resources, therefore, understanding their spatial architecture is essential for successful resource modelling and extraction. Detailed models of basin-hosted stratigraphy are also vital for paleogeographic reconstructions (e.g., Cas & Wright, 1987; Busby & Bassett, 2007; Manville et al., 2009; Sohn et al., 2013; Downs et al., 2014a). Examining detailed stratigraphy of thick basin strata can be made difficult, however, when strata are buried, contain rapid facies variations, have undergone hydrothermal alteration and have limited lateral correlations. Basin stratigraphy analysis requires large outcrop exposures or availability of comprehensive drill samples to directly assess spatial and temporal variations.

At Wairakei-Tauhara Geothermal Field (Wairakei-Tauhara) in the Taupo Volcanic Zone (TVZ), New Zealand, is a sequence of buried ignimbrites, lavas and lacustrine sediments assigned to the Huka Group (Grindley, 1959). Deposition occurred over ~300 kyrs in subsiding basins intersecting southern Whakamaru caldera (Fig. 6.1A-B; Grindley, 1965; Wilson et al., 1986; Rosenberg et al., 2009a). Today the strata host and cap the geothermal system, thus influencing fluid migration in the geothermal field (Bixley et al., 2009). Over sixty years of drilling >300 wells up to 3 km deep at Wairakei-Tauhara has thoroughly established the field's stratigraphy and structure (Rosenberg et al., 2009a; Bignall et al., 2010a). A resurgence in drilling over the past decade (2005 – 2015) has returned new samples identifying that existing geological interpretations of the Huka Group may be somewhat oversimplified and incomplete (e.g., Grindley 1965; Healy 1965). As most TVZ geothermal fields occur in filled basins (Fig. 6.1B; Bibby et al., 1995), increased knowledge on ancient sedimentation patterns and depocentre settings could enhance our understanding of other geothermal fields. Additionally, an improved awareness of these settings could allow the future geothermal potential of other basins to be evaluated. Given the new data source availability at Wairakei-Tauhara, ancient processes and events can now be investigated to locally explain the history of volcanism and basin tectonism in the TVZ.

Utilising a mix of new insights (previous chapters) and existing data, outcomes have identified the types of transport processes and the relative order of Huka Group deposition. Inferences are made on the timing of major depositional events, field subsidence rates and ancient depositional environments. Interpretations are presented as conceptual time-series evolutionary block models for Wairakei-Tauhara. Overall, refined insights on the field's geological evolution further explain its complex stratigraphic distribution. The results improve our understanding of ancient processes and environments prevailing in TVZ's history.

GEOLOGICAL SETTING AND TVZ ERUPTIVE HISTORY

Taupo Volcanic Zone (TVZ)

The TVZ is a rifted continental arc in the North Island of New Zealand (Fig. 6.1A). The area developed over ~2 Myr in response to westward oblique subduction of the Pacific Plate beneath the Australia Plate (Fig. 6.1A; Beavan et al., 2002; De Mets et al., 2010; Mortimer et al., 2010). The rate of rifting increases from the south towards the north promoting crustal thinning (Bibby et al., 1995; Lamarche et al., 2006), basin formation (Villamor & Berryman 2001; Nicol et al., 2006) and volcano-tectonic collapse (Houghton et al., 1995; Wilson et al., 1995; 2009; Gravley et al., 2007). Arc volcanism in TVZ includes andesite cone-building that are geographically concentrated in the north and south (Fig. 6.1A). Wairakei-Tauhara is located in a 120 × 60 km central section characterised by 8 rhyolitic calderas (Figs. 6.1A & 6.2; Wilson et al., 2009).

Extension in TVZ is mainly accommodated by NE-SW-trending, high-angle normal faults assigned to the Taupo Fault Belt (TFB) between Lakes Taupo and Okataina (Fig. 6.1A; Villamor & Berryman, 2001; 2006). The TFB is a regional active rift subsiding at 3 – 4 mm/yr (since ~61 ka; Bryan et al., 1999; Rowland & Sibson 2001; Villamor & Berryman 2006; Downs et al., 2014a) and hosts the Kaiapo Graben local to Wairakei-Tauhara. In eastern central TVZ is the Taupo-Reporoa Basin (TRB), a rift-basin bound by caldera centres and subsiding in the north at ~4 mm/yr (Fig. 6.1A; Manville, 2001; Wallace et al., 2004; Downs et al., 2014a). Drilling in TVZ has intersected basin depocentres filled with 1 – >3 km of mainly caldera-derived ignimbrites (Rosenberg et al., 2009a; Downs et al., 2014a). These basins host most of the TVZ's ~23 active geothermal systems (Fig. 1B; Rowland & Sibson 2004; Rowland et al., 2010; 2012).

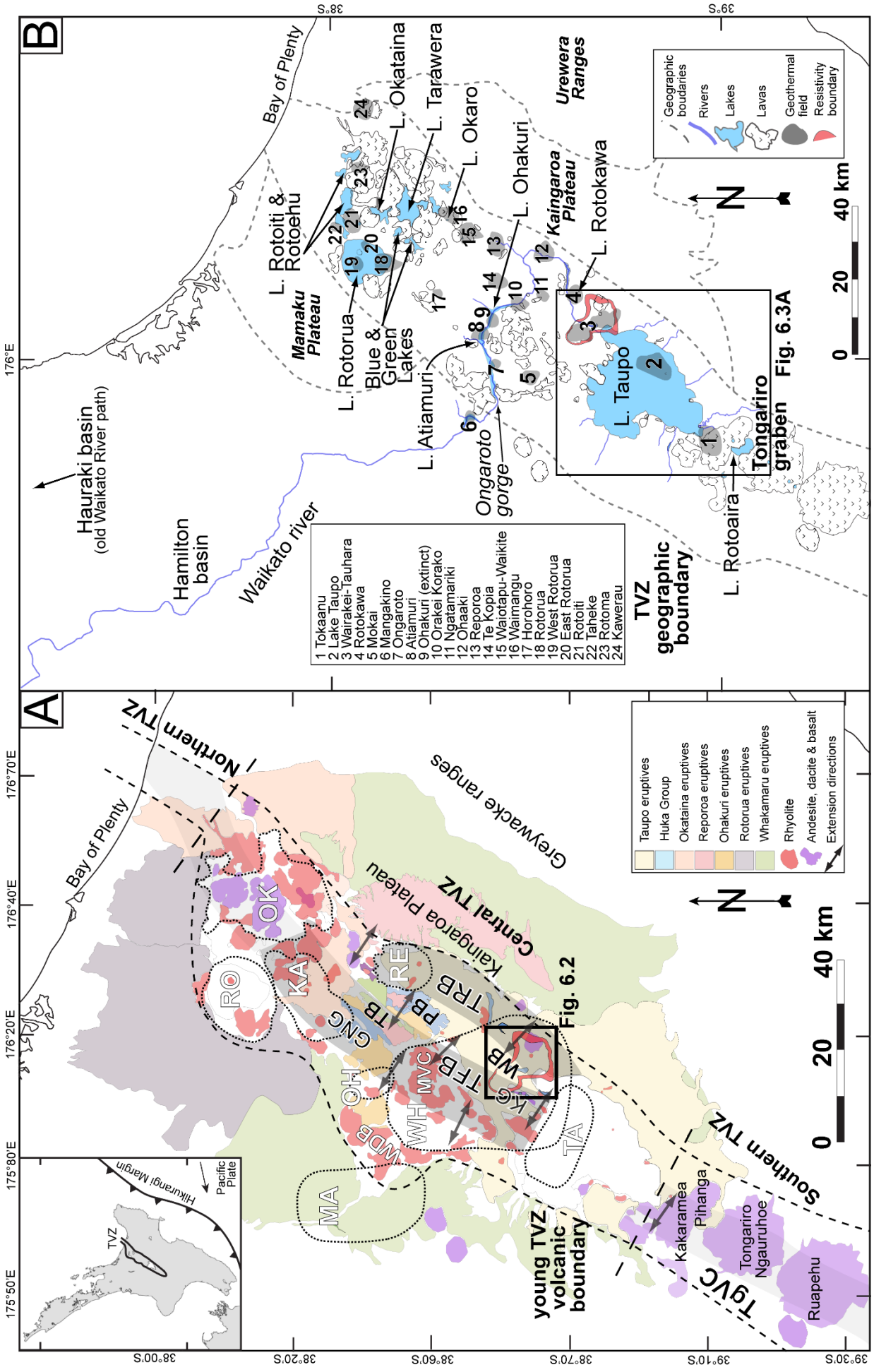

Figure 6.1. A. Geology of young TVZ boundary including inferred caldera structures (Wilson et al., 1995), surface outcrop geology (Leonard et al., 2010; Downs et al., 2014a) and extension directions (Seebeck et al., 2014). TVZ eruptive centres: OK = Okataina, RO = Rotorua, KA = Kapenga, MA = Mangakino, OH = Ohakuri, RE = Reporoa, WH = Whakamaru, TA = Taupo and TgVC = Tongariro Volcanic Centre. Abbreviations: MVC = Maroa Volcanic Centre, PB = Paeroa Fault Block, TB = Te Weta Block, WB = Wairakei Block, TFB = Taupo Fault Belt basin, KG = Kaiapo Graben and TRB = Taupo-Reporoa Basin (greyed zones); GNG = Ngakuru-Guthrie grabens. *Insert* location of TVZ and subduction of Pacific Plate along Hikurangi Margin (HM). **B.** Physiography and geographic boundary of present-day TVZ including lake, river and lava dome features.

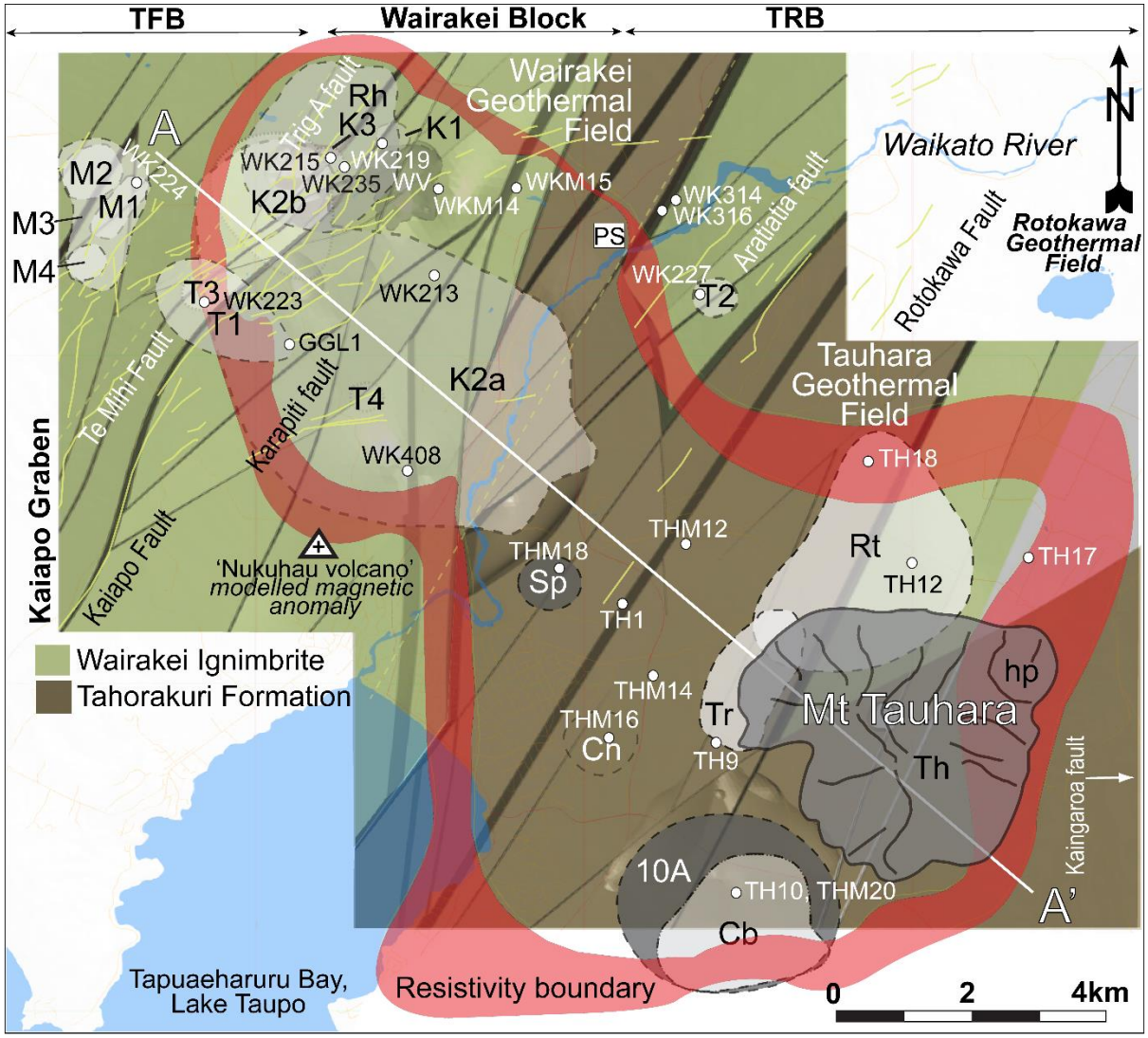

Figure 6.2. Wairakei-Tauhara Geothermal Field DC resistivity boundary (Risk, 1984). The modelled structure below the Huka Group includes the Kaiapo Graben within Taupo Fault Belt (TFB) Wairakei Block and the Taupo-Reporoa Basin (TRB). Yellow lines = surface fault traces (GNS Active Fault Database, 2014). Grey = inferred distributions of buried lavas. White dots = referenced well locations. Lava abbreviations: M1 – M4 = Mapara Rhyolite lavas 1 – 4, T1 – T4 = Te Mihi Rhyolites 1 – 4, K1 = Karapiti 1 Rhyolite, K2a = Karapiti 2a Rhyolite, K2b = Karapiti 2b Rhyolite, K3 = Karapiti 3 Rhyolite, WV = Waiora Valley Andesite, Sp = Spa Andesite, Cn = Crown Breccia, Rt = Racetrack Rhyolite, Tr = Trig Rhyolite, Cb = Crowbar Rhyolite, 10A = 10A Andesite, Th = Tauhara Dacite, hp = Hipaua dome, PS = Wairakei Power Station. A–A' cross section line corresponds with Fig. 6.6.

MAJOR VOLCANISM IN SOUTHERN CENTRAL TVZ

Historically, caldera eruptions in TVZ have occurred as intense syn-eruptive flare-up clusters from several vents. These events rapidly emplaced major stratigraphic units and modify existing landscapes (Manville & Wilson, 2004). Understanding the deposit and structural framework of the TVZ is fundamental for unravelling the history of volcanism and inter-eruptive environments controlling the evolution of its geothermal fields (Manville & Wilson, 2004; Rosenberg et al., 2009a; Wilson et al.,

2009). The last flare-up in central TVZ between ~350 – 280 ka consisted of eight widespread ignimbrites from six caldera sources (Fig. 6.1A; Wilson et al., 2005; 2009; Gravley & Wilson, 2006). The timing, styles and environments during ancient eruptions at Whakamaru, Ohakuri, and Reporoa calderas near Wairakei-Tauhara (Fig. 6.1A) provide valuable details for evaluating contemporaneous Huka Group evolution (Fig. 6.1A).

The Whakamaru caldera eruption commenced a flare-up at ~349 ka (Downs et al., 2014a). Over >1500 km^3 of magma was erupted by >3 phreatoplinian-plinian phases and transported >50 km throughout central TVZ (Brown et al., 1998a; Wilson et al., 1986; 1995; 2009). Whakamaru deposits are distinct between eastern and western TVZ and reflect phases of the eruption and transport (Brown et al., 1998a). Local to Wairakei-Tauhara, Wairakei Ignimbrite is a formally named Whakamaru Group member at the field consisting of ~3 separate sheets (Grindley, 1965; 1982). Drilling has identified that its distribution, thickness and elevation is highly variable (Rosenberg et al., 2009a). Petrographic and geochemical similarities suggest the upper section correlates with Rangitaiki ignimbrite (Whakamaru Member; Martin, 1961; Grindley, 1965; 1982; Wilson et al., 1986; Chapter 4). East of Wairakei-Tauhara, Rangitaiki ignimbrite outcrops on Kaingaroa Plateau (Fig. 6.1A; Grindley, 1960; Stagpoole, 1994).

Kaingaroa Ignimbrite erupted from Reporoa caldera at ~281 ka (Fig. 6.1A; Nairn et al., 1994; Beresford & Cole 2000; Downs et al., 2014a). The eruption commenced with a phreatomagmatic phase, probably interacting with an ancient lake that covered the vent, and later became replaced by plinian column collapse. The variably welded to unwelded 100 km^3 ignimbrite caps Kaingaroa Plateau (Fig. 6.1A; Nairn et al., 1994). Previously Kaingaroa Ignimbrite had been suggested to be interbedded with Waiora Formation near Wairakei (Wood, 1994a).

Ohakuri caldera erupted 100 km^3 of Ohakuri pyroclastics between 280 – 290 ka (Fig. 6.1A; Gravley et al., 2006; Downs et al., 2014a). The eruption commenced with an early phreatomagmatic phase followed by plinian phases. These were deposited in both terrestrial and lacustrine environments (in paleo-Lake Ohakuri?) >20 km from the source vent (Fig. 6.1A; Gravley, 2004). Contemporaneous eruptions from Ohakuri and Rotorua calderas ended the flair-up event (Gravley et al., 2007).

Maroa Volcanic Centre (MVC) is a hilly area of rhyolite lava domes surrounded by pyroclastic fans (Fig. 6.1A). Eruptive activity was dominantly between 251 – 222 ka during a period of reduced caldera activity in TVZ (Leonard, 2003). Limited stratigraphic, facies and structural evidence preclude a caldera collapse origin for MVC, excluding it from the flare-up event (Wilson et al., 1986; Leonard, 2003). However, MVC is relevant to understanding Wairakei-Tauhara because of its eruptive proximity (<10 km), their similar landforms and deposits (Grindley, 1965; Wood & Browne, 2000; Rosenberg et al., 2009a) and it is also located within Whakamaru caldera boundary (Fig. 6.1A; Wilson et al., 1986).

ASSESSMENT OF MAJOR LANDFORMS IN THE TVZ

Common landform features in present-day central TVZ and Taupo Volcanic Centre include lava domes and volcanogenic lakes drained by rivers (Figs. 6.1B). Understanding of the present-day distribution and controls on landforms and environments provide a useful context for helping decipher the types and longevity of ancient Huka Group environments (Chapter 2).

Lakes

Present-day TVZ is a locus for volcanogenic dammed, subsidence and explosion crater lake types (Manville, 2001; Manville et al., 2005; 2007; 2009). Drainage valleys blocked by volcanogenic flow deposits form unstable ignimbrite dams, which last only short geological time periods (less than a few thousand years) or relatively stable lava dams (>10 kyrs; Manville, 2001; Manville et al., 2007; Downs et al., 2014a; in press). Lava damming at present-day Okataina Volcanic Centre has formed multiple, hydraulically-connected lakes (e.g., Lakes Rotoiti, Rotoehu, Tarawera, Okataina; Fig. 6.1B).

Lakes formed by small-scale explosive eruptions are frequent in TVZ, but typically only form local sedimentary footprints several hundred metres wide (e.g., Lakes Rotokawa and Okaro; Fig. 6.1B; Collar & Browne, 1985; Bixley & Browne, 1988; Browne & Lawless, 2001).

Collapsed calderas form large depressions that can later host large lakes 50 – 185 m deep, such as lakes at Rotorua and Taupo (Fig. 6.1B). The morphology and sedimentology of Lake Taupo (Fig. 6.3A) is directly relevant for inferring characteristics of paleo-Lake Huka that covered the Wairakei-Tauhara area (Manville & Wilson, 2004). Northern Lake Taupo is controlled by caldera collapse structures and is >120 m deep (185 m maximum). The southern section is controlled by a structural

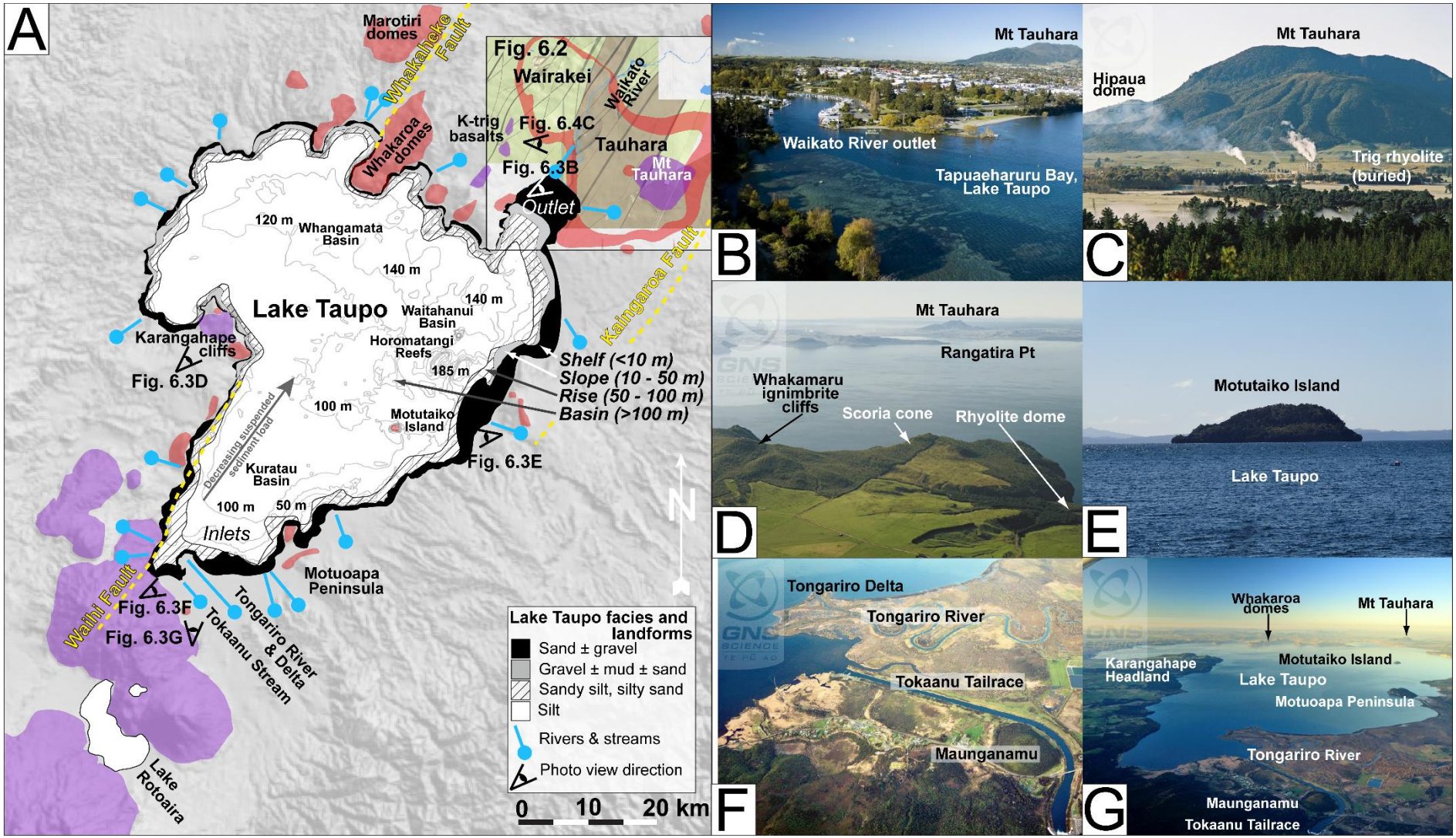

Figure 6.3. A. Physiography and relief map of Lake Taupo in the Taupo Volcanic Centre, including lacustrine topography and facies (Nelson & Lister, 1995), surface hydrology and surrounding landforms. Purple polygons are basaltic and andesitic volcanic centres. Photographs of landscapes surrounding and within Lake Taupo include: **B.** Waikato River outlet draining Lake Taupo in foreground and Mt Tauhara in background (image from: *http://www.greatlaketaupo.com*); **C.** Mt Tauhara composite dacite domes, northeast of Lake Taupo (Photographer: Lloyd Homer, GNS); **D.** steep Karangahape lava and ignimbrite cliffs, western Lake Taupo (Photographer: Lloyd Homer, GNS); **E.** Motutaiko Island rhyolite dome, eastern Lake Taupo; **F.** Tongariro and Tokaanu Rivers feeding Lake Taupo and Tongariro delta in the south (Photographer: Dougal Townsend, GNS); **G.** wide-angle northern oblique view of Lake Taupo physiography (Photographer: Dougal Townsend, GNS).

graben regulated by northeast-striking regional faults where the lake is <120 m deep (100 m average; Figs. 6.3A & F-G). The western and eastern lake margin profiles of Lake Taupo are non-symmetrical, resulting in a different lacustrine lithofacies distribution (Fig. 6.3A). The lake's western (and northern) shoreline is bound by steep faulted ignimbrite cliffs that plunge steeply into the lake and sheds talus into the basin (Fig. 6.3D; Nelson & Lister, 1995). In contrast, the eastern shoreline gradually drops into the lake forming a typical shallow shelf (0 – 10 m deep), slope (10 – 50 m) and rise (50 – 100 m) profile leading to the deep basin (>100 m; Nelson & Lister, 1995). These depth intervals are respectively characterised by dominantly sand (± gravel), gravel and mud (± sand), sandy silt and silty sand, and silt; each with increasing organic matter (Nelson & Lister, 1995).

Rivers

Rivers draining the southern andesite cones and greywacke ranges transport terrigenous sediments and connect lacustrine depocentres in TVZ (Figs. 6.1B & 6.3F-G). Fluvial activity is most evident on the ring plains around the stratovolcanoes to the south and is most active following large volcanic events when sediments are remobilised (Smith et al., 1993; Manville et al., 2007). Fluvial deposits are diagnostically coarser and more rounded than lacustrine sediments, usually consisting of planar to cross-bedded reworked gravelly to sandy volcanogenic fragments (Smith et al., 1993).

Lake Taupo is fed by >60 established rivers and streams (Fig. 6.3A; Nelson & Lister, 1995; McCraw, 2011). In the south, Tongariro River is the dominant feeder to the lake and maintains the Tongariro delta (Fig. 6.3F; Nelson & Lister, 1995). The Waikato River drains the lake at a single outlet in the northeast (Fig. 6.3A-B) and connects lakes Ohakuri and Atiamuri before exiting the TVZ at Ongaroto Gorge (Fig. 6.1B). Present western drainage through the Hamilton Basin resulted from disruption of its original course by the 25.4 ka Oruanui eruption (Wilson, 2001; Vandergoes et al., 2013).

Lava domes and cones

Rhyolite and andesite lava domes and dome complexes are common landforms that surround and dam lakes in central TVZ (Fig. 6.1A). Wilson et al. (1995) provides an overview of the composition and the distribution of volcanic landforms in TVZ. The distribution of domes are closely associated with regional faults and local caldera centres (Fig. 6.1A; Leonard, 2003; Ashwell et al., 2013). Dome

complexes near Wairakei-Tauhara include: Mt Tauhara, a composite of six dacite lava domes (Worthington, 1985); and MVC, dominantly two linear rhyolite dome complexes comprised of >30 domes (Fig. 6.1A; Leonard, 2003). Lava flow, clastic talus fans and co-eruptive pyroclastic material accumulate around these domes and provide material to nearby basins (e.g., Kaharoa pyroclastics; Leonard et al., 2002).

In southern TVZ, Tongariro Volcanic Centre (TgVC) contains four main andesite edifices, 2 – 2.8 km high and 10 – >200 km^3 in volume (Fig. 6.1A; Kakaramea, Pihanga, Tongariro-Ngauruhoe and Ruapehu; Cole, 1978). Dominant effusive eruptions from the cones generate eruptive volumes of 1 – 10 km^3 (Wilson et al., 1995). These cones may be similar to the large ancient buried edifices identified from some deep drilling (<2 km) and inferred from geophysical surveys in TVZ (Browne et al., 1992; Hunt et al., 2009). Poorly preserved basaltic cones in TVZ are small (<0.1 km^3) scoria or tuff cones (Wilson et al., 1995; Brown et al., 1994). Volumetrically these deposits are insignificant; however, their inferred eruption styles and resulting deposits can preserve the distribution of ancient water in TVZ (Brown et al., 1994).

INFERRED PHYSIOGRAPHY OF PALEO-LAKE HUKA

Huka Group lacustrine and phreatomagmatic deposits in TRB reflect locations of paleo-Lake Huka (Manville & Wilson, 2004). Understanding the morphology and early evolution of Lake Huka is restricted to a few outcrop exposures and poorly correlated drill samples. The greatest uncertainty of the ancient lake's evolution is its distribution, the number of lakes and their connectivity (Smith et al., 1993; Manville & Wilson, 2004; Downs et al., 2014a). An early conceptual interpretation of Lake Huka's evolution was proposed by Timperley (1983) including an inferred regional lake that evolved into two separate but connected lakes. Aspects of this model remain valid, however, the temporal distribution of lakes can now be refined (Fig. 6.4A-D) from the identification of hydrovolcanic and water-settled deposits since identified in central TVZ (Brown et al., 1994; Nairn et al., 1994; Wilson, 2001; Leonard, 2003; Gravley, 2004; Downs et al., 2014a; in press). Volcanic damming of late Lake Huka forming several lakes in the TRB (northern and southern) is supported by geological findings by

Manville and Wilson (2004). The ancient lakes may be similar to present-day lakes dammed in the Okataina Volcanic Centre (Fig. 6.1B).

Evidence for the early existence of Lake Huka in Wairakei-Tauhara exists prior to emplacement of Wairakei Ignimbrite at ~349 ka (Chapter 2). Later Waiora Formation deposits reflect material filling the lake between <200 ka – 300 ka. Huka Falls Formation then represents the following ~200 kyr of lacustrine sedimentation (Chapter 2). Distributions of the Oruanui Formation (Wilson, 1991) appear to preserve the morphology of the Lake Huka basin (Fig. 6.1A, Taupo eruptives). These suggest the late lake(s) was situated between the Tongariro graben and Waiotapu (Fig. 6.1B)

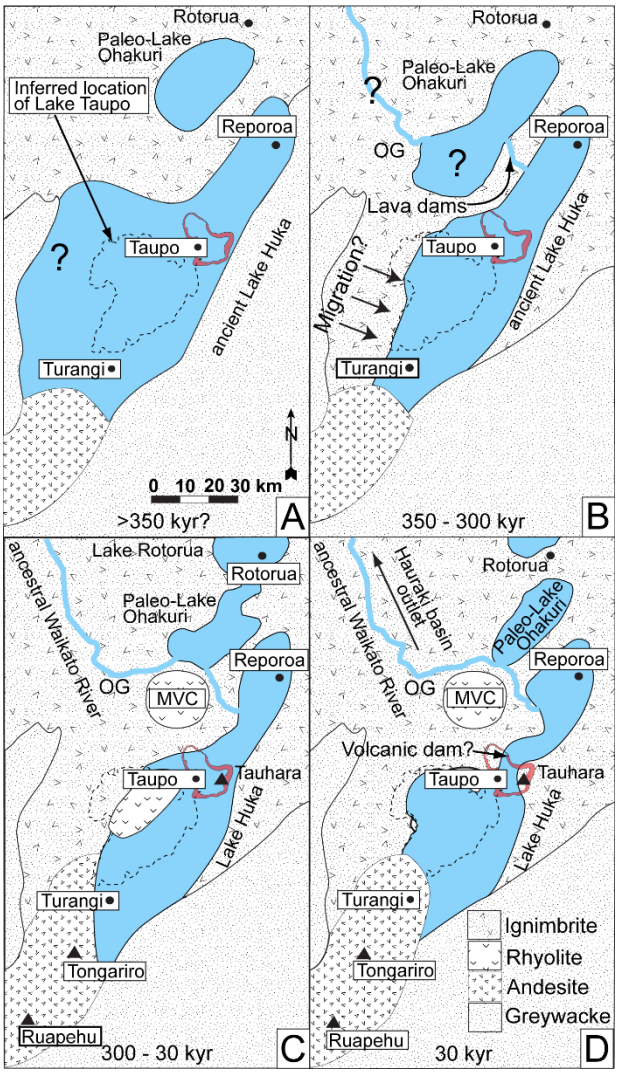

Figure 6.4. An early conceptual interpretation of Lake Huka and Lake Taupo evolution modified from Timperley (1983). **A.** ancient Lake Huka at >350 ka accommodated by the broad single TVZ basin (Downs et al., 2014a). **B.** 350 – 300 kyr easterly Lake Huka migration into TRB following the Whakamaru eruption. **C.** Between 300 – 30 kyr Lake Huka was dominantly hosted by TRB and **D.** Young Lake Huka at 30 kyr prior to Oruanui eruption MVC = Maroa Volcanic Centre, OG = Ongaroto Gorge.

Given the limited evidence on the form, structure and morphology of Lake Huka, its properties may be inferred from present-day Lake Taupo given their similar tectonic and volcanic location. Like Lake Taupo, the eastern and western ancient lake's margins were probably maintained by major NE-trending faults (e.g., Waihi, Whakaheke and Kaingaroa Faults; Fig. 6.3A) maintaining steeply faulted cliffs surrounding the lake (e.g., Fig. 6.3D). Bordering cliffs, together with intra-lacustrine lava dome islands and peninsulas (e.g., Fig. 6.3E-F), were likely major contributing sedimentary sources at the lake margin. Siltstone and fine sandstone dominating the Huka Falls Formation and interbedded within the Waiora Formation are consistent with deposition in the deep basinal facies of Lake Taupo (Nelson & Lister, 1995). These deep water facies identify areas of Lake Huka covering Wairakei-Tauhara originally >150 m deep (Chapter 3). The ancient catchment area and drainage pattern has probably remained near similar between Lake Taupo and Lake Huka. Lake Huka is also inferred to have utilised a dominant southern feeder river and a northern drainage outlet (e.g., Fig. 6.3B). The path of an ancestral Waikato River is inferred to have drained Lake Huka at its western margin. Ancestral Waikato River probably connected with proto-Lake Ohakuri before passing through the Ongaroto Gorge and draining in the north at Hauraki Basin (Fig. 6.4C-D; Leonard, 2003; Manville & Wilson, 2004; Manville et al., 2005; McCraw 2011; Downs et al., 2014a).

HISTORY AND STRATIGRAPHY OF THE HUKA GROUP

The long history of drilling at Wairakei-Tauhara has resulted in numerous descriptions of Huka Group deposits and suggestions of its geological origins (Grindley, 1965; Steiner, 1977; Healy, 1984; Wood, 1994a; Wood & Browne, 2000; Rosenberg et al., 2009a; Bignall et al., 2010a). Recent drilling has refined the field's stratigraphic architecture and new local units have been identified (Bignall et al., 2010a). The following section reviews all currently identified geological units and interpretations of their histories from Bignall et al. (2010a) and drilling data provided by Contact Energy (Table 6.1). This assessment uses Reference Section stratigraphy from WKM15 (Chapter 2) for field-wide stratigraphic correlation (Fig. 6.5A-B). Comparisons are made between the type of Huka Group strata and plausible regional analogues in the TVZ highlighting depositional similarities.

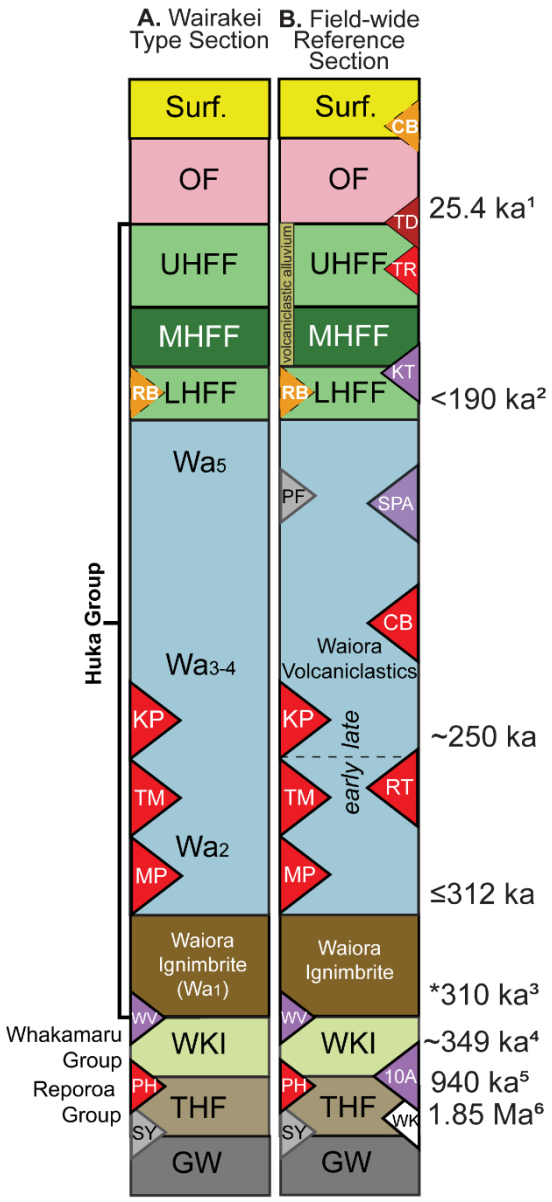

Figure 6.5. Comparison between the existing **A.** Type Section (after Rosenberg et al., 2009a) and **B.** Reference Section stratigraphic models for Wairakei-Tauhara. Interbedded and local units are in triangles. Surf. = surficial sediments and tephra, OF = Oruanui Formation; U/M/LHFF = Upper/Middle/Lower Huka Falls Formation; CB = Crown Breccia, TD = Tauhara Dacite, TR = Trig Rhyolite, KT = K-Trig Basalts, RB = Rautehuia Breccia, PF = Polo Flats Ignimbrite, SPA = Spa Andesite, CB = Crowbar Rhyolite, KP = Karapiti Rhyolite, RT = Racetrack Rhyolite, TM = Te Mihi Rhyolite, MP = Mapara Rhyolite. WKI = Wairakei Ignimbrite, WV = Waiora Valley Andesite, THF = Tahorakuri Formation, 10A = 10A Andesite, PH = Poihipi Rhyolite, WK = Waikora Formation, SY = Stockyard Ignimbrite. Ages are inferred from: 1: Vandergoes et al. (2013); 2: Wilson et al. (1995); ~250 ka is approximated in this chapter; 3: Rosenberg et al. (2014); 4: Downs et al. (2014a); 5: Wilson et al. (2015); 6: Chambefort et al. (2014).

Waiora Ignimbrite

The Waiora Ignimbrite at Tauhara (in TRB) occurs as ~4 composite sheets (TH9; Milicich et al., 2008a) and has only been drilled in one area of western Wairakei (WK215, WK219; Table 6.1; 2014 Contact). Models estimate a total volume of ~150 km^3, a volume comparable to other caldera-derived ignimbrites

in TVZ (Wilson et al., 1995; 2009). The great thicknesses of Waiora and the underlying Wairakei Ignimbrites at Wairakei-Tauhara indicate they are over-thickened intra-caldera deposits (Table 6.1; Wilson et al., 1986). Between the two ignimbrites, Wood (1994a) recognised a similar mineral assemblage (but in different proportions). He suggested Waiora Ignimbrite could be a late stage ignimbrite from Whakamaru caldera that locally erupted and collected in an accommodating depression (i.e., TRB subsidence or caldera depression; Wood, 1995). Recent whole-rock geochemistry support a Whakamaru-type magma source (Chapter 4).

Age constraints for stratigraphy at Wairakei-Tauhara are currently limited. Rosenberg et al. (2014) has reported a preliminary age of ~310 ka for Waiora Ignimbrite following ~349 ka Wairakei Ignimbrite. This age marks the commencement of Huka Group volcanism at Wairakei-Tauhara (Fig. 6.5B).

Waiora Volcaniclastics

Existing bracketing dates indicates that the Waiora Volcaniclastics represents up to 100 kyr of pyroclastic, lava, reworked volcanogenic and lacustrine deposition within a long-lived lacustrine environment (Table 6.1; Chapters 2 – 4; Wood & Browne, 2000; Rosenberg et al., 2009a). Coring at the Wairakei Block intersected at least seven, 20 – 40 m thick Waiora Volcaniclastics beds (Fig. 6.2, WKM14, WKM15; Chapter 2). Facies relationships identified all Huka Group deposits at Wairakei-Tauhara, and some vents, are sublacustrine (Chapters 2 and 3).

As similar stratigraphic grouping of thick, mixed composition, nondescript volcaniclastic and sedimentary basin-fill occurs in ~1.85 Ma Tahorakuri Formation from central TVZ (Gravley et al., 2006; Eastwood et al., 2013). Both Tahorakuri and Waiora Formations preserve insights into temporally-dominant caldera inter-eruption landscapes and volcanic and sedimentary processes in early TVZ (Chambefort et al., 2014). Major distally sourced tephras have previously been thought to be interbedded within Waiora Volcaniclastics (Wood, 1994a). Wood (1994a) suggested that distally-sourced ~281 ka Kaingaroa Ignimbrite (Nairn et al., 1994; Downs et al., 2014a) may occur in well WK227 (Fig. 6.2; here termed ‘Polo Flats Ignimbrite’; Table 6.1). However, subsequent mineral chemistry (Beresford, 1997), whole-rock geochemistry and the stratigraphic position (Chapter 4) have

since discounted this suggestion and indicate that Polo Flats Ignimbrite is likely younger and more locally sourced (Fig. 6.5B; Chapter 4).

Rhyolitic lavas buried within Waiora Volcaniclastics are geographically clustered in western Wairakei where intersecting TFB faults likely serve as eruptive pathways (Fig. 6.2; Table 6.1; Rosenberg et al., 2009a). Their morphology and eruptive history can be inferred when multiple drilled intersections and correlations have been made. Most lavas in Wairakei-Tauhara have thicknesses consistent with rhyolite dome morphologies (e.g., Te Mihi 1 – 4; Mapara 1 – 4; Karapiti 1, 2a, 2b, 3;). However, lava morphologies consistent with composite andesite lava flows (e.g., Waiora Valley and Spa Andesites) and rhyolite intrusions types (e.g., Racetrack Rhyolite) have also been previously recognised (Chapter 2).

Huka Falls Formation

Lower and Upper Huka Falls Formation Members record lacustrine sedimentation deep in central Lake Huka (Fig. 6.4A-D; Table 6.1). Equivalent local stratigraphic units in Wairakei-Tauhara include Rautehuia Breccia in northwestern Wairakei: a muddy, localised lithic breccia that erupted in Lake Huka (Figs. 6.5B; Grindley 1965; Rosenberg et al., 2009a). South of Wairakei-Tauhara local K-Trig basalts include 100 – 200 ka phreatomagmatic Acacia Bay and Kaiapo tuffs and the ~140 ka magmatic Punatekahi scoria cones (Fig. 6.3A; Brown et al., 1994). The shallow pyroclastic Middle Huka Falls Formation is local to Wairakei-Tauhara and pinches laterally from near central Tauhara (Rosenberg et al., 2009a). Its distribution and internal lithological variations is well constrained by many well intercepts, allowing for an eruption, transport and depositional history to be established (Chapter 3).

Siltstone, sandstone and pebbly silt comprising Upper Huka Falls Formation outcropping along the Waikato River valley preserve ancient turbidite gravity flows deposited deep in Lake Huka (Table 6.1; Chapter 2). Similar ancient lacustrine deposits occur elsewhere in TVZ beyond the TRB (Manville, 2001; Downs et al., 2014a; in press) including Kawerau (Fig. 6.1B; Grindley, 1986; Milicich et al., 2013), Ngakuru-Guthrie grabens (Fig. 6.1A; Grindley, 1963; Langridge, 1990) and in northern Whakamaru caldera (Fig. 6.1A; Leonard, 2003; Gravley, 2004). Their prevalence identifies the widespread occurrence of lakes in central TVZ during the past >300 kyr inter-eruptive period (Fig. 6.4A-D).

Widespread stratigraphic units (Fig. 6.5B)	Local stratigraphic units (Figs. 6.2 & 6.5B)	Estimated age (ka)	Intersected locations (Fig. 6.2)	Average (& max) drilled thickness (m)	Composition & lithology	Interpreted deposit	TVZ analogue example
Oruanui Formation	→	25.4 [A]	Field-wide	120 (170)	Rhyolite ash & accretionary lapilli	PDC and air fall deposits	Comprehensively studied[1]
Huka Falls Formation (Huka Group)	→	>190-28[B]	Field-wide	200-300 (600)	Volcanogenic & biogenic siltstone	Lacustrine suspension & turbidite	Lake Taupo sediments[2]
	Trig	28[B,C]	E. Tauhara	109	Rhyolite lava (quartz-bearing)	Dome	TVZ rhyolite domes[3]
	K-trig	~140[D]	Out-field	80-100	Basalt lava & tephra	Magmatic & phreatomagmatic	Tarawera Basalts[4]
	Middle Huka Falls	~150	Field-wide	80-100 (200)	Rhyolite pumice-lapilli tuff	Sublacustrine density current	Rautehuia Breccia[5]
	Hipaua	≤190[E]	E. Tauhara	>170 m	Dacite lava	Cryptodome & dome components	Kawerau Andesite[6]
	Rautehuia Breccia	<190	N. Wairakei	130 (228)	Angular lithic breccia, silty matrix	Magmatic & hydrothermal eruption	Rotomahana mud[7]
Waiora Volcaniclastics (Huka Group)	→	<310->190	Field-wide	300-400 (1085)	Primary & reworked volcaniclastics	Basin-fill volcaniclastics	Tahorakuri Formation[8]
	Mapara 4	<150	Out-field	98	Rhyolite lava (quartz-poor)	Dome or cryptodome	TVZ rhyolite domes[3]
	Te Mihi 1	<200	W. Wairakei	420	Rhyolite lava (quartz-bearing)	Cryptodome, partially extrusive	Hipaua dome[9]
	Racetrack	200-150	E. Tauhara	200 (285)	Rhyolite lava (quartz-poor)	Cryptodome (or laccolith)	Putauaki intrusions[6]
	Polo Flats*	250-200	Out-field	25 (40)	Welded to sintered grey ignimbrite	Local ignimbrite	Kaingaroa Ignimbrite[10]
	Crowbar	250-200	S. Tauhara	368	Rhyolite lava (quartz-free)	Dome or cryptodome	TVZ rhyolite domes[3]
	Mapara 3	250-200	Out-field	445	Rhyolite lava (quartz-poor)	Dome or cryptodome	TVZ rhyolite domes[3]
	Karapiti 1	~220	N. Wairakei	112	Rhyolite lava (quartz-free)	Brecciated dome	TVZ rhyolite domes[3]
	Te Mihi 2	≤250	Out-field	44	Rhyolite lava (quartz-bearing)	Dome or cryptodome	TVZ rhyolite domes[3]
	Spa	~250	W. Tauhara	200	Andesite lava	Ponded composite lava flows	Tongariro lavas[11]
	Karapiti 2a	~250	Wairakei	140 (490)	Rhyolite lava (quartz-free)	Dome composite (± flows)	Maroa dome complex[12]
	Karapiti 2b	≤310	W. Wairakei	120 (390)	Rhyolite lava (quartz-free)	Dome composite (± flows)	Maroa dome complex[12]
	Karapiti 3	≤310	N. Wairakei	150	Rhyolite lava (quartz-free)	Brecciated domes & flows	TVZ rhyolite domes[3]
	Te Mihi 3	≤310	W. Wairakei	235	Rhyolite lava (quartz-bearing)	Brecciated domes & flows	TVZ rhyolite domes[3]
	Mapara 1	≤310	Out-field	25	Rhyolite lava (quartz-poor)	Brecciated domes & flows	TVZ rhyolite domes[3]
	Mapara 2	≤310	Out-field	335	Rhyolite lava (quartz-poor)	Brecciated domes & flows	TVZ rhyolite domes[3]
	Te Mihi 4	350-310	S. Wairakei	28	Rhyolite lava (quartz-bearing)	Brecciated domes & flows	TVZ rhyolite domes[3]
Waiora Ignimbrite (Huka Group)	→	~310 [F]	Tauhara	600-700 (1500)	Rhyolitic ignimbrite	3-4 ignimbrite sheets	Whakamaru ignimbrites[13]
	Waiora Valley	≤310	N. Wairakei	182	Andesite lava	Composite lava flows?	Tongariro lavas[11]
	10A	>310	S. Tauhara	693	Andesite lava	Andesite cone	Rolles Peak Andesite[14]
Wairakei Ignimbrite (Whakamaru Group)	→	~349[F]	Wairakei	500-600 (1115)	Rhyolitic ignimbrite	~3 ignimbrite sheets	Rangitaiki ignimbrite[13]
	Nukuhau Andesite(?)	*>350*	*Magnetic anomaly only*	*~1500*	*Composite andesite lavas?*	*Stratocone*	*Mt. Ngauruhoe cone[11]*

Table 6.1. Summary of drilled thicknesses, locations and deposit analogues of widespread and local Huka Group lithostratigraphic units mentioned in the text identified in Wairakei-Tauhara from Bignall et al. (2010a) and 2014 Contact. Actrix (*) denotes new or redefined units discussed in the text. Age estimates are both confirmed and inferred TVZ stratigraphic correlatives: A. Vandergoes et al. (2013); B. Rosenberg et al. (2009a); C. Vucetich and Howorth (1976); D. Grindley (1960; 1961); E. Wilson et al. (1995); F. inferred age by Downs et al. (2014a). TVZ analogue deposits are identified to be lithologically or morphologically similar to deposits or landforms in the Huka Group: 1. Wilson (2001); 2. Nelson and Lister (1995); 3. Wilson et al. (1995); 4. Walker et al. (1984) 5. Bignall et al. (2010a); 6. Milicich et al. (2013); 7. Nairn (1979); 8. Gravley et al. (2006); 9. Rosenberg and Kilgour (2003); 10. Beresford and Cole (2000); 11. Cole (1978); 12. Leonard (2003); 13. Brown et al. (1998a); 14. Browne et al. (1992).

Depositional and structural order of events

Underlying Wairakei-Tauhara is a horst (block ridges) and graben (basins) structural arrangement (Grindley, 1965; Rosenberg et al., 2009a). Beneath central Wairakei field is Wairakei Block and to the west is Kaiapo Graben, the southeastern section of TFB (Fig. 6.2). The Tauhara field is underlain by TRB. The distribution of Huka Group indicates a spatially complex depositional history within the Kaiapo Graben (in TFB) and TRB, with later modification by faulting, differential subsidence and erosion (Rosenberg et al., 2009a; Bignall et al., 2010a). Stratigraphy of the ridge between the two basins (Kaiapo Graben and TRB) suggests Wairakei Block remained stable following ~349 ka (since Wairakei Ignimbrite emplacement), relative to the flanking basins. Following the field's structural interpretation by Rosenberg et al. (2009a) and regional structural correlation, a major horst structure is interpreted to occur along the centre of TVZ separating subsiding rift basins (Fig. 6.1A, Paeroa-Wairakei Blocks; Wilson et al., 2010; Downs et al., 2014a). Sedimentary features identified in the Huka Group for this study allows for proposal of deposition sequences, sediment sources and the structural development, illustrated as stages in Fig. 6.6A-H.

Taupo-Reporoa Basin, Tauhara

Emplacement of ~349 ka Wairakei Ignimbrite coincided with formation of the regional TFB and TRB (Fig. 6.6A; Downs et al., 2014a). Prior to Wairakei Ignimbrite, 10A Andesite (Fig. 6.5) erupted along eastern TRB and the TVZ margin where it probably utilised basement fault pathways (Fig. 6.6B). Drilling has intersected highly offset Wairakei Ignimbrite west (Kaiapo Graben) and east (TRB) of Wairakei Block. Wairakei Ignimbrite is rarely intercepted by drilling in Tauhara. Directly north of Tauhara at Rotokawa Geothermal Field, 200 – 390 m of Wairakei Ignimbrite has been drilled (Rae, 2007). At this location it may be preserved from erosion or high subsidence by occurring on a stable local structure (Fig. 6.2). The ignimbrite's distribution support its original emplacement across Wairakei-Tauhara, likely followed by very high subsidence in TRB (beyond current drilling depths), subsiding over ~37 kyr before Huka Group deposition commenced (Fig. 6.6B).

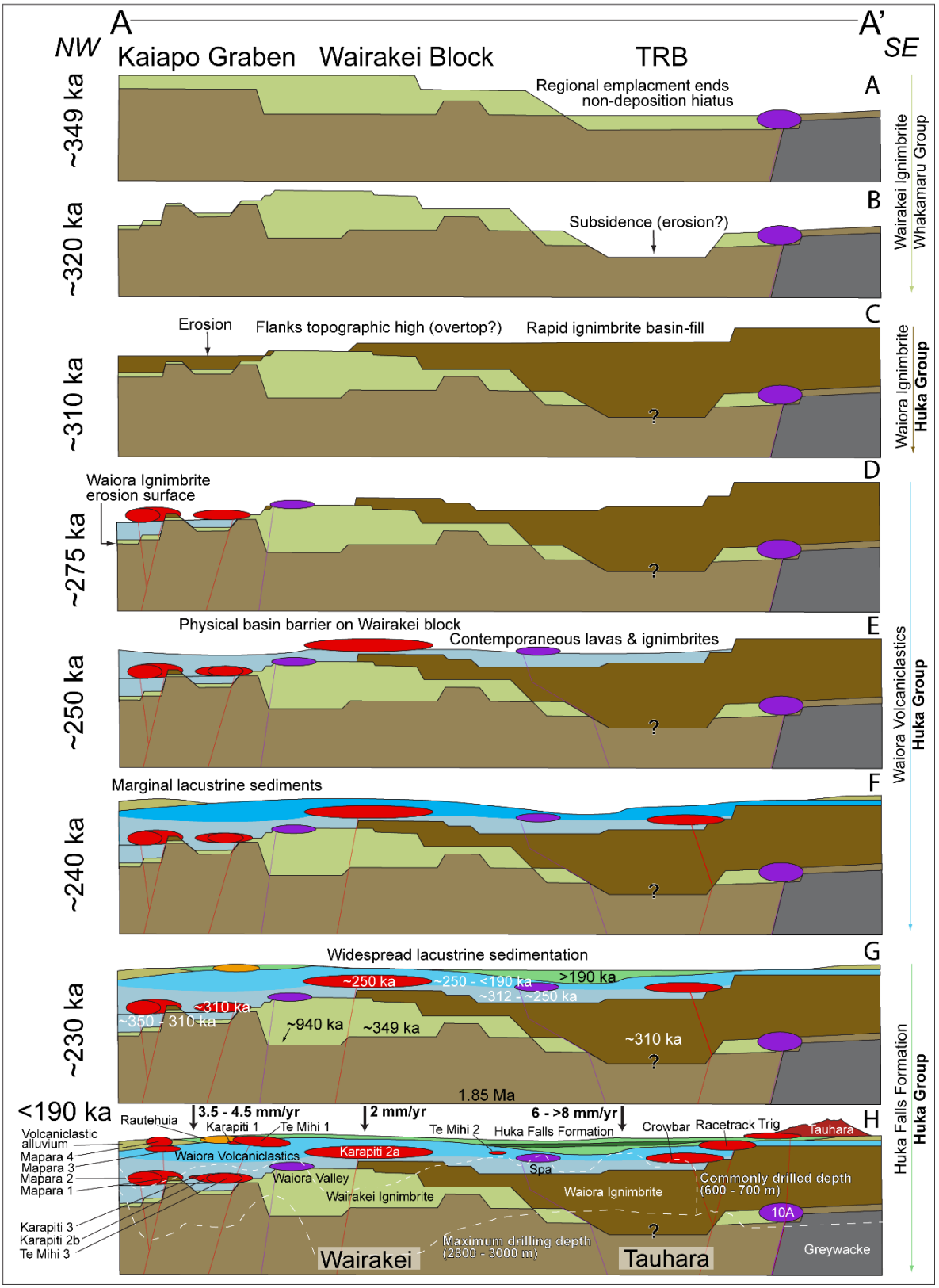

Figure 6.6. Interpreted emplacement sequence cross-section A–A' (through Fig. 6.2) of **A.** Whakamaru ignimbrite emplacement; **B.** and subsidence followed by Pre-Waiora sediments basin-fill; **C.** Waiora Ignimbrite sheets fill TRB and flank Wairakei Block; **D.** Waiora Ignimbrite erosion (or non-deposition) and lava extrusion in Kaiapo Graben; **E.** Early Waiora Volcaniclastics gradually fill Kaiapo Graben and TRB contemporaneous with lava extrusion; **F.** Late Waiora Volcaniclastics continue to fill Kaiapo Graben and TRB; **G.** Lower Huka Falls Formation sedimentation and lava accumulation. **H.** Middle and Upper Huka Falls Formation deposition with contemporaneous lavas. Black arrows represent field-local subsidence and estimated rates from geology well logs. Stratigraphic colours and inferred dates are in Fig. 6.5B and discussed in the text. Dikes using faults as feeder pathways is inferred. Conceptual figure made using 3D Geological model. Ages referenced in Fig. 6.5.

Huka Group deposition commenced as four or more successive Waiora Ignimbrite sheets inferred at ~310 ka. The sheets episodically filled TRB, eventually following over or around Wairakei Block paleo-high thinly covering Kaiapo Graben area (Fig. 6.6C). These events may have 'levelled off' the TRB and Kaiapo Graben depressions, temporarily forming a broad depocentre across Wairakei-Tauhara. Following Waiora Ignimbrite, reworked clastic material accumulated in the basins forming early Waiora Volcaniclastics (Fig. 6.6E). High deposition rates filled the subsiding basins and buried the Wairakei Block.

Lava emplacement mechanisms are inferred from lithostratigraphic relationships and textural analysis (Chapter 2). Contemporaneous extrusion with Waiora Volcaniclastics involved >4 now buried lavas (Fig. 6.6G; Mapara, Te Mihi, Karapiti, Spa, ± Crowbar) and at least 1 cryptodome/laccolith (Racetrack). Racetrack Rhyolite was previously suggested to be a cryptodome, probably post-dating Waiora Volcaniclastics and possibly ~190 ka Hipaua dome, Tauhara Dacite (Chapter 2; Fig. 6.6H; Rosenberg & Kilgour, 2003; Rosenberg et al., 2009a). Near cental Tauhara, Spa Andesite lava flows were emplaced on to ~300 m of early Waiora Volcaniclastics (Fig. 6.6E; 2014 Contact). A common stratigraphic elevation (~-200 mRL) exists between Spa Andesite and much of Karapiti 2a. This could reflect a coeval depositional surface if minimal differential offset has occurred since extrusion. Extrusion of voluminous Karapiti 2a lavas are interpreted to have formed a physical depositional barrier between the basins on the buried Wairakei Block (Fig. 6.6E; see next sub-section). Waiora Volcaniclastics deposition, following Karapiti 2a emplacement, filled Kaiapo Graben and TRB eventually overwhelming the rhyolite barrier and burying Karapiti 2a (Fig. 6.6F).

Later, the basins became filled with reworked volcaniclastic and interbedded lacustrine sediments gradually depositing 50 – 150 m of Lower Huka Falls Formation (Fig. 6.6G). Local eruption of the Middle Huka Falls Formation pyroclastic deposits ending Lower Huka Falls Formation sedimentation (Fig. 6.6H; Chapter 3). When lacustrine quiescence resumed, lacustrine sedimentation gradually deposited 50 – 100 m of Upper Huka Falls Formation. Coalesced Mt Tauhara Dacite domes periodically extruded contemporaneously with Huka Falls Formation sedimentation. Prior to Huka Falls Formation termination by the 25.4 ka Oruanui eruption, in the east Trig Rhyolite, the youngest rhyolite

at Wairakei-Tauhara, extruded onto the shallow soft lacustrine sediments (Fig. 6.6H; Rosenberg et al., 2009a).

Kaiapo Graben (TFB) and Wairakei Block, Wairakei

The numerous geothermal wells at Wairakei have intersected a distinct, structurally-influenced stratigraphic sequence (Rosenberg et al., 2009a). In Kaiapo Graben, west of the stable Wairakei Block, Wairakei Ignimbrite is offset by erosion and extensional thinning of underlying Tahorakuri Formation (Figs. 6.2 & 6.6B).

In western Wairakei, located between underlying Wairakei Ignimbrite and overlying Mapara Rhyolite lavas (1 and 2; <~900 m depth), is a 350 – 500 m thick volcaniclastic sequence currently assigned to Waiora Formation (Rosenberg et al., 2013; WK224). Lithic clasts petrographically consistent with reworked Wairakei Ignimbrite have previously been identified as comprising the unit (Rosenberg et al., 2013). The deposit could insted reflect older re-worked Wairakei Ignimbrite that rapidly accumulated in the subsiding Kaiapo Graben prior to Waiora Ignimbrite emplacement (>310 ka) but after Wairakei Ignimbrite (<349 ka), rather than during the younger Waiora Volcaniclastics period (<310 ka). However, comprehensive isotopic dating of interbedded or overlying marker units is needed before such stratigraphic relationships can be confidently established for this deposit. Overlying Mapara Rhyolites 1 and 2 are inferred to have then erupted onto an ancient depositional surface between <310 and approximately >275 ka (Fig. 6.6D; Table 6.1). Limited chronostratigraphic evidence restricts interpretation of Te Mihi 3 and Karapiti 2b and 3 lavas in western Wairakei (Fig. 6.2). Using their stratigraphic positions, the three lavas are tentatively inferred to have been extruded (*cf.* activity at MVC; Leonard, 2003) over a short time period (i.e., between <310 – 275 ka; Fig. 6.6D), but better understanding of their histories requires detailed dating and further drilling.

Waiora Ignimbrite is infrequently intersected by drilling at Wairakei. Its absence is likely due to thin primary emplacement (Fig. 6.6C), probably followed by a period of erosion (Fig. 6.6D).

While Waiora Volcaniclastics deposition was contemporaneous between Kaiapo Graben and TRB, sedimentary and pyroclastic material intersected by drilling in each of the basin is interpreted to have been dominantly locally sourced. Local sources, together with the Wairakei Block physically

limiting basin sediment exchange, resulted in distinct stratigraphic sequences between the basins underlying the Wairakei and Tauhara Fields (restricting use of detailed stratigraphic models between the two; Chapter 2). Early Waiora Volcaniclastics deposits in Kaiapo Graben (Grindley's (1965) Member 2) are petrographically similar to the quartz-bearing Waiora and Wairakei Ignimbrites. The early deposit may consist of these early reworked ignimbrites (Brown, 1994), mixed with local pyroclastics and sediments (Fig. 6.6E), such as from early Mapara and Karapiti lavas. Late Waiora Volcaniclastics beds are yet to be correlated with specific source vents. Contemporaneous local lava eruptions (late Te Mihi, Karapiti, Mapara Rhyolites) and prevailing lacustrine environments are probably major contributing sources.

In northwestern Wairakei several shallow rhyolites (<-400 mRL) are interbedded with Waiora Volcaniclastics including Mapara 3 and 4, Karapiti 1, Te Mihi 1 and 2 (Fig. 6.2). The lavas are late domes or younger shallow cryptodomes (Fig. 6.6H); however, interpreting their emplacement origins (intrusion or extrusion) is difficult given limited sample and restricted evidence from drill cuttings and core. Highly offset elevations of Te Mihi 1 Rhyolite between Wairakei wells (Fig. 6.3; Grindley, 1965) may reflect significant faulting. Alternatively, the offset is a primary depositional feature forming a lava with significant surface topography resulting and a dome with both primary cryptodome and extrusive characteristics (Fig. 6.6H; *cf.* Hipaua dome; Rosenberg & Kilgour, 2003).

Huka Falls Formation first accumulated deep in the submerged basins (Fig. 6.6G; Grindley. 1965). West of Wairakei, shallower drilling (<0 mRL) intersected coarser grained volcaniclastic alluvium that is a lateral facies correlative of the Huka Falls Formation (Fig. 6.6F). In northwest Wairakei, up to 100 m of Lower Huka Falls Formation was locally excavated through phreatic to phreatomagmatic eruptions forming the 228 m thick Rautehuia Breccia deposit (Fig. 6.6G; 2014 Contact). Middle Huka Falls Formation was later emplaced across eastern Wairakei area (50 – 100 m thick), followed by sedimentation of Upper Huka Falls Formation (50 – 100 m thick) in the TRB.

DISCUSSION

Huka Group subsidence and depositional rates

Subsidence across the Wairakei-Tauhara district is controlled by regional extension and inferred caldera collapse (Grindley, 1965; 1982; Wilson et al., 1986; Villamor & Berryman, 2001; Rosenberg et al., 2009a). The relative contribution of these two mechanisms on the structure of Wairakei has long been debated (Grindley, 1982; Healy, 1984; Wood et al., 1997; Wood, 1998; Rosenberg et al., 2009a). More than 3 km of ignimbrites, lavas and sediments have been intersected by drilling at Wairakei-Tauhara (WK408; 2014 Contact). As some stratigraphic ages used in this study are correlated from strata elsewhere in TVZ, calculated long-term subsidence rates made for Wairakei-Tauhara are approximate net values.

Dominant volcaniclastic deposits at Wairakei filling Kaiapo Graben support a history of gradual subsidence balanced by gradual basin filling in the west. In contrast, thick Waiora Ignimbrite in Tauhara supports a history of rapidly formed accommodation space and over-thickened episodic basin-fill (Fig. 6.6C). Presently, deepest drilling at Wairakei terminates in ~1.85 Ma Tahorakuri Formation at 3011 m (WK408; Fig. 6.2; Chambefort et al., 2014; 2014 Contact). Assuming long-term sedimentation rates are comparable to subsidence (and erosion) rates, 3011 m of total subsidence over 1.85 Ma yields a long-term net rate of >1.7 mm/yr in Wairakei. As regional comparisons, Tahorakuri Formation deposition at Ngatamariki has been calclated between ~0.3 – 10 mm/yr (Chambefort et al., 2014) and long-term gradual lake sedimentation in TVZ is ~0.3 – 1.4 mm/yr (Smith et al., 1993; Nelson & Lister, 1995).

The Huka Group at Wairakei-Tauhara is up to 1000 – 1300 m thick in Wairakei, 1800 – >2300 m thick in Tauhara and 550 – 600 m thick on Wairakei Block (2014 Contact). Tentative depositional age constraints proposed for Huka Group between 310 ka and 28 ka yield ~282 kyrs of total deposition. (Rosenberg et al., 2009a; 2014) Calculated cumulative maximum subsidence rates are, therefore, between 3.5 – 4.5 mm/yr at Wairakei, 6.3 – >8 mm/yr at Tauhara, and 1.9 – 2.1 mm/yr at Wairakei Block (Fig. 6.6H). Estimated subsidence rates for Kaiapo Graben (southern TFB) and Wairakei Block are comparable to existing calculated rates in central TVZ basins (3 – 5 mm/yr; Manville, 2001;

Villamor & Berryman, 2001; Rosenberg et al., 2009a; Downs et al., 2014a). Excluding Wairakei Block subsidence, rates at Wairakei-Tauhara are higher than those previously calculated for other TVZ geothermal fields located outside the active basins (<0.2 – 2 mm/yr; Wilson et al., 2010).

Subsidence at western Wairakei during deposition of the Huka Group (3.5 – 4.5 mm/yr between 310 – 28 ka) is twice the calculated long-term rate (1.7 mm/yr after 1.85 Ma). The increase could reflect major episodic subsidence caused by Whakamaru caldera collapse. Subsidence at Tauhara has occurred at twice the rate identified at northern TRB (Downs et al., 2014a). Gravity studies in the TRB have identified internal depression centres (sub-basins) including Reporoa caldera (Nairn et al., 1994) and Mihi volcanic depression (Soengkono, 2012). Regional gravity studies identify a negative gravity anomaly at southern TRB beneath Tauhara (Bibby et al., 1995). Subsidence in Tauhara may be localised in a sub-basin (Tauhara depression?), possibly overprinted by Whakamaru caldera-related subsidence. Dating of specific Waiora Ignimbrite and Huka Group marker units in Wairakei-Tauhara will refine these rates allowing relative volcano-tectonic and tectonic controls to be more confidently estimated (e.g., Rosenberg et al., 2014).

Complete Huka Group dynamic chronology

Depositional environments at Wairakei-Tauhara have been controlled by long-term tectonism and episodic large-scale volcanism. The order of these processes and their influence on surface environments are interpreted and illustrated as a series of conceptual 3D diagrams in Fig. 6.7A-F.

Prior to emplacement of Wairakei Ignimbrite was a 600 kyr volcanic hiatus at Wairakei-Tauhara (Wilson et al., 2015). The depositional hiatus allowed regional extension to extensively thin Tahorakuri Formation regulating the broad basin originally occupying central TVZ (Downs et al., 2014a). Andesite cones and lava flows, likely analogous to volumetrically more significant TgVC andesites (Cole, 1978), were prevalent in TVZ until the ~349 ka Whakamaru eruption (e.g., 10A and Waiora Valley Andesites; Browne et al., 1992; Sanders et al., 2013; Chambefort et al., 2014). The regional geographic extent of the Whakamaru caldera must have had a considerable, but poorly understood influence on the structure and long-term subsidence of central TVZ (Fig. 6.1A; Wilson et al., 1986; Brown, 1994). Wairakei Ignimbrite emplacement, ending the field-local volcanic hiatus, is

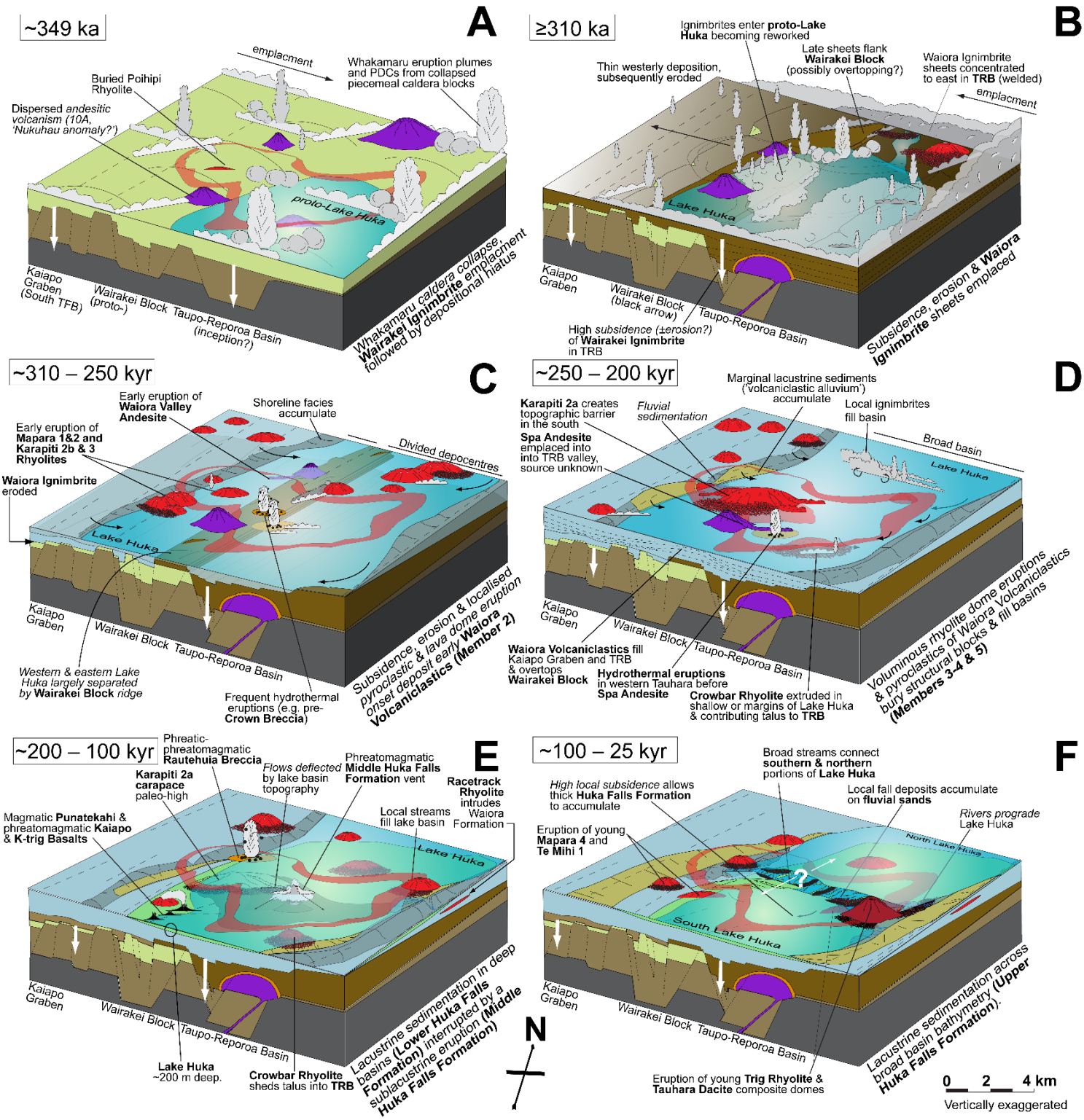

Figure 6.7. Time-series conceptual reconstruction of the events forming the Huka Group in Wairakei-Tauhara. **A.** Wairakei Ignimbrite emplaced by Whakamaru caldera ~349 ka and offsets stratigraphy. Proto-Lake Huka likely existed prior to this event. **B.** Waiora Ignimbrite sheets erupted ~310 ka covering Wairakei-Tauhara. **C.** Waiora Ignimbrite becomes eroded in Kaiapo Graben and capped by Mapara lavas. Early Waiora Volcaniclastics likely derived from reworked ignimbrites and local eruptions. **D.** Late Waiora Volcaniclastics likely sourced from local rhyolite eruptions. Wairakei block becomes buried. **E.** Lower and Middle Huka Falls Formations deposited in Lake Huka. Rautehuia Breccia, local rhyolites and K-trig basalts emplaced locally. **F.** Upper Huka Falls Formation sedimentation in Lake Huka. Lake become volcanically dammed and becomes increasingly fluvial. Mt Tauhara develops and young rhyolites erupt in Wairakei. Stratigraphic colours and inferred dates are in Fig. 6.5B.

petrographically, chemically and temporally consistent with the Rangitaiki Member (Briggs, 1976; Wilson et al., 1986; Brown et al., 1998a). Its eruption coincided with formation of TFB (local Kaiapo Graben) and TRB (Fig. 6.7A; Downs et al., 2014a).

Following Wairakei Ignimbrite emplacement, a submerged Wairakei Block acted as a depositional barrier between the flanking basins for ~100 kyr (Fig. 6.7B). Regional extension concentrated subsidence of Wairakei Ignimbrite in the basins to depths beyond current drilling at Tauhara (Figs. 6.6B & 6.7B; Rosenberg et al., 2009a).

Deposition of Waiora Ignimbrite at ~310 ka mostly occurred in the TRB (Fig. 6.7B). Its significant volume (modelled at >150 km^3) and over-thickened stratigraphy (1500 m) are equivalent to other TVZ intra-caldera deposits (Wilson et al., 1995; 2009). At least four variably-welded ignimbrite sheets are inferred to have erupted from a common, probably local source vent (*cf*. Paeroa fissure eruption; Downs et al., 2014b). Sheets were accommodated by a rapidly subsiding southern TRB separated by short sedimentation periods (e.g., ~10 kyr periods; Milicich et al., 2008a), gradually flooding the basin (Fig. 6.7B; Wood, 1995). The vent location is probably within or near the TRB and may coincide with southern Whakamaru caldera (Wilson et al., 1986). As the latest Waiora Ignimbrite sheet was deposited around the flaks of Wairakei Block (possibly overtopping), the density stratified currents overran Lake Huka (Chapter 2). Ignimbrite deposits may have been eroded or highly subsided in Kaiapo Graben, but were preserved on the upstanding Wairakei Block and in the TRB. The Waiora Ignimbrite erosion surface in the west may coincide with deposition surfaces of Mapara 1 and 2, Te Mihi 3 and Karapiti 2b and 3 lava domes (Fig. 6.7C), but comprehensive dating in the local area is required to confirm this relationship. Cored samples provided evidence for a TRB-hosted Lake Huka from at least this period (Chapter 2), but deeper, older lacustrine strata identified elsewhere in the field indicate lakes existed in the area prior to the Huka Group (e.g., Fig.6.4A-D; Rosenberg et al., 2009a; Downs et al., 2014a).

Following the late Waiora Ignimbrite sheet, there was deposition of layered volcaniclastic and lacustrine deposits that comprise the Waiora Volcaniclastics. Early deposits were likely a mixture of reworked Waiora Ignimbrite and local pyroclastic eruptions. A source for the late Waiora Volcaniclastics remain unclear. It is, however, temporally consistent with pyroclastic material

associated with lavas (Mapara (1 and 2), Te Mihi (3), Karapiti (2b and 3) and Waiora Valley), local pyroclastic and hydrothermal eruptions (*cf.* Rautehuia Breccia and Middle Huka Falls Formation eruptions; Chapters 2 & 3; Fig. 6.7C).

Prior to eruption of Karapiti 2a, estimated from stratigraphic constraints and sedimentation rates to be at ~250 ka, Waiora Volcaniclastics had filled the adjacent basins and buried Wairakei Block by 300 m (Fig. 6.7D; 2014 Contact; Chapter 3). Eruption of Karapiti 2a remains poorly understood. Its morphology is likely analogous to present-day lavas at MVC, consisting of amalgamated lava domes, flows and resedimented talus (Fig. 6.1A; Leonard, 2003). Important to note is its substantial thickness and lateral extent (Fig. 6.2; Table 6.1) which likely formed a local topographic barrier between the eastern and western lake basins in the Wairakei-Tauhara area (Fig. 6.7D). The thickness of Karapiti 2a suggest it was partially subaerial in Lake Huka forming an island similar, albeit probably larger, to those in present-day TVZ volcanogenic lakes (e.g., Motutaiko Island; Fig. 6.3E).

Subaqueously extruded lavas including Karapiti 2a and Crowbar Rhyolites (Fig. 6.7E-F) should include a hyaloclastite facies (e.g., McPhie et al., 1993, p. 54). To date no such facies are recognised in drillings. Clastic subaqueous facies would have contributed significant material to the filling basins (Manville et al., 2009). Evidence for quench fragmentation was previously identified in cored Waiora Volcaniclastics (e.g., THM18; Rosenberg et al., 2009b; Chapter 2). Brecciation and hyaloclastite between successive Spa Andesite lava flows support layered emplacement in a confined sublacustrine valley. (Fig. 6.7D; Chapter 2). Previously, Spa Andesite lava flows have been inferred to have been possibly sourced from a geophysical magnetic anomaly identified south of Wairakei (Rosenberg et al., 2009b) interpreted as a ~1500 m tall, buried andesite cone, "Nukuhau stratocone" (Fig. 6.2; Studt, 1958; Soengkono & Hochstein, 1992; Hunt et al., 2009). However, in the absence of direct evidence, this inferred relationship for the Spa Andesite source vent remains speculative.

Volcanic quiesence and continued subsidence allowed Huka Falls Formation lacustrine sedimentation to accumulate deep in Lake Huka (Fig. 6.7E). West of the Wairakei Field, contemporaneous coarser grained 'volcaniclastic alluvium' accumulated in a shallow lake shelf or margin environment where water energy was higher (*cf.* Lake Taupo shelf sediments; Nelson & Lister, 1995). Contemporaneous with Lower Huka Falls Formation sedimentation, eruption of Rautehuia

Breccia beneath Lake Huka commenced with a phreatomagmatic phase (Fig. 6.7E; Rosenberg et al., 2009a; Bignall et al., 2010a). As the eruption progressed, magmatic material decreased and the eruption became increasingly phreatic as it continued excavating overlying lacustrine substrate. Over-thickened Rautehuia Breccia deposits drilled along Te Mihi or Kaiapo faults (WK235, 205 m thick) could coincide with the vent location where radial subaqueous mass flows are interpreted to have transported material >1.2 km. Analogous to 1886 Tarawera scoria and the Rotomahana mud (Nairn, 1979; Bogie et al., 1995), Bogie et al. (1995) suggested Rautehuia Breccia and K-trig basalt eruptions may be contemporaneous with a common Kaiapo fault trigger. The absence of basalt in the breccia (Grindley, 1965; Bignall et al., 2010a), however, supports separate eruption mechanisms.

Lacustrine sedimentation was interrupted further from a ~200 m deep vent in northern Tauhara erupting Middle Huka Falls Formation (Chapter 3). The eruption occurred as a series of water-supported volcaniclastic density currents travelling up to 7 km beneath Lake Huka (Chapter 3). Density currents crossing the fields were controlled by subaqueous topography and lake bathymetry (e.g., Kokelaar et al., 2007). Directly north of the Karapiti 2a local high in Lake Huka, Middle Huka Falls Formation locally accumulated up to 200 m thick (Rosenberg et al., 2009a). The locality suggests density currents may have been confined to a narrow northern channel valley north of Karapiti 2a connecting TRB and Kaiapo Graben (Fig. 6.7E). When turbulence in the lake ceased, winnowed fines settled and lacustrine sedimentation resumed depositing Upper Huka Falls Formation (Fig. 6.7F; Chapter 3). Gradually, lacustrine deposits became progressively sandy and pebbly as the lake progressively shallowed and rivers established (Fig. 6.6H). Present-day lacustrine sedimentation rates in TVZ suggest maximum drilled Huka Falls Formation thicknesses (~300 m thick) would have required significant time to accumulate (~200 kyr; Smith et al., 1993; Nelson & Lister, 1995; Downs et al., 2014a; in press).

Growth of Tauhara dacite volcano was contemporaneous with Huka Falls Formation and initially erupted through and uplifted the saturated lacustrine sediments (Rosenberg & Kilgour, 2003; Rosenberg et al., 2009a). Trig Rhyolite later erupted onto the Huka Falls Formation sediments as small coalesced lava domes (Rosenberg et al., 2009a). Te Mihi 1 is inferred to be a cryptodome and, like Karapiti 2a, may have formed a small lake island (Fig. 6.7F). Prior to Huka Group termination at 25.4

ka, field evidence supports the development of a volcaniclastic barrier damming late Lake Huka into northern and southern portions (Fig. 6.7F; Manville & Wilson, 2004).

Outcomes and implications

Surface landscapes in TVZ are regulated by gradual, long-term extensional tectonism and large-scale episodic caldera-forming volcanism promote subsidence and create accommodation space. Our results estimate long-term (~1.85 ka) net subsidence and erosion in Wairakei-Tauhara occurred at ~1.7 mm/yr and are inferred to be controlled by gradual rifting. Subsidence became concentrated in elongate rift basins with possible early erosion (beyond current drilling depth) followed by rapid sedimentation phases. Over the last ~300 kyr subsidence occurred at high regional rates (2 – >8 mm/yr) controlled by both rifting and inferred caldera collapse.

Accommodation space development allowed exceptionally thick, basin-fill-type deposits to accumulate. Filled basins are preferred localities for geothermal systems in TVZ due to highly permeable fill, structurally maintained by active tectonism (Bignall et al., 2010b; Rowland & Simmons, 2012). Early Huka Group volcanism filling these basins are suggested to be associated with activity from the Whakamaru caldera. Younger material is inferred to have been mainly locally sourced.

Subsiding basins in the TVZ hosted ancient mature lacustrine systems as characterised by distributions of fine grained deposits interbedded with volcaniclastic basin fill. Their distribution can be useful for locating ancient basin depocentres where thick deposits may have accumulated. Basins presently filling in TVZ are sites with future potential for hosting large geothermal systems (e.g., Lake Taupo basin). Huka Group lithostratigraphy recording~300 kyr of depositional environments suggest the types and distributions of ancient landscapes were much the same as they are today. These environments characterised by lakes, rivers and effusive volcanism are created in response to gradual extension during intra-caldera eruption periods.

Effect on the Geothermal Reservoir

A detailed understanding of field's lithostratigraphy and structure influencing the reservoir is vital for successful and sustainable exploration and for explaining fluid flow. Lithologies and structures comprising the Huka Group reservoir and cap rock have a considerable influence on geothermal fluid

migration (Sepúlveda et al., 2012). Interbedded units control discrete lateral flow zones (Bixley et al., 2009). Deposition of vesicular pumice and highly fragmented tuffs in subsiding basins have produced effective reservoirs (Cattell et al., 2015). Above the depth of intense hydrothermal siliceous cementation (>~700 m), grain size influences matrix permeability as indicated by the highly productive pumice lapilli-tuffs between 300 – 900 m at Wairakei (Bixley et al., 2009). Low permeability cap rocks (Huka Falls Formation, Rautehuia Breccia) covering the high temperature resource control fluid flow in the field and separate groundwater from reservoir fluids. Faults cutting the impermeable cap strata allow warm upflows to mix with cool recharge. The permeability of primary lithological features are reduced by hydrothermal mineralisation (often >700 m; Mielke et al., 2010). Deep systems remain productive and dynamic when enhanced by gradual tectonism (Kissling et al., 2015) and episodic volcanic events (Henneberger & Browne, 1988; Chapter 5).

SUMMARY

Comprehensive geothermal drilling at Wairakei-Tauhara, TVZ, has provided abundant samples for establishing the field's structure and stratigraphy. Stratigraphic data from the field are assessed here to improve our understanding of the TVZ's volcanic and tectonic evolution. Results will also explain the architecture of deposits in basins hosting utilised geothermal systems. The Huka Group represents ~300 kyr of filling Kaiapo Graben (southern TFB) and TRB rift-basin depocentres intersecting Whakamaru caldera beneath Wairakei-Tauhara. Basin subsidence is estimated to be 3 – >8 mm/yr. The basins were filled by a locally-sourced caldera eruption at ~310 ka, ≤100 kyr of gradual volcaniclastic basin-fill and ≤200 kyr lacustrine sedimentation. Resulting lithostratigraphy suggest contemporaneous depositional environments between ~310 – 28 ka were analogous to the lakes, rivers and lava domes forming the present-day TVZ. A detailed understanding of the basin-fill architecture is established for Wairakei-Tauhara that is an important parameter for geothermal exploration. Additionally, the increased local understanding of volcanism and tectonism improves our knowledge of TVZ evolution and may be relevant for interpreting other continental arc settings.

Summary

Exploration at Wairakei-Tauhara Geothermal Fields has provided an ideal and unique opportunity to investigate the Huka Group in unique detail. New insights may enhance geothermal models and will provide new understanding of TVZ's volcanic evolution. Recently-drilled complete core samples allowed existing stratigraphic models to be evaluated through rigorous lithostratigraphic assessment. A robust approach of facies analysis, comprehensive geochemical and petrographic measurements characterised the field's spatial and temporal variation. Traditional methods and novel techniques are utilised in attempt to overcome sample type difficulties. Collectively they provided improved insight into the geological evolution of the field and the geothermal system. The achievements of each chapter are presented in the paragraphs below and outcomes to the initial research question are summarised in Table 7.1.

CHAPTER SUMMARY

To fulfil the aims of this thesis outlined in **Chapter 1**, each chapter presents results from traditional and innovative methods characterising the Huka Group to interpret its detailed geological history.

Chapter 2 documented the detailed stratigraphy of eleven continuous drill cores. A facies model summarised the complex stratigraphic sequence, depositional processes and their environments. This model was tested in following chapters. The Huka Group reflects ~300 kyr of volcanic and sedimentary deposition in long-lived subsiding TRB and Kaiapo Graben (southern TFB sector) depositional basins hosting Lake Huka. Products from explosive and effusive volcanism interacted with the lake, filling the basins over <100 kyr forming the Waiora Formation. Widespread ignimbrites covering the field form thick composite, lithologically similar and laterally graded units. These remain difficult to correlate between wells. Following the volcanic depositional period, Lake Huka accumulated mainly lacustrine sediments for ~200 kyr forming Huka Falls Formation. Later the lake became increasingly fluvial as rivers prograded the basin. Lake Huka was destroyed by the 25.4 ka Oruanui eruption. These interpretations align with, and add detail to, previous accounts on the Huka Falls Formation history and enhance the few existing explanations of the Waiora Formation (outlined in Chapter 2).

Chapter 3 focused on the detailed volcanic origins of the Middle Huka Falls Formation. Its low alteration intensity, shallow elevation and abundant cores allowing allowed for rigorous lateral stratigraphic assessments. A coarse lithic-rich facies drilled in central Tauhara was previously identified as a locality near an explosive source vent. Results from facies and textural analysis suggest water-supported density currents were fed from a collapsing column beneath Lake Huka. Currents transported pyroclastic material through the lake, principally towards the west (Wairakei). Bedding in the main pumice lapilli-tuff facies identified transport and deposition as a series of 'pulses'. Deposition of ~100 m Middle Huka Falls Formation (up to 200 m thick) was likely entirely subaqueous, suggesting the accommodating lake was at least this deep. This eruption style was the first of its kind to be recognised in the TVZ. Recently similar examples have been recognised in TRB (Downs et al., in press) and were likely prevalent in the region's past. These events potentially contributed uncorrelated pyroclastic strata in the Waiora Formation.

Characterising and correlating hydrothermally altered rocks in the TVZ is challenging owing to similar lithologies and alteration to distinctive chemical and textural properties. Limitations of macroscopic visual assessment were identified in Chapters 2 and 3. In an effort to improve stratigraphic model detail masked by hydrothermal alteration, vertical variations of remaining primary magmatic phases were measured in **Chapter 4.** These were trialled to assess suitability of recognising compositionally distinct emplacement units. Firstly, stratigraphic variations in phenocryst size and volume were useful for recognising the type of altered lithology (e.g., silicified volcaniclastic or silicified lava). Variations identified the vertical distribution of coarse particles within individual units (e.g., graded bedding) and reworking intensity (e.g., pyroclastic vs. volcanogenic sedimentary deposit). Secondly, chemostratigraphic distributions of immobile elements (Ti and Zr) identified the distribution of high density magmatic host minerals (titanite, ilmenite, leucoxene and zircon). Distributions were consistent with observable macroscopic textures, reflecting primary density stratification emplacement (normal grading) or reworking homogenisation (more evenly distributed). Lastly, Huka Group immobile elements were compared with TVZ juvenile pumice examples. Results support a possible Whakamaru magmatic correlative for Waiora Ignimbrite. Outcomes suggest that Whakamaru-type volcanism may have persisted for longer than earlier recognised, and included a quiescence period

allowing for some erosion of Whakamaru Ignimbrite. Overall, the methods supplemented macroscopic stratigraphic logs and identified new evidence of magmatic and volcanic processes. Additionally, recognise that regional Kaingaroa Ignimbrite is distinct to the previously correlated and local "Polo Flats Ignimbrite" from Wairakei.

During visual inspection of Huka Group in Chapter 2, a unique mineralised fracture containing pristine hydrothermal adularia was identified. Hydrothermal minerals in the Huka Group record reservoir and geothermal system evolution. A temporal constraint on the geothermal system within Huka Group was trialled in **Chapter 5** using $^{40}Ar/^{39}Ar$ dating of hydrothermal adularia. Such young material is typically difficult to date due to low radiogenic Ar concentrations. Using high-resolution $^{40}Ar/^{39}Ar$ methods, results identified samples were <30 ka. This was much younger than previous estimates of the system confirming a stage of late structural evolution in the presently active system. Fracture formation through the Waiora Formation host rock may be consistent with eruption of the post-25.4 ka Crown Breccia hydrothermal eruption deposits. This chapter identified the applicability of $^{40}Ar/^{39}Ar$ dating in complex geothermal settings for providing constraints on the system's temporal evolution.

Finally, **Chapter 6** utilises earlier findings and existing supporting information. These contribute to a geological model illustrating the depositional sequence, the distribution of strata and prevailing environments. Present-day TVZ landscapes are characterised by small to extensive lakes connected by rivers. Lithostratigraphic assemblages indicate post-300ka environments at Wairakei-Tauhara were relatively similar to landscapes present today (e.g., Maroa and Taupo Volcanic Centres). These are inferred to have remained relatively constant between landscape-forming caldera eruption periods. Localised vents, local sedimentary sources and ancient topographic sediment barriers (Wairakei Block and Karapiti 2a) explains the distinct lithostratigraphy between Kaiapo Graben (in TFB) and TRB. The basins evolved contemporaneously hosting lacustrine depositional environments. However, the Kaiapo Graben appears to have subsided and filled more gradually (~4.5 mm/yr). The TRB subsided rapidly (>8 mm/yr). The latter could relate to volcano-tectonic subsidence of Whakamaru caldera in southern TRB. Geological and paleo-geographical evolution at Wairakei-Tauhara is presented as time-series models.

The questions addressed by this research have enhanced our understanding of evolution at Wairakei-Tauhara and the broader evolution of the TVZ. Wairakei-Tauhara presented a unique opportunity with significant subsurface sample availability and 60 years of geological precedent that has established the field's geological architecture.

RESEARCH QUESTIONS

Outcomes to the key research questions are summarised below in Table 7.1.

Table 7.1. Summary of findings to the research questions presented in Chapter 1.

Research Questions	Outcome	
• ***What were the major transport and depositional processes?*** • ***How many emplacement events occurred?*** • ***What depositional environments prevailed?***	• Deposits are mainly subaerial and subaqueous pyroclastic density currents. • In Wairakei, ≥12 depositional events have been recognised, but this varies throughout the fields. • A developing lacustrine setting continually prevailed and was continually modified by volcanism.	**Chapters 2, 3 & 6**
• ***What processes do the facies variations represent?*** • ***How did the eruption progress?*** • ***What aspects of the physiography of Lake Huka can be inferred from the eruption?***	• Proximity to and development of the erupting vent. • Commenced as vent-clearing, followed by a collapsing water-supported column feeding density currents. • Lake Huka was ~200 m deep (150 – 250 m) across Wairakei-Tauhara.	**Chapter 3**
• ***Can magmatic phases be utilised to differentiate separate visually similar emplacement units?*** • ***Can immobile elements of Huka Group units be used to infer possible magmatic source origins with other TVZ eruptives?***	• Yes, but only when phases are stable and analytical resolution is high enough to recognise variations. • Probably, but additional evidence is required. Waiora Ignimbrite appears consistent with a Whakamaru magmatic source. Waiora Volcaniclastics units appear compositionally unique and are likely locally sourced. • "Polo Flats Ignimbrite" appears chemically affiliated with Waiora Volcaniclastics, not Kaingaroa Ignimbrite.	**Chapters 4 & 6**
• ***Can young hydrothermal minerals in the Huka Group be directly dated?*** • ***What geothermal processes can affect mineral dating?*** • ***How did the deep mineralised fracture likely form?***	• Yes, $^{40}Ar/^{30}Ar$ dating can be used in complex geothermal systems when suitable samples are available. • For argon to be lost from adularia, either high temperatures or short diffusion distances are needed. • It is consistent with hydrothermal fracturing, maybe associated with the Crown Breccia eruption.	**Chapter 5**
• ***What landscapes were present during Huka Group deposition?*** • ***Can regional deposits be used to constrain the relative timing of events?*** • ***How did the field's structure and stratigraphic architecture evolve?***	• Sedimentary basins and landscapes are similar to those in present-day TVZ (mainly lakes, rivers, lava domes). • Possible stratigraphic correlatives to the Huka Group may be inferred from elsewhere in TVZ until direct dating is undertaken at Wairakei-Tauhara. • The southern TFB (local Kaiapo Graben underlying Wairakei) evolved gradually, while TRB (beneath Tauhara) evolved rapidly. Both were locations of intense localised erosion followed by rapid deposition.	**Chapter 6**

References

Alcaraz S., Sepulveda F., Lane R., Rosenberg M., Rae A., Bignall G. 2010. A 3-D Representation of the Wairakei Geothermal System (New Zealand) using "Earth Research" Geothermal Visualisation and Modelling Software. GRC Trans 34:1119–1123.

Alcaraz S., Lane R., Spragg K., Milicich S., et al. 2011. 3D geological modelling using new LeapFrog Geothermal software. Proceedings, 36th Workshop on Geothermal Reservoir Engineering. January 31 – February 2, 2011, Stanford University, Stanford, USA. Stanford Geothermal Programme Workshop report SGP-TR-191: 351–356. Electronic Appendix 3.4.

Allen S.R., McPhie J. 2003. Phenocryst fragments in rhyolitic lavas and lava domes. Journal of Volcanology and Geothermal Research 126: 263–283.

Allen S.R., Fiske R.S., Cashman K.V. 2008. Quenching of steam-charged pumice: Implications for submarine pyroclastic volcanism. Earth and Planetary Science Letters 274: 40–48.

Allen S.R., McPhie J. 2009. Products of neptunian eruptions. Geology 37: 639–642.

Allen S.R., Freundt A., Kurokawa K. 2012. Characteristics of submarine pumice-rich density current deposits sourced from turbulent mixing of subaerial pyroclastic flows at the shoreline: field and experimental assessment. Bulletin of Volcanology 74: 657–675.

Arancibia G., Matthews S.J., Cornejo P., de Arce C.P., Kasaneva S., Zuluaga J.I. 2006. $^{40}Ar/^{39}Ar$ and K–Ar geochronology of magmatic and hydrothermal events in a classic low-suphidation epithermal bonanza deposit: El Peñon, northern Chile. Mineralium Deposita 41: 505–515.

Arehart G.B., Christenson B.W., Wood C.P., Foland K.A., Browne P.R.L. 2002. Timing of volcanic, plutonic and geothermal activity at Ngatamariki, New Zealand. Journal of Volcanology and Geothermal Research 116: 201–214.

Argyraki A., Ramsey M.H., Potts P.J. 1997. Evaluation of Portable X-ray Fluorescence Instrumentation for *in situ* Measurements of Lead on Contaminated Land. Analyst 122: 743–749.

Ashwell P.A., Kennedy B.M., Gravley D.M., et al. 2013. Insights into caldera and regional structures and magma body distribution from lava domes at Rotorua Caldera, New Zealand. Journal of Volcanology and Geothermal Research 258:187–202.

Barrett T.J., MacLean W.H. 1994. Chemostratigraphy and hydrothermal alteration in exploration for VHMS deposits in greenstones and younger volcanic rocks. In: Lentz D.R. ed. Alteration and Alteration Processes Associated with Ore-Forming Systems. GAC-MAC Annual Meeting, 1994, Waterloo, Canada. Geological Association of Canada, Short Course Notes 11. Pp. 433–467.

Bastos R.O., Melquiades F.L., Biasi G.E.V. 2012. Correction for the effect of soil moisture on *in situ* XRF analysis using low-energy background. X-Ray Spectrometry 41: 304–307.

Beavan J., Tregoning T., Bevis M., Kato T., Meetens C. 2002. Motion and rigidity of the Pacific Plate and implications for plate boundary deformation. Journal of Geophysical Research 107. 15 p.

Beresford S.W. 1997. Volcanology and geochemistry of the Kaingaroa Ignimbrite, Taupo Volcanic Zone, New Zealand. PhD theses, University of Canterbury, Christchurch, New Zealand. 363 p.

Beresford S.W., Cole J.W. 2000. Kaingaroa Ignimbrite, Taupo Volcanic Zone, New Zealand: Evidence for asymmetric caldera subsidence of the Reporoa Caldera. New Zealand Journal of Geology and Geophysics 43:471–481.

Best M.G., Christiansen E.H. 1997. Origin of broken phenocrysts in ash-flow tuffs. Geological Society of America 109: 63–73.

Bibby H.M., Caldwell T.G., Davey F.J., Webb, T.H. 1995. Geophysical evidence on the structure of the Taupo Volcanic Zone and its hydrothermal circulation. Journal of Volcanology and Geothermal Research 68: 29–58.

Bignall G., Browne P.R.L., Kyle P.R. 1996. Geochemical characterisation of hydrothermally altered ignimbrites in active geothermal fields from the central Taupo Volcanic Zone, New Zealand. Journal of Volcanology and Geothermal Research 73: 79–97.

Bignall G, Milicich S, Ramirez L, Rosenberg M, Kilgour G, Rae A 2010a. Geology of the Wairakei-Tauhara Geothermal System, New Zealand. Proceedings of the World Geothermal Congress, Bali, Indonesia, 25 – 29 April 2010. Pp. 25–30.

Bignall G., Rae A., Rosenberg M. 2010b. Rationale for Targeting Fault Versus Formation-Hosted Permeability in High-Temperature Geothermal Systems of the Taupo Volcanic Zone, New Zealand,. Proceedings of the World Geothermal Congress 2010, Bali, Indonesia, 25-30 April 2010. 7 p.

Bixley P.F., Browne P.R.L. 1988. Hydrothermal eruption potential in geothermal development. Proceedings of the 10th New Zealand Geothermal Workshop. Pp. 195–198.

Bixley P.F., Clotworthy A.W., Mannington W.I. 2009. Evolution of the Wairakei geothermal reservoir during 50 years of production. Geothermics 38:145–154.

Bogie I, Lawless J.V., MacKenzie K.M. 1995. Geological Results from drilling in the Poihipi (western) Sector of the Wairakei Geothermal Field, New Zealand. Proceedings 17th New Zealand Geothermal Workshop 1995. Kingston Morrison Ltd, Auckland, New Zealand. Pp. 55–60

Bolton R.S. 2009. The early history of Wairakei (with brief notes on some unforeseen outcomes). Geothermics 38:11–29.

Branney M.J., Kokelaar P. 2002. Pyroclastic density currents and the sedimentation of ignimbrites. Geological Society, London, Memoirs 27. 152 p.

Brathwaite R.L. 2003. Geological and Mineralogical Characterization of Zeolites in Lacustrine Tuffs, Ngakuru, Taupo Volcanic Zone, New Zealand. Clays and Clay Minerals 51: 589–598.

Briggs N.D. 1976. Recognition and correlation of subdivisions within the Whakamaru Ignimbrite, central north island, New Zealand. New Zealand Journal of Geology and Geophysics 19: 463–501.

Brockamp O., Clauer N., Zuther M. 2003. Authigenic sericite record of a fossil geothermal system: the Offenburg trough, central Black Forest, Germany. International Journal of Earth Sciences 92: 843–851.

Bromley C.J., Currie S., Manville V.R., Rosenberg M.D. 2009. Recent ground subsidence at Crown Road, Tauhara and its probable causes. Geothermics 38:181–191.

Bromley C., Currie S., Ramsay G., Rosenberg M., Pender M. et al. 2010. Tauhara Stage II Geothermal Project: Subsidence Report. GNS Science Consultancy Report 2010/151 154 p. http://www.contactenergy.co.nz/aboutus/pdf/environmental/P5SubsidenceReport.pdf

Brown S.J.A. 1994. Geology and geochemistry of the Whakamaru Group ignimbrites, and associated rhyolite domes, Taupo Volcanic Zone, New Zealand. Unpublished PhD thesis, Department of Geological Sciences, University of Canterbury, Christchurch, New Zealand, 194 p.

Brown S.J.A., Smith R.T., Cole J.W., Houghton B.F. 1994. Compositional and textural characteristics of the strombolian and surtseyan K-Trig basalts, Taupo Volcanic Centre, New Zealand: Implications for eruption dynamics. New Zealand Journal of Geology and Geophysics 37:113–126.

Brown S.J.A., Wilson C.J.N., Cole J.W., Wooden, J. 1998a. The Whakamaru group ignimbrites, Taupo Volcanic Zone, New Zealand: evidence for reverse tapping of a zoned silicic magmatic system. Journal of Volcanology and Geothermal Research 84: 1–37.

Brown S.J.A., Burt R.M., Cole J.W., Krippner S.J.P., Price R.C., Cartwright I. 1998b. Plutonic lithics in ignimbrites of Taupo Volcanic Zone, New Zealand; sources and conditions of crystallisation. Chemical Geology 148:21–41.

Browne P.R.L., Ellis A.J. 1970. The Ohaaki-Broadlands hydrothermal area, New Zealand: mineralogy and related geochemistry. American Journal of Science 269: 97–131.

Browne P.R.L. 1979. Minimum age of the Kawerau geothermal field, North Island, New Zealand. Journal of Volcanology and Geothermal Research 6: 213–215.

Browne P.R.L., Graham I.J., Parker R.J., Wood C.P 1992. Subsurface andesite lavas and plutonic rocks in the Rotokawa and Ngatamariki geothermal systems, Taupo Volcanic Zone, New Zealand. Journal of Volcanology and Geothermal Research 51: 199–215.

Browne P.R.L., Lawless J.V. 2001. Characteristics of hydrothermal eruptions, with examples from New Zealand and elsewhere. Earth-Science Reviews 52: 299–331.

Browne P.R.L., Graham I.J., Parker R.J., Wood C.P. 1992. Subsurface andesite lavas and plutonic rocks in the Rotokawa and Ngatamariki geothermal systems, Taupo Volcanic Zone, New Zealand. Journal of Volcanology and Geothermal Research 51: 199–215.

Bryan C.J., Sherburn S., Bibby H.M., et al. 1999. Shallow seismicity of the central Taupo Volcanic Zone, New Zealand: Its distribution and nature. New Zealand Journal of Geology and Geophysics 42:533–542.

Busby C.J., Bassett K.N. 2007. Volcanic facies architecture of an intra-arc strike-slip basin, Santa Rita Mountains, Southern Arizona. Bulletin of Volcanology 70: 85–103.

Busby-Spera C.J. 1986. Depositional features of rhyolitic and andesitic volcaniclastic rocks of the Mineral King submarine caldera complex, Sierra Nevada, California. Journal of Volcanology and Geothermal Research 27: 43–76.

Cas R.A.F., Wright J.V. 1987. Volcanic successions, modern and ancient: A geological approach to processes, products, and successions. Allen & Unwin Publishes Ltd., London, UK. 528 p.

Cas R.A.F., Allen R.L., Bull S.W., Clifford B.A., Wright J.V. 1990. Subaqueous, rhyolitic dome-top tuff cones: a model based on the Devonian Bunga Beds, southeastern Australia and a modern analogue. Bulletin of Volcanology 52: 159–174.

Cas R.A.F., Wright J.V. 1991. Subaqueous pyroclastic flows and ignimbrites: an assessment. Bulletin of Volcanology 53: 357–380.

Cas R.A.F., Edgar C., Allen R.L., Bull S. Clifford B.A., Giordano G., Wright J.V. 2001. Influence of Magmatism and Tectonics on Sedimentation in an Extensional Lake Basin: The Upper Devonian Bunga Beds, Boyd Volcanic Complex, South-Eastern Australia. In: White J., Riggs N. eds. Volcaniclastic Sedimentation in Lacustrine Settings. Blackwell Publishing Ltd, Oxford, UK. Pp. 83–108.

Cas R.A.F., Van Otterloo J. 2011. Introduction to the IUGG excursion guide. In: Cas R., Blaikie T., Boyce J. et al. eds. Factors that influence varying eruption styles (from magmatic to phreatomagmatic) in intraplate basaltic volcanic provinces: the Newer Volcanics Province of south-eastern Australia. Field trip guide. XXV IUGG General Assembly. IAVCEI, Melbourne. Pp. 7–31.

Cashman K.V., Sturtevant B., Papale P., Navon O. 2000. Magmatic Fragmentation. In: Sigurdsson H., Houghton B., McNutt S., Rymer H., Stix J. eds. Encyclopedia of Volcanoes. San Diego, Academic Press. Pp. 421–430.

Cattell H., Cole J., Bignall G., Sepúlveda F. 2015. Influences of Geological Depositional Processes and Environments on Geothermal Strata from Wairakei-Tauhara Geothermal Field , New Zealand. Proceedings of the World Geothermal Congress 2015, Melbourne, Australia, 19-25 April 2015, International Geothermal Association. Pp. 19–25.

Chambefort I., Lewis B., Wilson C.J.N., Rae A.J., Coutts C., Bignall G., Ireland T.R. 2014. Stratigraphy and structure of the Ngatamariki geothermal system from new zircon U-Pb geochronology: Implications for Taupo Volcanic Zone evolution. Journal of Volcanology and Geothermal Research 274: 51–70

Cole J.W. 1978. Andesites of the Tongariro Volcanic Centre, North Island, New Zealand: Journal of Volcanology and Geothermal Research 3: 121–153 .

Cole J.W., Lewis K. 1981. Evolution of the Taupo-Hikurangi subduction system. Tectonophysics 72:1–21.

Cole J.W., Darby D.J., Stern T.A. 1995. Taupo Volcanic Zone and Central Volcanic Region: Back arc structures of North Island, New Zealand. In: Taylor B. ed. Backarc Bains: Tectonics and Magmatism. Plenum Publishing, New York. Springer. Pp. 1–28

Cole R.B., Decelles P.G. 1991. Subaerial to submarine transitions in early Miocene pyroclastic flow deposits, southern San Joaquin basin, California. Geological Society of America 103: 221–235.

Collar R.J., Browne P.R.L. 1985. Hydrothermal eruptions at the Rotokawa Geothermal Field, Taupo Volcanic Zone, New Zealand. Proceedings of the 7th New Zealand Geothermal Workshop. Pp. 171–175.

Contact Energy. 2010. Tauhara II Geothermal Wairakei-Tauhara Geothermal System Draft System Management Plan. February 2010. 101 p.

Cuney M., Friedrich M. 1987. Physicochemical and crystal-chemical controls on accessory mineral paragenesis in granitoids: implications for uranium metallogenesis. Bulletin de Minéralogie 110:235–247.

Craig N., Speakman R.J., Popelka-Filcoff R.S., et al. 2007. Comparison of XRF and PXRF for analysis of archaeological obsidian from southern Perú. Journal of Archaeological Science 34: 2012–2024.

Dalrymple G.B., Grove M. 1999. Age and thermal history of the Geysers plutonic complex (felsite unit), Geysers geothermal field, California: a $^{40}Ar/^{39}Ar$ and U–Pb study. Earth and Planetary Science Letters 173: 285–298.

Darby D.J., Meertens C. 1995. Terrestrial and GPS measurements of deformation across the Taupo back arc and Hikurangi forearc regions in New Zealand. Journal of Geophysical Research 100: 8221–8232.

De Mets C., Gordon R.G., Argus D.F. 2010. Geologically current plate motions. Geophysical Journal International 181: 1–80.

Downs D.T., Rowland J. V., Wilson C.J.N., Rosenberg M.D., Leonard G.S., Calvert A.T. 2014a. Evolution of the intra-arc Taupo-Reporoa Basin within the Taupo Volcanic Zone of New Zealand. Geosphere 10: 185–206.

Downs D.T., Wilson C.J.N., Cole J.W., Rowland J. V, Calvert A.T., Leonard G.S., Keall J.M. 2014b. Age and eruptive center of the Paeroa Subgroup ignimbrites (Whakamaru Group) within the Taupo Volcanic Zone of New Zealand. Geological Society of America 126: 1131–1144.

Downs D.T., Wilson C.J.N., Leonard G.S., Rowland J.V. in press. Stratigraphic architecture of the Paeroa fault block, Taupo Volcanic Zone, New Zealand. New Zealand Journal of Geology and Geophysics. Pagination unknown.

Duffield W.A., Dalrymple G.B. 1990. The Taylor Creek Rhyolite of New Mexico: a rapidly emplaced field of lava domes and flows. Bulletin of Volcanology 52: 475–487.

Eastwood A.A., Gravley D.M., Wilson C.J.N., Chambefort I., Oze C., Cole J.W., Ireland T.R. 2013. U-Pb dating of subsurface pyroclastic deposits (Tahorakuri Formation) at Ngatamariki and Rotokawa geothermal fields. Proceedings, 35th New Zealand Geothermal Workshop, Rotorua, New Zealand, November, p. 17–23.

ECNZ 1990. Water Right Applications and Impact Assessment: Wairakei Geothermal Power Station. Report by Electricity Commission of New Zealand Limited, Wairakei.

Ewart A., Cole J.W. 1967. Textural and Mineral Significance of the Granitic Xenoliths from the Central Volcanic Region, North Island, New Zealand Journal of Geology and Geophysics 10:31–54.

Fisher R.V. 1961. Proposed classification of volcaniclastic sediments and rocks. Geological Society of America Bulletin 72: 1409–1414.

Fisher R.V. 1979. Models for pyroclastic surges and pyroclastic flows. Journal of Volcanology and Geothermal Research 6: 305–318.

Fisher R.V., Schmincke H.U. 1984. Pyroclastic Rocks. Springer. Berlin. 472 p.

Fiske R.S. 1963. Subaqueous pyroclastic flows in the Ohanapecosh Formation, Washington. Geological Society of America Bulletin 74: 391–406.

Fiske R.S. Matsuda T. 1964. Submarine equivalents of ash flows in the Tokiwa Formation, Japan. American Journal of Science 262: 76–106.

Forster N., Grave P., Vickery N., Kealhofer L. 2011. Non-destructive analysis using PXRF: Methodology and application to archaeological ceramics. X-Ray Spectrometry 40: 389–398.

Freundt A. 2003. Entrance of hot pyroclastic flows into the sea: experimental observations. Bulletin of Volcanology 65: 144–164. Kokelaar

Gasquet D., Bertrand J., Paquette J., et al. 2010. Messinian deformation and hydrothermal activity in a pre-Alpine basement massif of the French western Alps: new U-Th-Pb and argon ages from the Lauzière massif. Bulletin de la Societe Geologique de France 181: 227–241.

Gazley M.F., Vry J.K., du Plessis E., Handler M.R. 2011. Application of portable X-ray fluorescence analyses to metabasalt stratigraphy, Plutonic Gold Mine, Western Australia. Journal of Geochemical Exploration 110: 74–80.

Ge L., Lai W., Lin Y. 2005. Influence of and correction for moisture in rocks, soils and sediments on *in situ* XRF analysis. X-Ray Spectrometry 34: 28–34.

Gifkins C.C. 2001. Submarine volcanism and alteration in the Cambrian, northern Central Volcanic Complex, western Tasmania. Unpublished PhD thesis, University of Tasmania. 335 p.

Gifkins C.C., Allen R.L. 2001. Textural and chemical characteristics of diagenetic and hydrothermal alteration in glassy volcanic rocks: examples from the Mount Read Volcanics, Tasmania. Economic Geology 96: 973–1002.

Gifkins C.C., Allen R.L., McPhie J. 2005a. Apparent welding textures in altered pumice-rich rocks. Journal of Volcanology and Geothermal Research 142: 29–47.

Gifkins C., Herrmann W., Large R. 2005b. Altered volcanic rocks: a guide to description and interpretation: Centre for Ore Deposit Research, University of Tasmania, Hobart, Tasmania, Australia. 275 p.

Glynn-Morris T., Winmill R. 2009. Tauhara Subsidence Project: Field Setup and Operational Procedures. 22 p. http://www.contactenergy.co.nz/web/pdf/our_projects/tauhara/tauhara_phase_two/04ContactFieldProcedures.pdf

Goodale N., Bailey D.G., Jones G.T., et al. 2012. PXRF: A study of inter-instrument performance. Journal of Archaeological Science 39: 875–883.

Grange L.I. 1937. The Geology of the Rotorua-Taupo subdivision, Rotorua and Kaimanawa divisions. New Zealand Geological Survey Bulletin 37.

Gravley D.M. 2004. The Ohakuri pyroclastic deposits and the evolution of the Rotorua-Ohakuri volcanotectonic depression. Unpublished PhD thesis, University of Canterbury: Christchurch, New Zealand. 227 p.

Gravley D.M., Wilson C.J.N. 2006. An ignimbrite flare-up event at 340-240 ka in the Taupo Volcanic Zone, New Zealand: Implications for magmatic, volcanic, and tectonic linkages. Sapporo, Japan: 5th Biennial Workshop on Subduction Processes Emphasizing the Japan-Kurile-Kamchatka-Aleutian Arcs, 9-14 Jul 2006. Pp 25–28

Gravley D.M., Wilson C.J.N., Rosenberg M.D., Leonard G.S. 2006. The Nature and age of Ohakuri Formation and Ohakuri Group rocks in surface exposures and geothermal drillhole sequences in the central Taupo Volcanic Zone, New Zealand. New Zealand Journal of Geology and Geophysics 49: 305–308.

Gravley D.M., Wilson C.J.N., Leonard G.S., Cole J.W. 2007. Double trouble: Paired ignimbrite eruptions and collateral subsidence in the Taupo Volcanic Zone, New Zealand. Geological Society of America Bulletin 119: 18–30.

Gravley D.M., Leonard G.S., Wilson C.J.N., Rowland J.V., Hikuroa D.C.H. 2009. Build-up to an ignimbrite flare-up: geologic evidence for magmatic-tectonic-volcanic interplay in the central Taupo Volcanic Zone, New Zealand. Geological Society of America Abstracts with Programs 41. Pp. 57.

Grimes S., Rickard D., Hawkesworth C., Calsteren P.v., Browne P. 1998. A U–Th calcite isochron age from an active geothermal field in New Zealand. Journal of Volcanology and Geothermal Research 81: 327–333.

Grindley G.W. 1959. Sheet N85 – Waiotapu. Geological Map of New Zealand 1:63,360. Wellington, New Zealand. New Zealand Department of Scientific and Industrial Research, Wellington, New Zealand.

Grindley G.W. 1960. Sheet 8 – Taupo. Geological map of New Zealand 1:250,000. Wellington, New Zealand. New Zealand Department of Scientific and Industrial Research, Wellington, New Zealand.

Grindley G.W. 1961. Sheet N94 – Taupo. Geological map of New Zealand 1:63,360. Sheet N94 - Taupo. New Zealand Geological Survey. New Zealand Department of Scientific and Industrial Research, Wellington, New Zealand.

Grindley G.W. 1963. Geology and structure of Waiotapu Geothermal Field. Department of Scientific and Industrial Research Bulletin 155, New Zealand. Pp. 10–25

Grindley G.W. 1965. The Geology, Structure, and Exploitation of the Wairakei Geothermal Field, Taupo, New Zealand. New Zealand Geological Survey Bulletin, Wellington, New Zealand 75. 131 p.

Grindley G.W. 1982. The deeper structure of the Wairakei Geothermal Field. Proceedings of the Pacific Geothermal Conference, Lower Hutt, New Zealand. Pp. 69–74.

Grindley G.W. 1986. Subsurface geology and structure of the Kawerau Geothermal Field. In: Mongillo, MA eds. The Kawerau Geothermal Field : contributions from the 1982 seminar and other recent scientific investigations. New Zealand Department of Scientific and Industrial Research Geothermal Report 10. Pp. 49–65.

Hacker B.R., Mosenfelder J.L., Gnos E. 1996. Rapid emplacement of the Oman ophiolite: Thermal and geochronologic constraints. Tectonics 15: 1230–1247.

Hall G.E.M., Bonham-Carter G.F., Buchar A. 2014. Evaluation of portable X-ray fluorescence (pXRF) in exploration and mining: Phase 1, control reference materials. Geochemistry: Exploration, Environment, Analysis 14: 99–123.

Hames W., Unger D., Saunders J., Kamenov G. 2009. Early Yellowstone hotspot magmatism and gold metallogeny. Journal of Volcanology and Geothermal Research 188: 214–224.

Healy J. 1965. Geology of the Wairakei Geothermal Field. Proceedings of the Eighth Commonwealth Mining and Metallurgical Congress in Australia and New Zealand. Paper 218, Pp. 1–11.

Healy J. 1984. Wairakei Geothermal Field in review. Unpublished Geothermal Circular JH/10, New Zealand Geological Survey. New Zealand Department of Scientific and Industrial Research, Wellington, New Zealand. 34 p.

Healy J., Schofield J., Thompson B. 1964. Sheet 5 – Rotorua. Geological map of New Zealand 1:250,000. New Zealand Department of Scientific and Industrial Research, Wellington, New Zealand.

Henneberger R.C., Browne P.R.L. 1988. Hydrothermal alteration and evolution of the Ohakuri hydrothermal system, Taupo Volcanic Zone, New Zealand. Journal of Volcanology and Geothermal Research 34: 211–231.

Hochstein M.P., Hunt T.M. 1980. Guide to geophysics of the volcanic and geothermal areas of the North Island, New Zealand. The Royal Society of New Zealand, Wellington, New Zealand. 93 p.

Houghton B.F., Wilson C.J.N. 1989. A vesicularity index for pyroclastic deposits. Bulletin of Volcanology 51: 451–462.

Houghton B.F., Wilson C.J.N., McWilliams M.O., Lanphere M.A., Weaver S.D., Briggs R.M., Pringle M.S. 1995. Chronology and dynamics of a large silicic magmatic system: central Taupo Volcanic Zone, New Zealand. Geology 23: 13–16.

Houghton BF, Wilson CJN, Smith RT, Gilbert JS 2000. Phreatoplinian Eruptions. In: Sigurdsson H, Houghton B., McNutt S., Rymer H., Stix J. eds. Encyclopedia of Volcanoes. San Diego, Academic Press. Pp. 513–525.

Hunt T.M., Bromley C.J., Risk G.F., Sherburn S., Soengkono S. 2009. Geophysical investigations of the Wairakei Field. Geothermics 38: 85–97.

Jourdan, F., Mark, D.F., and Verati, C., 2014, Advances in $^{40}Ar/^{39}Ar$ Dating: From Archaeology to Planetary Sciences. Geological Society, London, Special Publications. 378 p.

Jutzeler M., McPhie J., Allen S.R. 2014. Facies architecture of a continental, below-wave-base volcaniclastic basin: The Ohanapecosh Formation, Ancestral Cascades arc (Washington, USA). Geological Society of America Bulletin 126: 352–376.

Kano K., Yamamoto T., Takeuchi K. 1993. A Miocene island-arc volcanic seamount: the Takashibiyama Formation, Shimane Peninsula, SW Japan. Journal of Volcanology and Geothermal Research 59: 101–119.

Kano K., Yamamoto T., Ono K. 1996. Subaqueous eruption and emplacement of the Shinjima Pumice, Shinjima (Moeshima) Island, Kagoshima Bay, SW Japan. Journal of Volcanology and Geothermal Research 71: 187–206.

Kelley S., Turner G., Butterfield A.W., Shepherd T.J., 1986, The source and significance of argon isotopes in fluid inclusions from areas of rnineralization. Earth and Planetary Science Letters 79: 303–318.

Kelley S. 2002. Excess argon in K-Ar and Ar-Ar geochronology. Chemical Geology 188: 1–22.

Kissling W.M., Weir G.J. 2005. The spatial distribution of the geothermal fields in the Taupo Volcanic Zone, New Zealand. Journal of Volcanology and Geothermal Research 145: 136–150.

Kissling W., Rae A., Villamor P., Ellis S. 2015. Hydrothermal Fluid Flow in a Structurally-controlled Basin , Ngakuru Graben, Taupo Rift , New Zealand. Proceedings World Geothermal Congress 2015, Melbourne, Australia, 19-25 April 2015. Pp. 19–25.

Kokelaar B.P. 1983. The Mechanism of Surtseyan Volcanism. Journal of the Geological Society 140: 939–944.

Kokelaar P. 1986. Magma-water interactions in subaqueous and emergent basaltic volcanism. Bulletin of Volcanology 48: 275–289.

Kokelaar P., Busby C. 1992. Subaqueous explosive eruption and welding of pyroclastic deposits. Science 257: 196–201.

Kokelaar P., Königer S. 2000. Marine emplacement of welded ignimbrite: the Ordovician Pitts Head Tuff, North Wales. Journal of the Geological Society 157: 517–536.

Kokelaar P., Raine P., Branney M.J. 2007. Incursion of a large-volume, spatter-bearing pyroclastic density current into a caldera lake: Pavey Ark ignimbrite, Scafell caldera, England. Bulletin of Volcanology 70: 23–54.

Lamarche G., Barnes P.M., Bull J.M. 2006. Faulting and extension rate over the last 20,000 years in the offshore Whakatane Graben, New Zealand continental shelf. Tectonics 25: 1–24.

Langridge R.M. 1990. The Geology of the Upper Atiamuri Region, Taupo Volcanic Zone (Southern Kapenga Caldera). Unpublished MSc thesis, University of Waikato, New Zealand. 168 p.

Large R.R., Allen R.L., Blake M.D., Herrmann W. 2001. Hydrothermal alteration and volatile element halos for the Rosebery K lens volcanic-hosted massive sulfide deposit, western Tasmania. Econmic Geology 96: 1055–1072.

Leonard G.S., Cole J.W., Nairn I.A., Self S. 2002. Basalt triggering of the c. AD 1305 Kaharoa rhyolite eruption, Tarawera Volcanic Complex, New Zealand Journal of Volcanology and Geothermal Research 115:461–486.

Leonard G.S. 2003. The evolution of Maroa Volcanic Centre, Taupo Volcanic Zone, New Zealand. Unpublished PhD thesis, Department of Geological Sciences, University of Canterbury, Christchurch, New Zealand. 335 p.

Leonard G.S., Begg J.G., Wilson C.J.N. 2010. Geology of the Rotorua area: scale 1:250,000. Lower Hutt: Institute of Geological & Nuclear Sciences Limited. Institute of Geological & Nuclear Sciences 1:250,000 geological map 5. 99 p. + 1 folded map

Lovera O.M., Grove M., Mark Harrison T., Mahon K.I. 1997. Systematic analysis of K-feldspar step heating results: I. Significance of activation energy determinations. Geochim Cosmochim Acta 61: 3171–3192.

Lowe D.R. 1982. Sediment gravity flows; II, Depositional models with special reference to the deposits of high-density turbidity currents. Journal of Sedimentary Research 52: 279–297.

MacLean W.H., Barrett T.J. 1993. Lithogeochemical techniques using immobile elements. Journal of Geochemical Exploration 48: 109–133.

Manville V., White J.D.L., Houghton B.F., Wilson C.J.N. 1998. The saturation behaviour of pumice and some sedimentological implications. Sedimentary Geology 119: 5–16.

Manville V., White J.D.L., Houghton B.F., Wilson C.J.N. 1999. Paleohydrology and sedimentology of a post–1.8 ka breakout flood from intracaldera Lake Taupo, North Island, New Zealand: Geological Society of America Bulletin 111: 1435–1447.

Manville V. 2001. Sedimentology and history of Lake Reporoa: an ephemeral supra-ignimbrite lake, Taupo Volcanic Zone, New Zealand. In: White J., Riggs N. eds. Volcaniclastic Sedimentation in Lacustrine Settings, International Association of Sedimentologists, Blackwell Science, Malden, MA, USA. Pp. 109–140.

Manville V. 2010. An overview of break-out floods from intracaldera lakes. Global and Planetary Change 70: 14–23.

Manville V., Segschneider B., White J.D.L. 2002. Hydrodynamic behaviour of Taupo 1800a pumice: implications for the sedimentology of remobilized pyroclasts. Sedimentology 49: 955–976.

Manville V., Wilson C.J.N. 2004. The 26.5 ka Oruanui eruption, New Zealand: A review of the roles of volcanism and climate in the post-eruptive sedimentary response. New Zealand Journal of Geology and Geophysics 47: 525–548.

Manville V., Newton E.H., White J.D.L. 2005. Fluvial responses to volcanism: resedimentation of the 1800a Taupo ignimbrite eruption in the Rangitaiki River catchment, North Island, New Zealand. Geomorphology 65: 49–70.

Manville V., Hodgson K.A., Nairn I.A. 2007. A review of break-out floods from volcanogenic lakes in New Zealand. New Zealand Journal of Geology and Geophysics 50: 131–150.

Manville V., Németh K., Kano K. 2009. Source to sink: A review of three decades of progress in the understanding of volcaniclastic processes, deposits, and hazards. Sedimentary Geology 220: 136–161.

Markey A.M., Clark C.S., Succop P.A., Roda S. 2008. Determination of the feasibility of using a portable X-ray fluorescence (XRF) analyzer in the field for measurement of lead content of sieved soil. Journal of environmental health 70: 24–29.

Martin R.C. 1961. Stratigraphy and structural outline of the Taupo Volcanic Zone. New Zealand Journal of Geology and Geophysics 4: 449–478.

Márton I., Moritz R., Spikings R. 2010. Application of low-temperature thermochronology to hydrothermal ore deposits: Formation, preservation and exhumation of epithermal gold systems from the Eastern Rhodopes, Bulgaria. Tectonophysics 483: 240–254.

Mauk J.L., Hall C.M. 2010. $^{40}Ar/^{39}Ar$ ages of adularia from the Golden Cross, Neavesville, and Komata epithermal deposits, Hauraki Goldfield, New Zealand. New Zealand Journal of Geology and Geophysics 47: 227–231.

Mauk J.L., Hall C.M., Chesley J.T., Barra F. 2011. Punctuated evolution of a large epithermal province: the Hauraki Goldfield, New Zealand. Economic Geology 106: 921–943.

Mauriohooho K., Barker S.L.L., Rae A.J., Simpson M.P. 2014a. Hydrothermal alteration and whole rock geochemistry of the Tauhara Geothermal Field: traditional versus rapid techniques.

Proceedings 36th New Zealand Geothermal Workshop, 24 - 26 November 2014, Auckland, New Zealand. 8 p.

Mauriohooho K., Barker S.L.L., Rae A.J., Simpson M.P. 2014b. Hydrothermal Alteration of the Tauhara Geothermal Field, an active hydrothermal system. AusIMM New Zealand Branch Annual Conference 2014. Pp. 371–381.

Mazor E., Bosch A., Stewart M., Hulston J. 1990. The geothermal system of Wairakei, New Zealand: physical processes and age estimates inferred from noble gases. Applied Geochemistry 5: 605–624.

McCraw J. 2011. The Wandering River: Landforms and geological history of the Hamilton Basin. Geoscience Society of New Zealand. 88 p.

McHenry L. 2005. Phenocryst composition as a tool for correlating fresh and altered tephra, Bed I, Olduvai Gorge, Tanzania. Stratigraphy 2: 101–115.

McNabb A. 1992. The Taupo-Rotorua hot-plate. Proceedings of the 14th New Zealand Geothermal Workshop. Pp. 111–114.

McNamara D.D., Massiot C., Lewis B. 2013. A Structural Review of the Wairakei-Tauhara Geothermal Field. GNS Science Report 2013/03. 20 p. http://www.gns.cri.nz/static/pubs/2013/SR%202013-003.pdf.

McPhie J., Allen R.L. 2003. Submarine, silicic, syn-eruptive pyroclastic units in the Mount Read volcanics, western Tasmania: Influence of vent setting and proximity on lithofacies characteristics. In: White J., Smellie J., Clague D. (eds) Explosive Subaqueous Volcanism. American Geophysical Union Geophysical Monograph 140. Pp. 245–258

McPhie J., Doyle M., Allen R. 1993. Volcanic textures: a guide to the interpretation of textures in volcanic rocks. Centre for Ore Deposit and Exploration Studies. University of Tasmania, Hobart. 189 p.

Mielke P., Bignall G., Sass I. 2010. Permeability and Thermal Conductivity Measurements of Near Surface Units at the Wairakei Geothermal Field, New Zealand. Proceedings of the World Geothermal Congress 2010, Bali, Indonesia 25-29 April 2010. Abstract 1228. 7 p.

Milicich S.D., Rosenberg M.D., Ramirez E., Kilgour G.N. 2008a. Geology of Exploration Well TH9 Tauhara Geothermal Field. GNS Science Consultancy Report 2008/56. 44 p.

Milicich, S.D., Ramirez, L.E., and Rosenberg, M.D., 2008b, Geology of Injection Wells WK314 and WK315 Wairakei Geothermal Field. GNS Science Consultancy Report 2008/235. 18 p.

Milicich S.D., Rae A.J., Ramirez L.E. 2009. Geology of Injection Wells WK313 and WK316 Wairakei Geothermal Field. GNS Science Consultancy Report 2009/23. 17 p.

Milicich S.D., Wilson C.J.N., Bignall G., Pezaro, B., Bardsley C. 2013. Reconstructing the geological and structural history of an active geothermal field: A case study from New Zealand. Journal of Volcanology and Geothermal Research 262: 7–24.

Milicich S.D., Chambefort I., Bignall G., Clark J., 2014. Overprinting Hydrothermal Systems in the Taupo Volcanic Zone. GRC transactions 38: 511–516.

Mortimer N. 1994. Origin of the Torlesse terrane and coeval rocks, North Island, New Zealand. International geology review 36:891–910.

Mortimer N., Gans P.B., Palin J.M., Meffre S., Herzer R.H., Skinner D.N.B. 2010. Location and migration of Miocene–Quaternary volcanic arcs in the SW Pacific region. Journal of Volcanology and Geothermal Research 190: 1–10.

Müller A., Breiter K., Seltmann R., Pécskay Z. 2005. Quartz and feldspar zoning in the eastern Erzgebirge volcano-plutonic complex (Germany, Czech Republic): evidence of multiple magma mixing. Lithos 80: 201–227.

Nairn I.A. 1979. Rotomahana—Waimangu eruption, 1886: base surge and basalt magma. New Zealand Journal of Geology and Geophysics 22: 363–378.

Nairn I.A., Wood C.P, Bailey R.A. 1994. The Reporoa caldera, Taupo volcanic zone: source of the Kaingaroa ignimbrites. Bulletin of volcanology 56: 529–537.

Nelson C.E., Giles D.L. 1985. Hydrothermal eruption mechanisms and hot spring gold deposits. Economic Geology 80: 1633–1639.

Nelson C.S., Lister G.S. 1995. Surficial bottom sediments of Lake Taupo, New Zealand: texture, composition, provenance, and sedimentation rates. New Zealand Journal of Geology and Geophysics 38: 37–41.

Nicol A., Walsh J., Berryman K., Villamor P. 2006. Interdependence of fault displacement rates and paleoearthquakes in an active rift. Geology 34: 865–868.

Norrish K., Chappell B.W. 1967. X-ray fluorescence spectrography. In: Zussman J ed. Physical Methods in Determinative Mineralogy. Academic, San Diego, Calif. Pp. 161 – 214.

Norrish K., Hutton J.T. 1969. An accurate X-ray spectrographic method for the analysis of a wide range of geological samples. Geochimica et cosmochimica acta 33: 431–453.

Paulick H., Vanko D.A., Yeats C.J. 2004. Drill core-based facies reconstruction of a deep-marine felsic volcano hosting an active hydrothermal system (Pual Ridge, Papau New Guinea, ODP Leg 193). Journal of Volcanology and Geothermal Research 130: 31–50.

Peinado F.M., Ruano S.M., González M.G.B., Molina C.E. 2010. A rapid field procedure for screening trace elements in polluted soil using portable X-ray fluorescence (PXRF). Geoderma 159: 76–82.

Piercey S.J., Devine M.C. 2014. Analysis of powdered reference materials and known samples with a benchtop, field portable X-ray fluorescence (pXRF) spectrometer: evaluation of performance and potential applications for exploration lithogeochemistry. Geochemistry: Exploration, Environment, Analysis 14: 139–148.

Potts P.J. 1987. A handbook of silicate rock analysis. Glasgow, Blackie, New York : Chapman and Hall, 1987. 622 p.

Potts P.J., Williams-Thorpe O., Webb P.C. 1997. The bulk analysis of silicate rocks by portable X-ray fluorescence: Effect of sample mineralogy in relation to the size of the excited volume. Geostandards Newsletter 21: 29–41.

Prasetyo I.M., Browne P.R.L., Zarrouk S.J., Sepúlveda F. 2012. Petrology and Hydrothermal Alteration of the Spa Andesite from the Wairakei-Tauhara Geothermal System, Taupo Volcanic zone, New Zealand. Proceedings of the New Zealand Geothermal Workshop 2012, Auckland, New Zealand. 9 p.

Rae A. 2007. Rotokawa Geology and Geophysics. GNS Science Consultancy Report 2007/83. 11 p.

Ramirez L.E., Rosenberg M.D. 2009. Geology of Monitor Well THM19 Tauhara Geothermal Field. GNS Science Consultancy Report 2009/221. 42 p.

Ramirez L.E., Alcaraz S.A., Rosenberg M.D., Rae A.J. 2009. Geology of Exploration Well TH18 Tauhara Geothermal Field. GNS Science Consultancy Report 2009/277. 146 p.

Risk G.F. 1984. Electrical resistivity survey of the Wairakei geothermal field. Proceedings of the 6th New Zealand Geothermal Workshop, University of Auckland, Auckland, New Zealand. Pp. 123–128.

Rosa C.J.P., McPhie J., Relvas J.M.R.S. 2009. Sediment-matrix igneous breccias at the top contacts of felsic units in the IPB: implications for VHMS exploration. Society for Geology applied to Mineral Deposits 3 p.

Rosa C.J.P., McPhie J., Relvas J.M.R.S. 2010. Type of volcanoes hosting the massive sulfide deposits of the Iberian Pyrite Belt. Journal of Volcanology and Geothermal Research 194:107–126.

Rosenberg M.D., Kilgour G.N. 2003. Explosive Volcanism at Tauhara Volcanic Complex: implications for the emplacement of Hipaua dome. Programme and Abstracts, Geological Society of New Zealand Annual Conference 2003, University of Otago, Dunedin, New Zealand, 1 – 4 December. Pp. 125.

Rosenberg M.D., Bignall G., Rae A.J. 2009a. The geological framework of the Wairakei Tauhara Geothermal System, New Zealand. Geothermics 38: 72–84.

Rosenberg M.D, Ramirez L.E., Kilgour, G.N., Milicich S.D., Manville V.R. 2009b. Tauhara Subsidence Investigation Project : Geological Summary of Tauhara Wells THM12-18 and THM21-22. GNS Science Consultancy Report 2009/309. 52 p.

Rosenberg M.D., Chambefort I., Lewis B. 2013. Stratigraphic Review of Well WK224, Poihipi West Area, Wairakei Geothermal Field. GNS Science Consultancy Report 2013/16. 16 p.

Rosenberg M.D., Wilson C.J.N., Bignall G., Alcaraz S.A., Sepúlveda F., Ireland T.R. 2014. Volcano-tectonic evolution of the Wairakei-Tauhara geothermal system: insights from U-Pb dating of zircons. Proceedings, Annual New Zealand Geosciences Conference, 24-27 November, New Plymouth. Pp. 92.

Ross P.-S., Bourke A., Fresia B. 2014. Lithological discrimination in exploration drill-cores using portable X-ray fluorescence measurements: (1) testing three Olympus Innov-X analysers on unprepared cores. Geochemistry: Exploration, Environment, Analysis 14:171–185.

Rowland J.V., Sibson R.H. 2001. Extensional fault kinematics within the Taupo Volcanic Zone, New Zealand: Soft-linked segmentation of a continental rift system. New Zealand Journal of Geology and Geophysics 44:271–283.

Rowland J. V., Sibson R.H. 2004. Structural controls on hydrothermal flow in a segmented rift system, Taupo Volcanic Zone, New Zealand. Geofluids 4: 259–283.

Rowland J.V., Wilson C.J.N., Gravley D.M. 2010. Spatial and temporal variations in magma-assisted rifting, Taupo Volcanic Zone, New Zealand. Journal of Volcanology and Geothermal Research 190:89–108.

Rowland J. V., Simmons S.F. 2012. Hydrologic, magmatic, and tectonic controls on hydrothermal flow, Taupo Volcanic Zone, New Zealand: Implications for the formation of epithermal vein deposits. Economic Geology 107: 427–457.

Rowland J., Bardsley C., Downs D., Sepúlveda F., Simmons S., Scholz C. 2012. Tectonic controls on hydrothermal fluid flow in a rifting and migrating arc, Taupo Volcanic Zone, New Zealand. Proceeding of the New Zealand Geothermal Workshop 2012, Auckland, New Zealand. 6 p.

Sanders F., Chambefort I., Rosenberg M., Bignall, G., Rae A., Sepúlveda F. 2013. Characterisation and stratigraphic correlation of the andesites encountered in the Wairakei Geothermal Field. Proceedings of the 35th New Zealand Geothermal Workshop 2013, 17-20 November 2013, Rotorua, New Zealand. 7 p.

Schindlbeck J.C., Kutterolf S., Freundt A., Scudder R.P., Pickering K.T. et al. 2013. Emplacement processes of submarine volcaniclastic deposits (IODP Site C0011, Nankai Trough). Marine Geology 343: 115–124.

Schneider J-L., Ruyet A-L., Chanier F., Buret C., Ferriere et al. 2001. Primary or secondary distal volcaniclastic turbidites: how to make the distinction? An example from the Miocene of New Zealand (Mahia Peninsula, North Island). Sedimentary Geology 145: 1–22.

Schneider J-L., Pérez Torrado F.J., Gimeno Torrente D.G., Wassmer P., Santana Md.C.C. et al. 2004. Sedimentary signatures of the entrance of coarse-grained volcaniclastic flows into the sea: the example of the breccia units of the Las Palmas Detritic Formation (Mio–Pliocene, Gran Canaria, Eastern Atlantic, Spain). Journal of Volcanology and Geothermal Research 138: 295–323.

Seebeck H., Nicol A., Villamor P., Ristau J., Pettinga J. 2014. Structure and kinematics of the Taupo Rift, New Zealand. Tectonics 1178–1199.

Self S., Sparks R.S.J. 1978. Characteristics of widespread pyroclastic deposits formed by the interaction of silicic magma and water. Bulletin of Volcanology 41: 196–212.

Sepúlveda F., Rosenberg M.D., Rowland J.V., Simmons, S.F. 2012. Kriging predictions of drill-hole stratigraphy and temperature data from the Wairakei geothermal field, New Zealand: Implications for conceptual modeling. Geothermics 42: 13–31.

Shane P., Wright I.C. 2011. Late Quaternary tephra layers around Raoul and Macauley Islands, Kermadec Arc: implications for volcanic sources, explosive volcanism and tephrochronology. Journal of Quaternary Science 26:422–432.

Sheppard P.J., Irwin G.J., Lin S.C., McCaffrey C.P. 2011. Characterization of New Zealand obsidian using PXRF. Journal of Archaeological Science 38:45–56.

Smith G. 1991. Facies sequences and geometries in continental volcaniclastic sediments. In: Fisher RV, Smith GA (eds) Sedimention in Volcanic Settings. SEPM Special Publication. 45: 109–121

Smith R.C.M., Smith I.E.M., Browne P.R.L., Hochstein M.P. 1993. Volcano-tectonic controls on sedimentation in the Taupo Volcanic Zone, New Zealand. In: Ballance P.F. ed., South Pacific sedimentary basins. Pp. 143–156.

Soengkono S., Hochstein M.P. 1992. Magnetic anomalies over the Wairakei Geothermal Field, central North Island, New Zealand. Geothermal Resources Council Transactions. Pp. 273–278.

Soengkono S. 2011. Deep interpretation of gravity and airborne magnetic data of the central Taupo Volcanic Zone. In: Proceedings of the 33rd New Zealand Geothermal Workshop 2011, 21-23 November 2011, Auckland, New Zealand. 6 p.

Soengkono S. 2012. Gravity modeling of Reporoa basin, eastern Taupo Volcanic Zone TVZ. New Zealand. In: Proceedings of the 34th New Zealand Geothermal Workshop 2012, 19-21 November 2012, Auckland, New Zealand. 6 p.

Sohn Y.K., Ki J.S., Jung S., Kim M-C., Cho H., Son M. 2013. Synvolcanic and syntectonic sedimentation of the mixed volcaniclastic–epiclastic succession in the Miocene Janggi Basin, SE Korea. Sedimentary Geology 288: 40–59.

Song S-R., Lo H-J. 2002. Lithofacies of volcanic rocks in the central Coastal Range, eastern Taiwan: implications for island arc evolution. Journal of Asian Earth Sciences 21: 23–38.

Stagpoole V. 1994. Interpretation of refraction seismic and gravity data across the eastern margin of the Taupo Volcanic Zone, New Zealand. Geothermics 23: 501–510.

Steiner A. 1970. Genesis of hydrothermal K-feldspar (adularia) in an active geothermal environment at Wairakei, New Zealand. Mineralogical Magazine 37: 916–922.

Steiner A. 1977. The Wairakei Geothermal Area, North Island, New Zealand. New Zealand Geological Survey Bulletin 90. 136 p.

Takemura K., Kamp P. 1991. A Sedimentological Study of Huka Group Sediments: Preliminary Report to Electricorp Production, Wairakei Geothermal Area. 43 p.

Thompson A.J.B., Thompson J.H.F. 1996. Atlas of alteration: a field and petrographic guide to hydrothermal alteration minerals (A. J. B. Thompson & J. F. H. Thompson, Eds.): Geological Association of Canada. 119 p.

Tian Y., Shan Y 2011. The diversity of flow structures in felsic dykes. Journal of the Geological Society 168: 1001–1011.

Timperley M. 1983. Geological history of Lake Taupo. In: Forsyth D.J., Howard-Williams C.O. eds. Lake Taupo: ecology of a New Zealand lake. Division of Marine and Freshwater Science, DSIR, Taupo, New Zealand, Wellington. Pp. 5–15.

Valenzuela A., Donaire T., González-Roldán M.J., Toscano M., Pascual E. 2011. Volcanic architecture in the Odiel river area and the volcanic environment in the Riotinto–Nerva Unit, Iberian Pyrite Belt, Spain. Journal of Volcanology and Geothermal Research 202: 29–46.

Van der Marel H.W. 1947. Diatomaceous deposits at Lake Toba. Journal of Sediment Research 17: 129–134.

Vandergoes M.J., Hogg A.G., Lowe D.J., et al. 2013. A revised age for the Kawakawa/Oruanui tephra, a key marker for the Last Glacial Maximum in New Zealand. Quaternary Science Reviews 74: 195–201.

Verati C., Patrier-Mas P., Lardeaux J.M., Bouchot V. 2013. Timing of geothermal activity in an active island-arc volcanic setting: First $^{40}Ar/^{39}Ar$ dating from Bouillante geothermal field (Guadeloupe, French West Indies):. Geological Society, London, Special Publications 378. Pp. 285–295.

Villa I.M., Ruggieri G., Puxeddu M., Bertini G. 2006. Geochronology and isotope transport systematics in a subsurface granite from the Larderello–Travale geothermal system (Italy). Journal of Volcanology and Geothermal Research 152: 20–50.

Villamor P, Berryman K 2001. A late Quaternary extension rate in the Taupo Volcanic Zone, New Zealand, derived from fault slip data. New Zealand Journal of Geology and Geophysics 44: 243–269.

Villamor P., Berryman K. 2006. Evolution of the southern termination of the Taupo Rift, New Zealand. New Zealand Journal of Geology and Geophysics 49: 23–37.

Vucetich C.G., Howorth R. 1976. Late Pleistocene tephrostratigraphy in the Taupo district, New Zealand. New Zealand Journal of Geology and Geophysics 19: 37–41.

Walker G.P.L., Croasdale R. 1971. Characteristics of some basaltic pyroclastics. Bulletin of Volcanology 35: 303–317.

Walker G.P.L. 1973. Explosive volcanic eruptions – a new classification scheme. Geologische Rundschau 62: 431–446.

Walker G.P.L. 1981. Characteristics of two phreatoplinian ashes, and their water-flushed origin. Journal of Volcanology and Geothermal Research 9: 395–407.

Walker G.P.L., Self S., Wilson L. 1984. Tarawera 1886, New Zealand — A basaltic plinian fissure eruption. Journal of Volcanology and Geothermal Research 21: 61–78.

Walker G.P.L. 1985. Origin of coarse lithic breccias near ignimbrite source vents. Journal of Volcanology and Geothermal Research 25: 157–171.

Wallace L.M., Beavan J., McCaffrey R., Darby D. 2004. Subduction zone coupling and tectonic block rotations in the North Island, New Zealand. Journal of Geophysical Research 109. 21 p.

White J.D.L. 2000. Subaqueous eruption-fed density currents and their deposits. Precambrian Research 101: 87–109.

White J.D.L. 2001. Eruption and reshaping of Pahvant Butte volcano in Pleistocene Lake Bonneville. In: White J., Riggs N. eds. Volcaniclastic Sedimentation in Lacustrine Settings, International Association of Sedimentologists, Blackwell Science, Malden, MA, USA. Pp 61–80.

White J.D.L, Houghton B.F. 2006. Primary volcaniclastic rocks. Geology 34: 677–680.

White N.C., Hedenquist J.W. 1990. Epithermal environments and styles of mineralization: Variations and their causes, and guidelines for exploration. Journal of Geochemical Exploration 36: 445–474.

Whitham A.G. 1989. The behaviour of subaerially produced pyroclastic flows in a subaqueous environment: evidence from the Roseau eruption, Dominica, West Indies. Marine geology 86: 27–40.

Wilson C.J.N., Houghton B.F., Lloyd E.F. 1986. Volcanic history and evolution of the Maroa-Taupo area, central North Island. In: Smith I.E.M. ed. Late Cenozoic Volcanism in New Zealand, Royal Society New Zealand Bulletin 23. Pp. 194–223.

Wilson C.J.N. 1991. Ignimbrite morphology and the effects of erosion: a New Zealand case study. Bulletin of Volcanology 533: 635–644.

Wilson C.J.N. 1993. Stratigraphy, Chronology, Styles and Dynamics of Late Quaternary Eruptions from Taupo Volcano, New Zealand. Philosophical Transactions: Physical Sciences and Engineering 343: 205–306.

Wilson C.J.N., Houghton B.F., McWilliams M.O., Lanphere M.A., Weaver S.D., Briggs R.M. 1995. Volcanic and structural evolution of Taupo Volcanic Zone, New Zealand: a review. Journal of Volcanology and Geothermal Research 68: 1–28.

Wilson C.J.N. 2001. The 26.5 ka Oruanui eruption, New Zealand: an introduction and overview. Journal of Volcanology and Geothermal Research 112: 133–174.

Wilson C.J.N., Gravley D.M., Leonard G.S., et al. 2005. The 340-240 ka Ignimbrite Flare-up Event in Taupo Volcanic Zone, New Zealand. EOS, Transactions American Geophysical Union 86(52), Fall Meeting Supplementary Abstracts V53B-1549.

Wilson C.J.N., Blake S., Charlier B.L.A., Sutton, A.N. 2006. The 26.5 ka Oruanui Eruption, Taupo Volcano, New Zealand: Development, Characteristics and Evacuation of a Large Rhyolitic Magma Body. Journal of Petrology 47: 35–69.

Wilson C.J.N., Rowland J.V., Gravley D.M. 2008. The Taupo Volcanic Zone, New Zealand: a geological and geophysical review, with emphasis on its central segment. Institute of Earth Science & Engineering, University of Auckland, New Zealand. Report 2008-01. 135 p.

Wilson C.J.N., Gravley D.M., Leonard G.S., Rowland J.V. 2009. Volcanism in the central Taupo Volcanic Zone , New Zealand : tempo, styles and controls. In: Thordarson T., Self S., Larsen G., Rowland S.K., Hoskuldsson A. eds. Studies in Volcanology: The Legacy of George Walker. Geological Society for IAVCEI. Pp. 225–247.

Wilson C.J.N., Charlier B.L.A., Rowland J.V., Browne P.R.L. 2010. U–Pb dating of zircon in subsurface, hydrothermally altered pyroclastic deposits and implications for subsidence in a magmatically active rift: Taupo Volcanic Zone, New Zealand. Journal of Volcanology and Geothermal Research 191: 69–78.

Wilson C.J.N., Bignall G., Chambefort I., Cole J.W., Charlier B.L.A., Eastwood A.A., Gravley D.M. 2015. Insights into Geothermal Systems from U-Pb Dating of Zircons in Hydrothermally Altered Rocks: the New Zealand Experience. In: Proceedings World Geothermal Congress 2015, Melbourne, Australia, 19-25 April 2015. 11 p.

Wood C.P. 1994a. The Waiora Formation geothermal aquifer, Taupo Volcanic Zone, New Zealand. Proceedings of the 16th New Zealand Geothermal Workshop 1994. Pp. 121–126.

Wood C. 1994b. Aspects of the geology of Waimangu, Waiotapu, Waikite and Reporoa geothermal systems, Taupo volcanic zone, New Zealand. Geothermics 23: 401–421.

Wood C.P. 1995. Calderas and geothermal systems in the Taupo volcanic zone, New Zealand. In: Barbie E., Frye G., Iglesias E., Palmason G. eds. Worldwide utilization of geothermal energy: an indigenous, environmentally begin renewable energy resource. Proceedings World Geothermal Congress, 1995, Florence, Italy. Auckland, International. Pp. 1331–1336.

Wood C.P., Mroczek E.K., Carey B.S. 1997. The boundary of Wairakei geothermal field: geology and chemistry. Proceedings of the 19th New Zealand Geothermal Workshop, University of Auckland, Auckland, New Zealand, University of Auckland, Auckland, New Zealand. Pp. 25–30.

Wood C.P. 1998. Water-rock interaction at the boundary of Wairakei geothermal field. In: Arehart G.B., Hulston J.R. eds. Water-rock Interact. Water-rock Interaction: Proceedings of the 9th International Symposium on Water-Rock Interaction -- WRI-9, Taupo, New Zealand, 30 March-3 April 1998. Pp. 705–708

Wood C.P., Browne P.R.L. 2000. Wairakei Geothermal Power Project 40th Anniversary: Geology and Hydrothermal Alteration. Proceedings 22nd New Zealand Geothermal Workshop 2000, Auckland University, Auckland, New Zealand. Pp. 285–290.

Worthington T.J. 1985. Geology and petrology of the Tauhara Volcanic Complex, Taupo, New Zealand. Unpublished MSc thesis. Victoria University of Wellington, New Zealand.

Youngman K.J. 1988. Hydrothermal Alteration and Thermal Evolution of the Wairakei-Tauhara Geothermal Area. Unpublished PhD thesis. University of Auckland. 352 p.

A1. Appendix

SUMMARY OF APPENDIX CONTENT

A1.1.Terminology

A1.2. Calibrating pXRF and comparisons with lab XRF

A2.1. – A2.8 Digital appendix files

The following files used in this research are the property of Contact Energy:

- Wairakei and Tauhara Subsidence Project core photographs (1108 photos)
- Geological and geothermal well data (spreadsheets)
- 2014 Geological model of Wairakei-Tauhara Geothermal Field (Leapfrog 3D)
- Client geological drilling reports (see references)

A1.1. TERMINOLOGY

Key terms are defined here to clarify their usage in this thesis. For volcanic textures or processes consult McPhie et al. (1993). All *volcaniclastic* grain size terminology follows the classification scheme of White and Houghton (2006), also evaluated in Manville et al. (2009).

- ***Autoclastic deposit:*** volcaniclastic deposits (*autoclastic lava*) generated by mechanical shearing fragmentation.
- ***Caldera:*** the surface and subsurface manifestation of structural collapse or subsidence associated with mass magma withdraw generating explosive volcanism.
- ***Diatomaceous:*** (or diatomite) rock rich in siliceous diatom shells within the Huka Group deposited in a lacustrine setting.
- **Density current:** see pyroclastic density current
- ***Facies association:*** a collection of facies that are spatially, mineralogically or texturally related, and may be genetically related.
- ***Facies/lithofacies:*** a distinctive rock that is lithologically, mineralogically or texturally characterised by a common depositional process or environment.
- ***Geothermal:*** a geothermal field defined at the surface by an electrical resistivity boundary (<500 m depth) above an active geothermal system characterised by descending meteoric water and ascending heated fluids.
- ***Hyaloclastic deposit:*** volcaniclastic deposits (*hyalocastite or peperite*) generated by quench fragmentation contacting or mixing with cold sediments or water.
- ***Hydrothermal:*** term associated with the processes and products within the geothermal system and field area. E.g., hydrothermal alteration, hydrothermal, mineralisation, hydrothermal eruption.
- ***Juvenile:*** Clast formed from magma genetically related to an erupted magmatic deposit (e.g., pumice, plutonic lithic clast).
- ***Ignimbrite:*** the characteristic deposit generated from a pyroclastic density current from column collapse that may be welded or unwelded. The use of *'Ignimbrite'* with a capitalised name in this thesis is a stratigraphic term for units consisting dominantly of ignimbrites (e.g., Wairakei Ignimbrite).
- ***Primary:*** refers to either a *mineral* crystallising directly from a magma, or a *volcanic deposit* deposited directly by volcanic processes with no temporary storage.
- ***Pumice:*** originally highly *vesicular* (>60 vol.%) *rhyolite clasts*. At Wairakei-Tauhara pumice clasts are almost always altered to white clays.
- ***Pyroclastic density current:*** a gravity-driven current comprised of hot material generated and deposited by a subaerial explosive eruption or series of related eruptions.

- ***Pyroclastic deposit:*** volcaniclastic deposits (*pyroclast*) generated by explosive fragmentation and transported by pyroclastic density currents.
- ***Pyroclastic flow:*** a concentrated pyroclastic density current.
- ***Reworked deposit:*** a deposit modified (grain size, shape, sorting, bedding) following an initial period of deposition involving re-sedimentation transport.
- ***Secondary:*** refers to either a *mineral* crystallising following the primary (magmatic) mineral assemblage from hydrothermal fluids *(secondary mineral)*, also synonymous with a reworked *volcanic* deposit *(secondary deposit).*
- ***Stratigraphy:*** is the combined layered sequence of volcanic and sedimentary rock (strata or beds) usually formally defined by a stratigraphic hierarchy: Group>Formation>Member.
- ***Subaqueous volcaniclastic density current:*** base-hugging, mainly water-supported density currents dominantly comprised of volcanic particles. Currents may be eruption-fed or not, and sourced from subaerial (traversing a shoreline) or subaqueous vents.
- ***Unit:*** informal term describing a discrete or sequence of related deposits comprising a stratigraphic succession.
- ***Volcanic deposit:*** includes coherent lava (lava flow, dome or intrusion) and volcaniclastic deposits effusively or explosively erupted from a vent source.
- ***Volcaniclastic deposit:*** umbrella term for lithified or nonlithified clastic deposits (pyroclastic, autoclastic and hyolaclastic) derived from the transport and deposition of the products of volcanic activity. Descriptive grain size terminology used is after White and Houghton (2006).
- ***Volcanogenic:*** material derived from temporarily stored nonlithified volcanic martial and deposited by normal sedimentary processes.

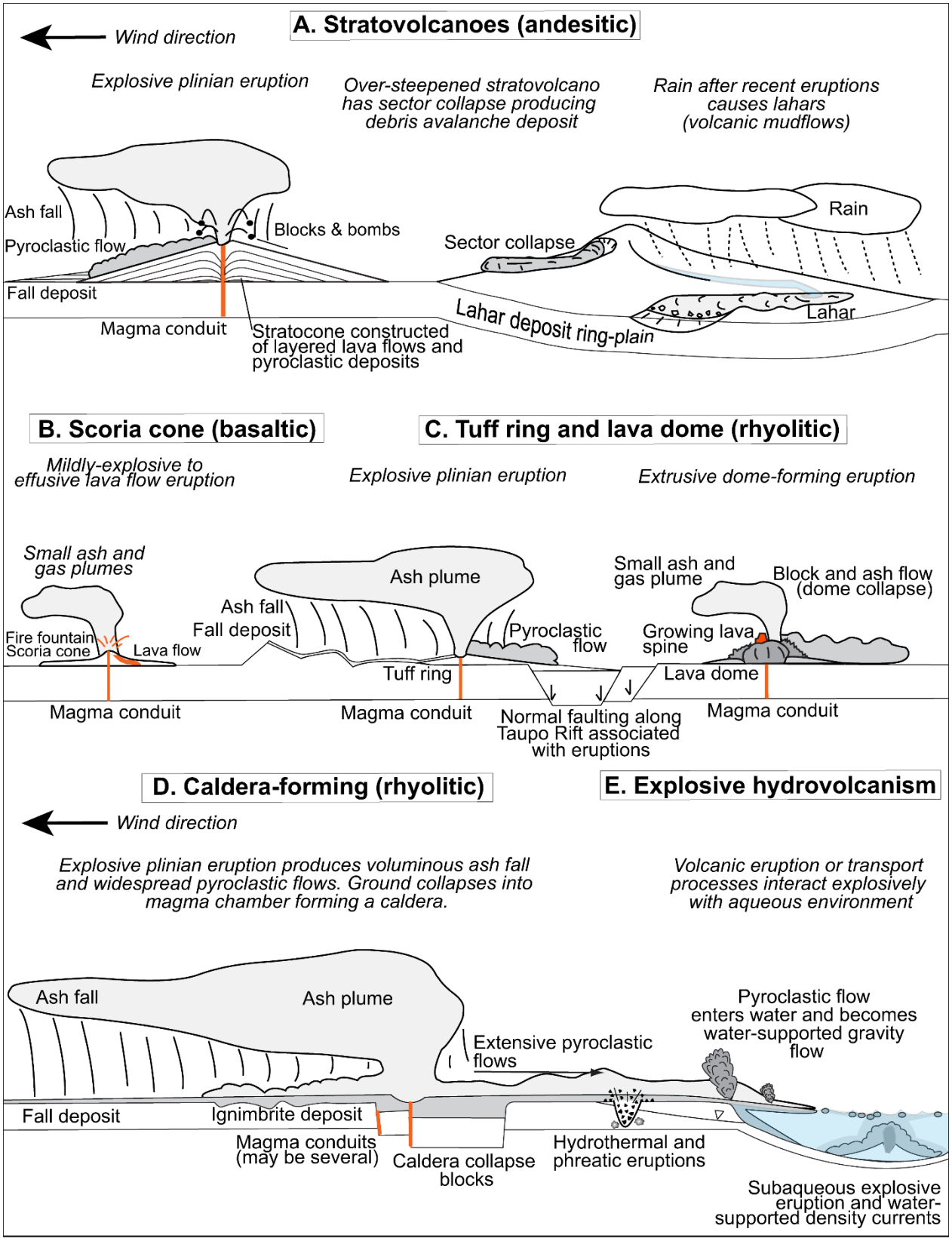

Figure A.1.1 Schematic illustrations of representative TVZ volcanic eruption styles, processes and deposits. Eruptive styles are principally influenced by magma composition. **A.** Andesitic compositions commonly involve explosive eruptions, pyroclastic flows and cone-building. **B.** Basaltic compositions result in weakly explosive fire-fountaining to effusive eruptions building scoria cones. **C.** Rhyolitic compositions build lava domes, commonly with block-and-ash flow collapse, and generate large explosive plinian eruptions from **D.** calderas forming pyroclastic flows. **E.** Smaller scale explosive eruptions or transported material may involve interaction with ground or surface water. Figure modified from Leonard et al. (2010).

A1.2. CALIBRATING pXRF AND COMPARISONS WITH LAB XRF

pXRF: machine-automated results

A full understanding of the pXRF model's analytical capabilities is needed to accurately understand and assess the collected data set (Chapter 4; Appendix A2.4). Twenty elements were analysed (Appendix A2.4), but only the results of elements Ti and Zr are used in Chapter 4. Geochemical pXRF results are exported as a spreadsheet file format. Each analysis includes the detected element's concentration, a calculated error (both in ppm). Results include if the test is a pass (reliable) or fail (unreliable; pass rate shown in Table A1.1) determined by a factory-defined acceptable concentration range compared to the detected concentration. From the large data set gathered (Appendix A2.4), the pXRF limit of detection (LOD), pass rate value and machine error can be empirically estimated (Table A1.1). The LOD is approximated from the lowest observed detected concentration that passed (Table A1.1). The lowest possible pass rate where the size error is compared to the detected concentration is estimated <30 % for Ti (e.g., 450/600 ppm = fail) and <<1 % for Zr. The error variation of the pXRF between tests was estimated by: $(\frac{\sigma\ error}{\mu\ error})$, and is 5 – 11 % for Ti and Zr (Table A1.1; σ = standard deviation; μ = mean)

pXRF: dry sample calibration

Preliminary pXRF tests were undertaken in to determine optimal pXRF test times that balanced efficiency and accuracy for the different sample types tested (e.g., powder, core; dry, moist). Inhomogeneous sample types and pXRF detection limitations returned results were less accurate than the lab XRF equivalent (Chapter 4). The precision the pXRF (replicability) were estimated by repeat tests on near homogeneous powder samples (Table A1.1). Variation between repeat tests ($\frac{\sigma\ conc.}{\mu\ conc.}$) reflects the instrument's

Table A1.1. Comparison of pXRF Ti and Zr pass rate and selected element detection on powder (homogeneous), dry core (inhomogeneous) and moist core (inhomogeneous) pyroclastic Huka Group samples. Note: the increased count time for the moist tests.

Element	Detection at 60 s (ppm)		Powder (60 s, n= 42)				Dry core (dry, 60 s, n= 39)				Moist core (**90 s**, n=55)			
	Observed LOD	Machine error (±)	Pass rate	Variation between tests	Average test error	Total machine error variation	Pass rate	Variation between tests	Average test error	Total machine error variation	Pass rate	Variation between tests	Average test error	Total machine error variation
Ti	600	200	82%	16%	17%	7%	81%	23%	16%	5%	83%	21%	18%	7%
Zr	64	3	100%	5%	2%	8%	100%	10%	2%	5%	100%	10%	2%	11%

consistency together with sample variations (conc. = concentration). On average, 60 s tests on 42 powder samples varied by 16 % for Ti and 5 % for Zr, further suggesting pXRF has reasonable precision (Table A1.1). Averaged 60 s analyses of selected dry core samples (n = 39) varied by 23 % for Ti and 10 % for Zr between tests. Repeat 90 s analyses on moist core (n = 55) returned similar results to the 60 s dry core (Table A1.1).

Tests of the resulting variation between sample states were made at 60 s (n = 39) between equivalent prepared powder (homogeneous) and unprepared core (inhomogeneous). Results suggest up to 30 % of Ti ($[23-16]/23$) and 50 % of Zr ($[10-5]/10$) repeat test variation could be due to the inhomogeneous sample type (including calculated machine error; Table A1.1). These values are lithology-dependent (i.e., more severe in coarse grained lithologies), but provide approximate constraints for assessing possible effects of sample inhomogeneity on results discussed below ('possible effect of inhomogeneity' in Table A2). Furthermore, the high variation between tests comparing equivalent powder and core samples may be attributed to sample coarseness. This outcome further supports the EDS results in that Ti and Zr within the samples are concentrated in small (local) mineral phases. Overall, the pXRF consistently provides highly consistent results when analysing ideal (prepared) powder and returns adequate consistency when analysing non-ideal (unprepared) core samples.

pXRF: moist sample calibration

Dry samples are optimal for pXRF detection as sample moisture reduces element detection proportional to its content level. Previous studies have suggested low moisture contents (<20 %) have a minimal effect on the overall pXRF error, and can be corrected for if they are significant (Peinado et al., 2010). Maximum sample moisture content was measured by weight at 2.5 wt.% for lavas and up to 20 wt.% for pumice lithic lapilli-tuffs and sediments (average <5 wt.%). Results were not corrected for moisture as water contents varied between each sample and were usually far below the maximum measured moisture content.

The pXRF analysis time was increased to 90 s for moist core samples to increase the accuracy of the results. Estimates on the effect of moisture on element detection are made using the mean and

standard deviation (SD at 1σ) of moist and dry collected pXRF data (Table A1.2). Repeat analysis of moist core samples (n = 55, 90 s) had Ti and Zr values varied by 21 % and 10 %, respectively (Table A1.1). Tests on powder have already indicated sample inhomogeneity is responsible for a fraction.

The following sections estimate the possible influence moisture may have had on pXRF detection. Traditionally, the effect of moisture on pXRF detection are determined by varying moisture while other parameters remain static. Given the available data set, the effect of moisture in these samples on pXRF detection is estimated using its precision on an inhomogeneous sample. More accurate estimates are beyond the scope of this investigation and have been comprehensively described and quantified (e.g., Argyraki et al., 1997; Ge et al., 2005; Markey et al., 2008; Peinado et al., 2010).

The effect of moisture alone is estimated using selected core samples (n = 14; Table A1.2). The dry 90 s SD of Ti and Zr are considered to be an acceptable maximum range within which the wet mean value must fall for wet and dry results to be considered 'comparable'. Mean moist test values outside the dry SD range are considered too variable to be used to reasonably estimate the effect of moisture. Table A1.2 shows that over half the Ti and Zr moist sample tests fall outside their equivalent dry SD. Mean moist tests values within the dry test SD are suitable to estimate the effect of moisture and sample inhomogeneity. Collectively, the 14 samples have high SD for their moist/dry ratios: Ti has a 36 % SD and Zr a 22 % SD. The effect of moisture together with sample inhomogeneity is ~20 – 30 % for Ti and Zr detection (Table A1.2). However, if only the results whose wet test mean fell inside the dry test SD are selected to provide a more reliable data set, the SD of Ti is 16 % and Zr 9 % (Table A1.2). These values are a reasonable conservative estimates for the effect moisture on element detection.

The effect of average sample inhomogeneity for medium to coarse grained samples was earlier empirically estimated and now can be broadly 'corrected' for in Huka Group lithologies. Sixty-second tests on ~40 powder and core samples suggested sample inhomogeneity (and pXRF error) had an average 30 % effect on Ti and 50 % effect on Zr concentration and detection (Table A1.1). Applying this value to the samples whose moist test concentration was with the dry test SD over or underestimated error (i.e.,$[(100\% - concentration) \times (inhomogency\ effect\ value) + concentration]$), SD values become 11 % for Ti (n = 7) and 4 % for Zr (n = 5). These values are comparable with the 60 s

homogeneous powder test SD's (Table A1.2), but are only estimates. Standard moisture testing procedures per sample would yield more accurate results.

Nonetheless, given the results from the sample suite, conservative estimates suggest moisture has a maximum ~10 – 20 % effect on pXRF detection of Ti and ~5 – 10 % effect on Zr (Table A2). Overall, tests identify moisture impacts pXRF element detection significantly less when detection times are higher (e.g., 60 s vs. 90 s). Results from inhomogeneous dry core tests (60 s) and moist tests (90 s) are comparable, but still require multiple analyses ($n \geq 4$) and averaged results to reduce the effect of inhomogeneity (Potts et al., 1997).

Table A1.2. Selected analyses of dry and moist core samples (n = 14) demonstrating the effect of moisture on pXRF detection at 90 s count time. **Bolded** moist analyses are those that exceed the 'acceptable' dry SD range (1σ standard deviation, SD), *italic* values are below this SD range. Column captions (see text): Dry = oven dried samples; Moist = *in situ* moist samples; Moist/dry conc. = moist test result concentration (conc.) divided by the dry test result concentration; Moist/dry (≤dry SD) = selected data where the moist concentration is within the dry SD range; Minus possible effect of inhomogeneity = the empirically estimated effect (difference between powder and core pXRF analyses) sample inhomogeneity has on the test result. Lithology abbreviations: *f = fresh/minimal alteration, a = altered/cemented, T = tuff/volcanic sandstone, Plt = pumice-lapilli-tuff, PLlt = Pumice and Lithic lapilli-tuff.*

Sample (n = 14)	**Core lithology**	**Ti (90 s)**				Selected data analysis			**Zr (90 s)**				Selected data analysis		
		Dry (n = 4)		Moist (n = 4)		Moist/dry conc.	Moist/dry (≤dry SD) n = 7	Minus possible effect of inhomogeneity (30 %)	Dry (n = 4)		Moist (n = 4)		Moist/dry conc.	Moist/dry (≤dry SD) n = 5	Minus possible effect of inhomogeneity (50 %)
		Conc.	Test SD (±)	Conc.	Test SD (±)				Conc.	Test SD (±)	Conc.	Test SD (±)			
WKM14-436	aT	1590	823	*1029*	213	0.65	-	-	197	2	*126*	26	0.64	-	-
WKM14-516	aT	2372	1171	*1125*	412	0.47	-	-	166	10	*138*	6	0.83	-	-
WKM14-529	aPLlt	1718	407	**2132**	662	1.24	-	-	176	37	*142*	9	0.81	-	-
WKM14-532	aPLlt	1378	186	1537	405	1.12	1.12	1.08	165	22	151	16	0.91	0.91	0.96
WKM14-543	aPLlt	1632	61	1426	293	0.87	0.87	0.91	220	19	*156*	9	0.71	-	-
WKM14-546	aPLlt	1131	280	1336	197	1.18	1.18	1.13	119	21	**153**	10	1.28	-	-
WKM14-592	aT	1409	208	1460	392	1.04	1.04	1.02	189	33	166	17	0.88	0.88	0.94
WKM14-620	aT	1923	341	*628*	49	0.33	-	-	244	47	*133*	8	0.54	-	-
WKM15-149	fT	1080	123	*719*	15	0.67	-	-	112	21	**142**	10	1.27	-	-
WKM15-176	fT	933	184	824	330	0.88	0.88	0.92	149	33	*100*	3	0.67	-	-
WKM15-489	aT	1284	199	992	239	0.77	0.77	0.84	184	26	166	15	0.90	0.90	0.95
WKM15-508	aT	974	279	**1329**	332	1.36	-	-	167	21	167	27	1.00	1.00	1.00
WKM15-512	aPlt	1649	280	1914	617	1.16	1.16	1.11	150	25	165	25	1.10	1.10	1.05
WKM15-515	aPLlt	1448	447	**2333**	87	1.61	-	-	174	25	*147*	14	0.84	-	-
Average (SD/Result)			0.23		0.22					0.14		0.09			
Total data set SD						0.36	**0.16**	**0.11**					0.22	**0.09**	**0.04**

A2. Digital appendix

SUMMARY OF DIGITAL APPENDIX FILES

The supplementary digital appendix on the supplied CD contains the following data files:

A2.1. Detailed **thesis methodologies and data sources** (below)

A2.2. A list of **collected** and provided **samples** from this research

A2.3. Photograph **clast size** measurement data (>5000 measurements)

A2.4. Laboratory X-ray Fluorescence (XRF) and portable XRF **geochemistry** data (>1400 analyses)

A2.5. Photomicrograph **crystal size** and volume measurement data (>2500 measurements)

A2.6. **EDS** thin section analysis reports

A2.7. Crystal **Raman** spectroscopy analyses (accessory data)

A2.8. Crystal **Electron Microprobe** (EMP) data (accessory data)